

July 2016

A Paleobathymetric Model and Evolution of the Brazilian Marginal Basins during the Late Maastrichtian to Eocene based on Benthic Foraminiferal Biofacies

Renata Moura de Mello
Umass Amherst

Follow this and additional works at: https://scholarworks.umass.edu/dissertations_2



Part of the [Geology Commons](#), [Oceanography Commons](#), and the [Paleontology Commons](#)

Recommended Citation

de Mello, Renata Moura, "A Paleobathymetric Model and Evolution of the Brazilian Marginal Basins during the Late Maastrichtian to Eocene based on Benthic Foraminiferal Biofacies" (2016). *Doctoral Dissertations*. 622.

https://scholarworks.umass.edu/dissertations_2/622

This Open Access Dissertation is brought to you for free and open access by the Dissertations and Theses at ScholarWorks@UMass Amherst. It has been accepted for inclusion in Doctoral Dissertations by an authorized administrator of ScholarWorks@UMass Amherst. For more information, please contact scholarworks@library.umass.edu.

**A PALEOBATHYMETRIC MODEL AND EVOLUTION OF THE BRAZILIAN
MARGINAL BASINS DURING THE LATE MAASTRICHTIAN TO EOCENE BASED
ON BENTHIC FORAMINIFERAL BIOFACIES**

A Dissertation Presented

By

RENATA MOURA DE MELLO

Submitted to the Graduate School of the
University of Massachusetts Amherst in partial fulfillment
of the requirements for the degree of

DOCTOR OF PHILOSOPHY

May 2016

Geosciences

© Copyright by Renata Moura de Mello 2016

All Rights Reserved

**A PALEOBATHYMETRIC MODEL AND EVOLUTION OF THE BRAZILIAN
MARGINAL BASINS DURING THE LATE MAASTRICHTIAN TO EOCENE BASED
ON BENTHIC FORAMINIFERAL BIOFACIES**

A Dissertation Presented

by

RENATA MOURA DE MELLO

Approved as to style and content by:

R. Mark Leckie, Chair

Robert DeConto, Member

Stephen J. Burns, Member

Cristina Cox Fernandes, Member

Julie Brigham-Grette, Department Head
Geosciences

DEDICATION

To **Ana Luisa**, my lovely daughter and the best part of me – you always will be my *cheerleader!*

To **Ivan & Madalena**, my parents and my foundation.

To **Flávia & Bruna**, my sisters and my best friends in life.

To **Mark & Pam Leckie**, my family and my heart in the USA.

Words cannot express how much I love you all.

ACKNOWLEDGMENTS

I would like to address my thanks in a distinct and unique way, such as the significance of this work in my life.

Initially, to my high school teacher Prof. Paulo Roberto, who first caught my attention on geosciences and its wonders about our planet. On my college years, to my professors Cristiane Castañeda, José Ricardo Maizatto and Maria Paula Delicio, who definitely guided me through my first steps on science and research.

To Oscar Strohschoen Jr. who first introduced me the most fascinating microfossils: the foraminifera, and always has been supportive and cheering for my success.

To Ellen Thomas, who has been teaching me so much about benthic foraminifera and we shared the love of these unique microfossils.

I would like to express my gratitude to Professor Mark Leckie who joined me on this project that seemed almost impossible to achieve, but we made it happen! Mark, you are the best mentor and advisor I could ever have. I've learned so much from you!

To Brian Huber that made my visit possible to the Foraminifera Collection at Smithsonian Museum, Washington DC.

To my MicroLab fellow mates Serena, Khalifa, Chris, Ali, Amanda, Rachel and Adriane for the stimulating discussions, coffee-coke breaks, and for all the fun we have had in the last three years. In particular, to Andy Frass who helped me through the statistics analysis, Thanks a lot ANDY!

To my UMass brothers and sisters Mateus, Mika, Priscilla, and all CsF people – Go Umass!

To my friends Eduardo Koutsoukos and Claudia Cetan who helped me in such interesting discussions and supported me before I even started the PhD.

To my ForamsSister Fabiana Almeida who helped me with bright discussions and always dreamed with me. Sis, your day is coming!

To my parents, Ivan & Madalena, my daughter Ana Luisa, my sisters in life (Flávia, Bruna, Silvinha, Bárbara), Candida & Carlos, Renato, and my spiritual family for taking the blows and giving me a chance to thrive.

To my BPApeople Antônio, Marcinha, Henrique (chefinho!), Vivi, Ariany, Fabinho, Ana Cláudia, Beurlen, Denize, galera do laboratório (Luciano, Anderson, Luiz Mauro e cia), Carolzinha and so many others who encourage me during this project.

Last but not least, I would like to thank PETROBRAS without which financial support it would not be possible to conduct this research.

ABSTRACT

A PALEOBATHYMETRIC MODEL AND EVOLUTION OF THE BRAZILIAN MARGINAL BASINS DURING THE LATE MAASTRICHTIAN TO EOCENE BASED ON BENTHIC FORAMINIFERAL BIOFACIES

MAY 2016

RENATA MOURA DE MELLO, B.A., STATE UNIVERSITY OF RIO DE JANEIRO, BRAZIL

M.A., FEDERAL UNIVERSITY OF RIO DE JANEIRO, BRAZIL

Ph.D., UNIVERSITY OF MASSACHUSETTS AMHERST

Directed by: Professor R. MARK LECKIE

Benthic foraminiferal biofacies were delimited for the Maastrichtian to upper Eocene of five Brazilian marginal basins (Sergipe-Alagoas, Mucuri, Campos, Santos and Pelotas) and two DSDP Sites 356 and 20C of the western South Atlantic. Five biofacies, denoted with letters A to E, were defined using Q-mode cluster analysis and correspondence analysis for all of the 11 sites.

The benthic foraminiferal biofacies were used to establish a paleobathymetric and paleoenvironmental model for the Brazilian marginal basins. The model tracks the evolution of the margin as it built seaward and transitioned from abyssal (2000-3000 m) to bathyal (<2000 m) and neritic (<200 m) depositional environments during the Maastrichtian – late Eocene. It is a powerful predictive tool for reconstructing depositional systems in deep-water and for correlation in tectonically disturbed and complex hydrocarbon basins.

The Maastrichtian – Paleocene interval was dominated by Biofacies E, which consists almost exclusively of agglutinated benthics and is also known as a flysch-type assemblage, and secondarily by Biofacies D consisting of a mix of agglutinated and calcareous benthic taxa. Sea level fluctuations may have contributed in downslope transport, as well as a shallow calcite compensation depth (CCD) along the continental margin resulting in dissolution of planktic and calcareous benthic taxa, and the alternation between biofacies E and D. An abrupt change in biofacies across the Paleocene/Eocene boundary is observed in all the Brazilian marginal basins, with the exception of the Campos Basin. The Eocene interval is characterized by calcareous-dominated biofacies A, B and C in the Sergipe-Alagoas, Mucuri, Santos and Pelotas basins due to progradation of the margin and shoaling of the slope above the CCD, allowing for better preservation of carbonate. Biofacies D and E continued to dominate the Campos Basin during the Eocene due to its continued deep-water setting and distal location relative to major centers of deposition. Major progradation of the Campos Basin segment of the margin occurred during the Oligocene and Miocene.

TABLE OF CONTENTS

	Page
ACKNOWLEDGEMENTS.....	v
ABSTRACT.....	vii
LIST OF TABLES.....	xii
LIST OF FIGURES.....	xiv
CHAPTER	
1 - INTRODUCTION.....	1
1.1 – INTRODUCTION.....	1
1.2 – OBJECTIVES.....	7
1.3 – MATERIALS AND METHODS.....	8
2 - UPPER MAASTRICHTIAN-EOCENE BENTHIC FORAMINIFERA FROM THE WESTERN SOUTH ATLANTIC.....	12
2.1 – ABSTRACT.....	12
2.2 – INTRODUCTION.....	13
2.3 – MATERIALS AND METHODS.....	16
2.4 – STUDY AREA.....	21
2.4.1 – The Proximal Brazilian Marginal Basins Setting.....	21
2.4.2 – The Distal DSDP Setting.....	23
2.4.2.1 – Leg 39 Site 356 – São Paulo Plateau.....	23
2.4.2.2 – Leg 3 Site 20C – Rio Grande Rise.....	28
2.5 – BENTHIC FORAMINIFERA ASSEMBLAGES.....	25
2.5.1 – Sergipe-Alagoas Basin.....	26
2.5.2 – Mucuri Basin.....	27
2.5.3 – Campos Basin.....	28

2.5.4 – Santos Basin.....	29
2.5.5 – Pelotas Basin.....	30
2.5.6 – DSDP Sites	31
2.6 – BENTHIC FORAMINIFERA ASSEMBLAGES EVOLUTION IN THE MAASTRICHTIAN THROUGH EOCENE OF THE WESTERN SOUTH ATLANTIC	32
2.7 – BENTHIC FORAMINIFERA EXTINCTION IN THE BRAZILIAN MARGINAL BASINS	38
2.8 – CONCLUSION	40
2.9 – BENTHIC FORAMINIFERA TAXONOMIC CLASSIFICATION.....	41
2.9.1 – Systematics:	43
3 - UPPER MAASTRICHTIAN – EOCENE BENTHIC FORAMINIFERAL BIOFACIES IN THE BRAZILIAN MARGIN, WESTERN SOUTH ATLANTIC	107
3.1 – ABSTRACT	107
3.2 – INTRODUCTION	109
3.3 – MATERIALS AND METHODS	111
3.4 – GEOLOGICAL SETTING	119
3.4.1 – The Proximal Brazilian Marginal Basins.....	119
3.4.2 – The Distal DSDP Sites.....	121
3.5 – PALEOCEANOGRAPHIC SETTING OF THE SOUTH ATLANTIC.....	123
3.6 – BENTHIC FORAMINIFERAL BIOFACIES AND PALEOBATHYMETRY	127
3.6.1 – Sergipe-Alagoas Basin.....	133
3.6.1.1 – Well SEAL-01	133
3.6.1.2 – Well SEAL-02	137
3.6.1.3 – Paleobathymetry of Sergipe-Alagoas Basin	138
3.6.2 – Mucuri Basin.....	140
3.6.2.1 – Well BA-01.....	140
3.6.2.2 – Paleobathymetry of Mucuri Basin	142
3.6.3 – Campos Basin	144
3.6.3.1 – Well CAM-01	145

3.6.3.2 – Well CAM-02	146
3.6.3.3 – Well CAM-03	147
3.6.3.4 – Well CAM-04	150
3.6.3.4 – Paleobathymetry of Campos Basin	152
3.6.4 – Santos Basin.....	156
3.6.4.1 – Well SAN-01	156
3.6.4.2 – Well SAN-02	158
3.6.4.3 – Paleobathymetry of Santos Basin	159
3.6.5 – Pelotas Basin.....	160
3.6.5.1 – Well PEL-01	160
3.6.5.2 – Paleobathymetry of Pelotas Basin	162
3.6.6 – Abyssal Basin	163
3.6.6.1 – Site 356 – São Paulo Plateau	164
3.6.6.2 – Site 20C – Rio Grande Rise	166
3.6.6.3 – Paleobathymetry	168
3.7 –BIOFACIES DISTRIBUTION IN THE WESTERN SOUTH ATLANTIC	170
3.8 –THE FLYSCH-TYPE BIOFACIES E – DISTRIBUTION AND SIGNIFICANCE	181
3.9 – SUMMARY AND CONCLUSION	187

4 - A PALEOBATHYMETRIC MODEL AND THE EVOLUTION OF THE BRAZILIAN MARGINAL BASINS DURING THE LATE MAASTRICHTIAN – EOCENE BASED ON BENTHIC FORAMINIFERAL BIOFACIES	192
4.1 – ABSTRACT	192
4.2 – INTRODUCTION	194
4.3 – MATERIALS AND METHODS	196
4.4 – GEOLOGICAL SETTING	199
4.5 – PALEOCEANOGRAPHIC SETTING OF THE SOUTH ATLANTIC.....	203
4.6 – BENTHIC FORAMINIFERAL BIOFACIES	206
4.7 – THE PALEOBATHYMETRIC MODEL.....	211

4.8 – PALEOENVIRONMENT	219
4.9 – DISCUSSION	220
4.10 – LYSOCLINE AND CCD ALONG THE BRAZILIAN MARGIN	226
4.11 – COMPARISON WITH THE NORTHERN GULF OF MEXICO	232
4.12 – CONCLUSIONS	234
5 - SUMMARY AND CONCLUSIONS	237
APPENDICES	
1 - STRATIGRAPHIC DISTRIBUTION CHART OF THE BENTHIC FORAMINIFERA.....	241
2 - PLATES OF THE BENTHIC FORAMINIFERA	243
3 - ABSOLUTE PERCENTAGE OF THE BENTHIC FORAMINIFERA.....	268
BIBLIOGRAPHY	279

LIST OF TABLES

Table	Page
1.1: Present geographic locations of samples in this study.	10
2.1: Present geographic locations of samples in this study.	19
2.2: Paleocene and Eocene benthic foraminiferal diversity based on the number of species (S), extinction and origination rates of the most representative sites and wells of the study area.....	36
3.1: Present geographic locations of samples in this study.	112
3.2: Flysch-type assemblages reported from numerous locations in the Cretaceous – Paleogene interval.....	184
3.3: The two types of Biofacies E recognized in the Maastrichtian-Paleogene of the Brazilian marginal basins.....	186
4.1: Present geographic locations of samples in this study.	198
4.2: Thicknesses of the sequences for the Brazilian marginal basins (thickness in meters).	202
4.3: Biofacies characteristics associated with the lithofacies in the Brazilian marginal basins.	216

LIST OF FIGURES

Figure	Page
1.1: Present-day bathymetric map of the marginal Brazilian basins with the locations included in this study.	11
2.1: Present bathymetric map of the study area including the five Brazilian marginal basins (Sergipe-Alagoas, Mucuri, Campos, Santos, and Pelotas) and the DSDP Sites 20C and 356.	16
2.2: Stratigraphic range and lithofacies of the ten wells of the Brazilian margin and the two DSDP sites.	20
2. 3: Main events and benthic foraminiferal assemblage recognized in the Brazilian margin and the western South Atlantic.	34
3.1: Present bathymetric map of the study area including the five Brazilian marginal basins (Sergipe-Alagoas, Mucuri, Campos, Santos, and Pelotas) and DSDP Sites 20C and 356.	111
3.2: Number of Specimens X Number of Species plot including the whole sample of the upper Maastrichtian through Paleocene interval. Despite the low number of specimens, the number of species does not increase drastically on the samples with more than 50 specimens.	114
3.3: Number of Specimens X Number of Species plot including the whole sample of the Eocene interval.	115
3.4: Dendrograms of the Q-mode cluster analysis of the Pelotas (left) and Sergipe-Alagoas (right) basins, using samples with number > 35 specimens (top), >100 specimens (middle) and all the samples (bottom). Note that the yellow (agglutinant-rich) and blue (calcareous-rich) contrasts are consistent among all cluster analysis.	117
3.5: Results of two correspondence analyses (CA) for DSDP Site 356 with all taxa (left) and with 5% cut off (right), showing the more pronounced grouping of samples after the cut. Blue = benthic taxa, black = samples depth.	118
3.6: Interpretative Atlantic Ocean circulation during the Paleogene. White arrows: surface water currents, red: intermediate water, grey: deep water. GS – Gulf Stream, NAD – North Atlantic Drift, WSW – Warm Saline Water,	

BC – Brazil Current, FC – Falkland Current, PC – Peru Current, ACC – proto-Antarctic Circumpolar Current, SCW – Southern Component Water, CC – Canary Current. Paleooceanographic map from Ron Blakey (https://www2.nau.edu/). Surface currents from Bice et al. (2000), WSW from Bice (2000), SCW from Thomas et al. (2003) and Thomas (2004).....	126
3.7: Benthic foraminiferal biofacies distributed by age for all wells and sites. The wells are organized northern and shallower (Sergipe-Alagoas) through southern (Pelotas) and deeper (DSDP Sites 356 and 20C). Nannofossil biozones after Gradstein et al. (2012), planktic foraminiferal biozones from Wade et al. (2011).....	131
3.8: Lithology and biofacies of the study locations from the late Maastrichtian through Eocene of the western South Atlantic and Brazilian marginal basins.	132
3.9: Dendrogram classifications of the samples produced by the Q-mode cluster analysis and correspondence analysis showing the seven major biofacies for the well SEAL-01.....	136
3.10: Dendrogram classifications of the samples produced by Q-mode cluster analysis and the correspondence analysis showing the three major biofacies of the well SEAL-02.....	138
3.11: Age vs Depth Model of the well SEAL-01 plotted with the benthic foraminiferal biofacies with correlated paleobathymetric range and sedimentation rates.	139
3.12: Age vs Depth Model of the well SEAL-02 plotted with the benthic foraminiferal biofacies with correlated paleobathymetric range and sedimentation rates.	140
3.13: Dendrogram classifications of the samples produced by Q-mode cluster analysis and correspondence analysis showing the three major biofacies of the well BA-01.	142
3.14: Age vs Depth Model of the well BA-01 plotted with the benthic foraminiferal biofacies with correlated paleobathymetric range and sedimentation rates.....	144
3.15: Dendrogram classifications of the samples produced by Q-mode cluster analysis and correspondence analysis showing the major biofacies recognized for the well CAM-01.	145

3.16: Dendrogram classifications of the samples produced by Q-mode cluster analysis and correspondence analysis (CA) showing the major biofacies and the interval with poor recovery of the well CAM-02.....	147
3.17: Dendrogram classifications of the samples produced by Q-mode cluster analysis and correspondence analysis showing the five major biofacies recognized for the well CAM-03.....	150
3.18: Dendrogram classifications of the samples produced by Q-mode cluster analysis and correspondence analysis showing the two major biofacies recognized for the well CAM-04.....	152
3.19: Age vs Depth Model of the well CAM-01 plotted with the benthic foraminiferal biofacies with correlated paleobathymetric range and sedimentation rates.....	154
3.20: Age vs Depth Model of the well CAM-02 plotted with the benthic foraminiferal biofacies with correlated paleobathymetric range and sedimentation rates.....	154
3.21: Age vs Depth Model of the well CAM-03 plotted with the benthic foraminiferal biofacies with correlated paleobathymetric range and sedimentation rates.....	155
3.22: Age vs Depth Model of the well CAM-04 plotted with the benthic foraminiferal biofacies with correlated paleobathymetric range and sedimentation rates.....	155
3.23: Dendrogram classifications of the samples produced by Q-mode cluster analysis and correspondence analysis showing the four major biofacies recognized for the well SAN-01.....	158
3.24: Age vs Depth Model of the well SAN-01 plotted with the benthic foraminiferal biofacies with correlated paleobathymetric range and sedimentation rates.....	159
3.25: Dendrogram classifications of the samples produced by Q-mode cluster analysis and correspondence analysis showing the three major biofacies recognized for the well PEL-01.....	161
3.26: Age vs Depth Model of the well PEL-01 plotted with the benthic foraminiferal biofacies with correlated paleobathymetric range and sedimentation rates.....	163

3.27: Dendrogram classifications of the samples produced by Q-mode cluster analysis and correspondence analysis showing the four major biofacies recognized for the Site 356.	166
3.28: Dendrogram classifications of the samples produced by Q-mode cluster analysis and correspondence analysis showing the four major biofacies recognized for the Site 20C.	168
3.29: Age vs Depth Model of the DSDP Site 356 plotted with the benthic foraminiferal biofacies with correlated paleobathymetric range and sedimentation rates.	169
3.30: Age vs Depth Model of the DSDP Site 20C plotted with the benthic foraminiferal biofacies with correlated paleobathymetric range and sedimentation rates.	169
3.31: Benthic foraminiferal biofacies distribution in the late Maastrichtian of the western South Atlantic.	172
3.32: Benthic foraminiferal biofacies distribution in the early to middle Paleocene of the western South Atlantic.	173
3.33: Benthic foraminiferal biofacies distribution in the late Paleocene of the western South Atlantic.	177
3.34: Benthic foraminiferal biofacies distribution in the early Eocene of the western South Atlantic.	178
3.35: Benthic foraminiferal biofacies distribution in the middle to late Eocene of the western South Atlantic.	179
3.36: Benthic foraminiferal biofacies distribution in the Paleogene of the western South Atlantic. Brazilian marginal wells are displayed from northern (SEAL-01) to southern (PEL-01) and the distal DSDP Sites 356 and 20C. BEE: Benthic Extinction Event.	180
3.37: Benthic foraminifera biofacies correlation with sea level and events from the Maastrichtian through the Eocene of the western South Atlantic.	191
4.1: Present bathymetric map of the study area including the five Brazilian marginal basins (Sergipe-Alagoas, Mucuri, Campos, Santos, and Pelotas) and the DSDP Sites 20C and 356.	198
4.2: Interpretative Atlantic Ocean circulation during the Paleogene. White arrows: surface water currents, red: intermediate water, grey: deep water. GS –	

Gulf Stream, NAD – North Atlantic Drift, WSW – Warm Saline Water, BC – Brazil Current, FC – Falkland Current, PC – Peru Current, ACC – proto-Antarctic Circumpolar Current, SCW – Southern Component Water, CC – Canary Current. Paleoceanographic map from Ron Blakey (https://www2.nau.edu/). Surface currents from Bice et al. (2000), WSW from Bice (2000), SCW from Thomas et al. (2003) and Thomas (2004).	206
4.3: Benthic foraminiferal biofacies distributed by age for all wells and sites. Note the implied presence of hiatuses in the studied marginal basins wells and deep-sea sites. Nannofossil biozones from Ogg et al. (2010), planktic foraminiferal biozones from Wade et al. (2011).....	211
4.4: Biofacies distribution in the Maastrichtian through upper Eocene interval for the Brazilian marginal basin.	217
4.5: The paleobathymetric and paleoenvironmental model for the Brazilian marginal basins based on benthic foraminiferal biofacies.	218
4.6: Age vs. depth models of Campos (CAM-01) and Santos (SAN-01) basins, with sedimentation rates and benthic foraminiferal biofacies. The age-depth model was based on nannofossils datums from PETROBRAS.	221
4.7: Brazilian continental margin progradation in the Paleogene based on benthic foraminiferal biofacies and the relative position of the marginal basins included in this study.	224
4.8: Sediment supply for the Brazilian marginal basins and the benthic foraminiferal biofacies. Width of the arrows shows relative sediment supply.	225
4.9: Berger (1970a, b) proposed model of the relationship between the lysocline and the CCD in the southeast Pacific. The red lines highlight the model for near the continent where the lysocline and CCD shoal along the margin.	227
4.10: Benthic foraminiferal biofacies comparison with the benthic assemblage of the Ross Sea, Antarctica, related to the position of the CCD (modified from Kennett, 1966).	229
4.11: CaCO ₃ (wt%) of the Walvis Ridge showing the shallow lysocline and CCD at the PETM and during the Eocene (modified from Zachos et al., 2004).	230
4.12: Sketch with the position of representative wells of the Brazilian marginal basins showing the change in agglutinant-dominated Biofacies E (I) to calcareous-dominated Biofacies A, B and C (II) and fluctuation of the CCD during the Paleogene.	231

4.13: Brazilian continental margin model progradation. Modified from Contreras (2011).....	233
4.14: Schematic paleoceanographic map for the upper Paleocene-lower Eocene Wilcox Formation in the Gulf of Mexico that compares with the Brazilian continental margin progradation. Black dots are the hypothetical positions of the Brazilian marginal basins relative to the major sources of siliciclastic sediment. Modified from McDonnell et al. (2008).....	234
4.15: Interpreted seismic section of Gulf of Mexico (A) and Santos Basin (B) showing the influence of salt tectonics influencing the deposition in both regions. Modified from McMoran Exploration Company (2009) and Modica and Brush (2004), A and B respectively.....	235

CHAPTER 1

INTRODUCTION

1.1 – INTRODUCTION:

Deep-sea benthic foraminifera assemblages have long been studied for their use in paleoenvironmental reconstructions, paleobiography, paleoceanography, and evolution (e.g., Heron-Allen, 1915, Cole and Gillespie, 1930, Finlay and Marwick, 1940, Parker, 1954, Bandy and Arnal, 1960, Buzas and Gibson, 1969, Lipps and Valentine, 1970, Berggren, 1972, Natland et al., 1974, Sliter, 1975, Corliss, 1985, Thomas, 1985, Van Morkhoven et al. 1986, Loeblich and Tappan, 1955, 1964, 1986, 1988, 1994, Berggren and Miller, 1989, Jorissen et al., 1995, Gooday and Rathburn, 1999, Alegret and Thomas, 2001, 2005, 2007, 2013, Gooday, 2003, Pawlowski et al., 2003, Thomas, 2003, Kaminski and Gradstein, 2005). However, relatively little documentation exists for the western South Atlantic (Boersma, 1977, Sliter, 1977, Tjalsma, 1977, Lohmann, 1978, Dailey, 1983, Tjalsma and Lohmann, 1983, Muller-Merz and Oberhansli, 1991). The publications on the Brazilian marginal basins are mostly focused on one basin (Campos or Sergipe-Alagoas), but no proper treatment of benthic foraminiferal taxonomy and paleoenvironmental analysis has been published (Tinoco, 1971, Koutsoukos and Hart, 1990, Koutsoukos et al., 1990, Koutsoukos, 1992, Mesquita, 1998, Koutsoukos, 2000, Viviers and Ferreira, 2005, Costa and Viviers, 2012).

Most of the information on the South Atlantic benthic foraminifera has been derived from the Deep-Sea Drilling Program (DSDP) or Ocean Drilling Program (ODP) publications, and a few others (e.g., Boersma, 1977, Sliter, 1977, Tjalsma, 1977, Lohmann, 1978, Dailey, 1983, Tjalsma and Lohmann, 1983, Muller-Merz and Oberhansli, 1991). The Brazilian Petroleum Company Petrobras has been drilling the marginal basins of the continental shelf and slope since 1953, but a paleobathymetric and paleoenvironmental model based on the benthic foraminifera has never been published. The Brazilian marginal basins provide an excellent study area to document the benthic foraminiferal assemblage distributions and relate assemblage changes to the evolution of this passive continental margin and the paleoceanography of the western South Atlantic. This study focuses on latest Cretaceous (Maastrichtian) through Eocene time (~70-35 Ma).

During the Maastrichtian through Eocene, changes in sea level, opening of ocean gateways at the northern and southern ends of the Atlantic, global climate change, and the sites of deep water formation that filled the Atlantic affected the depth of the lysocline (partial calcite dissolution depth) and calcite compensation depth (CCD, depth where rain of carbonate from the surface ocean is balanced by dissolution at the seafloor, Pälike et al., 2012). For example, drilling on the Walvis Ridge in the eastern South Atlantic has demonstrated large excursions in the depth of the CCD during the Paleogene, including the abrupt short-lived shoaling of the CCD during the Paleocene-Eocene Thermal Maximum (PETM) (e.g., Zachos et al., 2004). The depth of the CCD has a profound influence on the composition of benthic foraminiferal assemblages that live on the seafloor. The Brazilian passive continental margin provides a unique opportunity to test

the hypothesis of Berger (1970) stating that the CCD and the lysocline rise (shoal) along the continental margin due to higher productivity relative to more distal sites. It is a chance to have a better understanding on how the CCD behaved during the Paleogene in the Brazilian continental margin, because most of the published data come from deep-sea sites (e.g., Berger, 1970a, 1970b, Corliss and Honjo, 1981, Kelly et al., 2010, Pälke et al., 2012).

In addition, the study interval includes the abrupt and short-lived (<200-kyr) warming event known as the Paleocene-Eocene Thermal Maximum (PETM) that marks the Paleocene-Eocene boundary (e.g., Thomas et al., 2000, Katz et al., 2001, Alegret and Thomas, 2001, 2005, Zachos et al., 2005, Hancock et al., 2006, Thomas, 2007, d'Haenens et al., 2010, DeConto et al., 2012). This transient event is characterized by the mass extinction of the deep-sea benthic foraminifera, also known as Benthic Extinction Event (BEE), and I will investigate the record of this event along the Brazilian continental margin and compare it to well-established BEE records from the deep-sea. Was the extinction and subsequent recovery similar to other deep-sea records? How is it similar, and how is it different?

The three main parts of this dissertation provide the essential information to achieve my goal: (1) detailed taxonomy of the benthic foraminifera in the Maastrichtian to upper Eocene interval, (2) establishment of the benthic foraminiferal biofacies for the Brazilian marginal basins and the western South Atlantic, based on statistical analysis of assemblage census data, characterizing the flysch-type and calcareous-dominated assemblages in relation with the CCD, and (3) development of a paleobathymetric and

paleoenvironmental model based on benthic foraminiferal biofacies that would improve our understanding of the geological evolution of the Brazilian margin and assist in characterizing deep-waters reservoirs of the Brazilian marginal basins.

This dissertation is divided into three chapters representing manuscripts that are intended for publication in academic journals. The study area comprises five Brazilian marginal basins (Sergipe-Alagoas, Mucuri, Campos, Santos, and Pelotas) and two DSDP Sites 20C (Rio Grande Rise) and 356 (São Paulo Plateau). Since the contents of each chapter represent manuscripts in preparation, there are redundancies in these chapters especially with regards to the materials and methods, study area, figures and in some of the text.

Chapter 1 (this chapter) provides the Introduction, Objectives and Materials and Methods used in this research.

Chapter 2 presents the benthic foraminiferal taxonomic classification for the western South Atlantic and their distribution patterns, including the systematic paleontology and a suite of plates with Scanning Electron Microscope (SEM) images of the most relevant species. The benthic foraminiferal assemblage change through time, from primarily agglutinate dominated in the Maastrichtian-Paleocene of the marginal basins and calcareous dominated in the Eocene. The agglutinate dominated flysch-type assemblage (*Psammosiphonella cylindrica*, *Rhizammina* sp., *Haplophragmoides* sp., *Recurvoides* sp., *Bathysiphon* sp., *Nothia* sp.) is well developed and documented in the Maastrichtian-Paleocene of the Brazilian marginal basins. This assemblage does not occur in the distal DSDP Sites 20C and 356. A Velasco-type calcareous assemblage

(*Cibicidoides velascoensis*, *Nuttallides truempyi*, *Stensioeina beccariiformis*, *Gyroidinoides globosus*, *Cibicidoides hyphalus*, *Osangularia velascoensis*) dominated in the same interval of the DSDP Sites 20C and 356, as well as in some deep sections in the marginal basins. The Eocene assemblage is similar to the Barbados-type assemblage (*Cibicidoides eocaenus*, *Osangularia mexicana*, *Hanzawaia ammophila*, *Planulina costata*, *Nuttallides truempyi*, *Globocassidulina subglobosa*), especially in DSDP Sites 20C and 356, where the calcareous taxa dominate.

In **Chapter 3**, the benthic foraminifera were grouped into biofacies for each site/well. The major biofacies groups are not composed of exactly the same taxa due to basin-to-basin differences (niches). The biofacies are primarily distinguished by the agglutinated/calcareous percentage and the dominant three or four species for each biofacies. Five major biofacies were recognized based on Q-mode cluster analysis combined with correspondence analysis that were designated by letters A to E. **Biofacies A** is composed 100% of calcareous benthic taxa and is most frequent and abundant in the Eocene. **Biofacies B** has up to 10% of agglutinated taxa and occurs from the middle Paleocene to upper Eocene. **Biofacies C** has 11% to 25% of agglutinated taxa in its composition and occurs from the upper Maastrichtian to upper Eocene. **Biofacies D** contains a balanced mix of calcareous and agglutinated taxa and always occurs in association with Biofacies E in the marginal basins. **Biofacies E** is dominated by agglutinated taxa, especially tubular forms (*Bathysiphon*, *Nothia*, *Rhizammina*, *Psammosiphonella*). This biofacies correlates with the flysch-type biofacies of Berggren and Gradstein (1981). Biofacies E dominates the Maastrichtian through upper Paleocene in the marginal basins, although it occurs in the Campos Basin until the mid-upper

Eocene. The biofacies distributions reveal distinct and changing environmental settings through the study interval. In particular, the agglutinant-rich biofacies dominated in the Maastrichtian-Paleocene and calcareous-rich biofacies dominate in the Eocene. This transition is supported by the increase of the siliciclastic input associated with a sea level fall in the late Paleocene, followed by continued seaward progradation of the Brazilian margin and shoaling in the continental slope.

In **Chapter 4**, a paleobathymetric and paleoenvironmental model was developed based on the benthic foraminiferal biofacies presented in the Chapter 3. The model reveals the progradation of the Brazilian marginal basins during the Paleogene. An abrupt change in biofacies across the Paleocene/Eocene boundary is observed in all the Brazilian marginal basins, with the exception of the Campos Basin. The Eocene interval is dominated by biofacies A, B and C in the Sergipe-Alagoas, Mucuri, Santos and Pelotas basins due to progradation of the margin and shoaling of the slope allowing for better preservation of carbonate. Biofacies D and E continued to dominate the Campos Basin during the Eocene due to its continued deep-water setting and distal location relative to major centers of deposition.

In **Chapter 5**, I summarize the conclusions presented in the three main chapters.

1.2 – OBJECTIVES:

The overall purpose of this study is to investigate the benthic foraminiferal assemblages along the Brazilian passive margin and the western South Atlantic in order to understand their distribution that provides a paleoenvironmental reconstruction of the ancient depositional systems. The legacy of this study is to integrate the benthic foraminiferal assemblages of the Brazilian marginal basins with DSDP sites of the upper Maastrichtian through the upper Eocene, and to compare these assemblages with other continental margins.

In addition, the benthic foraminiferal assemblages help us to understand the history of the CCD along the paleo-slope and rise of the Brazilian margin, the Maastrichtian-Paleocene was a special period when the agglutinat-rich flysch-type assemblages characterize several continental margins, such as in the western Tethys (Kaminski and Gradstein, 2005), and Labrador and North Seas (Gradstein and Berggren, 1981, Jones, 1988).

The aim of this dissertation is to use Maastrichtian through Eocene benthic foraminiferal assemblage to:

- Understand how the CCD behaved on the Brazilian margin, testing the Berger (1970) hypothesis that it shoals along the continental margin due to higher productivity near the continent.

- What is the record of the PETM and Benthic Foraminiferal Extinction Event (BEE) along the Brazilian continental margin, and how does the BEE compares with other deep-water sites?
- Record the flysch-type assemblage distribution of the Brazilian margin and compare the record with other occurrences in the Paleocene in a better attempt to understand why agglutinated assemblages are so common during this time.
- Develop a paleobathymetric and paleoenvironmental model to compare the Brazilian maginal basins with other deep-water hydrocarbon basins, in particular the Gulf of Mexico.

1.3 – MATERIALS AND METHODS:

The samples from the Brazilian marginal basins and the deep western South Atlantic Ocean represent a variety of sources: core, cutting and sidewall samples. Core samples were obtained from discrete cored intervals in an industry well or DSDP site. Cutting samples are formed by drilled rock fragments that are transported up the well bore by the mudstream in the well. Sidewall core samples are obtained by percussion sidewall coring systems that shoot cylindrical bullets into the borehole wall.

The core samples are from either Deep Sea Drilling Project (DSDP) or Petrobras petroleum industry wells and are the majority of the analyzed samples (Table 1.1). The

cuttings and sidewall samples are from the Petrobras petroleum industry wells and were selected of intercalated intervals where the coring was not continuous.

The Petrobras petroleum industry wells are located in five Brazilian marginal basins (Sergipe-Alagoas, Mucuri, Campos, Santos and Pelotas) and the DSDP samples are from Leg 39 Site 356 (São Paulo Plateau) and Leg 3 Hole 20C (Rio Grande Rise) (Fig.1). The locations were selected based on their stratigraphic continuity over the Paleocene-Eocene interval, although some locations also recovered the upper Maastrichtian interval (Table 1.1).

Approximately 700 samples were processed at the Biostratigraphy and Paleocology Department at Petrobras Research Center, Rio de Janeiro, Brazil. The industry well samples (core, cutting and sidewall) were crushed and soaked in solution of 40% hydrogen peroxide, washed over 63 μm sieves and dried. The DSDP core samples consisted of stiff, unconsolidated to weakly consolidated sediment, they were washed the over 63 μm sieves and dried. The industry samples were provided in slides, picked. The picking follows the procedure of the company where ~300 tests are picked (planktics and benthics). For the DSDP sites, all benthic foraminifera were picked in each sample.

Table 1.1: Present geographic locations and age interval of samples in this study.

Well/Site	Location	Present water depth (m)	Samples	Sample type	Age
20C	Rio Grande Rise	4506	28	core	Paleocene-Eocene
356	São Paulo Pupperau - Santos Basin	3203	107	core	Paleocene-Eocene
PEL-01	Pelotas Basin	151	15	core	middle to upper Eocene
			40	cuttings	lower Eocene
			8	core	lower Eocene
			28	cuttings	upper Paleocene
			14	core	lower Paleocene
			9	cuttings	upper Maastrichtian
SAN-01	Santos Basin	1515	13	cuttings	upper Eocene
			14	sidewall	lower Eocene
			16	core	upper Paleocene-lower Eocene
			11	cuttings	upper Maastrichtian
			12	core	upper Maastrichtian
SAN-02	Santos Basin	1733	48	core	lower Eocene
CAM-01	Campos Basin	791	4	core	upper Maastrichtian
CAM-02	Campos Basin	1336	6	sidewall	Paleocene-Eocene
			11	cuttings	upper Eocene
			22	core	lower to middle Eocene
CAM-03	Campos Basin	923	3	cuttings	upper Maastrichtian to lower Paleocene
			42	core	Paleocene-Eocene
CAM-04	Campos Basin	820	16	cuttings	upper Eocene
			46	core	Paleocene
			31	cuttings	upper Maastrichtian to lower/middle Paleocene
SEAL-01	Sergipe-Alagoas Basin	27	44	cuttings	Eocene
			30	core	Paleocene
SEAL-02	Sergipe-Alagoas Basin	24	30	cuttings	upper Paleocene-lower Eocene
			18	core	Paleocene
			16	cuttings	upper Maastrichtian

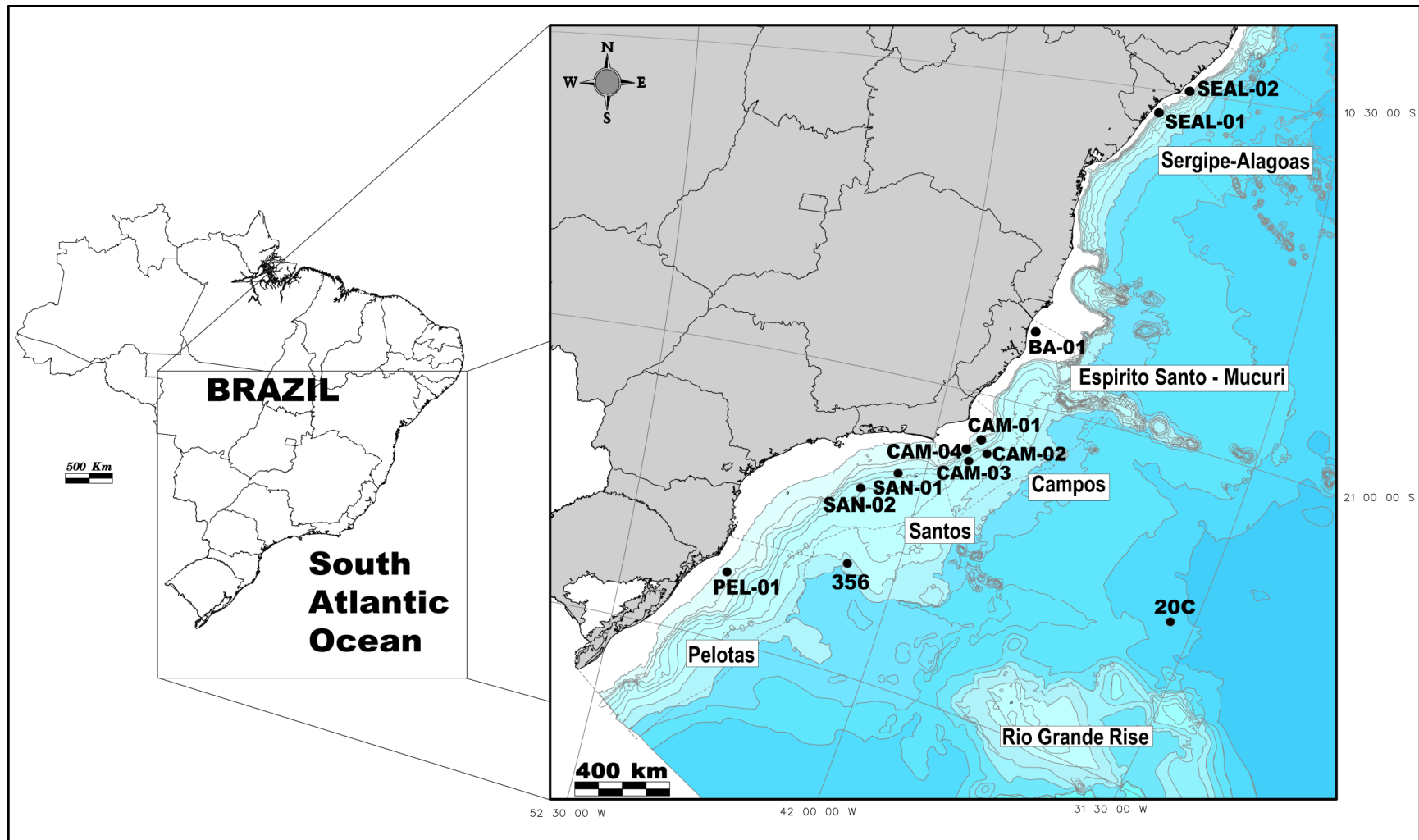


Figure 1.1: Present-day bathymetric map of the marginal Brazilian basins with the locations included in this study.

CHAPTER 2

UPPER MAASTRICHTIAN-EOCENE BENTHIC FORAMINIFERA FROM THE WESTERN SOUTH ATLANTIC

DE MELLO, RENATA MOURA^{1,2,*}, LECKIE, R.MARK¹, THOMAS, ELLEN³

¹ Department of Geosciences, University of Massachusetts, 611 N. Pleasant St., Amherst, MA 01003, USA

² PETROBRAS Research and Development Center, Av. Horacio de Macedo 950, Ilha do Fundão, Rio de Janeiro, RJ 21941-915, Brazil

³ Department of Geology and Geophysics, Yale University, New Haven, CT 06520-8109, U.S.A.

* Correspondence author: renatamouramello@yahoo.com.br.

2.1 – ABSTRACT:

The Brazilian marginal basins have not been the subject of benthic foraminiferal taxonomy and biofacies analysis in the context of paleoenvironmental reconstruction. The goal of this chapter is to present a detailed taxonomy and distribution of Maastrichtian through Eocene benthic foraminiferal species of the western South Atlantic integrating data from DSDP Sites 20C and 356 with data from ten industry wells in the Brazilian marginal basins. The deep-water Velasco-type assemblage is dominated by calcareous taxa (*Stensioeina beccariiformis*, *Nuttallides truempyi*, *Cibicidoides hyphalus*, *C. velascoensis*) and occurs from the Maastrichtian through the Paleocene, being better recorded at the deepest, most distal sites (DSDP 20C and 356). In the marginal basins, the Velasco-type assemblage occurs as a minor component associated with flysch-type assemblages dominated by agglutinated taxa (*Rhizammina*, *Psammosiphonella cylindrica*, *Nothia*, *Haplophragmoides*, *Cribrostomoides*). During the Eocene, the benthic assemblages in the Brazilian marginal basins changed from agglutinate-dominated to

calcareous dominated assemblages with *Globocassidulina subglobosa*, *Nuttallides trumpeyi*, *Cibicidoides eocaenus*, *C. havanensis*, and *Paralabamina lunata*. At DSDP Sites 20C and 356 Paleocene assemblages were already dominated by calcareous taxa, so there is no such change from agglutinate- to calcareous-dominated assemblages across the Paleocene-Eocene boundary. The Benthic Extinction Event (BEE) associated with the PETM is more severe at the distal DSDP sites, but is also preserved as a major turnover event along the Brazilian margin. The extinction is ~35% and is more severe in the calcareous taxa (83% of the extinct taxa) than the agglutinate taxa. The extinct calcareous taxa include *Stensioeina beccariiiformis*, *Neoeponides hillebrandti*, *Aragonia velascoensis*, *Gyroidinoides globosus*, *Cibicidoides hyphalus*, *C. velascoensis*, *Pullenia coryelli*, *Osangularia velascoensis*, *Lenticulina whitei*, *Neoflabelina semireticulata*, *Nuttallinella florealis* and *Anomalinoides praeacuta*. The extinct agglutinated taxa are *Ammodiscus pennyi*, *Trochamminopsis altiformis*, *Reticulophragmium garcilassoii*, and *Recurvoides walteri*.

2.2 – INTRODUCTION:

The use of benthic foraminiferal assemblages and foraminiferal shell trace element and stable isotope geochemistry have proven to be powerful tools in paleoceanographic and paleoecologic investigations, such as estimating paleoproductivity and dissolved oxygen at the seafloor or within the sediments, paleotemperatures and ice volume, and in reconstructing past ocean circulation (e.g., Douglas and Woodruff, 1981, Sen Gupta, 2003, Gooday, 2003, Jorissen et al., 2007, Thomas, 2007, Pearson, 2012).

Approximately 40,000 foraminiferal species have been described (Ellis and Messine Catalogue <http://www.micropress.org>) and most of them are known only as fossils, with benthic species greatly outnumbering planktic species (Loeblich and Tappan, 1988, Sen Gupta, 2003, WORMS <http://marinespecies.org>). Among the many described species synonyms are of major concern in evaluation of benthic foraminiferal taxonomy and may comprise possibly up to 25% of species (Murray, 2007). In addition, correct identification of the species is a critical step in using benthic foraminifera as a tool in past climate investigations.

The purpose of this chapter is to present a detailed taxonomy of benthic foraminifera and their distribution for the upper Maastrichtian through upper Eocene of the western South Atlantic Ocean, with a focus on the Brazilian continental margin. Our data are from Deep Sea Drilling Project (DSDP) Leg 3 Hole 20C on the Rio Grande Rise, DSDP Leg 39 Site 356 on the São Paulo Plateau, and unpublished data from ten petroleum industry wells of Petrobras (Brazilian Petroleum Company). The Petrobras wells are from five distinct Brazilian marginal basins, from the Pelotas Basin (~30°S) in the south to the Sergipe-Alagoas Basin (~10°S) in the north (Fig. 2.1).

Research published on benthic foraminiferal taxonomy of the western South Atlantic is based on DSDP Leg 3 Sites 13-22 drilled in 1970, Leg 36 Sites 326-331 and; Leg 39 Sites 353-359 drilled in 1977; and Leg 72 Sites 515-518 drilled in 1983 (Sliter, 1977, Tjalsma, 1977, Tjalsma and Lohmann, 1983, Müller-Merz and Oberhänsli, 1991, Widmark, 2000). The Brazilian continental margin has not been the focus of academic analysis of benthic foraminiferal taxonomy and paleoenvironments analysis. Thus, the legacy of this study is to integrate the benthic foraminiferal assemblages of the Brazilian

marginal basins with DSDP sites of the upper Maastrichtian through the upper Eocene, and to compare these assemblages with other continental margins.

The detailed taxonomic classification, synonymy, species descriptions, and stratigraphic range data are presented in the Systematics section.

We report stratigraphic ranges of species in the western South Atlantic spanning the Maastrichtian through Eocene (nannofossil biozones NC23 to CP15 in Gradstein et al. (2012), planktic foraminiferal biozones P0 to E16 in Wade et al., 2011). The distribution chart (Appendix I) shows the main benthic foraminiferal taxa organized by last occurrence (LO) as shown in Van Morkhoven et al. (1986) and traditionally adopted by petroleum companies. Species stratigraphic ranges may include local ranges that are shorter than the known stratigraphic record and are highly affected by the nature of the record. The presence of unconformities, as shown in the figure 2.2, coupled with the low sampling resolution probably did not capture the full impact of the Benthic Extinction Event (BEE).

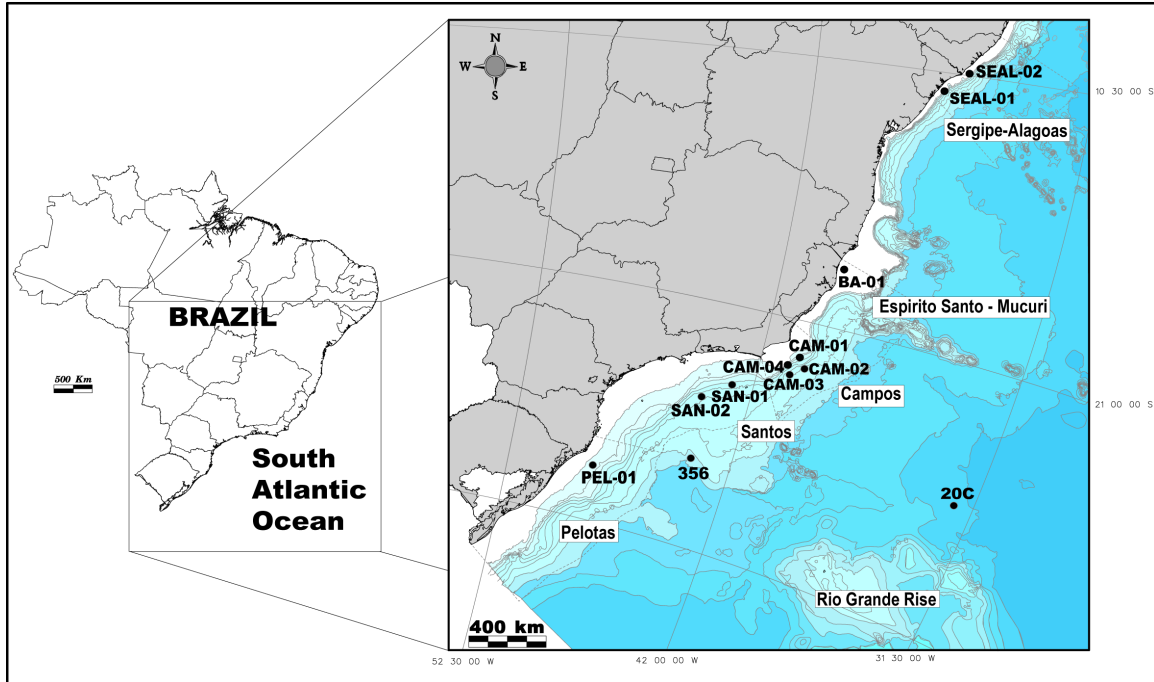


Figure 2.1: Present bathymetric map of the study area including the five Brazilian marginal basins (Sergipe-Alagoas, Mucuri, Campos, Santos, and Pelotas) and DSDP Sites 20C and 356

2.3 – MATERIALS AND METHODS:

The samples from the Brazilian marginal basins and the deep western South Atlantic Ocean represent a variety of sources: core samples, cuttings and sidewall samples. Core samples were obtained from discrete cored intervals in industry wells or DSDP sites. Cutting samples are formed by drilled rock fragments that are transported up the well bore by the drilling mudstream. Sidewall core samples are obtained by percussion sidewall coring systems that shoot hollow cylindrical bullets into the borehole wall.

The majority of the analyzed samples are core samples from Deep Sea Drilling Project (DSDP) and Petrobras petroleum industry wells (Table 2.1). Cuttings and sidewall samples from the Petrobras wells were selected from intercalated intervals where the coring was not continuous.

The Petrobras wells are located in five Brazilian marginal basins (Sergipe-Alagoas, Mucuri, Campos, Santos and Pelotas). The DSDP samples are from Leg 39 Site 356 (São Paulo Plateau) and Leg 3 Hole 20C (Rio Grande Rise) (Fig. 2.1). The locations were selected based on their stratigraphic continuity over the Paleocene-Eocene interval, although some locations also recovered the upper Maastrichtian (Table 2.1, Fig. 2.2). Approximately 700 samples were investigated, 66 samples from the upper Maastrichtian, 304 from the Paleocene and 344 from the Eocene.

The samples were processed at the Biostratigraphy and Paleocology Department at Petrobras Research Center, Rio de Janeiro, Brazil. The core/cutting samples of the petroleum wells were crushed and soaked in solution of 40% hydrogen peroxide washed over 63 μm sieves and dried. As the DSDP core samples consisted of unconsolidated sediment, they were washed the over 63 μm sieves and dried. The number of benthic foraminifera tests picked of each sample varies with the origin. All the benthic foraminiferal testes were picked from the DSDP sites samples (10cc of volume). The Petrobras samples were provided already picked, and the counts of the benthic foraminiferal tests are in the Appendix III.

Species identifications are based primarily on published papers and atlases by Tjalsma and Lohman (1983), Alegret and Thomas (2001), Van Morkhoven et al. (1986), Bolli et al. (1994), Kaminski and Gradstein (2005), and especially the online catalogue

Ellis & Messina (www.micropress.org). In many cases, species identification were compared with the type material (e.g., holotypes, paratypes, topotypes, etc.) from the collections of Cushman, Nuttall, Mello and others housed in the Department of Paleobiology, National Museum of Natural History, Smithsonian Institution in Washington, DC. The benthic foraminiferal assemblages comprise about 330 taxa identified at generic or specific level, including 180 calcareous taxa and 150 agglutinants taxa. Of the 330 taxa, 120 are presented here (63 calcareous and 58 agglutinants) with detailed taxonomic classification, stratigraphic range and SEM images.

Table 2.1: Present geographic locations and age interval of samples in this study.

Well/Site	Location	Present water depth (m)	Samples	Sample type	Age
20C	Rio Grande Rise	4506	28	core	Paleocene-Eocene
356	São Paulo Pupperau - Santos Basin	3203	107	core	Paleocene-Eocene
PEL-01	Pelotas Basin	151	15	core	middle to upper Eocene
			40	cuttings	lower Eocene
			8	core	lower Eocene
			28	cuttings	upper Paleocene
			14	core	lower Paleocene
			9	cuttings	upper Maastrichtian
SAN-01	Santos Basin	1515	13	cuttings	upper Eocene
			14	sidewall	lower Eocene
			16	core	upper Paleocene-lower Eocene
			11	cuttings	upper Maastrichtian
			12	core	upper Maastrichtian
SAN-02	Santos Basin	1733	48	core	lower Eocene
CAM-01	Campos Basin	791	4	core	upper Maastrichtian
CAM-02	Campos Basin	1336	6	sidewall	Paleocene-Eocene
			11	cuttings	upper Eocene
			22	core	lower to middle Eocene
CAM-03	Campos Basin	923	3	cuttings	upper Maastrichtian to lower Paleocene
			42	core	Paleocene-Eocene
CAM-04	Campos Basin	820	16	cuttings	upper Eocene
			46	core	Paleocene
			31	cuttings	upper Maastrichtian to lower/middle Paleocene
SEAL-01	Sergipe-Alagoas Basin	27	44	cuttings	Eocene
			30	core	Paleocene
SEAL-02	Sergipe-Alagoas Basin	24	30	cuttings	upper Paleocene-lower Eocene
			18	core	Paleocene
			16	cuttings	upper Maastrichtian

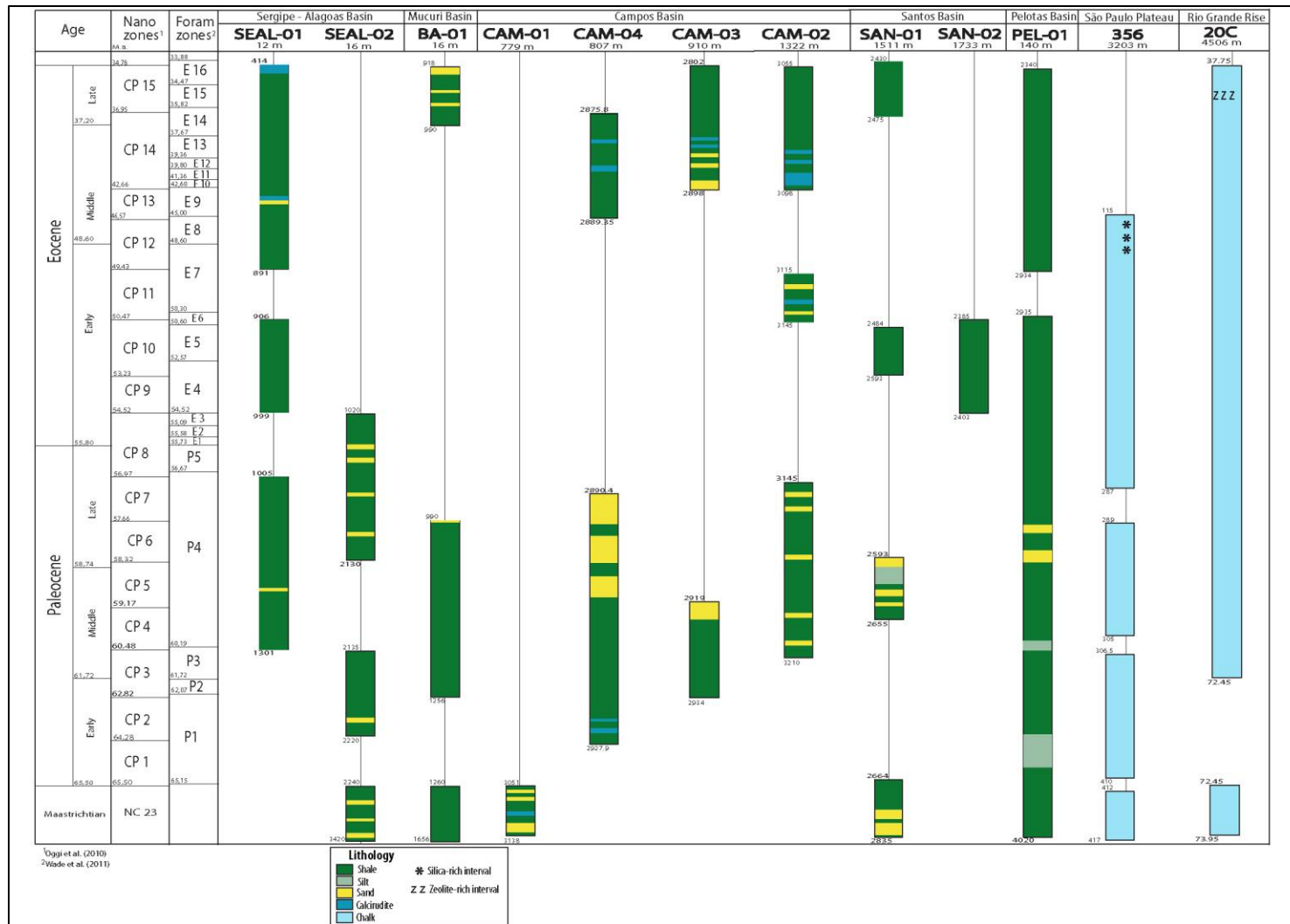


Figure 2.2: Stratigraphic range and lithofacies of the ten wells of the Brazilian margin and the two DSDP sites.

2.4 – STUDY AREA:

2.4.1 The Proximal Brazilian Marginal Basins Setting:

The eastern Brazilian continental margin is composed of a sequence of basins, well known as Brazilian Passive Marginal Basins. These sedimentary basins were formed during the continental drift phase of the African and South American plates as a result of the fragmentation of the supercontinent Gondwana (Asmus and Baisch, 1983, Milani et al., 2007). As a consequence, the tectonic and sedimentary evolution of the Brazilian marginal basins is quite similar although there are some regional differences on the development of each basin. The most expressive basins, from south to north, are: Pelotas, Santos, Campos, Mucuri, Bahia-Sul, Sergipe-Alagoas and Pernambuco-Paraíba.

Asmus and Ponte (1973) consolidated the vision that the eastern Brazilian margin evolved during four stages: pre-rift, rift, restricted marine and open marine. The pre-rift package (Late Jurassic-Early Cretaceous) occurs in the Sergipe-Alagoas basin and southward to the Pelotas Basin. This sequence is generally represented by reddish fluvial sediment deposited in a shallow lacustrine paleoenvironment (Milani et al., 2007). The rift section is recognized as diachronous lacustrine depocenters formed during the Early Cretaceous. These rift lakes contain shale deposits that are important as hydrocarbon source rocks. The syn-rift rocks are more abundant in the southern basins (Pelotas and Espírito Santo). During the Aptian, the opening became more expressive and a restricted marine section was deposited. This section is typically represented by a thick evaporites package (mostly halite and gypsum-anhydrite) and has importance in the Santos,

Campos, and Mucuri basins. A thinner succession of evaporites reaches the northern basin of the Sergipe-Alagoas. Evaporite deposition spanned the late Aptian to earliest Albian (Cainelli and Mohriak, 1999, Milani et al., 2001, Mohriak, 2003). Below the salts, a large proto-oceanic gulf accumulated carbonate and siliciclastic deposits with some locally associated magmatism. Such deposits, together with the evaporites, characterize the post-rift section of the eastern Brazilian margin. During the Albian, marine conditions became established, first represented by carbonates and then by thick siliciclastic sediment, predominantly shales and sandstones representing shallow platform, coastal fans, and slope and basin turbidites. This siliciclastic sequence consists of transgressive-regressive cycles that have been occurring since the Late Cretaceous (Asmus and Baisch, 1983, Milani et al., 2007).

During the Cenozoic, the Mucuri Basin experienced an important magmatic event that formed the Abrolhos Volcanic Complex, which was later capped by the Abrolhos coral reef. The Abrolhos carbonate sequence comprises the largest and the richest reef complex of the western South Atlantic (Leão, 1999). The carbonate bank was originally formed on volcanic rocks. The volcanics are intercalated with shales and carbonates. The Ar-Ar ages indicate that the volcanic activity spanned the Paleocene-Eocene (60-40 Ma, Szatmari et al., 2000, Milani et al., 2001, Zalan, 2004).

Salt tectonics played an important role in the evolution of the Brazilian marginal basins (Mohriak et al, 1990, Cainelli and Mohriak, 1999, Milani et al., 2001, Mohriak, 2003). The Campos and Santos basins are by far the most affected by salt mobilization, where it generated new depocenters basinwards. The Espírito Santo-Mucuri and Sergipe-Alagoas basins have reduced salt tectonics influence, mostly in deep-waters and onshore

respectively, while Pelotas Basin has incipient (northern part) or lacks salt tectonics (Cainelli and Mohriak, 1999).

2.4.2 – The Distal DSDP Setting:

2.4.2.1 – Leg 39 Site 356 – São Paulo Plateau:

DSDP Site 356 was drilled at the southeastern edge of São Paulo Plateau on the Brazilian continental margin (28°17.22'S, 41°05.28'W, 3175 m water depth), reaching sediments of late Albian age at 741m (Perch-Nielsen et al., 1977). According to Supko et al. (1977), the sediments of the Cretaceous/Tertiary boundary were deposited under oxidizing conditions and the supply of terrigenous material was cut off during the late Maastrichtian, the uppermost Maastrichtian to upper Paleocene sequence is relatively pure nannofossil and foraminifer chalk. During the Eocene, biogenic silica was deposited. Depositional hiatuses span the uppermost Paleocene to lowermost Eocene, and the upper middle Eocene to lower Miocene.

This site was selected for this study due to the relatively good recovery of the Paleocene section, represented by a thick and nearly complete sequence, although Boersma (1974) reported a gap spanning the lower Paleocene Zone P1b (Fig. 2.2). Boersma (1974) also highlights the impressive preservation in the Danian interval.

Paleocene sediments are recovered in Cores 356-29 to 16, where a hiatus of around 5 myr (~57 to 52 Ma) between the latest Paleocene and the earliest Eocene suggests either a break in the accumulation or deposition followed by erosion (Perch-Nielsen et al., 1977).

Eocene sediments were recovered in Cores 356-15 to 6. The lower Eocene sediments vary from chalky, foraminifer-rich sediments to radiolarian and diatom-rich sediments, which contain very small amount of foraminifera. The lower Eocene silicified chalks (cores 15 to 10) were deposited at the high rate of about 6 cm/kyr, and are overlain in core 10 by a thin sequence of siliceous calcareous ooze, which accumulated at very slow rate about 0.5cm/kyr. This decrease in the accumulation rate is probably associated to the high dissolution rate of biogenic sediments. The middle Eocene sediments vary from chalky, foraminifer-rich sediments to radiolarian and diatom-rich sediments, which contain very few foraminifera. The middle Eocene (cores 10 to 6) is characterized by sedimentation rates of about 4 cm/kyr (Perch-Nielsen et al., 1977).

2.4.2.2 – Leg 3 Site 20C – Rio Grande Rise:

This site is located at the Rio Grande Rise (28° 31.47'S and 26° 50.73'W – water depth 4506m), in the western South Atlantic. A relatively thin and incomplete uppermost Maastrichtian to Paleocene sequence was recovered in Hole 20C (Maxwell et al., 1970). The Cretaceous/Paleogene boundary interval is disturbed. The upper Paleocene to lower Eocene is nearly complete, although the dissolution interval that characterizes the Paleocene/Eocene boundary interval (PETM) at other South Atlantic sites was not recovered in the cored section. There is a stratigraphic break in the lower Paleocene (Fig. 2.2).

The upper Cretaceous to middle Eocene consists of very pale brown-pink and pink nannofossil chalky oozes. The lower to middle Eocene unit consists of nannofossil marl oozes and clays in various shades of brown and somewhat enriched in zeolites

(Maxwell et al., 1970). The authors suggest that this unit may have been deposited near the carbonate compensation depth, as the calcium carbonate content varies from 16% to 52%.

2.5 – BENTHIC FORAMINIFERA ASSEMBLAGES:

In general, the upper Maastrichtian to upper Eocene benthic foraminiferal assemblages of the western South Atlantic and eastern Brazilian marginal basins are composed of diverse agglutinated and calcareous taxa. The agglutinated species dominate the Brazilian marginal sites during Paleocene times, while the calcareous taxa dominate during the Eocene. The DSDP Sites 20C and 356 was dominated by calcareous taxa through the entire studied interval. The K/Pg boundary extinction of the benthic foraminifera is minimal when compared with Paleocene-Eocene boundary extinction, as it has been reported from middle bathyal and greater depths (Thomas, 1990; Kaiho, 1995; Alegret et al, 2001). Among the benthic foraminiferal taxa that went extinct across the PETM, the calcareous species were much more strongly affected (~83%) than the agglutinate species (~ 17%).

Among the most abundant benthic foraminiferal taxa (~330 taxa) studied, 32% occur exclusively in the Paleocene and 21% in the Eocene (Appendix A). Only 9.5% of the total benthic foraminiferal taxa occur from the late Maastrichtian through the upper Eocene interval, including *Nuttallides truempyi*, *Oridorsalis umbonatus*, *Bulimina trinitatensis*, *Recurvooides* sp., *Haplophragmoides* sp., *Gaudryina pyramidata*, *Gaudryina laevigata*, *Psammosiphonella cylindrica*, and *Cribrostomoides subglobosus*.

2.5.1 – Sergipe-Alagoas Basin:

SEAL-01 and SEAL-02 are the two wells that represent this basin, spanning the upper Maastrichtian to the upper Eocene.

The Maastrichtian-Paleocene boundary is marked exclusively by agglutinated taxa extinction (*Gaudryina expansa*, *G. inflata*, and *G. frankei*). The Maastrichtian-Paleocene interval is dominated by the agglutinated taxa, where the tubular forms (*Nothia*, *Rhizammina*, *Psammosiphonella*, *Bathysiphon*, *Hyperammina*) vary from 10% to 65% of benthics. *Haplophragmoides*, *Ammodiscus*, *Cribrostomoides*, *Budashevaella*, *Spiroplectammina*, and *Saccammina* are important agglutinated taxa. There are few calcareous taxa, including *Stensioeina beccariiformis*, *Nuttallides truempyi*, *Gavelinella* sp., *Anomalinoides* sp., and *Globobulimina* sp. This interval has high percentages of transported taxa (*Lenticulina*, *Amphistegina*, *Orthokarstenia*) from shallower depths. This interval is interpreted as middle to lower bathyal paleodepths, however SEAL-01 has a interval in the middle to upper Paleocene composed 100% of agglutinated (tubular forms ~30% of benthics) that corresponds to abyssal paleodepths, at or below the calcite compensation depth (CCD).

The Paleocene-Eocene boundary is marked by the extinction of the benthic taxa, mostly calcareous ones (~18% extinction rate), previously reported as the Benthic Extinction Event (BEE) associated with the Paleocene-Eocene Thermal Maximum (PETM). The extinct taxa in this basin are *Stensioeina beccariiformis*, *Cibicidoides velascoensis*, and *Gyroidindoides globosus* (calcareous), and *Reticulophragmium garcilassoii* (agglutinated).

The Eocene interval was recognized only in SEAL-01 and is composed mostly by calcareous taxa. The Eocene taxa includes a new group of taxa: *Cibicidoides eocaenus*, *Globocassidulina subglobosa*, *Hanzawaia ammophila*, and *Planulina costata*.

2.5.2 – Mucuri Basin:

This basin is represented by the well BA-01, spanning Maastrichtian to Eocene, with and unconformity from the lower to middle Eocene.

The agglutinated taxa (*Rhizammina* sp., *Haplophragmoides* sp., *Rzehakina epigona*, *Trochamminoides* sp., and *Saccammina placenta*) dominate the Maastrichtian through Paleocene interval associated with calcareous taxa (*Stensioeina beccariiformis*, *Nuttallides truempyi*, *Gyroidinoides globosus*, *Cibicidoides velascoensis*, *Pullenia coryelli*, *Oridorsalis umbonatus*, and *Osangularia velascoensis*).

In the middle to upper Paleocene (nannofossil biozone CP4 to CP8) the radiolarians appeared as 20% to 80% of total assemblage (planktics + benthics + radiolarians) and it was interpreted as the first radiolarian event (Fig. 2.3). The Maastrichtian-Paleocene interval is interpreted as middle to lower bathyal paleodepths.

The age could not be determined for a sandy interval on the top of the section because it lacked (planktic foraminifera and calcareous nannofossils). This interval is composed mostly of shallow water benthic taxa with evidence of transport (*Elphidium*, *Nodosaria*, *Lenticulina*, *Quinqueloculina*) and the age is no older than late Eocene, based on the presence of *Elphidium* sp. (first occurrence was in the late Eocene as reported by Loeblich and Tappan (1988)).

2.5.3 – Campos Basin:

Four wells from basin were studied (CAM-01, CAM-02, CAM-03, CAM-04 – Fig. 2.1), covering the Maastrichtian-Eocene interval. These wells have in common the high percentage of the agglutinated benthic foraminiferal taxa in the Maastrichtian through the upper Eocene. The Maastrichtian is recognized only at CAM-01 and is composed by agglutinated taxa (*Bathysiphon* sp., *Ammodiscus glabratus*, *Cribrostomoides trinitatensis*, *Glomospira charoides*, *G. serpens*, *Rzehakina epigona*, and *Gaudryina* sp.) associated with calcareous taxa (*Nuttallides truempyi*, *Stensioeina beccariiformis*, *Cibicidoides velascoensis*, *Gyroidinoides* sp., and *Lenticulina* sp.) interpreted as lower bathyal paleodepths.

The Paleocene was recognized at CAM-02 and CAM-04, which is dominated by agglutinated taxa dominated, especially the tubular forms (*Rhizammina* sp., *Bathysiphon* sp., *Psammosiphonella cylindrica*, *Kalamopsis grzybowskii* and *Nothia* sp.). *Haplophragmoides* sp., *Ammodiscus latus*, *A. glabratus*, *Glomospira charoides*, *Spiroplectammina* sp., and *Recurvoides* sp. are the other agglutinated taxa that occur in this interval. *Nuttallides truempyi*, *Stensioeina beccariiformis*, *Gyroidinoides globosus*, *Pullenia* sp., and *Cibicidoides velascoensis* are the calcareous taxa that are less abundant than the agglutinated taxa in the Paleocene interpreted as middle to lower bathyal paleodepths. There are some intervals in the Paleocene composed of 100% agglutinates (tubular forms 40% to 60% of benthics) and 0% of planktics that are interpreted as abyssal paleodepths, at or below the CCD.

The Eocene was recorded at CAM-02, CAM-03, and CAM-04 and new (post-BEE) calcareous taxa such as *Cibicidoides eoceanus*, *C. havanensis*, *C. mexicanus*,

Globocassidulina subglobosa, *Oridorsalis umbonatus*, and *Osangularia mexicana*, occur associated with the agglutinated *Haplophragmoides* sp., *Bathysiphon* sp., *Psammosiphonella cylindrica*, *P. discreta*, *Recurvoides* sp., *Saccamina placenta*, and *Ammodiscus* sp. The Eocene interval has a relatively balanced percentage of calcareous and agglutinated taxa interpreted as middle to lower bathyal paleodepths.

2.5.4 – Santos Basin:

The Santos Basin is represented by two wells (SAN-01 and SAN-02) that are ~500km apart. SAN-01 spans the upper Maastrichtian through the Eocene and SAN-02 the lower Eocene. The Santos Basin has three major unconformities that interrupt the record in the lower to middle Paleocene, in the lower Eocene and in the middle Eocene.

The upper Maastrichtian has a balanced percentage of calcareous and agglutinated taxa (*Psammosiphonella cylindrica*, *Globobulimina* sp., *Gyroidinoides globosus*, *Stensioeina beccariiformis*, *Gavelinella* sp., *Bulimina* sp., *Ammodiscus pennyi*, *Haplophragmoides eggeri*, *Bathysiphon* sp., and *Nuttallides truempyi*). The benthic assemblage in this interval is interpreted as middle to lower bathyal paleodepth zones.

The upper Paleocene is dominated by agglutinated taxa, especially the tubular forms (*Psammosiphonella cylindrica*, *Rhizammina* sp., *Spiroplectammina jarvisi*, *Ammodiscus glabratus*, *A. latus*, *Haplophragmoides* sp., *H. suborbicularis*, *Karrerulina conversa*, *Cribrostomoides trinitatensis*, *Psammosphaera fusca*, *Nuttallides truempyi*, *Anomalinoides capitatus*, and *Gyroidinoides globosus*). This assemblage is interpreted as lower bathyal to upper abyssal paleodepths.

The lower Eocene interval shows a decrease in diversity of the benthic taxa associated with the great percentage of radiolarians (40% to 100% of total assemblage). The radiolarian-rich interval is contemporaneous with Site 356, and it was interpreted as the second radiolarian event (Fig. 2.3). The Eocene benthic taxa are mostly represented by calcareous *Hanzawaia ammophila*, *Nuttallides truempyi*, *Oridorsalis umbonatus*, *Pullenia* sp., *Globobulimina* sp., *Gavelinella* sp., and *Stainforthia* sp. The assemblage is interpreted as middle to lower bathyal paleodepths.

2.5.5 – Pelotas Basin:

The Pelotas Basin is represented by the well PEL-01, and the samples cover the upper Maastrichtian through the upper Eocene.

From the Maastrichtian to the upper Paleocene, the benthic assemblage composed 100% of agglutinated taxa (*Bathysiphon* sp., *Haplophragmoides* sp., *Gaudryina pyramidata*, *Cyclamina placenta*, *Budashevaella multicamerata*, *Cribrostomoides subglobosus*, *Recurvoides* sp., *Nothia* sp., *Saccamina placenta*, *Psammosiphonella cylindrica*). This interval with no planktic foraminifera recovered and the benthic assemblage of 100% agglutinated is interpreted as lower bathyal to abyssal, at or below the CCD.

The lower Eocene shows an abrupt change in the benthic assemblage with the appearance of calcareous taxa, including new, post-BEE species (*Cibicidoides eoceanus*, *C. praemundulus*, *Hanzawaia ammophila*, *Anomalinoides garzaensis*, *Neoeponides byramensis*, *Planulina costata*, and *Bulimina alazanensis*) associated with survivors of the BEE (*Nuttallides truempyi*, *Oridorsalis umbonatus*, *Paralabamina lunata*). This

assemblage persists through upper Eocene and it is interpreted as middle to lower bathyal paleodepths.

2.5.6 – DSDP Sites:

DSDP Sites 356, on the São Paulo Plateau, and Site 20C on the Brazil Basin abyssal plain represent the most distal locations included in this study and provide a contrast with the deep-water settings along the Brazilian continental margin. Their benthic assemblages are somewhat similar and dominated by calcareous taxa.

The Paleocene benthic assemblage is composed by *Nuttallides truempyi*, *Stensioeina beccariiformis*, *Gyroidinoides globosus*, *Osangularia velascoensis*, *Aragonia velascoensis*, *Lenticulina whitei*, *Guttulina trigonula*, *Neoeponides hillebrandti*, *Quadratobuliminella pyramidalis*, *Oridorsalis umbonatus*, *Gaudryina pyramidata*, *G. laevigata*, *Dorothia trocoides*, *Marssonella* sp., *Pullenia coryelli*, *Spiroplectammina spectabilis*, *Buliminella grata*, *Cibicidoides velascoensis*, *C. hyphalus*, *Alabama midwayensis*, *Abyssamina poagi*, and *A. quadrata*. This assemblage is interpreted as middle to lower bathyal paleodepths.

The Benthic Extinction Event (BEE) is recorded in both sites and it affected mostly the calcareous taxa (*Stensioeina beccariiformis*, *Osangularia velascoensis*, *Aragonia velascoensis*, *Gyroidinoides globosus*, *Neoeponides hillebrandti*, *Cibicidoides velascoensis*, *C. hyphalus* and *Pullenia coryelli*), with extinction rate of ~37% at DSDP Site 20C and 33% at Site 20C.

In the lower Eocene, new, post-BEE species appear especially calcareous (*Cibicidoides eocaenus*, *C. havanensis*, *C. grimsdalei*, *C. micrus*, *C. mexicanus*,

Hanzawaia ammophila, *Globocassidulina subglobosa*, *Bolivina huneri*, *Osangularia mexicana*, and *Pullenia eocenica*,) that occur associated with the survivors (*Nuttallides truempyi*, *Oridorsalis umbonatus*, *Gaudryina pyramidata*, *Gaudryina laevigata*, and *Spiroplectammina spectabilis*). This assemblage is interpreted as lower bathyal.

At DSDP Site 356, there are two radiolarian events in the Eocene (2nd and 3rd, see figure 2.3) where they reached 60% in some samples (average 30-40% of total assemblage). The high percentage of biosiliceous sediments were also reported at DSDP Site 358 (Argentine Basin) in the lower Eocene where they have been interpreted as increased productivity (Van Andel et al., 1977).

2.6 – BENTHIC FORAMINIFERA ASSEMBLAGES EVOLUTION IN THE MAASTRICHTIAN THROUGH EOCENE OF THE WESTERN SOUTH ATLANTIC:

During the late Maastrichtian, the western South Atlantic had at least two major groups of benthic foraminiferal assemblages: one representing lower bathyal/abyssal depths and other representing outer neritic to middle bathyal depths. The deepest areas were inhabited by epifaunal species of the “Velasco-type assemblage” representing continental slope and abyssal plain paleodepths. This assemblage composition of epifaunal species (>60%) suggests generally oligotrophic conditions at the deepest locations in the western South Atlantic for this period of time (Gooday, 1993, Thomas, 1998, 2003).

The deeper regions of the Brazilian continental slope were populated chiefly by agglutinated taxa, especially the tubular forms (*Bathysiphon*, *Rhizammina*,

Psammosiphonella, and *Nothia*) typical of a classic flysch-type assemblage. The southern locations may or may not have developed a flysch-type assemblage in the late Maastrichtian.

Benthic foraminiferal extinction rates across the Cretaceous/Paleogene (K/Pg) boundary are relatively low (~10%) as typical for many deep-sea sites (e.g., Culver, 2003, Alegret and Thomas, 2005, 2012), for example, there was only 3% extinction at ODP Site 690 in the Weddell Sea (Alegret and Thomas, 2013). In the Sergipe-Alagoas, Pelotas and Santos basins, the K/Pg extinction was minor (~ 10%), with agglutinated taxa most affected (*Gaudryina expansa*, *G. ingens*, *G. inflata*, *G. frankei*, *Eggerellina brevis*, *Marssonella trochoides*, *Recurvoides nucleolus*, and *Pseudoclavulina chitinoso*). There were no extinction recognized across the K/Pg boundary at the deepest DSDP Sites 20C and 356.

The Paleocene benthic foraminiferal assemblages are dominated by agglutinated in wells of the Brazilian marginal basins (60% to 100% of the benthics). Calcareous taxa dominate the distal DSDP sites 20C and 356, accounting on more than 80% of the benthic foraminiferal assemblage. The Paleocene agglutinate-dominated benthic assemblages have a high percentage of tubular forms (*Bathysiphon*, *Rhizammina*, *Nothia*, *Psammosiphonella*, *Hyperammina*) reaching 70% of the benthic assemblages, with average of 35%. Agglutinated assemblages dominated by the tubular forms have been called as 'flysch-type' (Gradstein and Berggren, 1981, Kuhnt, 1987, Kaminski et al., 1988, Kuhnt & Kaminski, 1989, Kaminski et al., 1996, Kaminski and Gradstein, 2005).

The flysch-type assemblages dominate the Brazilian marginal basin during the late Maastrichian through the Paleocene, but persisted until the early late Eocene in the Campos Basin.

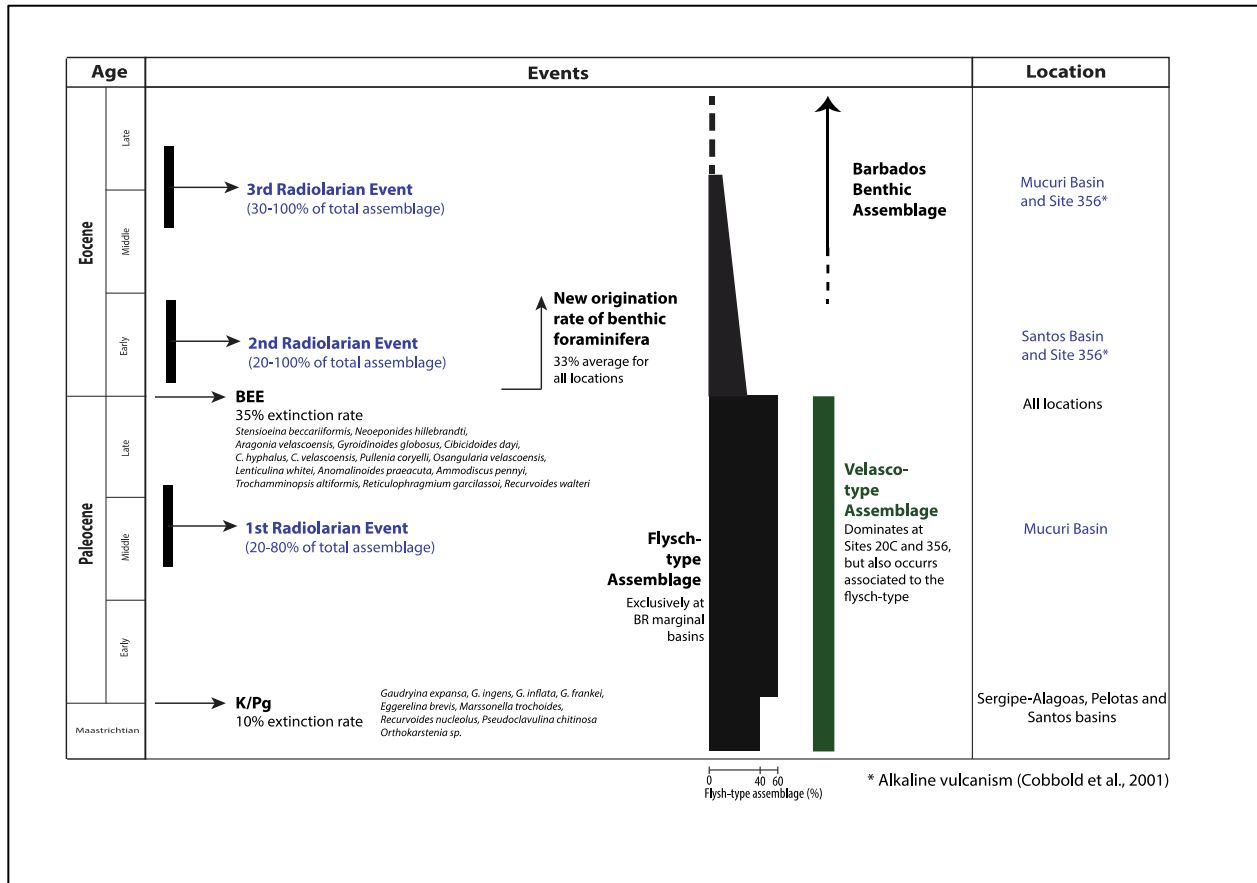


Figure 2. 3: Main events and benthic foraminiferal assemblage recognized in the Brazilian margin and the western South Atlantic.

The Paleocene calcareous assemblage is represented by the Velasco-type assemblage. The Velasco-type assemblage was first described by Berggren and Aubert (1975) for the Velasco Formation of Mexico. This assemblage is composed by *Stensioeina beccariiiformis*, *Nuttallides truempyi*, *Cibicidoides velascoensis*, *Osangularia*

velascoensis, *Aragonia velascoensis*, *Pullenia coryelli*, *Gyroidinoides globosus* and *Cibicidoides hyphalus*. The Velasco-type assemblage representing deep-water and dominates the distal sites 20C and 356 but also occurs as minor component associated to the flysch-type assemblage in the marginal basins (Fig. 2.3).

Nuttallides truempyi is by far the most abundant and frequent calcareous species in the studied interval (15-45% of benthics) and *Oridorsalis umbonatus* (10-23% of benthics) occurs in all locations but not always as abundant as *N. truempyi*.

The benthic extinction event (BEE) across the Paleocene-Eocene boundary is an important global extinction event affecting the benthic foraminiferal community at many deep water locations around the world, associated with the Paleocene-Eocene Thermal Maximum, or PETM (e.g., Tjalsma and Lohmann, 1983, Thomas, 1989, 1990, 1998, 2003, 2007, Pak and Miller, 1992, Ortiz, 1995, Thomas and Shackleton, 1996, Kaiho, 1998, Katz et al. 1999, Hancock et al., 2006, Takeda and Kaiho, 2007, McCarren et al., 2008, Alegret et al., 2009, d'Haenens et al., 2012, Speijer et al., 2012). The extinctions are much less pronounced in neritic and upper bathyal settings (e.g., Alegret and Ortiz, 2006, Stassen et al., 2015), and is ~16% in the Brazilian marginal basins (Table 2.2). The BEE is observed among all locations being much more pronounced on the calcareous taxa (~83%) than agglutinated taxa. The average extinction rate is ~35% at DSDP sites and is consistent with previous estimates 30-50% for the deep-sea (Tjalsma and Lohmann, 1983, Thomas, 1990, 1998, Pak and Miller, 1992, Thomas and Shackleton, 1996, Kaiho, 1998, Katz et al. 1999), however, the wells in the Brazilian marginal basins shows 16% average extinction rate across the Paleocene-Eocene boundary. The

difference between the DSDP sites and the marginal basins is due to the calcareous are more abundant in the DSDP sites than the basins in the Paleocene interval.

Table 2.2: Paleocene and Eocene benthic foraminiferal diversity based on the number of species (S), extinction and origination rates of the most representative sites and wells of the study area.

	Paleocene Taxa (S)			Extinct Taxa (S)			Extinction Rate		Eocene Taxa (S)			New Taxa (S)			Origination Rate	
	Calc.	Aggl.	Total	Calc.	Aggl.	Total			Calc.	Aggl.	Total	Calc.	Aggl.	Total		
20C	29	6	35	13	0	13	37%	35%	38	4	42	23	0	23	55%	47%
356	25	9	34	11	0	11	33%		25	7	32	12	0	12	38%	
SEAL-01	12	31	43	2	1	3	13%	16%	29	4	33	13	0	13	30%	25%
SEAL-02	12	16	28	3	0	3	21%		18	15	33	4	0	4	12%	
CAM-04	5	20	25	2	4	6	14%		32	16	48	4	0	5	35%	
SAN-01	23	25	48	2	5	7	15%		11	2	13	3	0	3	23%	

The calcareous benthic taxa that went extinct during the BEE include *Stensioeina beccariiformis*, *Neoeponides hillebrandti*, *Aragonia velascoensis*, *Gyroidinoides globosus*, *Cibicidoides dayi*, *C. hyphalus*, *C. velascoensis*, *Pullenia coryelli*, *Osangularia velascoensis*, *Lenticulina whitei* and *Anomalinoides praeacuta*. The agglutinate benthic taxa extinct during the BEE include *Ammodiscus pennyi*, *Trochamminopsis altiformis*, *Reticulophragmium garcilassoi*, and *Recurvoides walteri*.

In the early Eocene, origination of new, post-BEE calcareous species recorded in the Brazilian margin and at the DSDP sites. The origination rate is higher at DSDP sites 47% compared with the marginal basins 25% (Table 2.2).

A distinctive group of new species appeared during the latest Paleocene (nannofossil biozone CP7, planktic foraminiferal biozone P5), including *Hanzawaia ammophila*, *Cibicidoides eocaenus*, *Cyclamina placenta*, *Globocassidulina subglobosa*, and *Anomalinoides garzaensis*. A second group of new species emerged at the early

Eocene (nannofossil biozone CP8, planktic biozones E1/E3): *Stilostomella subspinoso*, *S. aculeata*, *Bulimina tuxpamensis*, *Cibicidoides havanensis*, *C. subspiratus*, *C. micrus*, *C. praemundulus*, *Osangularia mexicana*, and *Planulina costata*. These two distinct groups of originations were observed at all locations and suggest a progressive (or at least two-step event) response to changing conditions in the southwest Atlantic and along the Brazilian continental margin during the Paleocene-Eocene transition. These taxa are part of what is called the Barbados-type Assemblage (Wood et al., 1985, Van Markoven et al., 1986, Berggren and Miller, 1989, Bolli et al., 1994).

The calcareous taxa are mostly represented by epifaunal species of *Cibicidoides*, *Nuttallides*, *Planulina*, *Osangularia*, *Gyroidinoides* and *Neoeponides*. Common infaunal taxa are species of *Bulimina*, *Globocassidulina*, *Bolivina*, *Anomalinoidea* and *Pullenia*.

Of the two distinct groups of *Cibicidoides*, one occurs in the Paleocene (*C. velascoensis*, *C. hyphalus*, *C. dayi*) and the other in the Eocene (*C. eocaenus*, *C. micrus*, *C. havanensis*, *C. mexicanus*, *C. grimsdalei*, *C. praemundulus*). The Paleocene group became extinct during the BEE at the Paleocene-Eocene boundary and are most common at the deepest locations (Sites 20C and 356). The Paleocene *Cibicidoides* extinction has been reported from around the globe, in the Gulf of Mexico, Caribbean and South Atlantic by Tjalsma and Lohmann (1983), in the Gulf of Mexico by Van Morkhoven et al. (1986), in Trinidad by Bolli et al., 1994), in the western Tethys by Ortiz (1995), in northeastern Mexico by Alegret and Thomas (2001), and in the central equatorial Pacific by Nomura (2005). The Eocene *Cibicidoides* emerged after the P/E boundary and the diversity strongly increased at all locations.

2.7 – BENTHIC FORAMINIFERA EXTINCTION IN THE BRAZILIAN MARGINAL BASINS:

The deep-water benthic foraminiferal community experienced a major extinction event in the end of Paleocene (e.g., Tjalsma and Lohmann, 1983, Thomas, 1998, 2007, Kaiho, 2006, Stassen et al., 2012). The extinction event has been documented in the Atlantic Ocean (Tjalsma and Lohmann, 1983), in the Pacific Ocean (Miller et al., 1987), in the Indian Ocean (Nomura, 1991), Southern Ocean (Katz and Miller, 1991, Thomas, 1990) and the New Jersey coastal plain (Stassen et al., 2015). Benthic foraminiferal assemblages from shelf and upper slope depths were also affected by the PETM in the Tethys (e.g., Schmitz et al., 1996, Speijer et al., 1996, Scheibner and Speijer, 2008a, b).

There is no resolution in our record to discuss the benthic extinction event at the PETM in detail, however our results show the turnover of the benthic assemblage across the Paleocene-Eocene boundary. The Maastrichtian-Paleocene interval is dominated by the agglutinate-rich flysch-type assemblage in the marginal basins occasionally associated with the calcareous-dominant Velasco-type assemblage (Fig. 2.3). The Velasco-type assemblages have been reported as a pre-PETM benthic assemblage in the deep-water in several locations, e.g., Tethys and Atlantic Oceans (Berggren and Aubert, 1975), southern and southeastern Atlantic Oceans (Thomas and Shackleton, 1996), Atlantic Ocean (Tjalsma and Lohmann, 1983, Thomas, 1998), tropical Pacific Ocean (Kaiho et al., 2006), and New Jersey coastal plain (Stassen et al., 2015). They have in common the extinction of calcareous taxon *Stensioeina beccariiformis* that delimits the event in the deep-waters.

The extinction is less pronounced in the continental shelf as reported by Stassen et al. (2012) for the New Jersey coastal plain and Speijer et al. (1996) for the Red Sea coast. These works revealed that the Midway-type assemblage (*Cibicidoides*, *Anomalinoides midwayensis*, *A. acuta*, *Osangularia plummerae*, *Gavelinella danica*, nodosariids, lenticulariids, veginulinids, polymorphynids and textulariids; Berggren and Aubert, 1975) remained mostly unaffected by the extinction event. In our study area, the extinction is also less severe in the proximal locations of the Brazilian margin, accounting 16% of extinction rate contrasting 35% from the DSDP sites (Table 2.2). In both regions, proximal and distal, the calcareous taxa are by far the most affected by the event (~83%), that agrees with the rapid ocean acidification during the PETM (e.g., Zachos et al., 2005, Higgins et al., 2006, Thomas, 2007, Scheibner and Speijer, 2008a, b, Hoenisch et al., 2012).

The post-PETM benthic assemblage is composed of new calcareous taxa, dominated by *Globocassidulina subglobosa*, *Hanzawaia ammophila*, *Planulina costata* species of *Cibicidoides* and *Bulimina*. The survivors of the event are *Oridorsalis umbonatus*, *Bulimina trinitatensis*, and *Nuttallides truempyi*, in addition to the agglutinated taxa *Gaudryina pyramidata*, *Gaudryina laevigata*, *Cribrostomoides subglobosus*, *Recurvoides* sp., *Haplophragmoides* sp., and *Psammosiphonella cylindrica*. The new origination rate is higher at the DSDP sites than the marginal basins (47% and 25%, respectively).

2.8 – CONCLUSION:

Approximately 330 taxa are described from the upper Maastrichtian through to upper Eocene of the five Brazilian marginal basins and two distal DSDP sites. These taxa span lower abyssal to neritic paleodepths, and provide the basis of the assemblages analyzed in this study.

The Maastrichtian through Paleocene is dominated by the agglutinated flysch-type assemblage in the Brazilian marginal basins that occasionally occur associated with the Velasco-type calcareous assemblage. The Velasco-type assemblage dominates the distal DSDP Sites 20C and 356 in the same interval.

The Benthic Extinction Event (BEE) was recognized in the marginal basins and at DSDP sites and affected mostly the calcareous taxa (83%) than the agglutinated taxa. The Brazilian marginal basins revealed an abrupt change where the benthic assemblages changed from agglutinate-dominated in the Maastrichtian-Paleocene to calcareous-dominated in the Eocene. The extinction is less severe in the proximal marginal basins (~16% extinction) than in the distal DSDP sites (~35% extinction).

The agglutinated taxa are much more common and abundant in the proximal marginal basins compared with the distal DSDP sites, and one of the reasons could be the proximity to the siliciclastic input from continental areas associated with sea level fluctuations during upper Maastrichtian through Eocene. This siliciclastic input seems to be the main source for the particles used by agglutinated taxa to construct their tests. A relatively shallow CCD along the biologically productive continental margins may have

also contributed to the dominance of agglutinated taxa (e.g., Berger, 1979, Kaminski and Gradstein, 2005).

2.9 – BENTHIC FORAMINIFERA TAXONOMIC CLASSIFICATION:

Traditionally, the benthic foraminiferal taxonomic classification has long been based on the morphology and nature of the test, the hard shell that is preserved in the fossil record (see Sen Gupta, 2000 for a review). These classifications proposed evolutionary relationships between species and genera, also based on the morphology and type of the test (calcareous, aragonitic or agglutinated wall), which included both modern and ancient taxa. The most used taxonomic classifications (Galloway, 1933, Cushman, 1945, Loeblich & Tappan, 1955, 1964, 1987) argued that ‘the same chamber arrangement and form of the test may have parallel evolution, without indicating interrelationship of the similarly shaped shells’ (Loeblich & Tappan, 1964, p. 28), once again the nature of the test wall was the basis for classification. Sen Gupta (2000) proposed a new classification that follows Loeblich & Tappan (1987, 1994) but still used morphological criteria of the test as the basis for classification. Mikhalevich (2004) proposed a classification that is also based on the test morphology. However, she considered that some agglutinated tests are strikingly isomorphic analogues to some forms with calcareous secreted wall (see fig. 2 in Mikhalevich, 2004).

The advances in molecular systematics based on DNA sequences analysis provided a new perspective on the foraminifer systematics, which allowed phylogenetic links between organisms at different taxonomic levels (Pawłowski, 2000). This new approach challenged the traditional, test wall and morphology-based classification,

promoting total revision of the higher-level taxonomy and species identification (Pawlowski, 2000, Pawlowski et al., 2013). Pawlowski et al. (2013) proposed a new supraordinal classification of Foraminifera based on molecular phylogeny, where multi-chambered orders are organized into two classes: Tubothalamea and Globothalamea, both of which contain taxa with agglutinated or calcareous walls. The implication is that agglutinated and calcareous tests are polyphyletic, and according to Pawlowski et al. (2013), the calcareous wall appeared at least five different times. The single-chambered taxa are organized into a basal paraphyletic assemblage called “monothalamids”, placing agglutinated or organic-walled tests together. The multi-chambered lineages evolved independently two or three times from the monothalamids (Pawlowski et al., 2013).

Loeblich & Tappan (1987) placed Foraminifera as an Order while Sen Gupta (2000) placed as a Class. Meantime, other authors considered Foraminifera as Phylum, based on the fact that they sharply differ from all other protistan phyla and from other groups of the former Sarcodina (Margulis, 1974, Margulis & Schwarz, 1988, Mikhalevich, 2004, Pawlowski et al., 2013).

In this work, the benthic foraminiferal taxa described here follow the new classification scheme of Pawlowski et al. (2013), including the three Orders “Textulariida”, Rotaliida, and Lagenida. The Orders “Textulariida” and Rotaliida belong to the Class Globothalamea, while Lagenida was placed as Incertae Sedis. The genera *Ammodiscus* and *Glomospira* were placed as Class Tubothalamea by Pawlowski et al. (2013). The Superfamily, Family, and Genus-level classification follows that of Loeblich & Tappan (1988).

2.9.1 – Systematics:

Phylum FORAMINIFERA d'Orbigny (1826)
Class TUBOTHALAMEA Pawlowski et al. (2013)
Order Textulariida Pawlowski et al. (2013)
Superfamily AMMODISCCACEA Reuss, 1892
Family AMMOSDISCIDAE Reuss, 1862
Subfamily AMMODISCINAE Reuss, 1862
Genus *Ammodiscus* Reuss, 1862
Type species: *Ammodiscus infimus* Bornemann 1874

Ammodiscus cretaceous (Reuss, 1845)
Plate I, figs. 1a-b

Operculina cretacea Reuss, 1845, p. 35, pl. 13, figs. 64-65.

Cornuspira hoernesii Karrer 1866, p. 495, pl. 1, fig. 10.

Ammodiscus cretaceous (Reuss 1845) – Kaminski & Gradstein, 2005, pl.14, figs. 1-10.

Main features: Test agglutinated, planispiral, evolute, circular to slightly elliptical in outline with rounded periphery. First chamber followed by coiled tube with 9 to 11 whorls visible. The last whorls are thicker than the previous ones, tube gradually increasing in diameter. Test wall finely agglutinated, with smooth surface, aperture at open end of tubular chamber.

Remarks: We compared our specimens with the hypotype (USNM 302257) and plesiotypes (CC 39491, 61912) at the National Museum of Natural History, Smithsonian Institution and our material agrees with *Ammodiscus cretaceous* Reuss. This species is distinguished from other *Ammodiscus* species by its finely agglutinated wall, smoothly finished somewhat with some fine radial striations.

Stratigraphic distribution: This species is rare in the Campos and Santos basins in the middle Paleocene interval (CP5).

Distribution chart #: 101.

Ammodiscus glabratus Cushman & Jarvis, 1928

Ammodiscus glabratus Cushman & Jarvis, 1928, p. 86, pl. 4, fig. 66.

Ammodiscus glabratus Cushman & Jarvis, 1928 – Bolli et al., 1994, p. 68, figs. 18. 23-24, Kaminski & Gradstein, 2005, p. 32, figs 15-16.

Main features: Test agglutinated, planispiral, circular with ~10 whorls, increasing slowly in size. The sutures are weakly depressed, wall very finely agglutinated.

Remarks: This species is distinguished from other species in the genus by its number of whorls and thick and robust test, and the test finishing is usually smooth. Differs from *A. cretaceous* on having the incised sutures and more roughly finished wall.

Stratigraphic range: In our samples, it is rare to common in the Sergipe-Alagoas, Mucuri, and Santos basins and common to abundant in the Campos Basin from the Maastrichtian through middle Paleocene (NC23 to CP5).

Distribution chart #: 109.

Ammodiscus latus Grzybowski, 1898

Ammodiscus latus Grzybowski, 1898, p. 282, pl. 10, figs.27-28.

Lituoba eocenica Cushman & Renz, 1948, p.7, pl. 1, figs. 20-21.

Ammodiscus latus Grzybowski, 1890 – Kaminski & Gradstein, 2005, p. 150, pl. 16a-b, Bolli et al., 1994, p. 68, fig. 18.25, Holbourn et al., 2013, p. 34, fig. 1.

Main features: Test agglutinated, planispiral, with 3 to 5 whorls. The thickness of the test at the proloculus is less than in the coiled chamber, resulting in a depressed umbilicus on one or both sides. The diameter of the coiled chamber increases in size very slowly.

Kaminski & Gradstein (2005) distinguished microspheric and megalospheric types, but we did not recognize these in our specimens, which mainly have ~3-5 whorls.

Remarks: This species differs from *A. pennyi* by its depressed umbilical area, it sometimes has fewer whorls and is distinctly less coarsely agglutinated, and from other *Ammodiscus* by its large size, coarse wall and tendency to uncoil.

Stratigraphic range: In our samples, this species is very rare to rare in the middle in the lower through middle Paleocene (CP1 to CP4) of the Santos, Mucuri and Campos basins.

Distribution chart #: 106.

Ammodiscus macilentus (Myatlyuk, 1970)

Grzybowskiella macilenta Myatlyuk, 1970, p. 73, pl. 13, figs. 2-3.

Ammodiscus macilentus (Myatlyuk, 1970) – Bolli et al. 1994, p. 68, figs. 18. 26-27.

Main features: Test agglutinated, planispiral, almost elliptical outline, with 7 to 9 whorls and weakly depressed sutures.

Remarks: Frequently flattened due to the preservation. Differs from *A. glabratus* Cushman & Jarvis by its thinner test and usually larger size. Bolli et al. (1994) considered this taxon a transitional form between *A. planus* and *A. glabratus*, but we could not observe this transition in our samples. Differs from other species by its robust appearance and generally larger size.

Statigraphic range: This species is very rare and it was found only in the middle Paleocene (CP5) of the Santos Basin.

Distribution chart #: 102.

Ammodiscus pennyi Cushman & Jarvis, 1928
Plate I, figs. 2a-b

Ammodiscus pennyi Cushman & Jarvis, 1928, p. 87, pl. 12, figs. 4-5.

Ammodiscus pennyi Cushman & Jarvis, 1928 – Bolli et al., 1994, p.68, figs. 18.28, 36, Kaminski & Gradstein, 2005, pl. 17, figs. 1-6, Holbourn et al., 2013, p. 36, fig. 1.

Main features: Test agglutinated, planispiral, discoidal in outline, first chamber followed by coiled tube, 5-6 whorls visible. Wall coarsely agglutinated, robust, aperture at open end of tubular chamber.

Remarks: The holotype species for *Ammodiscus pennyi* Cushman & Jarvis is missing from the Cushman Collection at Smithsonian Institution. However, we compared our specimens with paratypes (CC 9670). The most distinct characteristics of this species are its few whorls and coarsely agglutinated particles (sometimes impossible to distinguished the sutures between the whorls in our material). Differs from other *Ammodiscus* by its fewer whorls and coarsely agglutinated wall.

Stratigraphic distribution: This species occurs only in two of the marginal basins, common to abundant in the Santos Basin and very rare in the Mucuri Basin from the lower through middle Paleocene interval (CP3 to CP5).

Distribution chart #: 104.

Subfamily AMMOVERTELLININAE Saidova, 1981
Genus *Glomospira* Rzehak, 1885

Type species: *Trochammina squamata* Jones and Parker var. *gordialis* Jones and Parker, 1860

Glomospira charoides (Jones and Parker, 1860)
Plate I fig. 3

Trochammina squamata var. *charoides* Jones and Parker, 1860, p. 304, no type figure given.

Repmanina charoides Jones and Parker var. *corona* Cushman & Jarvis, 1928 – Bolli et al., 1994, p. 70, fig. 19.3.

Glomospira charoides (Jones and Parker, 1860) – Koutsoukos, 2000, p. 252, pl. 2, figs. 1-3, Kaminski & Gradstein, 2005, p. 154, pl. 22, figs. 1-16, Holbourn et al., 2013, p. 268, fig. 1.

Main features: Agglutinated test, proloculus followed by a trochospirally enrolled, tubular second chamber, comprising about two to three whorls. The last part of the tube is irregularly coiled. Wall finely agglutinated, aperture at the end of the tube.

Remarks: This species differs from other *Glomospira* by its finely agglutinated wall and trochospirally coiling with last part irregularly coiled.

Stratigraphic distribution: This species is common to abundant in the Campos Basin through the lower Paleocene- upper Eocene interval (CP1 to CP14).

Distribution chart #: 56.

Glomospira gordialis (Jones and Parker, 1860)

Trochammina squamata Jones and Parker var. *gordialis* Jones and Parker, 1860, p. 11, fig. 4.

Glomospira gordialis (Jones and Parker, 1860) – Kaminski & Gradstein, 2005, p.153, pl. 25, figs. 1-8, Holbourn et al., 2013, p. 270, fig. 1.

Main features: Agglutinated test, almost spherical in shape, formed by a globular proloculus followed by undivided chamber coiled around the proloculus glomospirally, usually 5 to 6 whorls visible. Wall very finely agglutinated and aperture is the opening at the end of the tube.

Remarks: This species differs from others *Glomospira* on having more than one completely enveloping whorls of the tubal chamber.

Stratigraphic distribution: This species is common to abundant in the Mucuri, Campos, and Santos basins from the Maastrichtian through the lower Eocene (NC23 to CP8). It is rare in the lower Eocene of the Site 20C (planktic foraminifera biozones E5/E6).

Distribution chart #: 79.

Glomospira serpens (Grzybowski, 1898)

Ammodiscus serpens Grzybowski, 1898, p. 285, pl. 10, fig. 31.

Glomospira serpens (Grzybowski, 1898) – Kaminski & Gradstein, 2005, p. 155, pl. 27, figs. 1-6.

Main features: Test agglutinated, oval in outline formed by a tubular chamber coiled elliptically, miliolid-like. Wall very finely agglutinated and aperture as opening at the end of the tube.

Remarks: Differs from other *Glomospira* in its relatively large size and milioline-like coiling.

Stratigraphic distribution: This species is rare to frequent in the Paleocene (s CP3 to CP7) of the Campos Basin.

Distribution chart #: 87.

Class GLOBOTHALAMEA Pawlowski et al. (2013)

Order TEXTULARIINA Delage and Hérouard, 1896

Family BATHYSIPHONIDAE Avnimelech, 1952

Genus *Bathysiphon* M. Sars, 1872

Type species: *Bathysiphon filiformis* M. Sars, 1872

Bathysiphon sp.

Plate I fig. 4

Main features: Test agglutinated, thick straight and unbreached elongated tube, open at both ends. The annular constrictions are the main feature that differentiates this genus from other tubular forms. Annular constrictions resulting from periodic growth, thick wall may contain sponge spicules, sand grains, among other particules.

Remarks: Most of our specimens are fragments or are badly preserved, it is not possible to confidently assign specimens identification into species. *Bathysiphon* sp. is abundant in the flysch-type assemblage interval.

Stratigraphic distribution: *Bathysiphon* sp. is common to very abundant in the Paleocene interval among our samples, especially in the Mucuri, Campos, Santos and Pelotas basins. *Bathysiphon* sp. occurs from the Maastrichtian through the upper Paleocene/lower Eocene (NC23 to CP8). Highest abundance interval is in the middle to upper Paleocene (CP3 to CP6), reaching ~45% of benthics. This taxon, as most of the agglutinants, does not occur in the DSDP Sites 20C and 356.

Distribution chart #: 78.

Genus *Psammosiphonella* Avnimelech, 1952

Type species: *Bathysiphon arenaceous* Cushman, 1927

Psammosiphonella cylindrica (Glaessner, 1937)

Plate I, fig. 5.

Rhabdammina cylindrica Glaessner, 1937, p. 354, pl. 1, figs. 1.

Psammosiphonella cylindrica (Glaessner, 1937) – Kaminski & Gradstein, 2005, p. 145, pl. 6, figs. 1-5.

Main features: Test agglutinated, straight and cylindrical with uniform diameter. The test wall is thick and relatively coarse, and is composed mostly by quartz grains, evenly distributed. Inner circular wall is smooth, aperture at the end of the tube.

Remarks: This species seems to select the grains from the sediment to build its test. Due to the thick and well-cemented wall, the specimens are always better preserved than other tubular forms, almost never flattened, such as *Bathysiphon* and *Nothia*. This species is one of the tubular forms of the flysch-type biofacies.

Stratigraphic range: In our samples, this species is common to very abundant from the Maastrichtian through the upper Eocene (NC23 to CP15), with highest abundance and frequency in the Paleocene (~27% of benthics – CP1 to CP6) in the Brazilian marginal basins. *P. cylindrica* is rare in the Pelotas Basin (sparse occurrences in the upper Paleocene – CP6/7) and it absent at Sites 356 and 20C.

Distribution chart #: 43.

Psammosiphonella discreta (Brady, 1881)

Plate I, fig. 6.

Rhabdammina discreta Brady, 1881, pl. 22, figs. 8-10.

Psammosiphonella discreta (Brady, 1881) – Kaminski & Gradstein, 2005, p. 148, pl. 5, figs. 1-8.

Main features: Test agglutinated with fine grains of quartz, straight and with annular constrictions at irregular intervals. The elongated tube may taper toward one end. Wall thick, well-cemented, finely finished, aperture at the end of the tube.

Remarks: Kaminski & Gradstein (2005) reported the largest specimens might have as many as five constrictions, which was not observed in our material due to generally poor preservation. This species differs from *P. cylindrica* in having annular constrictions and in being finely agglutinated.

Stratigraphic range: *P. discreta* is common to very abundant and occurs from the middle Paleocene to upper Eocene (CP3 to CP15), with increased abundances in the middle through upper Paleocene (CP4 to CP7) of the Sergipe-Alagoas, Mucuri, Campos, and Santos basins, specially in the flysch-type assemblages. This species is absent in the Pelotas Basin and at Sites 356 and 20C.

Distribution chart #: 33.

Genus *Nothia* Pflaumann, 1964

Type species: *Rhizammina grilli* Noth, 1951

Nothia sp.

Main features: Agglutinated and tubular test with both open ends, may be sparsely and irregularly branched. Wall particles contain a wide variability in composition, but mostly fine sand grains in our specimens.

Remarks: Mostly specimens are flattened as a feature of preservation. The specimens placed as *Nothia* sp. are poorly preserved fragments. Differs from *Bathysiphon* sp. mainly by lacking any annular constrictions and being distinctly smoother.

Stratigraphic distribution: Through the Paleocene (CP1 to CP7) it is common in the Mucuri, Sergipe-Alagoas, and Campos basins. It is rare in the Pelotas Basin from the middle Paleocene through lower Eocene (CP4 to CP12). It is absent in the Santos Basin and at Sites 356 and 20C.

Distribution chart #: 88.

Nothia latissima (Grzybowski, 1898)

Plate I, fig. 7.

Dendrophyra latissima Grzybowski, 1898, p. 272, pl. 10, fig. 8.

Nothia latissima (Grzybowski, 1898) - Kaminski & Gradstein, 2005, p. 111, pl. 3, figs. 1-4.

Main features: Agglutinated and tubular form test with opening at both ends, thin wall composed mainly of finely agglutinated grains.

Remarks: Specimens usually flattened due to preservation. Differs from others by the very finely agglutinated wall, especially with mica grains.

Stratigraphic distribution: This species is very rare to rare and its occurrence is restricted to the middle to upper Paleocene (CP5 to CP6) in the Sergipe-Alagoas Basin.

Distribution chart #: 95.

Nothia robusta (Grzybowski, 1898)
Plate I, fig. 8.

Dendrophyra robusta Grzybowski, 1898, p. 273, pl. 10, fig. 7.

Nothia robusta (Grzybowski, 1898) – Kaminski & Gradstein, 2005, p. 114, pl. 4, figs. 1-8.

Main features: Agglutinated and robust test, generally straight and tubular form. Kaminski & Gradstein (2005) reported some rare branched fragments, which do not occur in our specimens. Thick test wall mostly composed of quartz grains (medium to coarsely agglutinated), and with inner brownish layer.

Remarks: Specimens usually flattened due to preservation. Differs from other *Nothia* species in having a thick wall and inner brownish layer, from *Bathysiphon* by the absence of the annular constrictions. Our specimens of *Nothia robusta* usually agglutinates medium- to coarse-size grains. Kaminski & Gradstein (2005) reported that the wall is often silicified, and may contain randomly oriented sponge spicules and occasionally fine mafic mineral grains on the test surface, but we could not observe those features among our specimens.

Stratigraphic distribution: This species is common to very abundant and occurs only in the Sergipe-Alagoas Basin, during upper Paleocene to lower Eocene (CP6 to CP8).

Distribution chart #: 76.

Family RHABDAMMINIDAE Brady, 1884
Subfamily RHABDAMMININAE Brady, 1884

Genus *Rhizammia* Brady, 1879
Type species: *Rhizammia algaeformis* Brady, 1879

Rhizammia sp.
Plate I, figs. 9a-b.

Main features: Test agglutinated, tubular, branching, slightly tapered toward one end, wall agglutinated, particles variable in size, slightly rough externally. Aperture at end of the tube.

Remarks: Not always readily differentiated between *Bathysiphon* and *Rhizammia*, but *Rhizammia* exhibits a more variable particle composition than *Bathysiphon*, including other foraminifera or radiolarians tests. In our material, the specimens included in this taxon are fragments, unlikely branched, mostly composed by quartz grains and other minerals particles, usually medium-to-coarse agglutinated. *Bathysiphon* specimens are finely agglutinated tubular forms. *Rhizammia* sp. is one of the most abundant taxa of the tubular forms as important component of the flysch-type assemblage.

Stratigraphic range: *Rhizammia* sp. is abundant to very abundant throughout the Maastrichtian to lower Eocene (NC23 to CP10), with highest abundance middle to upper Paleocene (CP3 to CP7) in the Sergipe-Alagoas, Mucuri, Campos, and Santos basins.

Distribution chart #: 68.

Family SACCAMMINIDAE Brady, 1884
Subfamily SACCAMMININAE Brady, 1884

Genus *Saccamina* Carpenter, 1869
Type species: *Saccamina sphaerica* Brady, 1871

Saccamina placenta (Grzybowski, 1898)

Reophax placenta Grzybowski, 1898, p. 276, pl. 10, figs. 9, 10.

Saccamina placenta (Grzybowski, 1898) – Bolli et al. 1994, p. 67, figs. 18. 14-15.

Main features: Agglutinated test, spherical, circular in outline, wall finely to moderately agglutinated. Aperture as single opening with short neck, not always preserved.

Remarks: Specimens usually compressed and flattened as preservation.

Stratigraphic range: This species is rare in the Pelotas Basin but it is relatively abundant in the other marginal basins, especially in the Paleocene interval (CP1 to CP7).

Distribution chart #: 89.

Genus *Hyperamma* Brady, 1878
Type species: *Hyperamma elongata* Brady, 1878

Hyperamma elongata Brady, 1878

Hyperamma elongata Brady, 1878, p. 433, pl. 20, fig. 2.

Hyperamma elongata Brady, 1878 – Jones, 1994, p. 33, pl. 23, fig. 8., Bolli et al., 1994, p. 67, figs. 18.18-19, Holbourn et al., 2013, p. 310, figs. 1-2.

Main features: Test agglutinated, elongated with large proloculus followed by undivided, tubular chamber, tapering slightly towards the aperture. Wall constructed of fine to medium grained size agglutinated particles, generally with organic cement as reported by Holbourn et al. (2013).

Stratigraphic range: This taxon is one of the tubular forms of the flysch-type assemblage and is very rare to rare in the Paleocene of the Sergipe-Alagoas and Pelotas basins (CP1 to CP7).

Distribution chart #: 90.

Superfamily RZEHAKINACEA Cushman, 1933
Family RZEHAKINIDAE Cushman, 1933

Genus *Rzehakina* Cushman, 1927
Type species: *Silicina epigone* Rzehak, 1895

Rzehakina epigona (Rzehak, 1895)
Plate II, fig. 1.

Silicina epigona Rzehak, 1895, 10, 213-230.

Rzehakina epigona (Rzehak, 1895) – Bolli et al. 1994, p. 71, figs. 19.7-8, Koutsoukos, 2000, p. 252, pl. 2, fig. 9, Kaminski & Gradstein, 2005, p. 72, figs. 31-32, Holbourn et al., 2013, p. 496, fig. 1.

Main features: Test agglutinated, planispiral, fusiform oval to sub-circular in outline, with two chambers per whorl. Median portion of the test slightly depressed, test wall very finely agglutinated with smooth surface. Aperture is a small oval opening, without a tooth.

Stratigraphic range: This species is common to abundant in almost all marginal basins, except for the Pelotas Basin, from the Maastrichtian through the upper Paleocene (NC23 to CP6). It is occasionally rare in middle Paleocene (CP3) samples of the Site 356.

Distribution chart #: 100.

Rzehakina inclusa (Grzybowski, 1901)

Plate II, fig. 2.

Spiroloculina inclusa Grzybowski, 1901, p. 260, pl. 8, fig. 20.

Rzehakina inclusa (Grzybowski, 1901) - Kaminski & Gradstein, 2005, p. 172, fig. 33, Holbourn et al., 2013, p. 500, fig. 1.

Main features: Test agglutinated, planispiral, biconvex, elliptical outline. The last two chambers cover the earlier whorls almost completely. Periphery acute to slightly rounded, aperture a slit at the end of a pronounced neck.

Remarks: Differs from *R. epigona* by its more biconvex and involute test, and by the fact that the later chambers cover the earlier ones completely.

Stratigraphic range: This species is very rare in the Sergipe-Alagoas Basin during the middle to upper Paleocene (CP5 to CP6).

Distribution chart #: 96.

Family HORMOSINIDAE Haeckel, 1894
Subfamily REOPHACINAE Cushman, 1910
Genus *Subreophax* Saidova, 1975
Type species: *Reophax aduncus* Brady, 1882

Subreophax scalaris (Grzybowski, 1896)

Plate II, fig. 3.

Reophax guttifera Brady var. *scalaria* Grzybowski, 1896, p. 277, pl. 8, fig. 26.

Subreophax scalaris (Grzybowski, 1896) – Bolli et al., 1994, p. 73, figs. 19. 28-29.

Subreophax scalaris (Grzybowski, 1896) – Kaminski & Gradstein, 2005, pl. 55, figs. 1-7.

Main features: Test agglutinated, uniserial, comprised of a series of globular chambers, which increase in size slowly as added. Chambers may be aligned rectilinearly or curved. Test wall finely to medium agglutinated, chambers usually compressed. Aperture is an opening in the last chamber, usually indistinct.

Stratigraphic range: This species is common and occurs from the Maastrichtian through the middle Paleocene (NC23 to CP4) and is rare in the upper Paleocene (CP8) in the Sergipe-Alagoas, Mucuri, Campos, and Santos basins.

Distribution chart #: 80.

Subfamily HORMOSININAE Haeckel, 1894

Genus *Hormosina* Brady, 1879

Type species: *Hormosina globulifera* Brady, 1879

Hormosina velascoensis (Cushman, 1926)

Plate II, fig. 4.

Nodosinella velascoensis Cushman (1926), p. 583, pl. 20, fig. 9.

Hormosina velascoensis (Cushman, 1926) – Kaminski & Gradstein, 2005, p. 243, pl. 44, figs. 1-8.

Main features: Test agglutinated, uniserial, usually up to 5 chambers, rarely more.

Chambers are cylindrical and slightly fusiform, and commonly compressed. Test wall finely to moderately agglutinated. Aperture a terminal opening in the last chamber.

Stratigraphic range: This species is very rare in the middle to upper Paleocene (CP5 to CP6) in the Sergipe-Alagoas and Santos basins.

Distribution chart #: 97.

Family HAPLOPHRAGMOIDIDAE Maync, 1952

Genus *Cribrostomoides* Cushman, 1910

Type species: *Cribrostomoides bradyi* Cushman, 1910

Cribrostomoides subglobosus (Cushman, 1910)

Plate II, figs. 5a-b.

Haplophragmoides subglobosum Cushman, 1910, p. 105, figs. 162-164.

Cribrostomoides subglobosus (Cushman, 1910) – Kaminski & Gradstein, 2005, pl. 92, figs. 1-3, Holbourn et al., 2013, p. 220, figs. 1-2.

Main features: Test agglutinated, coiling streptospiral becoming almost planispiral, globular in outline, involute, with broadly rounded periphery. Chambers increase rapidly in size, with 5 to 6 in the final whorl. Test wall coarsely agglutinated, aperture oval to slit-like, with a lip of fine, agglutinated grains. This species is easily recognized by its larger number of chambers than in other *Cribrostomoides* in the last planispiral whorl.

Remarks: Mostly specimens are flattened. Kaminski & Gradstein (2005) discussed the original description of *C. subglobosus* Cushman in detail, and described the syntype, since no holotype was designed. The syntype described by Cushman (1910) is missing. However, we examined some types of *Haplophragmoides subglobosum* Cushman from the Albatross expedition (no number) deposited at Smithsonian Institution.

Stratigraphic distribution: This species is common to abundant and occurs from the Maastrichtian through the upper Eocene (NC23 to CP15) in the Sergipe-Alagoas,

Campos, Santos and Pelotas basins, and is very abundant in the middle to upper Paleocene (CP5 to CP7) probably associated to the expansion of the flysch-type biofacies during this time.

Distribution chart #: 39.

Cribrostomoides trinitatensis Cushman & Jarvis, 1928
Plate II fig. 6.

Cribrostomoides trinitatensis Cushman & Jarvis, 1928, p. 91, pl. 12, figs. 12a-b.

Cribrostomoides trinitatensis Cushman & Jarvis, 1928 – Bolli et al. 1994, p.74, figs. 19-35, 41, Kaminski & Gradstein, 2005, pl.93, figs. 1-7.

Main features: Test agglutinated, planispiral coiling becoming streptospiral in large specimens, involute, globular in outline, 6 to 8½ chambers in the last whorl, distinct and slightly depressed sutures. Aperture an interior marginal slit at the base of the last chamber.

Remarks: The holotype (CC 4728) of *Cribrostomoides trinitatensis* Cushman & Jarvis is slightly compressed, but still has its characteristic features, circular and inflated test, high apertural face with diagnostic aperture. Kaminski & Gradstein (2005) reported that the original aperture as openings described by Cushman (1928) are actually grains of pyrite, which is not always very clear, forming a low slit-like aperture at the base of the last chamber. Some of the paratypes (CC 12607) are flattened, although it is possible to count the number of chambers (8-9) in the last whorl. We compared our specimens with the holotype and paratype and we agreed to assign them to *Cribrostomoides trinitatensis* Cushman & Jarvis.

Stratigraphic range: This species is common to very abundant from Maastrichtian through middle Eocene (NC23 to CP13) in the Sergipe-Alagoas, Mucuri, Campos, Santos, and Pelotas basins. At the Site 356 it is rare in the lower Paleocene (planktic foraminifera biozone P1c), and it is absent at Site 20C.

Distribution chart #: 62.

Genus *Haplophragmoides* Cushman, 1910
Type species: *Nonionina canariensis* d'Orbigny, 1839

Haplophragmoides eggeri Cushman, 1926
Plate III, figs. 1a-b.

Haplophragmoides eggeri Cushman, 1926, p. 583, pl. 15, figs. 1a-b.

Haplophragmoides eggeri Cushman, 1926 – Kaminski & Gradstein, 2005, p. 342, pl. 75, figs. 1-6.

Main features: Test moderately to coarsely agglutinated, planispiral, involute, slightly compressed with a depressed umbilicus and rounded periphery. Chambers added slowly, with 6 to 7 in the last whorl. Apertural face triangular, widest towards the base. Aperture an equatorial interior marginal slit, usually obscured by sediment filling.

Remarks: We compared our specimens with the holotype (CC 5134) of *Haplophragmoides eggeri* Cushman & plesiotypes (CC 15278, 46501) and agreed to assign them as *H. eggeri*. Differs from *H. stomatus* Grzybowski in its larger size, coarser agglutination, depressed umbilical area (Kaminski & Gradstein, 2005), and *H. horridus* has less chambers and more triangular chambers than *H. eggeri*.

Stratigraphic range: This species is common in two of the marginal basins: Campos and Santos in the lower to middle Paleocene (CP1 to CP5).

Distribution chart #: 110.

Haplophragmoides horridus Grzybowski, 1901
Plate III, figs. 12a-b.

Haplophragmium horridum Grzybowski, 1901, p. 54, pl. 7, fig. 12.

Haplophragmoides horridus Grzybowski, 1901 – Bolli et al., 1994, p.75, figs. 20.8-9, Kaminski & Gradstein, 2005, pl. 77, figs. 1-6.

Main features: Test moderately to coarsely agglutinated, planispiral, involute, and with 4½ triangular chambers in the last whorl. The last chamber is usually distinctly triangular, with straight and incised sutures. Aperture slit-like, at the inner edge of the last chamber.

Remarks: This species is distinguished by the coarsely agglutinated test and its large, triangular last chamber, comparing with other *Haplophragmoides* species. Kaminski & Gradstein (2005) consider *Haplophragmoides quadratus* Earland a junior synonym of *H. horridus*.

Stratigraphic range: This species is rare and its occurrence is restricted to the middle Paleocene (CP4 to CP5) of the Campos and Pelotas basins.

Distribution chart #: 103.

Haplophragmoides porrectus (Maslakova, 1955)
Plate III, figs. 3a-b.

Haplophragmoides porrectus Maslakova, 1955, p. 47, pl. 3, figs. 5-6.

Haplophragmoides porrectus Maslakova, 1955 – Bolli et al., 1994, p.76, figs. 20.15-16, Kaminski & Gradstein, 2005, pl. 79, figs. 1-6.

Main features: Test agglutinated, planispiral, rounded in outline, six triangular chambers in the last whorl. Wall usually formed by medium-size grains, aperture slit-like, located at the base of the last chamber.

Remarks: Bolli et al. (1994) reported that their *H. porrectus* specimens were usually compressed 5½ chambers in the last whorl. Kaminski & Gradstein (2005) notice that there are transitional forms between *H. porrectus* and *Recurvoidella lamella* Grzybowski emend. Charnock and Jones, which have 5½ chambers and those Paleocene specimens of *H. porrectus* have as many as 7 chambers in the last whorl. Differs from other *Haplophragmoides* by its rounded outline with inflated triangular chambers that increase rapidly in size, especially in the last whorl.

Stratigraphic range: This species is rare and is restricted to the middle Paleocene to lower Eocene (CP4 to CP12) of the Pelotas and Campos basins.

Distribution chart #: 65.

Haplophragmoides stomatus (Grzybowski, 1898)
emend Kaminski & Geroch, 1993
Plate III, figs. 4a-b.

Trochammina stomata Grzybowski, 1898, p. 290, pl. 11, fig. 26-27.

Haplophragmoides stomatus (Grzybowski, 1898) emend Kaminski & Geroch, 1993 – Kaminski & Gradstein, 2005, pl. 80, figs. 1-6.

Main features: Test planispiral, involute, circular in outline with rounded periphery and flat lateral sides. Triangular chambers 8 in the last whorl, increasing rapidly in size. The last chamber usually has high apertural face. Wall agglutinated often well silicified. Aperture an interiormarginal slit.

Remarks: According to Kaminski & Gradstein (2005) this species differs from *H. glabrus* and *H. horridus* in its finely agglutinated wall and from *H. walteri* in its thicker test, straight sutures and lack of a keel. Besides that, the inner chamber is easily seen when wet. This species differs from *H. suborbicularis* in its thicker and more robust test with fewer chambers.

Stratigraphic range: This species is rare to common and occurs from the middle Paleocene to the upper Eocene (CP4 to CP15) in the Sergipe-Alagoas, Campos and Pelotas basins.

Distribution chart #: 31.

Haplophragmoides suborbicularis (Grzybowski, 1896)
Emend. Kaminski & Geroch, 1993
Plate III, fig. 5.

Cyclammina suborbicularis Grzybowski, 1896, p. 284, pl. 9, figs. 5-6.

Haplophragmoides suborbicularis Grzybowski, 1896 – Kaminski & Gradstein, 2005, pl. 81, figs. 1-4.

Main features: Test moderately agglutinated, planispiral, with broadly rounded periphery, circular in outline, becoming more rhomboidal in outline in the later chambers, 5 to 7 chambers in the final whorl with flush or slightly depressed sutures. Apertural face low with an oval interiormarginal opening.

Remarks: This species differs from other *Haplophragmoides* by its broadly circular outline that becomes rhomboidal in the later chambers, more inflated than other species of this genus.

Stratigraphic range: This species is common to abundant and is restricted in the Santos Basin from the Maastrichtian to middle Paleocene (NC23 to CP5).

Distribution chart #: 111.

Haplophragmoides walteri (Grzybowski, 1898)
Plate III, fig. 6.

Trochammina walteri Grzybowski, 1898, p. 290, pl. 11, fig. 31.

Haplophragmoides walteri Grzybowski, 1898 – Kaminski & Gradstein, 2005, pl. 83, figs. 1-6, Holbourn et al., 2013, p. 292, figs. 1-2.

Main features: Test agglutinated, planispiral, involute, and circular in outline, with an acute periphery. Sutures incised, triangular chambers, 8 to 9 in the last whorl. Wall finely agglutinated and finely finished. Aperture an interior marginal slit.

Remarks: We examined holotype (USNM 627070) at the Smithsonian Institution and our specimens resemble them. This species differs from other *Haplophragmoides* by its very finely wall, and usually shows the inner structure when wet.

Stratigraphic range: This species is very rare to common and occurs from the lower Paleocene to the lower Eocene (CP1 to CP12) in the Sergipe-Alagoas, Campos and Pelotas basins.

Distribution chart #: 66.

Haplophragmoides sp.

Main features: Test agglutinated, planispiral, wall test variable but commonly coarsely agglutinated, aperture an equatorial slit.

Remarks: The specimens included here typically are poorly preserved, with flattened tests and do not show important morphological features.

Stratigraphic range: *Haplophragmoides* sp. is common to very abundant and occurs in all marginal basins as one of the main components of the flysch-type biofacies, from the Maastrichtian through the upper Eocene (NC23 to CP15). Its peak abundance (~ 28%) is in the lower to middle Paleocene (CP1 to CP5).

Distribution chart #: 42.

Superfamily HAPLOPHRAGMIACEA Eimer and Fickert, 1899
Family AMMOSPHAERIDINIDAE Cushman, 1927
Subfamily RECURVOIDINAE Alekseychik-Mitskevich, 1973

Genus *Budashevaella* Loeblich & Tappan, 1964
Type species: *Circus multicameratus* Voloshinova, 1961

Budashevaella multicamerata (Voloshinova, 1961)
Plate II figs. 7a-b.

Circus multicameratus Voloshinova, 1961, p. 201, pl. 7, figs. 6a-c, pl. 8, figs. 1a-c, 6a-c.

Budashevaella multicamerata (Voloshinova, 1961) – Kaminski & Gradstein, 2005, pl. 90, figs. 1-6.

Main features: Test moderately to coarsely agglutinated, coiling initially streptospiral, later planispiral, rounded periphery, with 2 to 2.5 whorls visible and 10 to 18 chambers visible in the last whorl. Chambers slightly inflated, sutures straight and incised in the planispiral part. The wall is thick, medium to finely agglutinated, commonly silicified. Aperture an interiomarginal slit, usually indistinct. This species is easily recognized by the large number of chambers on the last planispiral whorl.

Remarks: Mostly specimens are flattened as a preservation feature.

Stratigraphic distribution: This species is very rare to common and occurs in all five marginal basins from the lower through upper Paleocene (CP3 to CP8).

Distribution chart #: 75.

Genus *Recurvoides* Earland, 1934

Type species: *Recurvoides contortus* Earland, 1934

Recurvoides anormis Mjatluk, 1970

Plate III, fig. 7.

Recurvoides anormis Mjatluk, 1970, p. 84, pl. 18, fig. 4, pl. 19, figs. 1-4.

Recurvoides anormis Mjatluk, 1970 – Kaminski & Gradstein, 2005, pl. 95, figs. 1-6.

Main features: Test agglutinated, thick and partially involute, coiling streptospiral, with broadly rounded periphery. Chambers 6 to 7 in the final whorl with straight sutures. Aperture as an oval opening commonly surrounded by lip.

Remarks: Kaminski & Gradstein (2005) commented that *R. anormis* differs from other Late Cretaceous-Paleogene *Recurvoides* in having a subspherical, subplanispiral, robust test with relatively few chambers (around 5), features easily seen in our specimens.

Stratigraphic range: This species is rare in the Sergipe-Alagoas Basin and abundant in the Campos Basin, from the lower Paleocene through upper Eocene (CP1 to CP14).

Distribution chart #: 58.

Recurvoides azuaensis Bermudez, 1949

Plate III, figs. 8a-b.

Recurvoides azuaensis Bermudez, 1949, p. 49, pl. 1, fig. 35.

Recurvoides azuaensis Bermudez, 1949 – Sender et al. 2008, p. 126, pl. 10, figs. 2-3.

Main features: Test coarsely agglutinated, streptospirally enrolled, biconvex, slightly compressed, periphery rounded and slightly lobulate. Dorsal side broadly convex and ventral side excavated. Umbilical region covered by the last chamber, 4 chambers in the last whorl. Test wall thick, strongly silicified, aperture indistinct at the base of the last chamber.

Remarks: We compared our specimens with the holotype and paratypes (CC 62834/35) at the Smithsonian Institution, and we agreed to assign them as *R. azuaensis*. Differs from others by its coarsely agglutinated wall and a thick border in the last chamber as a preservation feature.

Stratigraphic range: This species is rare and is restricted to the upper Eocene (nannofossil biozone CP15) of the Campos Basin.

Distribution chart #: 5.

Recurvoides nucleolus (Grzybowski, 1898)
emend Samuel, 1977

Trochammina nucleolus Grzybowski, 1898, p. 265, pl. 11, fig. 4a-d.

Recurvoides nucleolus (Grzybowski, 1898) emend Samuel, 1977 – Kaminski & Gradstein, p. 408, 2005, pl. 97, figs.1-2.

Main features: Test agglutinated, inflated, planoconvex, circular in outline, streptospiral coiling without abrupt changes of direction followed by a planispiral or low trochospiral whorl with 7 to 9 chambers. The chamber lumina can be observed when the specimen is wetted, and appear to be sac-shaped connected by a thin tube. Wall thick, medium to finely agglutinated, surface smooth to somewhat rough. Apertural face high and narrow, aperture as a small, area slit.

Remarks: Differs from other *Recurvoides* by its nearly planispiral last whorl with 3 or 4 chambers streptospirally coiled in the central region, and the sac-shaped lumina observed when wet.

Stratigraphic range: This species is rare in the Maastrichtian through the lower Paleocene (NC23 to CP1) of the Segipe-Alagoas Basin.

Distribution chart #: 114.

Recurvoides walteri (Grzybowski, 1898)
emend. Mjatluk, 1970

Haplophragmium walteri Grzybowski, 1898, p. 280, pl. 10, fig. 24.

Recurvoides walteri (Grzybowski, 1898) emend. Mjatluk, 1970 – Kaminski & Gradstein, 2005, p. 415, pl. 100, figs. 1-3.

Main features: Test agglutinated, rounded in outline, streptospiral coiling with the direction of coiling changing gradually, 8 to 11 chambers visible in the last whorl increasing slowly in size. Wall thick, medium to coarsely agglutinated, aperture as a small round opening at the base of the last chamber.

Remarks: Chambers lumina best visible when specimens are immersed in water. Test frequently flattened. Differs from others *Haplophragmoides* by its thick and coarsely agglutinated wall, later chambers broader than high, and chambers lumina.

Stratigraphic range: This species is rare in the middle Paleocene (CP3 to CP5) of the Pelotas, Campos and Santos basins.

Distribution chart #: 105.

Recurvoides sp.

Recurvoides contortus Earland, 1934, p. 91.

Main features: Agglutinated test, streptospirally enrolled, later whorls may tend to be trochospiral to planispiral, or show an abrupt change in plane of coiling by 90° from previous whorls, earliest chambers not visible externally from either side (Kaminski & Gradstein, 2005).

Remarks: The typically flattened tests due to preservation make it impossible to assign a species name.

Stratigraphic range: This taxon is common to abundant and occurs in all of the marginal basins from the Maastrichtian through the middle Eocene (NC23 to CP14), but the highest abundances (~40% of benthics) occur in the middle Paleocene to lower Eocene (CP5 to CP8).

Distribution chart #: 40.

Family CYCLAMMINIDAE Marie, 1941

Subfamily ALVEOLOPHRAGMIINAE Saidova, 1981

Genus *Reticulophragmium* Maync, 1955

Type species: *Alveolophragmium venezuelanum* Maync, 1952

Reticulophragmium acutidorsatum (Hantken, 1868)

Plate IV, figs. 1a-b.

Haplophragmium acutidorsatum Hantken, 1868, p. 82, pl. 1, fig. 1a-b.

Reticulophragmium acutidorsatum (Hantken, 1868) – Kaminski & Gradstein, 2005, pl. 122, figs. 1-7.

Main features: Test finely agglutinated, planispirally coiled, involute, circular outline with a broad depressed umbilicus, 8 to 14 chambers in the outer whorl. Sutures straight or slightly sinuous and depressed, periphery acute to subacute. Aperture a broad interiormarginal slit.

Remarks: Kaminski & Gradstein (2005) describe *R. acutidorsatum* Hantken with coarse grains in the apertural face, and occasionally small pores between the grains, which were not classify as supplementary apertures, therefore they did not place *Cyclammina placenta* in the synonymy. Differs from *Cyclammina* on not having supplementary apertures, thinner in profile and more evolute, and from other *Reticulophragmium* by its internal structural when wet, broad and depressed umbilicus. We compared our specimens with some types (CC 56975) of *H. acutidorsatum* Hantken in the Cushman Collection at the Smithsonian Institution, and agreed to assign our specimens in this species.

Stratigraphic range: In our samples, this species is very rare to rare and occurs from the upper Paleocene through the upper Eocene (CP6 to CP14) in all marginal basins.

Distribution chart #: 53.

Reticulophragmium amplexens (Grzybowski, 1898)
Plate IV, fig. 2.

Cyclammina amplexens Grzybowski, 1898, p. 292, pl. 12, figs. 1-3.

Reticulophragmium amplexens (Grzybowski, 1898) – Kaminski & Gradstein, 2005, p. 491, pl.123, figs.1-6, Holbourn et al., 2013, p. 486, figs. 1-2.

Main features: Test agglutinated, planispirally coiled, involute test, disk-shaped in lateral view, shallowly depressed umbilicus. Chambers 12 to 17 in the last whorl, initial chambers triangular and commonly without alveoles, which are well-developed in later chambers. The alveoles are simple, unbranched, sutures straight sometimes curved in the early whorls and slightly depressed in later whorls. Aperture as interiomarginal slit with a thin lip. Wall finely agglutinated, with much cement. Specimens with test not strongly silicified may contain occasional large grains in a matrix of fine grains.

Remarks: Kaminski & Gradstein (2005) assigned this species to the genus *Reticulophragmium* based on the presence of an interiomarginal aperture. They also reported variations in the amount and position of the alveoles, which in general appear along the sutures in early chambers and then spread to the chamber lumen. We compared our specimens with some cotypes of Smithsonian Institution (USNM 627071) and decided to assign them to *Reticulophragmium amplexens* Grzybowski. We observed a wide variability of number of chambers (10-15) in the last whorl, and Kaminski and Geroch (1993) observed two distinct megalospheric and megalospheric forms that have 10-13 and 12-17 chambers in the last whorl, respectively.

Stratigraphic range: This species is very rare to rare and occurs in the Eocene interval (CP8 to CP13) in the Pelotas Basin.

Distribution chart #: 60.

Reticulophragmium garcilassoi (Frizzell, 1943)
Plate IV, figs. 3a-b.

Cyclammina garcilassoi Frizzell, 1943, p. 338, pl. 55, fig. 11.

Reticulophragmium garcilassoi (Frizzell, 1943) – Kaminski & Gradstein, 2005, pl. 124, figs. 1-6.

Main features: Test agglutinated, lenticular in shape, circular to lobate outline, planispirally coiled with subacute peripheral margin. Last whorl with 10 to 16 chambers, sinuous and slightly depressed sutures, umbilicus depressed. Chamber interior with small and evenly distributed alveoles, usually simple but occasionally branched. Test wall thick, finely agglutinated, well-cemented, smoothly finished surface, aperture as a low broad slit at the base of the last chamber.

Remarks: We examined the holotype (CC 39550) of *Cyclammina garcilassoi* Frizzell and other hypotypes (CC 47873, 47869, 47870) from the Santa Anita Formation (Venezuela) confirmed by Kaminski & Gradstein (2005) as true forms of *R. garcilassoi* Frizzell (see detailed discussion in Kaminski & Gradstein, 2005). Our specimens have 15 chambers in the last whorl, alveoles are small and completely filling the chamber as on

the typical *R. garcilassoi* Frizzel. The types examined are from the Cushman Collection at Smithsonian Institution.

Stratigraphic range: This species is very rare and occur in the middle to upper Paleocene (CP5 to CP6) of the Sergipe-Alagoas Basin.

Distribution chart #: 98.

Reticulophragmium rotundidorsatum (Hantken, 1875)

Plate IV, figs. 4a-b.

Haplophragmium rotundidorsatum Hantken, 1875, p. 12, pl. 1, fig. 2.

Reticulophragmium rotundidorsatum (Hantken, 1875) – Kaminski & Gradstein, 2005, pl. 127, figs. 1-5.

Main features: Test agglutinated, planispirally coiled, broadly rounded periphery, involute, with 7 to 9 chambers in the last whorl, alveoles evenly distributed throughout the interior of the chamber. Wall finely agglutinated, thick with a shallow depressed umbilicus, aperture an interiormarginal slit, but larger specimens may have supplementary areal pores (not always visible).

Remarks: Differs from other *Reticulophragmium* species by its rounded outline, relatively shallower umbilicus, and internal chamber structures (alveoles) visible when wet.

Stratigraphic range: This species is rare to abundant and occurs from the lower Paleocene through the lower Eocene (CP1 to CP8) of the Sergipe-Alagoas and Campos basins.

Distribution chart #: 77.

Genus *Reticulophragmoides* Gradstein & Kaminski, 1989

Type species: *Nonion jarvisi* Thalmann, 1932

Reticulophragmoides jarvisi (Thalmann, 1932)

Plate IV, fig. 5.

Nonion cretaceum Cushman & Jarvis (1932) was a previously occupied name and therefore invalid, and the species was renamed *Nonion jarvisi* by Thalmann (1932).

Reticulophragmoides jarvisi (Thalmann, 1932) emend. Gradstein & Kaminski, 1989 – Gradstein & Kaminski, 1989, p. 81, pl. 7, figs. 1a-8, text-fig. 4, Kaminski & Gradstein, 2005, pl.128, figs.1-8.

Main features: Test agglutinated, planispiral, biconvex and thickest near the umbilicus. Acute periphery, circular to slightly lobate in outline, 6 to 9 chambers in the last whorl. Sutures slightly depressed, slightly sinuous or curved and strongly limbate. The umbilical region is depressed. Chambers are typically simple but later chambers sometimes develop simple alveolar structure. Test wall finely agglutinated and well cemented, aperture is *Haplophragmoides*-like interiormarginal slit without a lip or supplementary pores.

Remarks: We compared our specimens with the holotype of *Nonion cretaceum* (CC 15327) Cushman & Jarvis (1932) and decided to assign them as *Reticulophragmoides jarvisi*. Differs from other *Reticulophragmoides* by its thicker and limbate sutures around the well-developed boss in the umbilical region, simple alveolar structure and finely agglutinated test wall.

Stratigraphic range: This species is rare in the Paleocene (CP1 to CP6) of the Sergipe-Alagoas and Campos basins.

Distribution chart #: 99.

Subfamily CYCLAMMININAE Marie, 1941

Genus *Cyclammina* Brady, 1879

Type species: *Cyclammina cancellata* Brady, 1879

Cyclammina placenta (Reuss, 1851)

Plate IV, figs. 6a-b.

Nonionina placenta Reuss, 1851, p. 72, pl. 5, figs. 33a-b.

Cyclammina placenta (Reuss, 1851) – Kaminski & Gradstein, 2005, pl. 119, figs. 1-10.

Main features: Test agglutinated, robust, almost circular in outline, planispiral and involute with rounded periphery. The umbilicus is usually depressed, especially in large specimens, with 8 to 13 chambers in the last whorl. Aperture as an interiormarginal slit. *Remarks:* Kaminski & Gradstein (2005) describe a morphological progressive evolution of *C. placenta* through time, with lower Eocene specimens small, relatively thin, with evenly distributed alveoles, straight sutures, flat apertural face and lack of supplementary apertures but with an interiormarginal aperture. Specimens from the lower middle Eocene are somewhat larger and thicker, with one or two areal openings. The middle to upper Eocene specimens have larger grains and more numerous pores in the apertural face, the areal openings develop distinct lips. Meanwhile, they become larger, and the number of chambers increased (10 to 13), as does the sinuosity of sutures and corresponding growing of curvature of the apertural face.

Remarks: The species *C. cancellata* Brady (CC 24789) is larger, thicker, has more chambers and has a more broadly rounded periphery than *C. placenta* Reuss. Kaminski & Gradstein (2005) consider that there are transitional forms between the species, especially in Oligocene and Miocene populations, and *C. placenta* may be the ancestral form, evolving into *C. cancellata* during the Eocene, although we do not observed this trend among our specimens.

Stratigraphic range: This species is common in the middle Paleocene (CP5) of the Pelotas Basin and in the Eocene (CP8 to CP15) of the Campos and Sergipe-Alagoas basins.

Distribution chart #: 25.

Family SPIROPLECTAMMINIDAE Cushman, 1927
Subfamily SPIROPLECTAMMININAE Cushman, 1927
Genus *Spiroplectammina* Cushman, 1927

Type species: *Textularia agglutinans* d'Orbigny var. *biformis* Parker & Jones, 1865

Spiroplectammina jarvisi Cushman, 1939
Plate IV, figs. 7a-b.

Spiroplectammina jarvisi Cushman, 1939, p. 90, pl. 16, fig. 1.

Quasispiroplectammina jarvisi (Cushman, 1939) – Bolli et al., 1994, p. 83, fig. 21.1-2.

Main features: Test agglutinated, about twice as long as broad, much compressed, periphery acute. Tapering earliest portion is planispiral, then biserial with distinct sutures, slightly depressed, straight. Test wall, finely arenaceous, smoothly finished, aperture a low arch at the base of the last chamber.

Remarks: The specimens designated as holotype (CC 15283) of *Spiroplectammina jarvisi* Cushman is somewhat compressed, but its characteristics can be seen. Microspheric and megalospheric forms are represented on Plate IV, figures 7a and 7b, respectively. Differs from *Quasispiroplectammina* in having more depressed sutures, and from other *Spiroplectammina* by having straighter sutures and nearly parallel sides without any spinose projections.

Stratigraphic range: This species is rare to very abundant in the middle Paleocene to the lower Eocene (CP5 to CP10) of the Santos Basin.

Distribution chart #: 67.

Spiroplectammina navarroana Cushman, 1932
emend. Gradstein & Kaminski, 1989
Plate IV, fig. 8.

Spiroplectammina navarroana Cushman, 1932, p. 96, pl. 11, fig. 14.

Spiroplectammina navarroana Cushman, 1932 emend. Gradstein & Kaminski, 1989, p. 83, pl. 9, figs. 1a-12, text-figure 5, Kaminski & Gradstein, 2005, pl. 103, figs. 1-13.

Main features: Test agglutinated, elongated, tapered and arched, initially planispiral, later biserial with rounded periphery. The later chambers may be somewhat more inflated than earlier ones. Test wall medium-coarse to finely agglutinated, aperture an interiomarginal arch.

Remarks: The holotype in the Cushman Collection although is not very well preserved (CC 26887), the paratype (371545) is also broken. However, we were able to compare them with our specimens and we are confident to assign them as *Spiroplectammina navarroana*. Differs from other species by its more inflated chambers, especially the last ones. Frequently found broken as part of the flysch-type assemblage.

Stratigraphic range: This species is abundant to very abundant in the middle Paleocene through the middle Eocene (CP5 to CP14), with highest abundances (~ 30%) in the upper

Paleocene (CP6 to CP7) of the Sergipe-Alagoas Basin, it is very rare in the Campos Basin.

Distribution chart #: 54.

Spiroplectamina spectabilis (Grzybowski, 1898)
emend. Kaminski, 1984

Spiroplecta spectabilis Grzybowski, 1898, p. 293, pl. 12, fig. 12.

Spiroplectamina spectabilis (Grzybowski, 1898) – Kaminski 1984, p. 29, pls. 12-13.

Spiroplectamina spectabilis (Grzybowski, 1898) emend. Kaminski, 1984 – Kaminski & Gradstein, 2005, p. 429 pl. 104, figs. 1-6, Holbourn et al., 2013, p. 522, figs. 1-3.

Main features: Test agglutinated, initially planispiral, later biserial. Peripheral margin acute, sometimes dentate. Sutures flush or slightly depressed, inclined approximately 60° to the central axis. Aperture as a narrow slit.

Remarks: Kaminski & Gradstein (2005) reported that in megalospheric forms, the planispiral portion consists of 4 to 7 chambers, and may be wider than the subsequent biserial portion, and the planispiral portion of microspheric forms is minute in comparison, and may also be wider than the biserial part. Also, chambers in the biserial part are low and numerous, as many as 36 biserial chambers have been observed in microspheric individuals. Megalospheric forms are rare to find among our specimens, however both megalospheric and microspheric forms have numerous chambers in the biserial part.

Stratigraphic range: This species is common to abundant in the Campos, Mucuri and Sergipe-Alagoas basins and rare at Sites 20C and 356, from the lower Paleocene to middle Eocene (CP1 to CP14). Khunt et al. (1998) and Kaminski and Gradstein (2005) reported an acme zone of *Spiroplectamina spectabilis* for the lower Paleocene (Danian) on the Atlantic and western Tethys, but this event was not observed among our samples.

Distribution chart #: 57.

Family TROCHAMMINIDAE Schwager, 1877
Subfamily TROCHAMMININAE Schwager, 1877
Genus *Ammoglobigerina* Eimer and Fickert, 1899
Type species: *Ammoglobigerina bulloides* Eimer and Fickert, 1899

Ammoglobigerina globigeriniformis (Parker & Jones, 1865)
Plate IV figs. 10a-b

Lituola nautiloidea Lamarck var. *globigeriniformis* Parker & Jones, 1865, p. 302, pl. 6, fig. 22.

Haplophragmium globigeriniforme (Parker, Jones & Brady), 1884, p. 312, pl. 35, figs. 10-11.

Ammoglobigerina bulloides Eimer and Fickert 1899, p.704.

Ammoglobigerina globigeriniformis (Cushman & Renz) – Bolli et al. (1994), p. 14, fig. 22.24-25.

Main features: Test agglutinated, trochospiral, globular chambers, 3 to 4 chambers visible on the involute side. Moderately to coarsely agglutinated wall, aperture an interiomarginal slit, not visible in all specimens due to sediment filling.

Stratigraphic distribution: This species is rare in the lower to middle Eocene of the Pelotas Basin (CP12), but it is rare to frequent in the Campos, Mucuri and Santos basins, from the Maastrichtian through the middle Eocene (NC23 to CP14).

Distribution chart #: 59.

Genus *Trochamminopsis* Brönnimann, 1976

Type species: *Trochammina pusilla* Höeglund, 1947

Trochamminopsis altiformis (Cushman & Renz, 1946)

Plate IV, fig. 9.

Trochammina globigeriniformis var. *altiformis* Cushman & Renz, 1946, p. 24, pl. 3, fig. 7-11.

Trochamminopsis altiformis (Cushman & Renz, 1946) – Kaminski & Gradstein, 2005, p. 458, pl. 112, figs. 1-3.

Main features: Globigerina-like coiling of the agglutinated test with a high spire, typically 4 chambers in the last whorl (adult form) and closed umbilical area. Test wall moderately to coarsely agglutinated, aperture umbilical, small, usually indistinct.

Remarks: We compared our specimens with the paratypes (CC 46565, 46566) in the Cushman Collection at Smithsonian Institution and agreed to assign them as *T. altiformis*.

Stratigraphic Range: This species is rare in the Pelotas and Santos basins, but relatively frequent in the middle to upper Paleocene (CP5 to CP7) in the Campos Basin.

Distribution chart #: 86.

Family VERNEUILINIDAE Suleymanov, 1973

Subfamily VERNEUILINOIDINAE Suleymanov, 1973

Genus *Eggerellina* Marie, 1941

Type species: *Bulimina brevis* d'Orbigny, 1840

Eggerellina brevis (d'Orbigny, 1840)

Bulimina brevis d'Orbigny, 1840, p. 41, pl. 4, figs. 12-13.

Main features: Test agglutinated, conical or ovoid in shape, triserial throughout, with inflated and subglobular chambers, rapidly increasing in size, sutures incised. Wall agglutinated non-caliculate smoothly finished. Aperture as a narrow hook-like slit extending up the apertural face.

Remarks: The characteristic feature of this species is the triserial arrangement of the chambers and the inflated final chambers that occupy about 4/5 the length of the test.

Stratigraphic range: This species is rare in the Maastrichtian through the lower Paleocene (NC23 to CP1) of the Pelotas and Santos basins.

Distribution chart #: 116.

Family VERNEUILINIDAE Cushman, 1911
Subfamily VERNEUILININAE Cushman, 1911
Genus *Gaudryina* d'Orbigny, 1839
Type species: *Gaudryina rugosa* 1840

Gaudryina expansa Israelsky, 1951
Plate V, Fig. 1.

Gaudryina (Gaudryina) expansa Israelsky, 1951, p. 16, pl. 5, figs. 21-24.

Gaudryina expansa Israelsky, 1951 – Bolli et al., 1994, p. 89, figs. 23.27-28.

Main features: Test moderate to coarsely agglutinated, early stage triserial and commonly pyramidal, later portion biserial, rounded margins, later sutures slightly depressed. Aperture in notch on the base of the last chamber, wall texture smoother on the apertural face than other parts of the chamber.

Remarks: We examined the holotype (USNM 560530) deposited in the Cushman Collection at the Smithsonian Institution and we agreed to assign them as *G. expansa*. Differs from other *Gaudryina* by its pyramidal shape and relatively inflated last chambers.

Stratigraphic range: This species is rare and occurs only in the Maastrichtian (NC23) of the Sergipe-Alagoas Basin.

Distribution chart #: 120.

Gaudryina frankei Brotzen, 1936
Plate V, fig. 2.

Gaudryina frankei Brotzen, 1936, p. 33, pl. 1, fig. 7.

Gaudryina frankei Brotzen, 1936 – Bolli et al., 1994, p. 89, figs. 23.29-30.

Main features: Test agglutinated, generally v-shaped, cuneiform, with early portion triserial (pyramidal) expanding to biserial portion, the pyramid part is long and the chambers high almost square shape in cross-section. Aperture semicircular to circular always connected with the basal suture.

Remarks: Bolli et al. (1994) reported some variability in shape between sub-angular and sub-rounded in the early triserial part, and our specimens are more sub-rounded. Differs from other *Gaudryina* by its very pronounced inflated chambers, especially the last ones, and incised sutures.

Stratigraphic range: This species is very rare and occurs only in the Maastrichtian of the Sergipe-Alagoas Basin (NC23).

Distribution chart #: 117.

Gaudryina inflata Israelsky, 1951
Plate V, fig. 3.

Gaudryina (Gaudryina) inflata Israelsky, 1951, p. 16, pl. 6, figs. 1-12.
Gaudryina sp. aff. *G. inflata* Israelsky, 1951, p. 89, figs. 23.31-32.

Main features: Test moderate to finely agglutinated, early triserial portion transforming to biserial expanding gradually to the final two chambers, which are strongly inflated and expanded. The inflated and enlarged last chambers are the characteristic features of this species. Test wall fairly smoothly cemented medium-grained sand. Aperture an elongate slit reentrant and lying between the final and penultimate chambers.

Remarks: We compared our specimens with the paratypes (USNM 560531, 560533) of *G. inflata* Israelsky and they are very similar. Differs from other species by its strongly inflated last chambers, especially the last two, increasing rapidly in size.

Stratigraphic range: This species is rare and occurs only in the Maastrichtian of the Sergipe-Alagoas Basin (NC23).

Distribution chart #: 118.

Gaudryina ingens Voloshinova, 1972
Plate V, fig. 4.

Gaudryina ingens Voloshinova, 1972, p. 55, pl. 1, fig. 1.
Gaudryina ingens Voloshinova, 1972 – Bolli et al., 1994, p. 89, figs. 23.33-34.

Main features: Test agglutinated, with the triserial part takes 1/3 to 1/2 of the total test, rectangular-shaped chambers arranged obtusely to each other. Test wall coarsely arenaceous, slightly rough and commonly covered with striae. Aperture slit-like located between the last and penultimate chambers.

Remarks: This species has a distinctly broader test and quadrangular outline than other *Gaudryina* species.

Stratigraphic range: This species is rare and occurs in the Maastrichtian (NC23) of the Santos Basin.

Distribution chart #: 119.

Gaudryina laevigata Franke, 1914
Plate V, fig. 5.

Gaudryina laevigata Franke, 1914, p. 431, pl. 27, figs. 1-2.
Gaudryina laevigata Franke, 1914 - Bolli et al., 1994, p. 89, figs. 23.35-37.

Main features: Test agglutinated, v-shaped, cuneiform, short triserial early portion transforming to biserial expanding to the final chambers. Chambers is rounded rectangular in cross-section. Test wall moderate to finely agglutinated, aperture a low arch the inner margin of chamber face.

Remarks: We examined some paratypes (CC 19573, 47897) of *G. laevigata* Franke from the Cushman Collection at the Smithsonian Institution, and our specimens are similar to *G. laevigata*. Differs from other *Gaudryina* by its v-shaped test and rounded rectangular chambers in cross-section.

Stratigraphic range: This species is rare to common in the Maastrichtian through early Eocene (NC23 to CP10) of the Pelotas and Santos basins. *G. laevigata* is very rare to common in the Campos and Sergipe-Alagoas basins and at Site 20C from the Maastrichtian through the upper Eocene (NC23 to CP15).

Distribution chart #: 45.

Gaudryina pyramidata Cushman, 1926

Plate V, fig.6.

Gaudryina laevigata Franke var. *pyramidata* Cushman, 1926, p. 587, pl. 16, fig. 8.

Gaudryina pyramidata Cushman, 1926 – Tjalsma & Lohmann, 1983, pl. 8, figs. 1a-1b, Bolli et al., 1994, p. 90, figs. 24.4-6, Alegret & Thomas, 2001, p. 285, pl. 6 fig. 4.

Main features: Test agglutinated, pyramidal in shape, stout, with acute periphery. Test triangular in cross-section in the early stages, becoming more sub-rectangular in its later stages. Depressed sutures, aperture a low interior marginal opening.

Remarks: The holotype is missing from the Cushman Collection at Smithsonian Institution. Bolli et al. (1994) reported a significant difference in size among specimens from Trinidad, where the larger ones have relatively few biserial chambers and in the smaller ones the biserial part is often better developed. We also observed some of these features in our specimens of *G. pyramidata*. *G. pyramidata* is a very distinctive species of *Gaudryina*, with small test and acute periphery.

Stratigraphic range: This species is rare to frequent in the Pelotas, Campos, Mucuri and Sergipe-Alagoas basins, and at Sites 356 and 20C from the Maastrichtian through the upper Eocene (NC23 to CP15).

Distribution chart #: 46.

Family EGGERELLIDAE Cushman, 1937

Subfamily DOROTHIINAE Balakhmatova, 1972

Genus *Marssonella* Cushman, 1933

Type species: *Gaudryina oxycona* Reuss, 1860

Marssonella trochoides (Marsson, 1878)

Plate V, fig.7.

Gaudryina crassa Marsson var. *trochoides* Marsson, 1878, p. 158, pl. 3, fig. 27.

Marssonella trochoides (Marsson, 1878) – Bolli et al., 1994, p. 94, fig. 25.7.

Main features: Test agglutinated, early stage trochospirally enrolled, later biserial, chambers increasing very slowly in size so that has nearly parallel sides, circular in

section. Test wall finely agglutinated and canaliculated (not easily visible, unless wet). Aperture an interiomarginal slit in a slight reentrance on the final chamber face.
Stratigraphic range: This species is abundant to very abundant and occurs only in the Maastrichtian through the lower Paleocene of the Pelotas Basin (NC23 to CP1).
Distribution chart #: 115.

Subfamily EGGERELLINAE Cushman, 1937
Genus *Karreriella* Cushman, 1933
Type species: *Gaudryina siphonella* Reuss, 1851

Karreriella cubensis Cushman & Bermudez, 1937
Plate V, fig. 8.

Karreriella cubensis Cushman & Bermudez, 1937, p. 4, pl. 1, figs. 4a-b.
Karreriella cf. *cubensis* Cushman & Bermudez, 1937 – Tjalsma & Lohmann, 1983, p. 33, pl. 9, figs. 4a-b.

Main features: Test agglutinated, almost entirely biserial, longer than broad, compressed, periphery in early stage subacute, later rounded. Sutures distinct, depressed and strongly oblique. Test wall finely arenaceous with much cement, smoothly finished, aperture an elongate opening bordered by a raised lip, at the base of the apertural face.
Remarks: Tjalsma & Lohmann (1983) reported that their specimens are, in general, more compressed and more strongly tapering, with also more inflated chambers, which we did not commonly see in our specimens. We examined the holotype (CC 23359) and paratype (CC 23360) of *Karreriella cubensis* Cushman & Bermudez in the Cushman Collection and our specimens are similar. Differs from *K. subglabra* by its shortest biserial test and faster growing of the chambers, last two chambers more inflated.
Stratigraphic range: This species is very rare and occurs only in the lower Eocene through the middle Eocene of Site 20C (CP8 to CP13).
Distribution chart #: 61.

Karreriella subglabra (Gümbel, 1868)
Plate V, fig. 11.

Gaudryina subglabra Gümbel, 1868, p. 602, pl. 1, figs. 4a-b.
Karreriella subglabra (Gümbel, 1868) – Tjalsma & Lohmann, 1983, p.34, pl.9, figs. 1a-b.
Main features: Test agglutinated, elongated, early trochospiral, later biserial. Test wall finely agglutinated, smoothly finished, aperture rounded, in terminal face of final chamber, bordered by lip or produced on a distinct neck.
Remarks: Differs from *K. cubensis* by its longest biserial part, depressed sutures forming zig-zag curve in front view.
Stratigraphic range: This species is rare to common and occurs only in the lower to middle Eocene of at Site 356 (CP10 to CP14).
Distribution chart #: 51.

Family PSEUDOGAUDRYINIDAE Loeblich & Tappan, 1985
Subfamily PSEUDOGAUDRYININAE Loeblich & Tappan, 1985
Genus *Clavulinoides* Cushman, 1936
Type species: *Clavulina trilatera* Cushman, 1936

Clavulinoides trilaterus (Cushman, 1926)
Plate V, fig. 10.

Clavulina trilatera Cushman, 1936, p. 588, pl. 17, fig. 2.

Clavulinoides trilaterus (Cushman, 1926) – Bolli et al. 1994, p. 96, figs. 25.21; Alegret & Thomas (2001), p. 283, pl. 5, figs. 6-8.

Main features: Test moderate to coarsely agglutinated, initially triserial, later arranged uniserial, triangular cross section, rounded periphery with circular terminal aperture.

Remarks: We compared our specimens with the holotype (CC 5155) of *Clavulinoides trilatera* Cushman at Smithsonian Institution and our specimens are very similar to the holotype. Alegret & Thomas (2001) described a juvenile form of *C. trilaterus* consisting of the early stages of the species, before the development of uniserial chambers, and are always associated to adult species. We do not recognized juvenile species among our specimens, possibly due to the low occurrence of this taxon.

Stratigraphic distribution: This species is very rare in the Paleocene (CP3 to CP7) of the Mucuri and Sergipe-Alagoas basins.

Distribution chart #: 94.

Genus *Pseudoclavulina* Cushman, 1936
Type species: *Gaudryina medwayensis* Parr, 1935

Pseudoclavulina chitinosa (Cushman & Jarvis, 1932)
Plate V, fig. 9.

Clavulina chitinosa Cushman & Jarvis, 1932, p. 20, pl. 5, figs. 9-11.

Pseudoclavulina chitinosa (Cushman & Jarvis, 1932) - Bolli et al. 1994, p. 97, fig. 25.28.

Main features: Test agglutinated, slender, early portion triserial with indistinct chambers becoming uniserial. Test wall finely agglutinated and smoothly finished (possibly to the organic cement reported by Kaminski & Gradstein (2005)), terminal aperture.

Remarks: Cushman & Jarvis (1932) described this deep-water species with a wall becoming almost entirely pure chitin (organic cement). Usually our specimens are much distorted because of the test composition and preservation.

Stratigraphic range: This species is abundant to very abundant in the lower Paleocene (CP1) of the Pelotas Basin.

Distribution chart #: 113.

Pseudoclavulina trinitatensis Cushman & Renz, 1948

Pseudoclavulina trinitatensis Cushman & Renz, 1948, p. 13, pl. 3, fig. 5.

Pseudoclavulina trinitatensis Cushman & Renz, 1948 - Bolli et al., 1994, p. 97, fig. 25.29, p. 330, fig. 65.13, 52.

Main features: Test agglutinated, elongate, and slender, with early portion triserial, later uniserial, circular in cross section. Wall finely agglutinated and strongly cemented, surface roughened, aperture terminal.

Remarks: We compared our specimens with the holotype (CC 57064) and paratypes (57065) of *Pseudoclavulina trinitatensis* Cushman & Renz and concluded we can assign them to this species.

Stratigraphic range: This species is very rare in the upper Eocene of the Pelotas Basin.

Distribution chart #: 4.

Order ROTALIINA Delage & Hérouard, 1896
Superfamily BOLIVINACEA Glaessner, 1937
Family BOLIVINIDAE Glaessner, 1937
Genus *Bolivina* d'Orbigny, 1839
Type species: *Bolivina plicata* d'Orbigny, 1839

Bolivina huneri Howe, 1939

Plate VI, fig. 1.

Bolivina huneri Howe, 1939, p. 66, pl. 9, figs. 3-4.

Bolivina huneri Howe, 1939 – Tjalsma & Lohmann, 1983, p. 23, pl. 11, figs. 5a-b, Holbourn et al., 2013, p. 68, figs. 1-3.

Main features: Test calcareous, biserial, elongate slightly compressed, with sides nearly parallel, chambers and sutures indistinct due to the surface ornamentation, wall ornamented with numerous, delicate, irregularly anastomosing costae, finely perforate, aperture as a slit extending from the base of the last chamber.

Remarks: Our specimens resemble with the delicate Oligocene types of *Bolivina huneri* Howe in the Boltoskoy & Watanabe Collection (397885) available in the Cushman Collection at Smithsonian Institution.

Stratigraphic distribution: This species is very rare to rare in the upper Eocene (CP15) at Site 20C.

Distribution chart #: 1.

Superfamily BOLIVINACEA Glaessner, 1937
Family BOLIVINIDAE Glaessner, 1937
Genus *Tappanina* Montanaro Gallitelli, 1955
Type species: *Bolivinita selmensis* Cushman, 1933

Tappanina selmensis (Cushman , 1933)
Plate VI, fig. 2.

Bolivinita selmensis Cushman, 1933, p. 58, pl. 7, figs. 3-4.

Tappanina selmensis (Cushman, 1933) – Tjalsma & Lohmann, 1983, p. 37, pl. 11, fig. 4,
Van Morkhoven et al., 1986, p. 332, pl. 108, Holbourn et al., 2013, p. 552, figs. 1-4.

Main features: Test calcareous, biserial, tapering from its initial end, rhomboid or rectangular in cross section, chambers distinct, increasing gradually in size as added, early chambers flat and compressed, later chambers concave, rounded periphery. The angled and sharply edged chambers give it a distinctive zigzag periphery. Aperture narrow, at the inner margin of the last chamber.

Remarks: Our specimens resemble the holotype (CC 19043) and paratype (CC 19046) of *Tappanina selmensis* Cushman at the Smithsonian Institution.

Stratigraphic range: This species is very rare in the upper Paleocene to lower Eocene (CP8) at Site 20C.

Distribution chart #: 74.

Superfamily LOXOSTOMATACEA Loeblich & Tappan, 1962
Family LOXOSTOMATIDAE Loeblich & Tappan, 1962
Genus *Aragonia* Finlay, 1939
Type species: *Aragonia zelandica* Finlay, 1939

Aragonia aragonensis (Nuttall, 1930)
Plate VI, fig. 3.

Textularia aragonensis Nuttall, 1930, p. 280, pl. 23, fig. 6.

Aragonia aragonensis (Nuttall, 1930) – Tjalsma & Lohmann, 1983, p. 23, pl. 11, figs. 2a-b, Van Morkhoven et al., 1986, p. 308, pl. 101A, figs. 1-3, pl. 101B, figs. 1-4, Bolli et al., 1994, p. 130, figs. 35.5, Ortiz & Thomas, 2006, p. 112, pl. 4, figs. 1-3, Holbourn et al., 2013, p. 58, figs. 1-3.

Main features: Test calcareous, biserially arranged, rhomboid in shape (slightly longer than broad), laterally very compressed. Chambers about three times as long as wide, ornamented with thin limbate sutures with fine raised projections. Aperture a narrow transverse slit at the base of the last chamber.

Remarks: This is a fairly compressed and fan-shaped species of *Aragonia* (Tjalsma & Lohmann, 1983). Our specimens resemble the holotype (CC 25691a) and the paratypes (CC 25691b) of *Aragonia aragonensis* Nuttall at Smithsonian Institution.

Stratigraphic distribution: This species is very rare to common in the Mucuri Basin and at Sites 356 and 20C, from the Maastrichtian through the upper Eocene (NC23 to CP15), with maximum abundances (~10%) from the middle to upper Paleocene (CP3 to CP6).

Distribution chart #: 41.

Aragonia velascoensis (Cushman, 1925)
Plate VI, fig. 4.

Textularia velascoensis Cushman, 1925, p. 280, pl. 23, fig. 6.

Bolivinooides ouezzaensis Rey, 1955, p. 210, pl. 12, fig. 2., Tjalsma & Lohmann, 1983, p. 4, pl. 5, figs. 4a-c.

Aragonia velascoensis (Cushman, 1925) – Tjalsma & Lohmann, 1983, p. 23, pl. 11, figs. 2a-b, Van Morkhoven et al., 1986, p. 340, pl. 111A, figs. 1-3, pl. 111B, figs. 1-3, Holbourn et al., 2013, p. 60, figs. 1-2.

Main features: Test calcareous, biserial, oval in front view, widest near the middle, sutures distinct and limbate, raised, surface ornamented by the limbate sutures between which are raised projections extending back from the sutures themselves onto the lateral surfaces of the chambers with other irregular sutures, aperture elongated, low.

Remarks: Our specimens resemble the holotype (CC 4343) of *Aragonia velascoensis* Cushman in the Cushman Collection at Smithsonian Institution. We agreed with Van Morkhoven et al. (1986) in placing *Aragonia ouezzaensis* Rey as a synonym of *Aragonia velascoensis* Cushman, although Tjalsma & Lohmann (1983) considered them as distinct species.

Stratigraphic distribution: This species is very rare to rare at Site 356 and rare to common at Site 20C, from the middle to upper Paleocene (CP3 to CP8, planktic foraminifera biozones P5 to E1).

Distribution chart #: 82.

Superfamily CASSIDULINACEA d'Orbigny, 1839
Family CASSIDULINIDAE d'Orbigny, 1839
Subfamily CASSIDULININAE d'Orbigny, 1839
Genus *Globocassidulina* Voloshinova, 1960
Type species: *Cassidulina globosa* Hantken, 1876

Globocassidulina subglobosa (Brady, 1881)
Plate VI, fig. 5.

Cassidulina subglobosa Brady, 1881, p. 60, pl. 54, figs. 17-a-c.

Globocassidulina subglobosa (Brady, 1881) – Tjalsma & Lohmann, 1983, p. 31, pl. 16, fig. 9, Holbourn et al., 2013, p. 264, figs. 1-2.

Main features: Test calcareous, chambers biserially arranged and enrolled, subglobular in outline, somewhat compressed on the two lateral faces, slightly inflated. Aperture an oblique or nearly erect loop-like slit on the face of the projecting terminal segment.

Remarks: Most of our specimens from the Eocene are smaller than Oligocene and younger specimens. Our specimens resemble the plesiotypes (USNM 688507, 377191, CC 23611) of *G. subglobosa* Brady from upper Eocene, Recent and Oligocene ages respectively.

Stratigraphic distribution: This species occurs in the Santos, Campos, and Sergipe-Alagoas basins and at Sites 20C and 356. *G. subglobosa* is rare in the lower Eocene becoming abundant through the upper Eocene (CP8 to CP15).

Distribution chart #: 24.

Superfamily TURRILINACEA Cushman, 1927

Family TURRILINIDAE Cushman, 1927

Genus *Praebulimina* Hofker, 1953

Type species: *Bulimina ovulum* Reuss, 1844

Praebulimina navarroensis (Cushman & Parker, 1935)

Plate VI fig. 8.

Bulimina reussi Morrow var. *navarroensis* Cushman & Parker, 1935, p. 100, pl. 15, fig. 11.

Main features: Test calcareous, fusiform in shape, triserially arranged, ovate in outline, circular in section, chambers overlapping the preceding ones, rapidly flaring from the more or less pointed initial part, sutures depressed, wall calcareous, smooth. Aperture comma shaped, arched, at the base of the inner margin of the last chamber.

Remarks: Our specimen is very similar to the holotype (CC 22372) of *Bulimina reussi* var. *navarroensis* Cushman & Parker, however due to the aperture shape we decided to assign as *Praebulimina navarroensis* Cushman & Parker. This species is less inflated and the chambers grow slowly than *P. reussi* Morrow, resulting in a more conical initial part of the test. Differs from *Bulimina* by its fusiform shape, more inflated than *Bulimina kugleri* Cushman & Renz. Thomas (2003) discuss the confusion among homonymic *Bulimina ovula* d'Orbigny, Reuss and Terquem, *B. kugleri* Cushman & Renz and *Praebulimina reussi* Morrow, which is in fact a very confusing taxa.

Stratigraphic distribution: This species is rare to common in the Pelotas, Santos and Sergipe-Alagoas basins, from the lower Paleocene through upper Eocene (CP1 to CP15).

Distribution chart #: 37.

Superfamily BULIMINACEA Jones, 1875

Family BULIMINIDAE Jones, 1875

Genus *Bulimina* d'Orbigny, 1826

Type species: *Bulimina marginata* d'Orbigny, 1826

Bulimina alazanensis Cushman, 1927

Plate VI, fig. 6.

Bulimina alazanensis Cushman, 1927, p. 161, pl. 25, fig. 4.

Bulimina alazanensis Cushman, 1927 – Tjalsma & Lohmann, 1983, p. 24, pl. 14, fig. 4, Bolli et al., 1994, p. 347, figs. 53.27, 78.30, 81.13, 75, Ortiz & Thomas, 2006, p. 114, pl. 4, figs. 12-13, Holbourn et al., 2013, p. 90, figs. 1-2.

Main features: Test calcareous, triserial, somewhat longer than broad, the greatest breadth near the apertural end, chambers and sutures obscured by the ornamentation which consists of prominent longitudinal costae ending at the basal end in somewhat spinose projections, aperture elongated, comma-shaped.

Remarks: The holotype of *Bulimina alazanensis* Cushman is missing (USNM 36307 – empty slide). The paratypes (CC 58965) and topotypes (CC 51870, 58963) were preserved and our specimens resemble them. This species is easily distinguished through its longitudinal costae.

Stratigraphic distribution: This species is common to abundant in the Sergipe-Alagoas and Pelotas basins from the lower to upper Eocene (CP12 to CP15).

Distribution chart #: 10.

Bulimina jarvisi Cushman & Parker, 1936

Plate VI, fig. 7.

Bulimina jarvisi Cushman & Parker, 1936, vol. 12, p.39, pl.7, fig.1.

Bulimina jarvisi Cushman & Parker, 1936 – Tjalsma & Lohmann, 1983, p. 25, pl. 13, figs. 4-5b, Van Morkhoven et al., 1986, p. 184, pl. 62, figs.1-5, Bolli et al., 1994, p. 349, figs. 53.30a-b, 87.19, Holbourn et al., 2013, p. 104, figs. 1-2.

Main features: Test calcareous, triserial, longer than wide, chambers around 6 to 7, inflated, sutures distinct, depressed, wall test covered with fine, irregular costae. Aperture loop-shaped with a slight lip.

Remarks: Comparing paratype (CC 51871) and cotypes (CC 59482) of *Bulimina semicostata* Nuttall and holotype (CC 23128) and paratypes (CC 58942) of *Bulimina jarvisi* Cushman & Parker it is clear that our specimens should be assigned to *Bulimina jarvisi* Cushman & Parker, which is more slender and has more inflated chambers. Tjalsma & Lohmann (1983) mentioned transitional forms between the two species occurring in the Zone P14 (upper middle Eocene), but we do not observed that among our specimens.

Stratigraphic distribution: This species is very rare to rare in the lower to middle Eocene of Site 20C (CP9 to CP12).

Distribution chart #: 64.

Bulimina trinitatensis Cushman & Jarvis, 1928

Plate VI, fig. 9.

Bulimina trinitatensis Cushman & Jarvis, 1928, p. 102, pl. 14, figs. 12a-b.

Bulimina trinitatensis Cushman & Jarvis, 1928 – Tjalsma & Lohmann, 1983, p. 7, pl. 3 figs.3-4, pl. 14, fig.1, Van Morkhoven et al., 1986, p. 299, pl. 98A, figs. 1-2, pl. 98B, figs. 1-4, Bolli et al., 1994, p. 136, figs. 36.28-29, Holbourn et al., 2013, p. 122, figs. 1-2.

Main features: Test calcareous, triserial in early stage, later uniserial, longer than broad, rounded in transverse section, chambers distinct, with spines placed irregularly, with reticulate areas, aperture elongate, comma-shaped, smooth apertural face.

Remarks: Our specimens resemble the holotype (CC 9682) and paratypes (CC 15414, 15415) of *Bulimina trinitatensis* Cushman & Jarvis in the Cushman Collection at Smithsonian Institution, Washington DC.

Stratigraphic distribution: This species is rare to abundant at Sites 356 and 20C from the lower Paleocene to upper Eocene (CP1 to CP15).

Distribution chart #: 47.

Bulimina tuxpamensis Cole, 1928

Bulimina tuxpamensis Cole, 1928, p. 123, pl. 32, fig. 23.

Bulimina tuxpamensis Cole, 1928 – Van Morkhoven et al., 1986, p. 155, pl. 51A, B, figs. 1-4, Bolli et al., 1994, p. 137, figs. 36.32-33, Holbourn et al., 2013, p. 124, figs. 1-2.

Main features: Test calcareous, chambers triserially arranged, slightly inflated, numerous, sutures limbate to very indistinct. Wall very finely perforate and aperture loop-like or comma shaped.

Stratigraphic distribution: This species is rare to common in the lower to upper Eocene of Sites 356 and 20C (CP9 to CP15).

Distribution chart #: 19.

Family BULIMINELLIDAE Hofker, 1951

Genus *Buliminella* Cushman, 1911

Type species: *Bulimina elegantissima* d'Orbigny, 1839

Buliminella grata Parker & Bermudez, 1937

Plate VI, fig. 10.

Buliminella grata Parker & Bermudez, 1937, vol.11, pl. 59, fig. 6.

Buliminella grata Parker & Bermudez, 1937 – Tjalsma & Lohmann, 1983, p. 26, pl. 12, figs. 7a-b, Bolli et al., 1994, p. 137, fig. 37.3, Holbourn et al., 2013, p. 130, figs. 1-2.

Main features: Test calcareous, with high trochospiral coil of 2-3 whorls tapering rapidly, 4 chambers in the last whorl, sutures broad, flush and usually incised. Wall smooth, finely perforate, aperture rounded with small narrow radial depressions.

Remarks: We examined the holotype (CC 23340) of *Buliminella grata* Parker & Bermudez in the Cushman Collection at Smithsonian Institution, and our specimens are similar to the holotype and we assigned them as *B. grata*.

Stratigraphic distribution: This species is very rare to rare in the middle Paleocene through middle/upper Eocene (CP6 to CP14) at Site 20C.

Distribution chart #: 52.

Genus *Quadratobuliminella* de Klsz, 1953
Type species: *Quadratobuliminella pyramidalis* de Klsz, 1953

Quadratobuliminella pyramidalis de Klsz, 1953
Plate VI, fig. 11.

Quadratobuliminella pyramidalis de Klsz, 1953, p. 435, figs. 1a-2c.
Quadratobuliminella pyramidalis de Klsz, 1953 – Tjalsma & Lohmann, 1983, p. 19, pl. 4, fig. 1, pl. 12, figs. 6a-b, Van Morkhoven et al., 1986, p. 320, pl. 104, Holbourn et al., 2013, p. 464, fig. 1.

Main features: Test calcareous, chambers arranged in a quadrilocular spiral, globular in early stages becoming more cylindrical in later stages. The finely perforate pyramid-shaped test is square in cross section, and has a loop-shaped aperture across the upper surface of the last chamber, which are distinguishing features of this species.

Remarks: We compared our specimens with the topotype (USNM 433512) of *Quadratobuliminella pyramidalis* de Klsz at Smithsonian Institution and assigned them into this species.

Stratigraphic range: This species is very rare to common and restricted to the lower Paleocene through middle Eocene (CP2 to CP14) of the Site 356.

Distribution chart #: 55.

Superfamily STILOSTOMELLACEA Finlay, 1947
Family STILOSTOMELLIDAE Finlay, 1947
Genus *Siphonodosaria* Silvestri, 1924
Type species: *Nodosaria abyssorum* Brady, 1881

Siphonodosaria jacksonensis (Cushman & Applin, 1926)
Plate VI, fig. 12.

Nodosaria jacksonensis Cushman & Applin, 1926, p. 170, pl. 7, figs. 14-16.
Ellipsonodosaria nuttalli Cushman & Jarvis var. *aculeata* Cushman & Renz, 1948, p.32, pl. 6, fig. 10.
Stilostomella aculeata (Cushman & Renz, 1948) – Tjalsma & Lohmann, 1983, p. 36, pl. 14, fig. 12, Holbourn et al., 2013, p. 532, figs. 1-2.
Siphonodosaria jacksonensis (Cushman & Applin, 1926) – Hayward et al. (2012), p. 173, pl. 17, figs. 32-37, pl. 18, figs. 1, 2.

Main features: Test calcareous, uniserial, rectilinear to slightly arched, chambers subglobular, increasing gradually in size, sutures distinct and constricted. Wall smooth with spinose projections on the lower part of all chambers. Aperture terminal on a short neck at the end of the last chamber, sometimes with a toothlike projection preserved.

Remarks: Our specimens resemble the holotype (CC 57461) and paratypes (CC 57461) of *Stilostomella aculeata* Cushman & Renz that were placed as a synonym of *Siphonodosaria jacksonensis* Cushman & Applin (1926) by Haward et al. (2012). We

agreed to place them as synonyms so then assigned our specimens as *Siphonodosaria jacksonensis* Cushman & Applin (1926).

Stratigraphic distribution: This species is very rare to common in the lower to upper Eocene of Site 20C (CP9 to CP15).

Distribution chart #: 20.

Siphonodosaria scripta (d'Orbigny, 1846)

Plate VI, fig. 13.

Dentalina scripta d'Orbigny (1846), p. 51, pl. 2, figs. 21-23.

Ellipsonodosaria subspinosa Cushman, 1943, p. 92, pl. 16, figs. 6-7b.

Stilostomella subspinosa (Cushman, 1943) – Tjalsma & Lohmann, 1983, p. 36, pl. 14, figs. 16-17, Holbourn et al., 2013, p. 550, figs. 1-2.

Siphonodosaria scripta (d'Orbigny, 1846) – Hayward et al. (2012), p. 180, pl. 19, fig. 17.

Main features: Test calcareous, uniserial, elongate, subcylindrical, slightly tapering with greatest breadth near the apertural end. Chambers distinct and inflated, increasing gradually in size as added, sutures strongly depressed, wall with short stout spines, either entirely covering the chamber or in the early stages confined to the lower portion of the chamber wall, aperture with subcylindrical neck and distinct lip with inwardly projecting tooth.

Remarks: Our specimens resemble the holotype (CC 21484) and paratypes (CC 21483) of *Stilostomella subspinosa* Cushman that we agreed to considered as synonym of *Siphonodosaria scripta* d'Orbigny as reported by Hayward et al. (2012), so then assigned our specimens as *S. scripta*.

Stratigraphic distribution: This species is very rare to rare in the lower to upper Eocene of Site 20C (CP9 to CP15).

Distribution chart #: 21.

Superfamily DISCORBACEA Ehrenberg, 1838

Family DISCORBIDAE Ehrenberg, 1838

Genus *Neoeponides* Reiss, 1960

Type species: *Rotalina schreibersii* d'Orbigny, 1846

Neoeponides byramensis (Cushman, 1922)

Plate VII, figs. 1a-c, 2a-c.

Pulvinulina byramensis Cushman, 1922, p. 99, pl. 22, figs. 4-5.

Eponides byramensis (Cushman, 1922) – Bolli et al., 1994, p. 363, figs. 55.19a-b.

Main features: Test calcareous, trochospirally coiled, biconvex to unequally biconvex with oblique and tangential, somewhat limbate sutures on the evolute dorsal side, circular outline, slightly lobate on the last chambers. Larger adult specimens usually have 8 to 9^{1/2} chambers in the last whorl, while small adult specimens have 6 to 7^{1/2} chambers, radial

sutures, almost straight and deeply marked sutures on the involute ventral side. Interiomarginal aperture on the ventral side with thin lip.

Remarks: There is a wide variability in the specimens we assigned to *Neoeponides byramensis* Cushman, as also seen in the paratypes in the Cushman Collection at Smithsonian Institution. The holotype (CC 25558) is not very well preserved, with the last chamber missing and some holes, possible due to dissolution. Possibly 7 chambers in the last whorl, spiral side evolute, more convex and elevated with tangential sutures, umbilical side involute somewhat flat with radial and slightly curved sutures. Preservation of the paratypes (CC 3017, 3018, 25559) is also not good, although it is possible to see the thickening of the sutures towards the umbilicus on the involute side (not clear in the holotype). The number of chambers in the last whorl varies widely (5 to 8). Paratypes (USNM 6648, 7372, 7671) with better preservation clearly show this range of chambers on the final whorl and the thickening of the radial sutures towards the umbilicus on the involute side. One topotype (CC 5942) of *Rotalina schreibersii* d'Orbigny (1846) has an inequally biconvex test, spiral side evolute and more conical convex with very oblique (almost tangential) sutures, umbilical side low convex, involute, straight and radial sutures becoming thicker towards the umbilicus, six chambers in the last whorl. The biconvex shape of those forms came from the raised central area on the spiral side. In conclusion, our specimens resemble the holotype and paratypes of *Neoeponides byramensis* Cushman. Differs from other species by its robust appearance, biconvex test, slightly lobate in the last chambers and the thickening of the sutures towards umbilicus.

Stratigraphic distribution: This species is rare to common in middle to upper Eocene in the Pelotas Basin (CP12 to CP15).

Distribution chart #: 11.

Neoeponides campester (Palmer & Bermudez, 1941)

Plate VII figs. 3a-c.

Eponides byramensis Cushman var. *campester* Palmer & Bermudez (1941) (new name for *Eponides byramensis* Cushman var. *cubensis* Palmer & Bermudez (1936) homonym of *Eponides cubensis* Palmer & Bermudez (1936).

Pulvinulina jacksonensis Cushman & Applin, 1926, pl. 9, figs. 24-25.

Neoeponides campester (Palmer & Bermudez, 1941) – Van Morkhoven et al., 1986, p. 152, pl. 50.

Main features: Test calcareous, trochospiral, asymmetrically biconvex with the umbilical side more vaulted. Periphery acute, oblique and somewhat limbate sutures on the evolute side and radial on the involute side, 7 to 10 chambers in the last whorl, radial sutures thickening towards the umbilicus. Aperture a long and narrow interiomarginal slit between the periphery and the umbilicus on the last chamber.

Remarks: We compared our specimens with the holotype of *Eponides byramensis* Cushman var. *cubensis* Palmer & Bermudez (USNM 448828), topotype of *Eponides byramensis* Cushman var. *campester* Palmer & Bermudez (CC 45925) and plesiotypes of *Eponides campester* Palmer & Bermudez (CC 62624). The diagnostic characteristics of

this species are the assymmetrically biconvex test with acute periphery and the thickening towards the umbilicus of the radial sutures on the umbilical side. Comparing the holotypes and paratypes cited above of *Neoeponides campester* Palmer & Bermudez (age Oligocene) and holotype (CC 5373) and paratypes (CC 5517) of *Eponides jacksonensis* Cushman & Applin (age upper Eocene), they are very similar, on having 7 chambers in the last whorl, thickened and straight sutures towards the umbilicus, *E. jacksonensis* Cushman & Applin could be a junior synonym of *Neoeponides campester* Palmer & Bermudez, being a small species in the upper Eocene increasing in size into the Oligocene.

Stratigraphic distribution: This species is very rare in the middle to upper Eocene (CP14 to CP15) of the Pelotas Basin.

Distribution chart #: 7.

Neoeponides elevatus (Plummer, 1926)

Plate VII, figs. 4a-c.

Truncatulina elevata Plummer, 1926, p. 142, pl. 11, fig. 1a-c.

Eponides elevatus (Plummer, 1926) – Fluegeman et al., 1990, p. 63, pl. 1, figs. 1-3.

Main features: Test calcareous, trochospiral, unequally biconvex, high spiral side and almost flat umbilical side giving a more conical shape on profile view. Periphery bluntly angular and ~7 chambers in the last whorl. Spiral side sutures curved and limbated, while the umbilical sutures are radiate forming a distinct and thick ridge surrounding a small excavated umbilicus. Aperture small, arched interior marginal slit near the periphery.

Remarks: Differs from other species by its high spiral side, unequally biconvex, that is conical shape on lateral view, radial sutures and thick ridge surrounding the umbilicus.

Stratigraphic distribution: This species is rare to common from the middle to upper Eocene (CP14 to CP15) in the Sergipe-Alagoas and Pelotas basins.

Distribution chart #: 9.

Neoeponides hillebrandti Fisher, 1962

Plate VII, figs. 5a-c.

Rotalia cf. partschiana d'Orbigny – White, 1928, p.288, pl. 38, figs. 10a-c.

Eponides whitei Von Hillebrandt, 1962, p. 106, pl. 8, fig. 11.

Neoeponides hillebrandti Fisher, 1962, p. 197.

'*Eponides*' cf. *hillebrandti* Fisher, 1962 – Bolli et al., 1994, p. 146, figs. 39.7-9.

Neoeponides hillebrandti Fisher, 1962 – Tjalsma & Lohmann, 1983, p. 16, pl. 7, figs. 9a-b, Holbourn et al., 2013, p. 364, figs. 1-3.

Main features: Test calcareous, trochospirally coiled, almost plano-convex, with the umbilical side nearly flat and the spiral side high cone-shaped, periphery subacute. Umbilical side involute with almost straight and radial sutures and may be thicken towards the large and granular umbilicus. Spiral side highly convex with oblique sutures,

7 ½ to 9 chambers in the last whorl. Aperture as a low arch beneath apertural face, possibly extending into the umbilical area.

Remarks: The name *Eponides whitei* von Hillebrandt (1962) was already taken by *E. whitei* Brotzen (1936), for this reason Fisher (1962) proposed a new name for Hillebrandt's species and placed it in the genus *Neoeponides*. This species is distinguished by its high spiral side, acute periphery and straight sutures on the umbilical side.

Stratigraphic distribution: This species is very rare to common in the Paleocene of the distal sites 356 and 20C (CP1 to CP8 - Planktic foraminifera biozones P1a to P5/E1), its extinction marks the benthic foraminiferal extinction at the Paleocene-Eocene boundary.

Distribution chart #: 81.

Family SPHAEROIDINIDAE Cushman, 1927

Genus *Sphaeroidina* d'Orbigny, 1826

Type species: *Sphaeroidina bulloides* d'Orbigny, 1826

Sphaeroidina bulloides d'Orbigny, 1826

Plate VII, fig. 6.

Sphaeroidina bulloides d'Orbigny, 1826, p. 16, pl. 2, fig. 58.

Sphaeroidina bulloides d'Orbigny, 1826 – Van Morkhoven et al., 1986, p. 80, pl. 24, Holbourn et al., 2013, p. 520, figs. 1-3.

Main features: Test calcareous, with coiling strongly embracing chambers, subglobular in outline. Few globular chambers, sutures depressed. Test wall smooth and imperforate. The small, rimmed, crescent-shaped aperture is distinct and usually situated slightly above the junction of three chambers.

Remarks: We examined upper Eocene hypotypes (USNM 688509) and Recent topotypes (CC 59393) of *Sphaeroidina bulloides* d'Orbigny at Smithsonian Institution, and our specimens were similar to them.

Stratigraphic range: This species is rare to common in the upper Eocene of the Pelotas Basin (CP15).

Distribution chart #: 6.

Superfamily DISCORBINELLACEA Sigal, 1952

Family PARRELOIDIDAE Hofker, 1956

Genus *Cibicidoides* Thalmann, 1939

Type species: *Truncatulina mundula* Brady, Parker & Jones, 1890

Cibicidoides dayi (White, 1928)

Plate VIII, figs. 1a-c.

Planulina dayi White, 1928, p. 300, pl. 41, figs. 3a-c.

Cibicidoides dayi White, 1928 – Tjalsma & Lohmann, 1983, p. 9, pl. 6, figs. 6-7, Van Morkhoven et al., 1986, p. 353, pl. 114, figs. 1a-c, Alegret & Thomas, 2001, p. 280, pl. 3, figs. 3-4.

Main features: Test calcareous, trochospiral, biconvex, sutures curved on both sides, limbate spiral sutures and slightly depressed dorsal sutures, spiral side with prominent umbo, finely perforate spiral side and imperforate umbilical side, periphery acute and imperforate.

Remarks: The depressed spiral suture and prominent umbo on the finely perforate spiral side, and relatively indistinct umbo on the smooth, imperforate, umbilical side are the distinctive features of *Cibicidoides dayi* White (Van Morkhoven et al., 1986). We compare our specimens to the paratypes (AMNH 19908-19910) at American Natural History Museum, NY, and they are similar.

Stratigraphic distribution: This species is rare to common in the Paleocene (CP2 to CP7) of the Campos and Mucuri basins and Site 356. Occasionally rare in the upper Paleocene-lower Eocene (CP8 to CP9) of the Pelotas Basin.

Distribution chart #: 73.

Cibicidoides eoacaenus (Gümbel, 1868)

Plate VIII, figs. 3a-c, 4a-c.

Rotalia eoacaenus Gümbel, 1868, p. 650, pl. 2, figs. 87a-b.

Cibicides tuxpamensis Cole, 1928, p. 219, pl. 2, figs. 2-3, pl. 3, figs. 5-6.

Cibicides perlucida Nuttall, 1932, p. 33, pl. 8, figs. 10-12.

? *Rotalia propinqua* Reuss, 1856, p. 241, pl. 4, fig. 53.

Cibicidoides tuxpamensis Cole, 1928 – Tjalsma & Lohmann, 1983, p. 28, pl. 18, figs. 3a-4c, pl. 22, figs. 1a-3c.

Cibicidoides eoacaenus Gümbel, 1868 – Van Morkhoven et al., 1986, p. 256, pl. 86A, figs. 1-4, pl. 86B, figs. 1-2, Ortiz & Thomas, 2006, p. 115, pl. 5, fig. 2, Holbourn et al. 2013, p. 172, figs. 1-3, Holbourn et al., 2013, p. 172, figs. 1-3.

Cibicidoides tuxpamensis tuxpamensis Cole, 1928 – Bolli et al., 1994, p. 148, figs. 40.1-3.

Cibicidoides perlucidus Nuttall, 1932 – Bolli et al., 1994, p. 366, figs. 79.21a-b, 88.3a-c.

Main features: Test trochospiral, plano-convex to biconvex, nearly circular in outline, umbilical side evolute and commonly more flattened than spiral side. Last whorl with 12 to 15 chambers, curved sutures on both sides, slightly depressed on umbilical side and limbate on the spiral side, dorsal wall coarsely perforate. Very distinct and prominent umbo with a spiral side suture line in the central part of the test. Periphery acute with imperforate keel. Primary aperture is a narrow equatorial slit bordered by a thin lip, extending onto the spiral side.

Remarks: Van Morkhoven et al. (1986) presented a historical overview of the taxonomy of this species, compared types of *Cibicidoides eoacaenus* Gümbel, *Cibicidoides tuxpamensis* Cole, and *Cibicidoides perlucidus* Nuttall and concluded that they were synonymous, because they could not consistently separate the peripherally rounded (*tuxpamensis-eoacaenus* type) and more angular (*perlucidus* type) morphotypes.

Comparing our specimens with the plesiotype (USNM 623850) and topotypes (CC 9527) of *Cibicides tuxpamensis* Cole, plesiotypes of Cushman Collection (CC 60531, 64489, 57929) of *Cibicides perlucida*, and topotypes (USNM 627093, 377282) of *Cibicides eocaenus* Gümbel we agree that it is difficult to differentiate them into three distinct species. One of the topotypes of *C. eocaenus* Gümbel (USNM 627093) has a very pronounced umbilical boss that is a characteristic feature for *C. tuxpamensis* Cole. For these reasons, we agree with van Morkhoven et al. (1986) that these three species should be considered as synonyms. Differs from other species by its very distinguished and prominent umbo with a spiral side suture line in the central part of the test, coarsely perforate on both sides.

Stratigraphic distribution: This species occurs from the lower to the upper Eocene (CP8 to CP15). It is rare to very abundant in the Pelotas and Santos basins, occasionally very abundant in the Campos Basin and common at Sites 20C and 356.

Distribution chart #: 26.

Cibicidoides grimsdalei (Nuttall, 1930)
Plate VIII, figs. 2a-c.

Cibicides grimsdalei Nuttall, 1930, p. 291, pl. 25, figs. 7-8, 11.

Cibicidoides grimsdalei (Nuttall, 1930) – Tjalsma & Lohmann, 1983, p. 26, pl. 18, figs. 2a-c, pl. 22, figs. 6-7, Van Morkhoven et al., 1986, p. 247, pl. 83A, figs. 1-3, pl. 83B, figs. 1-7, Ortiz & Thomas, 2006, p. 116, pl. 5, fig.3, Houlborn et al., 2013, p. 174, figs. 1-3, Houlborn et al., 2013, p. 174, figs. 1-3.

Main features: Test trochospiral, plano-convex, dorsally practically flat, ventrally much elevated. Umbilicus closed, sutures gently curved and limbate on the dorsal side. Ventral side with thick and limbate sutures with almost 10 chambers in the last whorl. Aperture is a narrow equatorial arch bordered by a thin lip extending onto the spiral side.

Remarks: We compared our specimens with the co-types (CC 59517, 59518, 59519, USNM 369263, 369264) and plesiotypes (CC 59629, 57499, 57040) at Smithsonian Institution, they all show the distinct characteristics of the plano-convex test, coarsely perforate evolute side and less perforate involute side. Douglas (1973) refers to the pitted and coarsely perforated spiral side as a very distinct feature of this species.

Stratigraphic distribution: *C. grimsdalei* is rare to common in the lower to the upper Eocene (CP10 to CP15) at Sites 356 and 20C.

Distribution chart #: 12.

Cibicidoides havanensis (Cushman & Bermudez, 1937)
Plate VIII, figs. 5a-c.

Cibicides havanensis Cushman & Bermudez, 1937, p. 28, pl. 3, figs. 1-3.

Cibicidoides havanensis Cushman & Bermudez, 1937 – Tjalsma & Lohmann, 1983, p. 27, pl. 22, figs. 4a-c, Van Morkhoven et al., 1986, p. 189, pl. 64A, figs.1-4, pl. 64B, figs. 1-2, Bolli et al., 1994, p. 366, figs. 88.1a-c, Houlborn et al., 2013, p. 180, figs. 1-4.

Main features: Test trochospiral, biconvex, periphery subacute and imperforate. Umbilicus filled with a mass of secondary calcite, ~12 chambers in the last whorl, sutures strongly oblique on the dorsal side. Wall smooth, except for the secondary layer over the spire, aperture as a small opening at the peripheral margin extending to the dorsal side.

Remarks: We compared our specimens with the holotype (CC 23424), paratype (CC23428) and plesiotype (USNM 642243) which clearly have the high spiral side and the secondary calcite on the dorsal side, and the umbilical calcite on the ventral side. Some of our specimens have very high dorsal spire, giving the mostly plano-convex profile.

Stratigraphic distribution: This species is common to abundant in the Eocene of the Campos Basin and at Site 20C (CP9 to CP15), increasing in abundance (~18%) on the upper Eocene (CP14 to CP15).

Distribution chart #: 18.

Cibicidoides hyphalus (Fisher, 1969)

Anomalinoides hyphalus Fisher, 1969, p. 197, figs. 3a-c.

Cibicidoides hyphalus Fisher, 1969 – Van Morkhoven et al., 1986, p. 359, pl. 116, figs. 1-2, Holbourn et al., 2013, p. 182, figs. 1-3.

Main features: Test calcareous, trochospiral, unequally biconvex to plano-convex with periphery subacute to rounded. Spiral side convex, smooth, with transparent umbo, umbilical side flat to slightly convex, almost completely involute, coarsely punctuate, deep umbilicus obscured by triangular flap-like extension of later chambers. Up to 12 chambers in the last whorl, sutures curved on both sides and somewhat limbate on the umbilical. Aperture a low arch at the base of the last chamber.

Remarks: We agree with Van Morkhoven et al. (1986) which reported that *C. hyphalus* and *C. velascoensis* are similar forms and have the same stratigraphic range, but *C. hyphalus* has more chambers in the last whorl. *C. velascoensis*, which is larger in diameter and has a more strongly convex evolute side.

Stratigraphic distribution: This species is common to abundant in the Paleocene at Sites 356 and 20C (CP1 to CP7).

Distribution chart #: 91.

Cibicidoides micrus (Bermudez, 1949)

Plate VIII, figs. 6a-c.

Cibicides micrus Bermudez, 1949, p. 302, pl. 24, figs. 34-36.

Cibicidoides micrus Bermudez, 1949 – Van Morkhoven et al., 1986, p. 267, pl. 88, figs. 1-2, Holbourn et al., 2013, p. 194, figs. 1-6.

Main features: Test calcareous, trochospiral, asymmetrically biconvex to plano-convex, with dorsal side slightly convex, ventral side nearly flat, subacute periphery. Last whorl with 12 chambers, spiral side sutures slightly depressed, the center of the dorsal surface

with some protruding shell growth usually circular in shape. Aperture narrow, at the base of the last chamber.

Remarks: We compared our specimens with three paratype specimens (CC 62431-62432). Distinguishing features are the protruding spiral suture over the initial chambers on the spiral side, the biconvex profile, and having numerous chambers in the last whorl (11-12).

Stratigraphic distribution: *C. micrus* is common to abundant in the lower through upper Eocene of the Campos Basin and rare in the Pelotas Basin and rare to common at Site 20C (CP10 to CP15).

Distribution chart #: 13.

Cibicidoides praemundulus (Berggren & Miller, 1986)
Plate VIII, figs. 7a-c.

Cibicidoides ungerianus (d'Orbigny, 1846) – Tjalsma & Lohmann, 1983, p. 28-29, pl. 18, figs. 1a-c, pl. 21, figs. 5-6.

Cibicidoides praemundulus Berggren & Miller, 1986, p. 264, pl. 87, figs. 1-3.

Cibicidoides praemundulus Berggren & Miller, 1986 – Van Morkhoven et al., 1986, p. 264, pl. 87, figs. 1-2, Holbourn et al., 2013, p. 200, figs. 1-3.

Main features: Test trochospiral, nearly circular in outline, low biconvex, acute periphery with an imperforate band. Spiral side evolute, coarsely perforate, 10 to 12 chambers in the last whorl, sutures often strongly curved on both sides. Umbilical side with glossy umbilical plug.

Remarks: Our specimens were compared with the holotype (USNM 406407) of *Cibicidoides praemundulus*, although some of them are a little more highly biconvex, but still lenticular and with acute periphery. They have 10 to 12 chambers in the last whorl, increasing gradually in size. All our specimens have the very characteristic glossy umbilical boss. Holbourn et al. (2013) reported that *C. praemundulus* differs from *Cibicidoides mundulus* Brady, Parker & Jones by the distribution of pores and more curved sutures on the spiral side. There are transitional forms between them at the end of the Oligocene (Miriam Katz, personal communication 2015).

Stratigraphic distribution: This species is very rare to common in the lower to upper Eocene in the Pelotas Basin and at Site 20C (CP10 to CP15).

Distribution chart #: 14.

Cibicidoides subspiratus (Nuttall, 1930)
Plate VIII, figs. 8a-c.

Cibicides subspirata Nuttall, 1930, p. 292, pl. 25, figs. 9, 10, 14.

Cibicidoides subspiratus (Nuttall, 1930) – Tjalsma & Lohmann, 1983, p. 28, pl. 18, figs. 5a-c, pl. 22, figs. 5a-b, Miller and Katz, 1986, p. 285, pl. 7, figs. 7-9; Van Morkhoven et al., 1986, p. 314, pl. 102, figs. 1a-c, Holbourn et al., 2013, p. 206, figs. 1-2.

Main features: Test trochospiral, asymmetrically biconvex to planoconvex. Lunate chambers on the involute side (very long and curved chambers), peripheral keel which sometimes is absent from the last 3-4 chambers, numerous chambers (12-14) in the last whorl, strongly curved, slightly depressed sutures and central boss on the umbilical side. Test wall finely perforate in both sides, aperture a short arch slit, extending over the peripheral margin to the base of the last chamber.

Remarks: Most of the cotypes (USNM 369278, 369279, CC 59520, 59521, 59522) examined have a central umbilical plug over the previous whorls on the evolute side. Our specimens all have the very lunate shape chambers, 12 to 13 chambers in the last whorl, the plug on the evolute side, and the peripheral keel.

Stratigraphic range: This species is rare to common in the lower through the upper Eocene of the Campos, Santos and Pelotas basins and at Site 356 (CP9 to CP15).

Distribution chart #: 16.

Cibicidoides velascoensis (Cushman, 1925)

Plate IX, figs. 1a-c.

Anomalina velascoensis Cushman, 1925.

Cibicidoides velascoensis (Cushman, 1925) - Van Morkhoven et al., 1986, p. 371, pl. 121, figs. 1-2, Holbourn et al., 2013, p. 208, figs. 1-3.

Main features: Test calcareous, trochospiral, asymmetrically biconvex with dorsal side nearly flat and ventral side broadly convex, broadly rounded periphery, 8 to 9 chambers in the last whorl. Dorsal side with central portion raised, sutures raised on the dorsal side and limbate on both sides, wall finely perforate on the umbilical side and coarsely punctuate, centrally thickened but relatively flat dorsal side. Aperture a low interiomarginal and equatorial arch at the base of the apertural face.

Remarks: Our specimens were compared to the holotype (CC4345) and topotypes (CC 38928) of *C. velascoensis*. Differs from other *Cibicidoides* by its very coarsely perforate and flat evolute side, and smoother and convex involute side.

Stratigraphic range: This species is common to abundant in the Campos, Sergipe-Alagoas and Mucuri basins and at Site 356, from the Maastrichtian through the upper Paleocene (NC23 to CP7).

Distribution chart #: 93.

Superfamily PLANORBULINACEA Schwager, 1877

Family PLANULINIDAE Bermúdez, 1952

Genus *Planulina* d'Orbigny, 1826

Type species: *Planulina ariminensis* d'Orbigny, 1826

Planulina costata (Hantken, 1875)

Plate VII, figs. 7a-c.

Truncatulina costata Hantken, 1875, p. 73, pl. 9, fig. 2a-c.

Planulina costata (Hantken, 1875) – Van Morkhoven et al., 1986, p. 212, pl. 72, Holbourn et al., 2013, p. 404, figs. 1-2.

Main features: This species is distinguished by its nearly plano-convex trochospirally coiled test, with low, convex umbilical side with a small umbonal depression, spiral side flat (sometimes slightly depressed). Periphery compressed and keeled, 10 to 12 chambers in the last whorl, sutures curved and limbate, those of umbilical side are notably thinner toward umbilicus, aperture a low interiomarginal arch with slight lip. The earlier whorls on the spiral side may be obscured by thickened suture material, somewhat wrinkled in appearance.

Remarks: Our specimens were compared with topotype (CC15770) and paratypes (CC7552, USNM 627354, 627128) of *Planulina costata* in the Smithsonian. They all show the very flat evolute side and low convex involute side. The chambers are long and curved, with limbate sutures and ~12 chambers in the last whorl. Our specimens differ from *C. subspiratus* Nuttall in their low convex spiral side and the lack of the umbilical plug. We examined topotypes (CC 9478, USNM 627095) of Eocene *Cibicidoides pseudowuellerstorfi* Cole. Our specimens differ from this species in their lack of a lobate outline and a knob on the umbilical side. Some types (CC 39311, 39415, 39443, USNM 377317) assigned to *Cibicidoides pseudowuellerstorfi* Cole were erroneously placed in this species.

Stratigraphic range: This species has its first occurrence in rare samples of the Sergipe-Alagoas and Santos basins in the lower Eocene (CP9) and becomes abundant in the upper lower Eocene through upper Eocene (CP10 to CP15). This species is common in the Campos and Pelotas basins in the upper lower Eocene to upper Eocene (CP10 to CP15), reaching maximum abundances (~12% of benthics) from middle to upper Eocene (CP12 to CP15).

Distribution chart #: 15.

Superfamily ASTERIGERINACEA d'Orbigny, 1839

Family EPISTOMARIIDAE Hofker, 1954

Subfamily NUTTALLIDINAE Saidova, 1981

Genus *Nuttallides* Finlay, 1939

Type species: *Eponides truempyi* Nuttall, 1930

Nuttallides truempyi (Nuttall, 1930)

Plate IX, figs. 3a-c, 4a-c.

Eponides truempyi Nuttall, 1930, p. 287, pl. 24, figs. 9, 13-14.

Astigerina crassaformis Cushman & Siegfus, 1935, p. 94, pl. 14, fig. 10.

Nuttallides truempyi (Nuttall, 1930) – Tjalsma & Lohmann, 1983, p. 17, pl. 6, figs. 4a-b, pl. 17, figs. 4a-5b, pl. 21, figs. 1a-4c, Miller and Katz, 1986, p. 287, pl. 4, figs. 1-3, Van Morkhoven et al., 1986, p. 288, pl. 96A-B, Holbourn et al., 2013, p. 378, figs. 1-2.

Nuttallides truempyi crassaformis Cushman & Siegfus, 1935 – Bolli et al., 1994, p. 149, figs. 40.24-26.

Nuttallides truempyi truempyi Nuttall, 1930 – Bolli et al., 1994, p. 149, figs. 40.27-28.

Main features: Test calcareous, trochospirally coiled with wide variability in shape in profile, from plano-convex to biconvex with a peripheral keel. They are recognized by its 6 to 13 chambers in the last whorl, almost flat evolute side with the tangential sutures almost radial, and the central boss on the involute side. The periphery of the last chambers may be slightly lobate. Aperture interiomarginal, extending from the umbilical boss nearly to the peripheral keel.

Remarks: Tjalsma & Lohmann (1983) and Van Morkhoven et al. (1986) confirmed Beckmann's (1954) observation of two end-member morphologies in *Nuttallides truempyi*, with many transitional forms in between. One is a lenticular, biconvex form with 8 to 13 chambers in the last whorl and large transparent umbilical boss (type 1 – Plate IX, figs. 3a-c), the other is nearly plano-convex form with 6-9 chambers in the last whorl and a small umbilical boss (type 2 – Plate IX, figs. 4a-c), which Tjalsma & Lohmann (1983) observed on having a larger proloculus and shorter coil than the lenticular form. They also describe a rare megalospheric form of *N. truempyi* with more compact and conical test and 1-2 convolutions on the evolute side. Our specimens range between these two end-members morphologies. The co-types (CC 59491, 59492, 59493) and paratypes (CC 57168, 57027, 57561) of *Nuttallides truempyi*, were compared with the holotype (CC 22358) and paratypes (CC 22359 – USNM 366119, 366120) of *Asterigerina crassaformis* Cushman & Siegfus, it is difficult to split them as distinct species. The holotype of *A. crassaformis* did not have the central boss, and Cushman & Siegfus did not mention a boss in its description, but it is visible in several of the paratypes. Both *N. truempyi* and *A. crassaformis* have the same main characteristics of plano-convex to biconvex profile, very peculiar arrange of chambers with tangential sutures on the evolute side and the central boss on the strongly convex involute side is almost always present.

Stratigraphic distribution: This species occurs from the Maastrichtian through the upper Eocene (NC23 to CP15) at all locations. *N. truempyi* is abundant to very abundant at Sites 20C and 356, with abundances ranging from 13% to 35% of benthics. In the proximal Brazilian marginal basin wells, *N. truempyi* is rare to abundant, reaching maximum abundance ~15%. In general, average abundance is ~20% for the Paleocene and 15% for the Eocene

Distribution chart #: 44.

Genus *Nuttallinella* Belford, 1959

Type species: *Nuttallina coronula* Belford, 1958

Nuttallinella florealis (White, 1928)

Plate IX, figs. 5a-c.

Gyroidina florealis White, 1928, p. 293, pl. 40, figs. 3a-c.

Nuttallinella florealis (White, 1928) – Van Morkhoven et al., 1986, p. 356, pl. 115, Bolli et al., 1994, p. 150, figs. 41.3-5.

Main features: This species is distinguished by its plano-convex profile and peripheral flange, oblique sutures on the flat to slightly concave evolute side and radial sutures on the strongly convex involute side, sutures thickened around the umbilicus on the involute side. Aperture interiomarginal, an elongate slit on the umbilical side, often with a narrow lip (although often difficult to see due to poor preservation).

Remarks: Our specimens were compared to a paratype (USNM 473146) at Smithsonian and the holotype (19899) at AMNH, NY, they all have a flat evolute side, with strongly oblique sutures and convex involute side with radial sutures slightly thickening towards the small umbilicus. This species is easily recognized by its sharp keel or flange, slightly lobate outline and thickening of the sutures on the involute side.

Stratigraphic distribution: This species is rare to common in the Maastrichtian through the middle Paleocene (NC23 to CP3) in the Mucuri Basin and at Sites 20C and 356.

Distribution chart #: 112.

Nuttallinella sp. 1
Plate IX, figs. 5a-c.

Main features: Test calcareous, trochospiral, asymmetrically biconvex, spiral side evolute, umbilical side involute and with 10 chambers in the last whorl, narrow umbilical boss, periphery carinate, aperture an elongate slit on the umbilical side.

Remarks: Those specimens have a very distinctive toothplate across their chambers, which is only visible in the last chambers, especially when wet. We compared our specimens with paratypes of *Nuttallinella disca* Mello (USNM 642668, 642669, 642670), the holotype of *N. disca* Mello is missing. *N. disca* has a more lobate outline and very low spiral side. We also compared them with paratypes of *Pulvinulinella ripleysis* Sandidge (CC 34079, 34080), which has fewer numbers of chambers in the last whorl and much less evolute side.

Stratigraphic range: This species is rare in the Sergipe-Alagoas Basin and at Site 20C and common to abundant in the Pelotas Basin from the lower to middle Eocene (CP12 to CP14).

Distribution chart #: 50.

Superfamily NONIONACEA Schultze, 1854
Family NONIONIDAE Schultze, 1854
Subfamily NONIONINAE Schultze, 1854
Genus *Nonion* de Montfort, 1808
Type species: *Nautilus faba* Fitchel and Moll, 1798

Nonion havanense Cushman & Bermudez, 1937
Plate VII, figs. 8a-b.

Nonion havanense Cushman & Bermudez, 1937, p. 19, pl. 2, figs. 13-14.

Nonion havanense Cushman & Bermudez, 1937 – Tjalsma & Lohmann, 1983, p. 17, pl. 7, figs. 6a-b, Holbourn et al., 2013, p. 370, figs. 1-2.

Main features: Test calcareous, planispiral and involute, somewhat compressed, slightly depressed in the umbilical region, rounded periphery, 8 to 9½ chambers in the last whorl increasing gradually in size as added, sutures distinct, slightly limbate, not depressed, gently curved, aperture low.

Remarks: Tjalsma & Lohmann (1983) observed a wide variation in the degree of lateral compression, as well as in the number of chambers (6-9), curvature of sutures, and test size. They reported larger specimens in the Paleocene than in the Eocene, which often have fewer chambers in the last whorl. Our specimens are similar to the holotype (CC 23417) and paratype (CC 23417) of *Nonion havanense* Cushman & Bermudez (Eocene), which have 9 and 8 chambers in the last whorl respectively.

Stratigraphic range: This species is rare to common at Site 20C and in the Sergipe-Alagoas Basin from the upper Paleocene through upper Eocene (CP6 to CP15), with first occurrence in the upper Paleocene (CP6) of the Sergipe-Alagoas Basin and upper Paleocene (CP8) at Site 20C.

Distribution chart #: 30.

Subfamily PULLENIINAE Schwager, 1877

Genus *Melonis* de Montfort, 1808

Type species: *Melonis etruscus* de Montfort, 1808 =
Nautilus pompilioides Fichtel and Moll, 1798

Melonis sp. 1

Plate X, figs. 1a-c.

Main features: Test calcareous, planispiral and involute, 10 to 11 chambers in the last whorl enlarging gradually in size, sutures curved and slightly limbate, narrow, open umbilicus on both sides, test wall coarsely perforate. Aperture an interior-marginal slit hidden in most specimens.

Remarks: Our specimens resemble *Melonis barleeanus* (Williamson, 1858), but they are thicker in profile with maximum width closer to the umbo in *M. barleeanus* and they are less inflated than *Melonis pompilioides* (Fichtel and Moll, 1798).

Stratigraphic range: This species is rare to common in the upper Eocene (CP15) of the Sergipe-Alagoas Basin.

Distribution chart #: 3.

Genus *Pullenia* Parker & Jones, 1862

Type species: *Nonionina bulloides* d'Orbigny, 1846

Pullenia coryelli White, 1929

Plate IX, figs. 6a-c.

Pullenia coryelli White, 1929, p. 56, pl. 5, fig. 22.

Pullenia sphaeroides Cushman, 1927 (not d'Orbigny)

? *Nonionina bulloides* d'Orbigny, 1846, p. 127, pl. 5, figs. 9-10.

? *Pullenia bulloides* d'Orbigny, 1846 – Jones, 1994, p. 92, pl. 84, figs. 12-13.

Pullenia coryelli White (1929) – Tjalsma & Lohmann, 1983, p. 18, pl. 5, figs. 5a-b, Bolli et al., 1994, p. 151, figs. 41. 23-24, Alegret & Thomas, 2001, p. 296, pl. 10, fig. 4, Holbourn et al., 2013, p. 444, figs. 1-3.

Main features: Calcareous, planispiral test, subspherical in outline, sutures distincts and slightly depressed in some specimens. Typically 5 to 5½ chambers in the final whorl, surface smooth, aperture low and over the apertural face. Aperture an interio-marginal slit extending from one umbilicus to the other.

Remarks: Our specimens are similar to the plesiotypes of *Pullenia coryelli* White (CC 46786, 42023, 15462) deposited at Smithsonian Institution and to the holotype (FI-19928) of *Pullenia coryelli* of the American Museum of Natural History, NY. In the original description, White (1929) cited that the number of chambers in the last whorl is 6 or 7 chambers, and the holotype has 6 chambers, but the plesiotypes have 4 to 5½. Comparing plesiotypes of *Pullenia coryelli* White with topotypes (CC 39057, 39146, 43929, 57564) of *Pullenia bulloides* d'Orbigny from Miocene, Oligocene and Eocene specimens respectively, we note that they are similar, but *P. bulloides* has generally fewer chambers (4 per whorl), and the chambers are lower than in *P. coryelli*.

Stratigraphic distribution: This species is rare to common in the Maastrichtian of the Mucuri and Santos basins (NC23) and very rare to common in the lower to upper Paleocene at Sites 20C and 356 (CP1 to CP7).

Distribution chart #: 92.

Pullenia eocenica (Cushman & Siegfus, 1939)
Plate IX, figs. 7a-b.

Pullenia eocenica Cushman & Siegfus, 1939, p.31, pl. 7, fig. 1.

Pullenia eocenica Cushman & Siegfus, 1939 – Tjalsma & Lohmann, 1983, p. 36, pl. 16, fig. 1, Bolli et al., 1994, p. 152, figs. 41.29-30.

Main features: Calcareous, planispirally coiled test with smooth wall, broadly rounded, slightly depressed at umbilicus. Chambers distinct, inflated and normally five in the last whorl, sutures distinct and slightly depressed on both sides. Aperture an interio-marginal slit extending from one umbilicus to the other.

Remarks: Our specimens were compared with the holotype (CC 25485), plesiotypes (CC 61855, 64481, 64482) and hypotype (USNM 687538) of *Pullenia eocenica* Cushman & Siegfus. Comparing the types of *P. eocenica* Cushman & Siegfus with the holotype of *P. jarvisi* Cushman, and the plesiotypes of *P. coryelli* White reveals a progressive transition in outline of the tests, from more lobate to more inflated in cross section. The *P. jarvisi* Cushman has the most lobate outline (and could possibly a synonym of *P. quinqueloba* Reuss), progressing to fully rounded and inflated test of *P. coryelli* White (synonymous with *P. bulloides* d'Orbigny?) and with *P. eocenica* Cushman & Siegfus the transitional form.

Stratigraphic distribution: Rare specimens occur in the upper Paleocene and lower Eocene of the Pelotas Basin (CP8) and in the middle to upper Paleocene of Sites 356 and

20C (planktic foraminiferal biozones P3/P4). *P. eocenica* is rare to abundant in the Pelotas Basin and at Sites 356 and 20C in the lower to upper Eocene (CP8/9 to CP15).
Distribution chart #: 32.

Pullenia jarvisi (Cushman, 1936)
Plate IX, figs.8a-b.

Pullenia jarvisi Cushman, 1936, p. 77, pl. 13, fig. 6.

Pullenia jarvisi Cushman, 1936 – Bolli et al., 1994, p. 152, figs. 42.1-3, Alegret & Thomas, 2001, p. 298, pl. 10, fig. 6.

Pullenia quinqueloba Reuss, 1851 – Bolli et al., 1994, p. 152, figs. 41.31-32.

Main features: Test calcareous, planispiral much compressed, involute and biumbilicate, subcircular to lobate outline, periphery rounded, 5 chambers in the last whorl, somewhat inflated and increasing gradually in size as added. Sutures distinct, slightly curved and depressed. Aperture an interio-marginal slit extending from one umbilicus to the other.

Remarks: Our specimens were compared with the holotype (CC 15459) of *Pullenia jarvisi* Cushman. Bolli et al. (1994) affirm that it is difficult to separate specimens of *P. quinqueloba* Reuss from *P. jarvisi*, and Alegret & Thomas (2001) considered them as synonyms. We agreed to place them as possible synonyms, with the distinguishing characteristics that *P. jarvisi* is more lobate.

Stratigraphic range: This species is rare in the middle to upper Eocene (CP14 to CP15) of the Campos Basin.

Distribution chart #: 8.

Superfamily CHILOSTOMELLACEA Brady, 1881
Family CHILOSTOMELLIDAE Brady, 1881
Subfamily PALLAIMORPHININAE Loeblich & Tappan, 1988
Genus *Abyssamina* Schnitker and Tjalsma, 1980
Type species: *Abyssamina quadrata* Schnitker and Tjalsma, 1980

Abyssamina quadrata (Schnitker and Tjalsma, 1980)
Plate X, figs. 2a-b.

Abyssamina quadrata Schnitker and Tjalsma, 1980, p. 237, pl. 1, figs. 1-6.

Abyssamina quadrata Schnitker and Tjalsma, 1980 – Tjalsma & Lohmann, 1983, p. 22, pl. 4, fig. 5, pl. 19 – figs. 1-2, Van Morkhoven et al., 1986, p. 285-288, pl. 95, figs. 1-4, Holbourn et al., 2013, p. 18, figs. 1-3.

Main features: Test calcareous, quadrate and spheroidal in lateral view, streptospiral but almost planispiral, unequally involute with the dorsal side nearly involute but occasionally early chambers visible in the central area. Sutures radial, straight to slightly curved, depressed. Aperture as a narrow half crescentic slit extending from toward umbilicus.

Remarks: Our specimens were similar to the holotype (USNM 305103) and paratype (USNM 305104) of *Abyssamina quadrata* Schnitker and Tjalsma. Tjalsma & Lohmann (1983) discussed similarity with *Pullenia jarvis* Cushman. *A. quadrata* has almost planispiral coiling, but it is possible to see the proloculus on the slightly more evolute side. Schnitker and Tjalsma (1980) differentiate *A. quadrata* from *P. jarvisi* Cushman (upper Paleocene) based on slanted apertural face and asymmetrical placement of the aperture.

Stratigraphic distribution: This species is rare to common in the middle Paleocene to upper Eocene of Sites 20C and 356 (CP3 to CP15).

Distribution chart #: 34.

Family ALABAMINIDAE Hofker, 1951

Genus *Alabamina* Toulmin, 1941

Type species: *Alabamina wilcoxensis* Toulmin, 1941

Alabamina dissonata (Cushman & Renz, 1948)

Plate X, figs. 3a-b.

Pulvinulinella atlantisae Cushman var. *dissonata* Cushman & Renz, 1948, p. 35, pl. 7, figs. 3a-b, pl. 20, fig. 5.

Abyssamina quadrata (Cushman & Renz, 1948) – Tjalsma & Lohmann, 1983, p. 22, pl. 17 – figs. 3a-b, pl. 20, fig. 5, Van Morkhoven et al., 1986, p. 283, pl. 94A, figs. 1-3, pl. 94B, figs. 1-5, Bolli et al., 1994, p. 154, fig. 42.30, Holbourn et al., 2013, p. 22, figs. 1-5.

Main features: Test calcareous, trochospirally coiled with very acute and keeled periphery, tangential sutures on the evolute side and almost triangular chambers on the involute side, 5 to 6 chambers in the last whorl, aperture an elongate slit extending up the apertural face at acute angle to the base of the final chamber.

Remarks: Our specimens are similar to the holotype (CC 57353) and paratypes (CC 57354, 57355) at the Smithsonian Institution. They displays variability in having 5 to 6 chambers in the last whorl, with triangular chambers on the involute side and very oblique (tangential) sutures on the evolute side. The peripheral keel may not be well developed on the final chamber, as observed on the holotype and some of our specimens.

Stratigraphic distribution: This species is rare to abundant in the middle Paleocene to upper Eocene of the Sergipe-Alagoas, Santos, and Pelotas basins and at Sites 20C and 356 (CP15).

Distribution chart #: 29.

Alabamina midwayensis Brotzen, 1948

Plate X, figs. 4a-b.

Alabamina midwayensis Brotzen, 1948, p. 99, pl. 16, figs. 1-2.

Alabamina midwayensis Brotzen, 1948 – Bolli et al., 1994, p. 155, figs. 42.33-34.

Main features: Test calcareous, trochospiral, almost equally biconvex, peripheral margin bluntly subacute, 5 to 6 chambers in the last whorl, sutures almost straight, radial and slightly curved on the umbilical side. A small central filling may be present in the umbilicus. Aperture narrow, at an acute angle to the base of the last chamber, wall smooth mostly glossy.

Remarks: This species has a more circular outline than *Alabamina dissonata* Cushman & Renz. In addition, the peripheral margin of *A. midwayensis* is more subacute than that of *A. dissonata*, and it has more radial sutures on the involute side. Our specimens are similar to the paratypes of the USNM (643150, 471901, 471902) at the Smithsonian Institution.

Stratigraphic distribution: This species is rare to common in the Maastrichtian through upper Paleocene/lower Eocene (NC23 to CP8) of Sites 20C and 356.

Distribution chart #: 85.

Family OSANGULARIIDAE Loeblich & Tappan, 1964

Genus *Osangularia* Brotzen, 1940

Type species: *Osangularia lens* Brotzen, 1940

Osangularia mexicana (Cole, 1927)

Plate X, figs. 5a-b.

Pulvinulinella culter Parker & Jones var. *mexicana* Cole, 1927, p. 31, pl. 1, figs. 15-16.

Osangularia mexicana (Cole 1927) – Tjalsma & Lohmann, 1983, p. 35, pl. 20, fig. 6, Bolli et al., 1994, p. 157, figs. 43.30-32.

Main features: Test calcareous, trochospiral, biconvex, lenticular in profile, carinate periphery, spiral side evolute, sutures thickened, curved and oblique, umbilical side involute, sinuate and radial sutures, slightly depressed, ~13 to 14 chambers in the last whorl. Narrow peripheral flange, test wall finely perforate, smooth and glassy. Aperture at an acute angle to the base of the last chamber.

Remarks: Cole (1927) differentiates this species from other *Osangularia* species by its larger size, narrow flange, less pronounced ventral sutures, greater convexity and very smooth and glassy dorsal surface. Tjalsma & Lohmann (1983) report that this species is generally larger than *O. velascoensis* Cushman and has fewer chambers in the last whorl, a small umbilical mass and more oblique dorsal sutures. Our specimens resemble the paratypes (USNM 243215) of *Osangularia mexicana* Cole. This species differs from *O. expansa* Toulmin on having more number of chambers in the last whorl (paratypes 11 to 12, our specimens 11) and more straight sutures on the umbilical side. Bolli et al., 1994 differentiates *O. mexicana* from *O. expansa* in its slightly larger size and greater number of chambers in the last whorl (8½ -11 against 7-9).

Stratigraphic range: This species occurs from lower to upper Eocene (CP9 to CP15) and it is very rare to common in the Campos and Santos basins and at Site 20C and very abundant at Site 356.

Distribution chart #: 17.

Osangularia plummerae (Brotzen, 1940)
Plate X, figs. 6a-c.

Osangularia plummerae Brotzen, 1940, p. 30, text-fig. 8.

Parrella expansa Toulmin, 1941, p. 604, text-fig. 3.

Osangularia expansa Toulmin, 1941 – Bolli et al., 1994, p. 156, figs. 43.20, 25-26.

Osangularia plummerae Brotzen, 1940 – Alegret & Thomas, 2001, p. 292, pl. 9, fig. 11.

Main features: Test calcareous, trochospiral, assymmetrically biconvex to planoconvex to low biconvex, subcircular outline with acute periphery formed by flange. Dorsal side nearly flat to convex with all chambers visible, sutures oblique and slightly elevated, spiral suture limbate. Ventral side convex, ~8 chambers in the last whorl, sutures radial and limbate in the earlier portion, depressed between the last chambers. Aperture consist of two slits, one extending obliquely from the base of the last chamber to the periphery across the apertural face, and the second slit forming an angle with the first one extending toward the umbilical area.

Remarks: Our specimens were compared with the paratypes (CC 38531) of *Osangularia expansa* Toulmin, which is an objective synonym of *O. plummerae* Brotzen, and both names were proposed as *nomina nova* for *Truncatulina culter* Plummer, not Parker & Jones (Alegret & Thomas, 2001). This species differs from *O. mexicana* Cushman by having less chambers (paratypes 6 to 7, our specimens 8) in the last whorl and more curved sutures on the umbilical side.

Stratigraphic range: This species is rare to common in the Pelotas Basin from the upper Paleocene through lower Eocene (CP8 to CP9).

Distribution chart #: 71.

Osangularia velascoensis (Cushman, 1925)
Plate X, fig. 7.

Truncatulina velascoensis Cushman, 1925, p. 20, pl. 3, figs. 2a-c.

Osangularia velascoensis (Cushman, 1925) – Tjalsma & Lohmann, 1983, p. 18, pl. 7, fig. 14, Alegret & Thomas, 2001, p. 292, pl. 9, fig. 12, Holbourn et al., 2013, p. 388, figs. 1-2.

Main features: Test calcareous, trochospiral, biconvex, nearly symmetrical. Periphery sharp with broad and flange, all chambers visible in the dorsal side, ~10 in the last whorl. Ventral side with sutures slightly depressed. Aperture narrow and elongate, visible on the ventral side.

Remarks: Alegret & Thomas (2001) differentiate this species from *O. plummerae* Brotzen by being more biconvex and having a wider keel.

Stratigraphic range: This species is very rare in the Campos Basin and Site 20C and common at Site 356 from the lower to upper Paleocene (CP1 to CP7/8, Planktic foraminifera biozones P1 to P5/E1).

Distribution chart #: 83.

Family ORIDORSALIDAE Loeblich & Tappan, 1984

Genus *Oridorsalis* Andersen, 1961
Type species: *Oridorsalis westi* Andersen, 1961

Oridorsalis umbonatus (Reuss, 1851)
Plate X, figs. 8a-c.

Rotalina umbonata Reuss, 1851, p. 75, pl. 5, fig. 35.

Oridorsalis umbonatus (Reuss, 1851) – Tjalsma & Lohmann, 1983, p. 18, pl. 6, figs. 8a-b, Bolli et al., 1994, p. 246, figs. 58.10-13, Alegret & Thomas, 2001, p. 291, pl. 9, figs. 8-9, Holbourn et al., 2013, p. 384, figs. 1-3.

Main features: Calcareous and trochospiral test, biconvex with subacute periphery and somewhat lobate outline. Spiral side evolute with distinct and straight sutures, umbilical side involute and with 5 to 6 chambers in the last whorl, umbo slightly elevated at the central portion of the test. Secondary apertures located at intersection of spiral and radial sutures on the spiral side are poorly developed.

Remarks: Our specimens are similar to the types (CC 54070, 54065, USNM 110789) of *Eponides umbonata* Reuss from the Miocene and Recent at Smithsonian Institution.

Stratigraphic range: This species occurs in all locations but with variable abundances, it is very rare to rare in the Pelotas, Campos and Sergipe-Alagoas basins, rare in the Santos Basins, rare to common in the Mucuri Basin and common to very abundant at Sites 20C and 356 from the Maastrichtian through the upper Eocene (NC23 to CP15).

Distribution chart #: 38.

Family HETEROLEPIDAE Gonzáles-Donoso, 1969
Genus *Anomalinoides* Brotzen, 1942
Type species: *Anomalinoides plummerae* Brotzen, 1942 =
Anomalinoides pinguis P.H. Jennings, 1936

Anomalinoides capitatus (Gümbel, 1868)
Plate XI, figs. 1a-b.

Rotalia capitata Gümbel, 1868, p. 653, pl. 2, fig. 92.

Anomalina rubiginosa Cushman, 1926, p. 607, pl. 21, fig. 6.

Anomalina dorri Cole aragonensis Nuttall, 1930, p. 291, pl. 24, fig. 18, pl. 25, fig. 1.

Anomalina dorri Cole aragonensis Nuttall, 1930 – Bolli et al., 1994, p. 157, figs. 44,3-5.

Gavelinella capitata (Gümbel, 1868) – Tjalsma & Lohmann, 1983, plate 16, figs. 4a-5b.

Anomalinoides rubiginosus Cushman, 1926 – Van Morkhoven et al., 1986, pg. 366, pl. 119, figs. 1a-c, 2a-b, Bolli et al., 1994, p. 157, figs. 44.6, 13, 18-19, Holbourn et al., p. 54, figs. 1-3.

Anomalinoides capitatus (Gümbel, 1868) - Holbourn et al., p. 50, figs. 1-6.

Main features: Test calcareous, almost planispiral, plano-convex, very coarsely perforate wall on both sides, spiral side flattened, umbilical side more convex, periphery broadly rounded, almost circular outline somewhat lobate on the last three chambers. Spiral side

evolute with straight depressed sutures becoming slightly curved on the last chambers. The number of chambers in the last whorl varies from 6 to 9. Secondary growth of calcite material covers the central part on the spiral side, possibly hiding the chambers in the earlier whorls. Sutures curved and depressed on the umbilical side, small open umbilicus, chambers wall with roughened surface in the last whorl and protruding last chamber on the involute side. Aperture an interior marginal arch, extending from the periphery onto the umbilical side.

Remarks: Tjalsma & Lohmann (1983) named this species as *Gavelinella capitata* (Gümbel) and considered *Gavelinella (Rotalia) capitata* Gümbel, *Anomalina rubiginosa* Cushman (1926), *Anomalina dorri* Cole (1928), *Anomalina dorri* Cole *aragonensis* Nuttall (1930) as synonyms. Van Morkhoven et al. (1986) considered *Anomalina dorri* Cole var. *aragonensis* Nuttall as a synonym of *Rotalia capitata* Gümbel, and *Anomalina rubiginosa* Cushman as a separate species, which they called *Anomalinoides rubiginosus* Cushman. Comparison of the holotype (CC 5226), topotype (CC 38927) and several plesiotypes (CC 15634, 42771, 42085, 48121, 46800, 41933, 46802, USNM 559735, 627322) of *Anomalina rubiginosa* Cushman with cotypes of *Anomalina dorri* Cole var. *aragonensis* Nuttall (CC 59511, 59512) clearly shows the similarity among these taxa. The holotype and topotypes of *A. rubiginosa* Cushman are moderately to poorly preserved, with their last chambers probably affected by dissolution. Some of the cotypes of the Nuttall species seem to have overgrowths of calcite on the initial part of the chamber. The plesiotypes are much better preserved, with a good preservation of the pitted area around the umbilicus. The holotype of *Rotalia capitata* Gümbel was originally deposited in the collections of the Institute for Historical Geology and Paleontology of University Munich and destroyed during the World War II. Since Van Morkhoven et al. (1986) considered *Anomalina dorri* Cole var. *aragonensis* Nuttall as a synonym of *Rotalia capitata* Gümbel and *Anomalina dorri* Cole var. *aragonensis* Nuttall and compare these with the holotype and other types of *Anomalina rubiginosa* Cushman. We consider all these species synonyms, and use the name *Anomalinoides capitatus* Gümbel, as first described.

Stratigraphic distribution: This species is very rare to rare in the upper Paleocene throughout upper Eocene (CP3 to CP15) in all locations, with an exception of Pelotas Basin (rare to common).

Distribution chart #: 36.

Anomalinoides garzaensis Cushman & Siegfus, 1939
Plate X, figs. 2a-c.

Anomalina garzaensis Cushman & Siegfus (1939), p. 32, pl. 7, fig. 3.

Main features: Test calcareous, almost planispiral somewhat depressed in the central portion of both sides, wall distinctly perforate, rounded periphery, numerous and narrow and long chambers in the last whorl (11 to 15), increasing gradually in size, curved sutures distinct on both sides becoming slightly limbate and thicker on the initial chambers of the last whorl. Aperture a small slit at the base of the last chamber.

Remarks: The holotype of *Anomalinoides garzaensis* Cushman & Siegfus is missing. Our specimens were compared with the paratypes (Ruby 1 and 3, Shaw 10 and 23, Mohr 72) in the Cushman Collection at Smithsonian Institution, from the Eocene upper part of Lower Agua Fresca Formation. Differs from *Anomalina alazanensis* Nuttall (Holotype CC 16461, paratypes 16463) by its more rounded periphery, less limbate sutures and less flattened ventral side.

Stratigraphic distribution: This species is rare to common in two of the basins: Pelotas and Santos, from the upper Paleocene to the upper Eocene (CP8 to CP15).

Distribution chart #: 22.

Anomalinoides praeacuta (Vasilenko, 1950)

Plate X, figs. 3a-c.

Anomalina praeacuta Vasilenko, 1950, p. 208, pl. 5, figs. 2a-3.

Anomalina praeacuta Vasilenko, 1950 – Tjalsma & Lohmann, 1983, p. 4, pl. 4, fig. 10, pl. 7, figs. 8a-b.

Main features: Test calcareous, almost planispiral, symmetrically convex, periphery rounded. Ventral side tightly coiled, 14 to 15 chambers in the last whorl, small umbilicus covered by a raised boss. Chambers somewhat triangular, narrow and strongly drawn out in the direction of coiling, sutures tapering toward the periphery. Test wall transparent, perforate, aperture extending onto the ventral side, with narrow lip.

Remarks: We could not have access to the holotype of *Anomalinoides praeacuta* Vasilenko which is deposited in the collection of All-Union Petroleum-Leningrad, but in the original description the author designed *Anomalina acuta* Plummer as synonym. Our specimens are similar to the hypotypes (USNM 492191, 492192) and plesiotypes (CC 38213, 46434) of *Anomalina acuta* Plummer preserved in the Cushman Collection at Smithsonian Institution.

Stratigraphic distribution: This species occurs from the middle Paleocene to lower Eocene (CP3 to CP9) and it is very rare to rare in the Mucuri and Campos basins and common at Sites 20C and 356.

Distribution chart #: 72.

Anomalinoides welleri (Plummer, 1926)

Plate X, figs. 4a-b.

Truncatulina welleri Plummer, 1926, p. 143, pl. 9, fig. 6.

Anomalinoides welleri Plummer, 1926 – Bolli et al., 1994, p. 158, figs. 44. 23-25.

Main features: Test calcareous, almost planispiral, equally biconvex, laterally considerable compressed, periphery eubounded, chambers narrow and curved, 10 to 11 chambers in the final whorl. Sutures distinct, narrow, tapering, slightly elevate, small umbilical depression, aperture as a low arch.

Remarks: Our specimens are similar to the hypotypes of *Anomalinoidea welleri* Plummer in the Browne and Herrick Collection (1963) at the Smithsonian Institution (639164, 639165) – Paleocene samples.

Stratigraphic distribution: This species is very rare to rare at Site 20C from the upper Paleocene to upper Eocene (CP8 to CP15, Planktic foraminifera biozones E2/E3 to E15).

Distribution chart #: 48.

Family GAVELINELLIACE Hofker, 1956
Subfamily GYROIDINOIDINAE Saidova, 1981
Genus *Gyroidinoidea* Brotzen, 1942
Type species: *Rotalia nitida* Reuss, 1844

Gyroidinoidea beisseli (White, 1928) emend Alegret & Thomas, 2001
Plate XII, figs. 1a-c.

Gyroidina beisseli White, 1928, p. 291-292, pl. 39, figs. 7a-c.

Gyroidina comma White, 1928, p. 292, pl. 39, figs. 8a-c.

Gyroidina mendezensis White, 1928, p. 293, pl. 40, figs. 4a-c.

Gyroidina nitida Reuss, 1851 – White, 1928, pl. 40, figs. 6a-c.

Gyroidina simplex White, 1928, p. 296, pl. 40, fig. 7.

Gyroidina sparski White, 1928, p. 297, pl. 40, fig. 8.

Gyroidina vortex White, 1928, p. 297, pl. 40, figs. 9a-c.

Gyroidina nitida (Reuss) – Morrow, 1934, p. 197, pl. 30, figs. 1a-c. -
Cushman 1946, p. 140, pl. 58, fig. 5.

Eponides bollii Cushman & Renz, 1946, p. 44, pl. 7, figs. 23-25.

Gyroidinoidea nitidus (Reuss) – Sliter, 1968, p. 121, pl. 22, figs. 7a-c.

Gyroidinoidea (Rotalina) nitidus (Reuss) – Loeblich & Tappan, 1988, p. 633, pl. 713,
figs. 7-9.

Oridorsalis nitidus (Reuss) – Thomas, 1990, p. 590, pl. 3, figs. 7-9.

Gyroidinoidea bollii (Cushman and Renz) – Kaiho, 1998, p. 292, pl. 1, fig. 2.

Gyroidina beisseli White, 1928 emend Alegret & Thomas 2001, p. 286, pl. 7, figs. 1-10.

Main features: Test calcareous, trochospiral coiling with considerable variability from planoconvex to almost biconvex, subcircular outline, subangular periphery. Dorsal side nearly flat to slightly convex, sutures curved not limbate, 6 to 8 chambers in the last whorl, central part of the dorsal side often covered with thick secondary layer, ventral side with radial and indistinct sutures. Umbilicus very narrow, open to hidden, aperture a slit at the middle of the base of the last chamber.

Remarks: Alegret & Thomas (2001) investigated various species of *Gyroidinoidea* and identified several intermediate species between *G. beisseli* White and *G. goudkoffii* (Trujillo). They defined *G. beisseli* on having subangular periphery, sometimes angular to subangular edge. Our specimens are similar to the plesiotypes of *G. beisseli* White (CC 46768, 48104) at Smithsonian Institution and holotype and paratypes of *G. beisseli* White (19897) at American Natural History Museum, NY, considering within the rather broad range of variation typical of this species.

Stratigraphic distribution: This species is rare to common in the middle Paleocene through upper Eocene of the Mucuri, Campos and Pelotas basins and at Site 20C (CP3/4 to CP15).

Distribution chart #: 35.

Gyroidinoides depressus (Alth, 1850)

Plate XII, fig. 2.

Rotalina depressa Alth, 1850, p. 266, pl. 13, fig. 21.

Gyroidinoides depressus (Alth, 1850) – Bolli et al., 1994, p. 159, figs. 44. 29-30, 32-34; Alegret & Thomas, 2001, p. 287, pl. 6, fig. 9.

Main features: Test calcareous, trochospiral, compressed, rounded periphery. Dorsal side flat to slightly convex, evolute with curved and depressed sutures. Ventral side convex with depressed umbo, sutures almost straight. Last whorl with 8 to 9 chambers, later ones somewhat inflated. Aperture as a lip extending from the periphery to the umbilicus.

Remarks: Alegret & Thomas (2001) compare several species of *Gyroidinoides* and they found that *G. depressus* Alth is distinguished from others by its flat, rounded periphery and depressed umbo. We examined some types (CC 33803, 33818) from the Cushman Collection at the Smithsonian Institution and they are similar.

Stratigraphic distribution: This species is very rare in the lower Eocene (CP8 to CP9) of the Site 20C.

Distribution chart #: 70.

Gyroidinoides girardanus (Reuss, 1851)

Plate XII, figs. 3a-c.

Rotalina girardana Reuss, 1851, p. 73, pl. 5, fig. 34.

Gyroidinoides girardanus (Reuss, 1851) – Alegret & Thomas, 2001, p. 287, pl. 6, fig. 10.

Main features: Test calcareous, trochospiral planoconvex, periphery subangled at the dorsal edge. Dorsal side flattened or slightly concave, ventral side strongly convex with an open umbilical area. Chambers distinct with radial and depressed sutures on both sides. Aperture low slit between the periphery and the umbilicus. Alegret & Thomas (2001) describe the shape of the apertural face is very typical in this species, flaring out a somewhat concave shape along the dorsal side.

Remarks: We examined plesiotypes (CC 16479, 59488) of *Gyroidinoides girardanus* Reuss at the Smithsonian Institute.

Stratigraphic range: This species is very rare in the upper Eocene of the Pelotas Basin (CP15).

Distribution chart #: 2.

Gyroidinoides globosus (Hagenow, 1842) emend Alegret & Thomas, 2001
Plate XII, figs. 4a-b.

Nonionina globosa Hagenow, 1842, p. 574.

Rotalina nitida Reuss, 1845, p. 35, pl. 8, fig. 52, pl. 12, figs. 8, 20.

Gyroidina nitida (Reuss, 1845) – White, 1928, p. 296, pl. 40, figs. 6a-c.

Gyroidinoides globosus (Hagenow, 1842) – Tjalsma & Lohmann, 1983, p. 14, pl. 7, fig. 5, Van Morkhoven et al., 1986, p. 329, 330, pl. 107, Alegret & Thomas, 2001, p. 288, pl. 8, figs. 1-5.

Main features: Test calcareous, trochospiral, globular and inflated, unequally biconvex, subcircular in outline, periphery broadly rounded. Dorsal side slightly convex, sutures distinct almost straight. Umbilical side strongly convex, 6 to 7 chambers in the last whorl, somewhat inflates and often lobate outline in the last chambers. Large apertural face with slit-like aperture.

Remarks: Alegret & Thomas (2001) discuss about the confusion in the literature between *G. globosus* Hagenow and *G. nitidus* Reuss. They argue that there is considerable overlap in morphology between the lectotype and paralectotypes of *G. nitidus* Reuss and the original description of *G. globosus* Hagenow in the Ellis and Messina Catalogue. We agreed that our specimens show considerable variability in lobateness of the last chambers and the roundness of the periphery. Alegret & Thomas (2001) considered *G. naranjoensis* White a junior synonym of *G. globosus* Hagenow and the specimens with bluntly angled periphery were placed in *G. beisseli* White, specimens with a very sharp periphery in *G. goudkoffi* Trujillo. Comparing our specimens with several secondary types (CC 33694, 33702, 33717, 33347, 33748) of *Gyroidinoides globosus* Hagenow in the Cushman Collection and with synonym *Rotalia nitida* Reuss' original collection (selected by F. Rögl for the USNM collection), we decided to place them in *G. globosus* Hagenow. Alegret & Thomas (2001) differentiate *G. globosus* Hagenow from other *Gyroidinoides* by its typical globular, unequally convex test and the interiomarginal slit-like aperture, as well as the low and broad apertural face (about 4 times as broad as high), and we agree with this distinction.

Stratigraphical range: This species was found from the Maastrichtian through the upper Paleocene (NC23 to CP9/10, Planktic foraminifera biozones P0 to E4), it is rare to common in the Sergipe-Alagoas, Mucuri, Campos, and Santos basins, and common at Sites 20C and 356. In our samples, this species ranged into the lower Eocene (Nannofossil biozone CP10, Planktic foraminifera biozone E5) at Site 20C, but usually becomes extinct at the end of the Paleocene (Thomas, 1998).

Distribution chart #: 69.

Gyroidinoides quadratus (Cushman & Church, 1929)
Plate XII, figs. 5a-c.

Gyroidina quadrata Cushman & Church, 1929, p. 516, pl. 41, figs. 7-9.

Gyroidinoides quadrata (Cushman & Church, 1929) – Bolli et al., 1994, p. 160, figs. 45. 19-21, Holbourn et al., 2013, p. 276, figs. 1-3.

Main features: Test calcareous, trochospiral coiling, 6 chambers in the last whorl, dorsal side concave with depressed spiral suture, ventral side strongly convex with peripheral view nearly quadrate. Aperture ventral between the umbilicus and the periphery.

Remarks: The main diagnostic characteristics of this species are the quadrate shape in side view, concave dorsal side and deeply excavated spiral suture.

Stratigraphic range: This species is very rare to rare in the middle Paleocene through the upper Eocene (CP5 to CP15) in the Mucuri, Santos and Pelotas basins. In the deep-sea, it generally becomes extinct at the end of the Paleocene (Thomas, 1998).

Distribution chart #: 28.

Gyroidinoides subangulatus (Plummer, 1926)

Plate XII, figs. 6a-c.

Rotalia soldanii d'Orbigny var. *subangulata* Plummer, 1926, p. 154, pl. 12, figs. 1a-c.

Gyroidinoides subangulatus (Plummer, 1926) – Alegret & Thomas, 2001, p. 289, pl. 6, fig. 11.

Main features: Test small, trochospiral almost planoconvex with periphery angular. Dorsal side flat to somewhat concave, sutures oblique, ventral side strongly convex with about two convolutions, 8 to 9 chambers in the last whorl, sutures slightly depressed between the last chambers on both sides and around the small umbilicus, otherwise faintly limbate moderately oblique dorsally and radiate ventrally. Test wall smooth and finely perforate, aperture a long narrow slit extending into the umbilicus.

Remarks: Our specimens are similar to several secondary types of *Gyroidinoides subangulatus* Plummer in the Cushman Collection at Smithsonian Institution (CC 58040, 46418, 4150).

Stratigraphic range: This species is very rare to rare in the Sergipe-Alagoas, Campos, Santos and Pelotas basins and at Site 20C, from the upper Paleocene through the upper Eocene (CP3 to CP15, planktic foraminifera biozones P3 to E15).

Distribution chart #: 49.

Genus *Stensioeina* Brotzen, 1936

Type species: *Rotalia exsculpta* Reuss, 1860

Stensioeina beccariiformis (White, 1928)

Plate X, figs. 5a-c.

Rotalia beccariiformis White, 1928, p.287, pl. 39, figs. 2a-c.

Anomalina beccariiformis (White, 1928) – Cushman & Renz, 1946, p. 48, pl. 8, figs. 21-22.

Gavelinella beccariiformis (White, 1928) – Tjalsma & Lohmann, 1983, p. 12, pl. 6, figs. 1a-3b, Bolli et al., 1994, p. 161, figs. 46.4-6

Stensioeina beccariiformis (White, 1928) – Van Morkhoven et al., 1986, p. 347, pl. 113A-B, Alegret & Thomas, 2001, p. 306, pl. 1, figs. 10-12, Holbourn et al., 2013, p. 526, figs. 1-3.

Main features: Test calcareous, trochospiral, biconvex with rounded periphery, spiral side smooth, relatively flat and finely perforate, sutures flush and gently curved, ventral side slightly convex with a narrow umbilicus, which is closely covered by an outgrowth of the final chamber. The ornamentation around the umbilicus radiates irregularly from the central area, to thick depressed lines. The ventral side is more coarsely and irregularly perforate than the dorsal side. The aperture extends from the periphery to the umbilicus at the base of the last chamber.

Remarks: We compared our specimens with the holotype of the species' two varieties (var. A AMNH 19892, var. B AMNH 19893) of White Collection at AMNH, NY and plesiotypes of *Anomalina beccariiformis* White (CC 46805, 46806) in the Cushman Collection at Smithsonian Institution and agreed to assign them in *S. beccariiformis*.

Stratigraphic range: This species occurs in the Maastrichtian through the upper Paleocene (NC23 to CP8, planktic foraminifera biozones P0 to P5/E1), and it is common in the Sergipe-Alagoas Basin, abundant in the Mucuri Basin, common to abundant in the Santos Basin and at Site 20C and common to very abundant in the Campos Basin and at Site 356. Its maximum abundances occurred in the middle Paleocene (~45%, CP3 to CP4). Its extinction at the end of the Paleocene (CP8) is one of the markers of the Benthic Extinction Event (BEE) at the base of the Paleocene-Eocene Thermal Maximum (PETM) (Tjalsma & Lohmann, 1983, Van Morkhoven et al., 1986, Berggren & Miller, 1989, Thomas and Shackleton, 1996, Thomas, 1989, 1990, 1998, 2000, 2003, 2007, Nomura, 2005, Wing et al., 2005, Alegret & Ortiz, 2006, Hancock et al., 2006, Alegret et al., 2009, Sluijs et al., 2011, d'Haenens et al., 2012).

Distribution chart #: 84.

Subfamily GAVELINELLINAE Hofker, 1956

Genus *Hanzawaia* Asano, 1944

Type species: *Hanzawaia nipponica* Asano, 1944

Hanzawaia ammophila (Gümbel, 1868)

Plate X, figs. 7a-c.

Rotalia ammophila Gümbel, 1868, p. 652, pl. 2, fig. 90a-b.

Cibicides cushmani Nuttall, 1930, p. 291, pl. 25, figs. 3, 5, 6.

Hanzawaia cushmani Nuttall, 1930 – Tjalsma & Lohmann, 1983, p. 32, pl. 17, figs. 1a-c.

Hanzawaia ammophila Gümbel, 1868 – Van Morkhoven et al., 1986, p. 168, pl. 56, Holbourn et al., 2013, p. 280, figs. 1-3.

Main features: Test calcareous, trochospiral, subrounded to subacute in edge view, slightly convex on spiral side, flattened towards the middle and slightly depressed, ~15 very narrow and curved chambers in the last whorl, separated by strongly curved and limbate sutures. Umbilical side flat, sutures slightly depressed. Test wall smooth and

glassy, aperture extending from the periphery to the umbilicus under umbilical flaps. The strongly curved and thick sutures, narrow and curved chambers and rounded periphery are the main characteristics of this species. Some specimens have a clear boss in the central area of the spiral side.

Remarks: Tjalsma & Lohmann (1983) do not consider *H. cushmani* Nuttall and *H. ammophila* Gümbel synonyms because they think that *H. ammophila* shows a more rapidly uncoiling spire, resulting in a flatter test than in *H. cushmani*. Van Morkhoven et al. (1986) designated a lectotype of *Cibicides cushmani* Nuttall, and follow Hagn (1956) in considering *C. cushmani* Nuttall a junior synonym of *Rotalia ammophila* Gümbel. We also consider *C. cushmani* Nuttall as a synonym of *Rotalia ammophila* Gümbel, and place it in the genus *Hanzawaia*. Our specimens resemble the cotypes (CC 59514, USNM 369259, 369260), paratypes (CC 57300, 57185, 57576) and plesiotypes (CC 26224, 57575) of *Cibicides cushmani* Nuttall at Smithsonian Institution. The rapidly uncoiling spire, which results in a flatter test, is seen in some specimens of both species, characterizing them as morphotypes of the same species.

Stratigraphic distribution: *H. ammophila* is rare to abundant in the upper Paleocene through the upper Eocene (CP8 to CP15) in the Campos and Sergipe-Alagoas basins and at Sites 20C and 356.

Distribution chart #: 27.

Hanzawaia mantaensis (Galloway & Morrey, 1929)
Plate X, figs. 8a-c.

Anomalina mantaensis Galloway and Morrey, 1929, p. 28, pl. 4, figs. 5a-c.

Hanzawaia mantaensis Galloway and Morrey, 1929 – Van Morkhoven et al., 1986, p. 8, pl. 32, Holbourn et al., 2013, p. 284, figs. 1-2.

Main features: This is a very distinct form with a calcareous test, trochospiral coiling, asymmetrical biconvex in edge view, with dorsal side flat and ventral side convex, ~10 chambers in the last whorl, thick and limbate periphery and clear umbilical boss, narrow, limbate and strongly curved sutures. Aperture at the base of the chamber toward the spire.

Remarks: Our specimens resemble with the plesiotype (USNM 625070) in its limbate sutures and very narrow and curved chambers.

Stratigraphic distribution: This species is common in the Pelotas Basin from the lower through middle Eocene (CP10 to CP12).

Distribution chart #: 63.

Genus *Paralabamina* Hansen, 1970
Type species: *Eponides lunata* Brotzen, 1948

Paralabamina lunata (Brotzen, 1948)
Plate X, figs. 6a-c.

Eponides lunata Brotzen (1948), p. 77, pl. 10, figs. 17-18.

Neoeponides cf. *lunata* (Brotzen, 1948) – Tjalsma & Lohmann, 1983, p. 16, pl. 7, figs. 10a-b.

Paralabamina lunata (Brotzen, 1948) – Alegret & Thomas, 2001, p. 294, pl. 9, fig. 14.

Main features: Test calcareous, trochospiral, unequally biconvex with umbilical side often higher than the spiral side, uneven lenticular in cross section. Periphery sharply acute with a hyaline border, outline lobate. Spiral side evolute, with crescent-shaped chambers and sutures between the last two or three somewhat depressed, umbilical side involute, chambers slightly inflated, sutures curved, depressed, 6 to 7 in the last whorl. Aperture under a narrow lip, wall smooth, very finely perforate.

Remarks: Our specimens are similar to the hypotypes (CC 58021, 547476, 547477) of *P. lunata* Brotzen in the Cushman Collection at Smithsonian Institute. Some of our specimens have slightly less lobate outline, but they comprise the most important features of this species: biconvex test, dorsal side evolute, more convex than the involute ventral side with often 6 chambers in the last whorl, sutures oblique on the evolute side and radial and almost straight on the involute side. Tjalsma & Lohmann (1983) reported some variability in the number of chambers in the last whorl (8 instead of 6-7), non-depressed and limbate sutures on the ventral side, which radiate more or less straight from a small umbilical boss to the periphery.

Stratigraphic range: This species has been reported to be extinct at the end of the Paleocene (Tjalsma & Lohmann, 1983, Alegret & Thomas, 2001), however we found them in the Brazilian marginal basins and at DSDP Site 20C. It is rare to abundant in the Sergipe-Alagoas, Santos and Pelotas basins and very rare at Site 20C from the lower to upper Eocene (CP8 to CP15).

Distribution chart #: 23.

Class INCERTAE SEDIS Pawlowski et al., 2013
Order LAGENINA Delage and Hérouard, 1896
Family VAGINULINIDAE Reuss, 1860
Subfamily LENTICULININAE Chapman, Parr & Collins, 1934
Genus *Lenticulina* Lamarck, 1804
Type species: *Lenticulites rotulatus* Lamark, 1804

Lenticulina whitei Tjalsma & Lohmann, 1983
Plate XII, fig. 7.

Lenticulina whitei Tjalsma & Lohmann, 1983, p. 15, pl. 7, figs. 1a-b.

Main features: Test calcareous, planispiral, with smooth wall and thin keel, which is less distinct in the last chamber, outline in axial view biumbonate and thin lenticular. Triangular apertural face and heart-shaped, bounded laterally by subacute rims. Five to six chambers in the last whorl increasing gradually in size, sutures flush and strongly curved, aperture as small opening at peripheral end.

Stratigraphic range: This species is very rare in the Santos Basin from the middle Paleocene (CP5), and very rare to common in the lower to middle Paleocene (CP1 to CP3) at Site 356.

Distribution chart #: 107.

Subfamily PALMULINAE Saidova, 1981
Genus *Neoflabellina* Barstenstein, 1948
Type species: *Flabellina rugosa* d'Orbigny, 1840

Neoflabellina semireticulata (Cushman & Jarvis, 1928)
Plate XII, fig. 8.

Flabellina semireticulata Cushman & Jarvis, 1928, p. 98, pl. 13, fig. 14.

Neoflabellina semireticulata (Cushman & Jarvis, 1928) – Tjalsma & Lohmann, 1983, p. 16, pl. 2, fig.9.

Main features: Test calcareous, early stage is a planispiral coil, later flaring and astacolite, finally uniserial and rectilinear, with very broad and low, inverted V-shaped chambers, rhomboid in front view, laterally compressed and with chambers obscured by the ornamented surface which consist of more or less irregular reticulation, aperture is a neck at the end of the last chambers.

Remarks: Our specimens resemble the holotype (CC 9227) of *Neoflabellina semireticulata* Cushman & Jarvis. Differs from *N. reticulata* by having smaller and irregular reticulate ornamentation (Cushman & Jarvis, 1928).

Stratigraphic range: This species is very rare in the Santos Basin and at Site 356 in the lower to the middle Paleocene (CP3 to CP5).

Distribution chart #: 108.

CHAPTER 3

UPPER MAASTRICHTIAN – EOCENE BENTHIC FORAMINIFERAL BIOFACIES IN THE BRAZILIAN MARGIN, WESTERN SOUTH ATLANTIC

DE MELLO, RENATA MOURA^{1,2,*}, LECKIE, R.M.¹, THOMAS, E.³

¹ Department of Geosciences, University of Massachusetts, 611 N. Pleasant St., Amherst, MA 01003, USA

² PETROBRAS Research and Development Center, Av. Horacio de Macedo 950, Ilha do Fundão, Rio de Janeiro, RJ 21941-915, Brazil

³ Department of Geology and Geophysics, Yale University, New Haven, CT 06520-8109, U.S.A.

* Correspondence author: renatamouramello@yahoo.com.br.

3.1 – ABSTRACT:

Benthic foraminiferal biofacies were delimited for the upper Maastrichtian through upper Eocene of five Brazilian marginal basins (Sergipe-Alagoas, Mucuri, Campos, Santos and Pelotas) and two DSDP Sites 356 and 20C of the western South Atlantic.

The biofacies were determined based on the benthic foraminiferal assemblages and associated parameters, including percentage of planktic foraminifera (% planktics), lithology, and percentage of radiolarians (% rads). The major biofacies groups are not composed of exactly the same taxa due to basin-to-basin differences (niches). The biofacies are primarily distinguished by the agglutinated/calcareous taxon percentage and the dominant three or four species for each biofacies. **Biofacies A** is composed 100% of calcareous taxa and predominates in the Eocene. **Biofacies B** has up to 10% agglutinated taxa and occurs from the middle Paleocene through upper Eocene. **Biofacies C** has 11% to 25% agglutinated taxa in its composition and is recorded from the upper Maastrichtian through upper Eocene. **Biofacies D** contains a more balanced percentage of calcareous

and agglutinated taxa (~50 % each) and is always associated with Biofacies E in the marginal basins. **Biofacies E** is dominated by agglutinated taxa, especially tubular forms (*Bathysiphon*, *Nothia*, *Rhizammina*, *Psammosiphonella*). This biofacies correlates with the so-called “flysch-type” biofacies of Berggren and Gradstein (1981) and it occurs exclusively in the marginal basins from the Maastrichtian through upper Eocene, although predominates in the Paleocene.

The biofacies distribution reveals distinct environmental settings as the Brazilian margin built outwards in response to tectonic activity and increased terrigenous input. The biofacies record a deep-water setting close to or below the calcite compensate depth (CCD) during the Maastrichtian-Paleocene along the entire eastern Brazilian margin. Progradation of the shelf and shoaling of the slope during the Eocene is the principal reason for the abrupt change from agglutinant-rich biofacies (E and D) to calcareous-rich biofacies (A, B, and C) in the early Eocene. The Campos Basin continued to record abyssal to lower bathyal conditions while the Sergipe-Alagoas and Mucuri basins shoaled to neritic paleodepths by late Eocene time. Changes in relative sea level, including a global sea level fall in the late Paleocene followed by global sea level rise in the early Eocene, as well as changes in the position of the CCD along the Brazilian margin also affected the development of foraminiferal biofacies in the marginal basins. Although the distal DSDP sites were at deeper paleodepths, they were never below the CCD during the Maastrichtian-Eocene and were dominated by calcareous benthic biofacies. These findings suggest that the CCD shoaled along the productive Brazilian continental due to the greater flux of organic matter.

3.2 – INTRODUCTION:

Biofacies are discrete stratigraphic units based on microfossil content, which differs significantly from units above and/or below. Biofacies are recognized in stratigraphic sequences and can be used as mappable horizons in seismic profiles (Fillon, 2009). In this study, benthic foraminiferal assemblages are the microfossil content used in the study of the Brazilian marginal basins.

Benthic foraminiferal biofacies analysis has proven to be a powerful tool for paleoenvironment and paleoecologic investigations. The benthic foraminiferal biofacies distribution are strongly correlated to export productivity thus organic flux to the seafloor, and depositional conditions at the seafloor, including seasonality of organic flux, lateral flux of refractory organic matter, oxygen levels at the seafloor, carbon content of the sediments, grain size, current activity, carbonate corrosivity in pore and bottom waters (e.g., Ingle et al., 1980, Peterson, 1984, Jorissen et al, 1995, Klitgaard and Sejrup, 1996, Kitazato et al., 2000, Heinz et al., 2001, Murray, 2001, 2006, 2014, Jorissen et al, 2007, Phipps et al., 2010, Nisha and Singh, 2012). Benthic foraminiferal biofacies have been applied to sequence stratigraphy (Christensen et al., 1995, Liu et al., 1997) and paleobathymetric models (Pekar and Kominz, 2001). Deep-water benthic foraminiferal studies demonstrate that benthic foraminifera distribution is strongly linked to type and quality of organic matter that reaches the seafloor and bottom current strength, lithology (grain size and mineralogy) and type of substrate, and oxygen levels in the bottom water (Gooday, 1993, 1996, 1999, 2003, Jorissen et al, 1995, Schonfeld, 2002, Fillon, 2003, 2005, Thomas, 2003, Jorissen et al, 2007, Schroder-Adams et al., 2008). In this study,

biofacies analysis is used to improve the interpretation of paleoenvironments recognized in marine sections in cores and borehole samples from the hydrocarbon-rich marginal basins of Brazil.

Sea-level fluctuations may have greatly influenced over the benthic foraminiferal biofacies distribution in the Maastrichtian through Eocene of the western South Atlantic. Lowstands of sea-level induce greater deposition of silicilastics on the slope and rise and in marginal basins due to increased erosion/weathering on land (Leckie and Olsson, 2003, Catuneanu, 2006). In contrast, deep-sea depositional rates during transgressions and sea-level highstands are lower and there is greater potential for sediment condensation and generation of unconformities on the slope and rise, and in the marginal basins (Leckie and Olsson, 2003, Miller et al., 2005, Catuneanu, 2006). A rise in the sea level may also cause a rise in lysocline and calcite compensation depth (CCD, Berger, 1970), providing an opportunity for the habitat space of abyssal agglutinated assemblages to expand into shallower depths along the continental margin. By contrast, lowering of sea level may cause the CCD to be depressed, thereby restricting dominantly agglutinated assemblages to deeper abyssal regions (Khunt, 1996, Kaminski and Gradstein, 2005).

The main objective of this chapter is to present a biofacies analysis of benthic foraminiferal assemblages combined with other parameters (planktic foraminiferal percentage, radiolarians, lithology). The biofacies provide the framework for investigation of Maastrichtian-Eocene evolution of the Brazilian margin in the western South Atlantic.

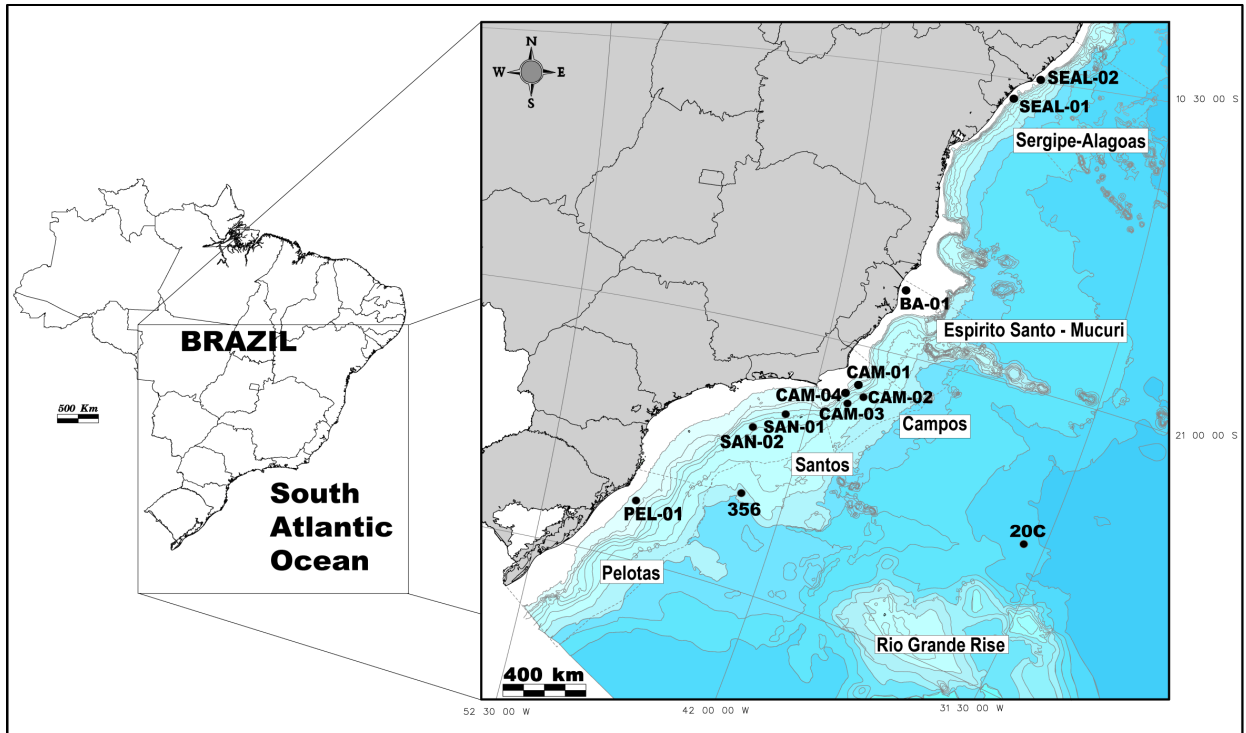


Figure 3.1: Present bathymetric map of the study area including the five Brazilian marginal basins (Sergipe-Alagoas, Mucuri, Campos, Santos, and Pelotas) and DSDP Sites 20C and 356.

3.3 – MATERIALS AND METHODS:

Biofacies were defined based on the benthic foraminiferal assemblages of wells from five Brazilian marginal basin and two Deep Sea Drilling Project (DSDP) sites in the western South Atlantic. The samples came from a variety of sources: cores, cuttings and sidewall samples. Core samples were obtained from discrete cored intervals in an industry well or DSDS site. Cutting samples are formed by drilled rock fragments that are transported up the well bore by the mudstream in the well. Sidewall core samples are obtained by percussion sidewall coring systems that shoot cylindrical bullets into the

borehole wall. The core samples are the majority of the analyzed samples. The cuttings and sidewall samples are from the Petrobras petroleum industry wells and were selected of intercalated intervals where the coring was not continuous.

The Petrobras petroleum industry wells are located in five Brazilian marginal basins (Sergipe-Alagoas, Mucuri, Campos, Santos, and Pelotas) and the DSDP samples are from Leg 39 Site 356 (São Paulo Plateau) and Leg 3 Hole 20C (Rio Grande Rise) (Fig. 3.1). The locations were selected based on their stratigraphic continuity over the Paleocene-Eocene interval, although some locations also recovered the upper Maastrichtian (Table 3.1).

Table 3.1: Present geographic locations and age interval of samples in this study.

Well/Site	Location	Present water depth (m)	Samples	Sample type	Age
20C	Rio Grande Rise	4506	28	core	Paleocene-Eocene
356	São Paulo Pupperau - Santos Basin	3203	107	core	Paleocene-Eocene
PEL-01	Pelotas Basin	151	15	core	middle to upper Eocene
			40	cuttings	lower Eocene
			8	core	lower Eocene
			28	cuttings	upper Paleocene
			14	core	lower Paleocene
SAN-01	Santos Basin	1515	9	cuttings	upper Maastrichtian
			13	cuttings	upper Eocene
			14	sidewall	lower Eocene
			16	core	upper Paleocene-lower Eocene
SAN-02	Santos Basin	1733	11	cuttings	upper Maastrichtian
			12	core	upper Maastrichtian
			48	core	lower Eocene
CAM-01	Campos Basin	791	4	core	upper Maastrichtian
CAM-02	Campos Basin	1336	6	sidewall	Paleocene-Eocene
			11	cuttings	upper Eocene
			22	core	lower to middle Eocene
CAM-03	Campos Basin	923	3	cuttings	upper Maastrichtian to lower Paleocene
			42	core	Paleocene-Eocene
CAM-04	Campos Basin	820	16	cuttings	upper Eocene
			46	core	Paleocene
			31	cuttings	upper Maastrichtian to lower/middle Paleocene
SEAL-01	Sergipe-Alagoas Basin	27	44	cuttings	Eocene
			30	core	Paleocene
SEAL-02	Sergipe-Alagoas Basin	24	30	cuttings	upper Paleocene-lower Eocene
			18	core	Paleocene
			16	cuttings	upper Maastrichtian

The samples were processed at the Biostratigraphy and Paleoecology Department at Petrobras Research Center, Rio de Janeiro, Brazil. The DSDP core samples consisted of stiff, unconsolidated to weakly consolidated sediment, they were washed the over 63 μm sieves and dried. The core/cutting samples of the petroleum wells were crushed and soaked in solution of 40% hydrogen peroxide washed over a 63 μm sieves and dried, as standard procedure of the company. The Brazilian marginal basins samples are from the industry and were provided in slides, picked. The picking follows the procedure of the company where ~300 tests are picked (planktics and benthics). We acknowledge that this is not the ideal process for studies focused on benthic foraminiferal assemblages where ~200 benthic foraminiferal tests would be a more representative number (see Fig 2 in Thomas, 1985), however the availability of these samples provides a unique opportunity to compare deep-sea sites with the Brazilian marginal basins. As a result, most of the samples have low numbers of benthic foraminiferal community that only partially represent the community (Fig. 3.2 and 3.3). Despite the relatively low number of specimens, it was still possible to recognize the main trends of the benthic foraminiferal assemblage as demonstrated by comparing Q-mode cluster analysis for all samples of the Pelotas and Sergipe-Alagoas basins, including samples that contain at least 35 specimens and at least 100 specimens. In all the cases, the same major clusters are generated, showing the main groups of samples persist, despite the low number of specimens in some samples (Fig. 3.4). Therefore, benthic foraminiferal assemblages were used to establish the biofacies, even though there are major limitations on the statistical significance of the samples analyzed here.

A low number of specimens was also observed in DSDP Sites 20C and 356 even though all the benthic foraminifera were picked in each sample. This low number of specimens collected is likely related to the small sample volume (~10cc). However, Site 20C has a relatively higher number of benthic specimens than Site 356 and the location could explain the distinction between them. Despite both sites being situated above the paleo-CCD, Site 20C was possibly deeper in the lysocline than Site 356, which likely affected the flux of fragile planktic foraminiferal tests and thereby increasing the concentration of benthics within the sediment. The very low sedimentation rates in Site 20C than Site 356 (1.42m/myr and 20m/myr for the upper Cretaceous-Paleocene respectively) support the deeper position in the lysocline for the Site 20C.

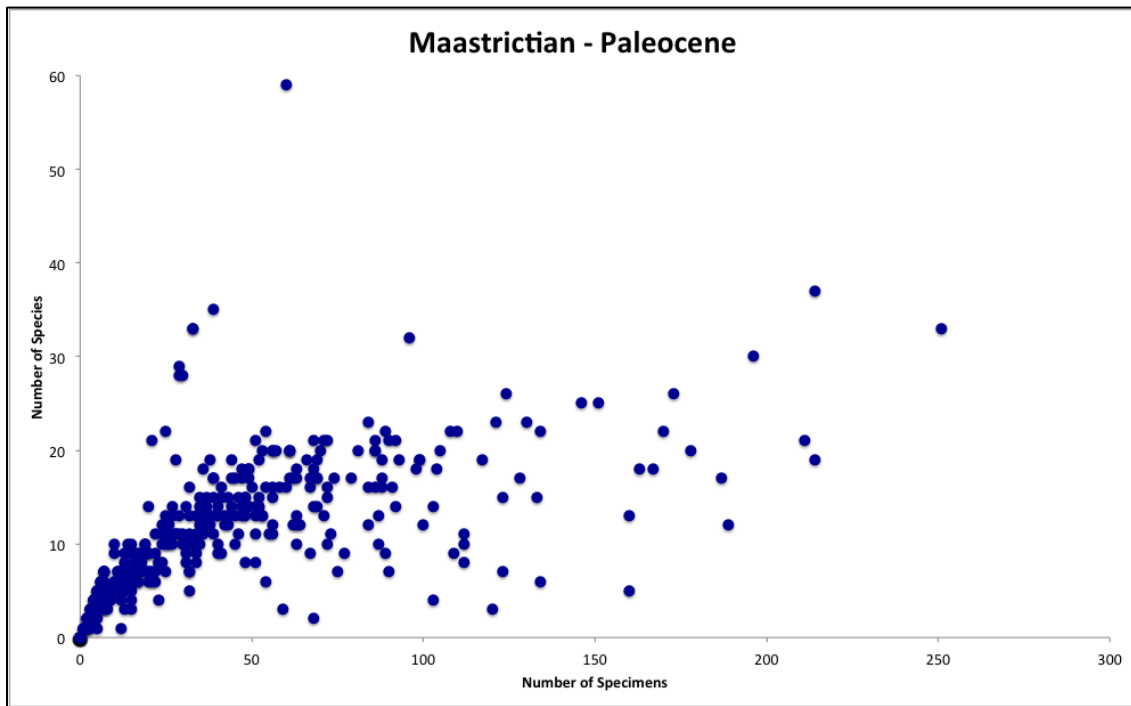


Figure 3.2: Number of Specimens X Number of Species plot including the whole sample of the upper Maastrichtian through Paleocene interval. Despite the low number of specimens, the number of species does not increase drastically on the samples with more than 50 specimens.

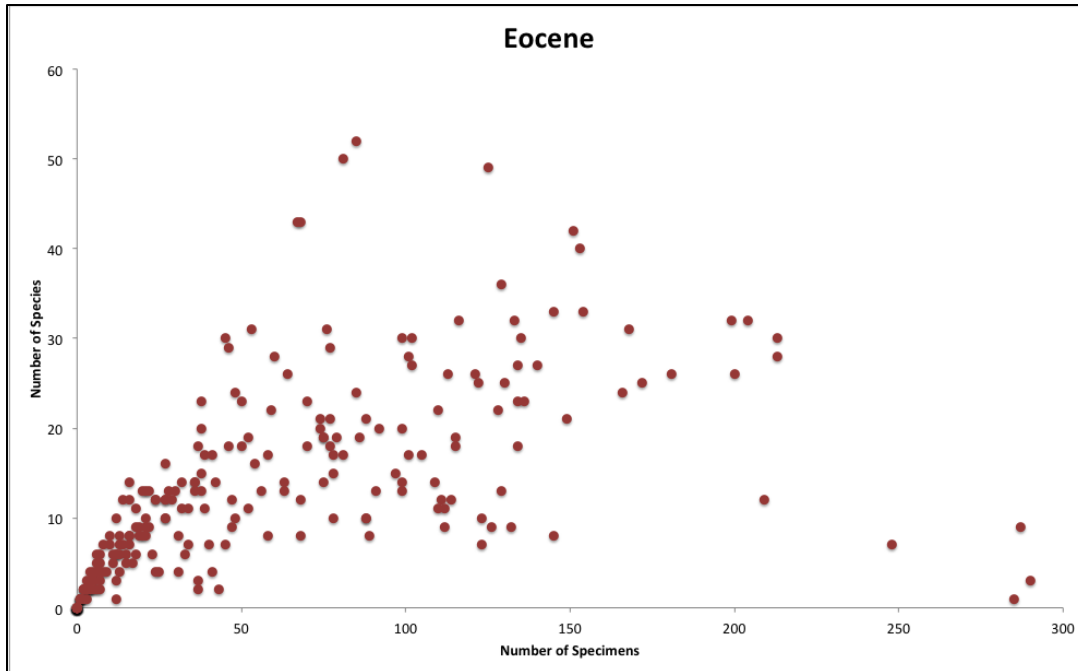


Figure 3.3: Number of Specimens X Number of Species plot including the whole sample of the Eocene interval.

The benthic foraminiferal taxonomy presented in the Chapter 2 is here used to establish the biofacies based on the benthic foraminifera absolute percentages (Appendix III). Every site was analyzed individually to group the samples (Q-mode cluster) and correlate the groups with the taxa present in the samples (Correspondence Analysis). Cluster analysis is a multivariate analytical technique that has been widely used to determine biofacies based on benthic foraminifera (Buzas, 1979, Parker and Arnold, 1999). It classifies the samples (Q-mode) or variables (R-mode) into a smaller number of categories (clusters) that are presented as dendrograms for each site (branching diagram that hierarchically nests objects into increasingly more inclusive groups) (Buzas, 1979, Valentin, 1995, Legendre and Legendre, 1998). Here, the Q-mode cluster analysis groups the samples into clusters by depth (m).

Correspondence analysis (CA) is a descriptive/exploratory technique designed to analyze simple two-way and multi-way tables containing some measure of correspondence between the rows and columns, here designed as samples (depth) and taxa (benthic foraminifera) (Valentin, 1995, Legendre and Legendre, 1998). The Q-mode cluster analysis and CA were performed using PAST 3 software (Hammer and Harper, 2006). The CA and Q-mode cluster analysis took into account the absolute percentage of the most abundant species, here defined as >5% absolute percentage in at least two samples. The cut off of 5% was adopted after repeated attempts in using CA for each well or site in order to make clearer separation of the biofacies, as exemplified by data of DSDP Site 356 in figure 3.5.

The percentage of total assemblage (% total assemblage) cited below when biofacies are defined includes: planktics and benthics foraminifera (% planktics + % benthics = % total assemblage) or planktics, benthics foraminifera and radiolarians (% radiolarians) when they occur. These counts were made in order to quantify the percentage of planktics foraminifera (% planktics) and/or radiolarians (% radiolarians) compared with the benthic foraminifera assemblage. The percentage of tubular forms (% tubular forms) was calculated from the benthic foraminiferal assemblage and includes the elongate, tubular agglutinant taxa (e.g., *Bathysiphon*, *Psammosiphonella*, *Nothia*, and *Rhizammina*).

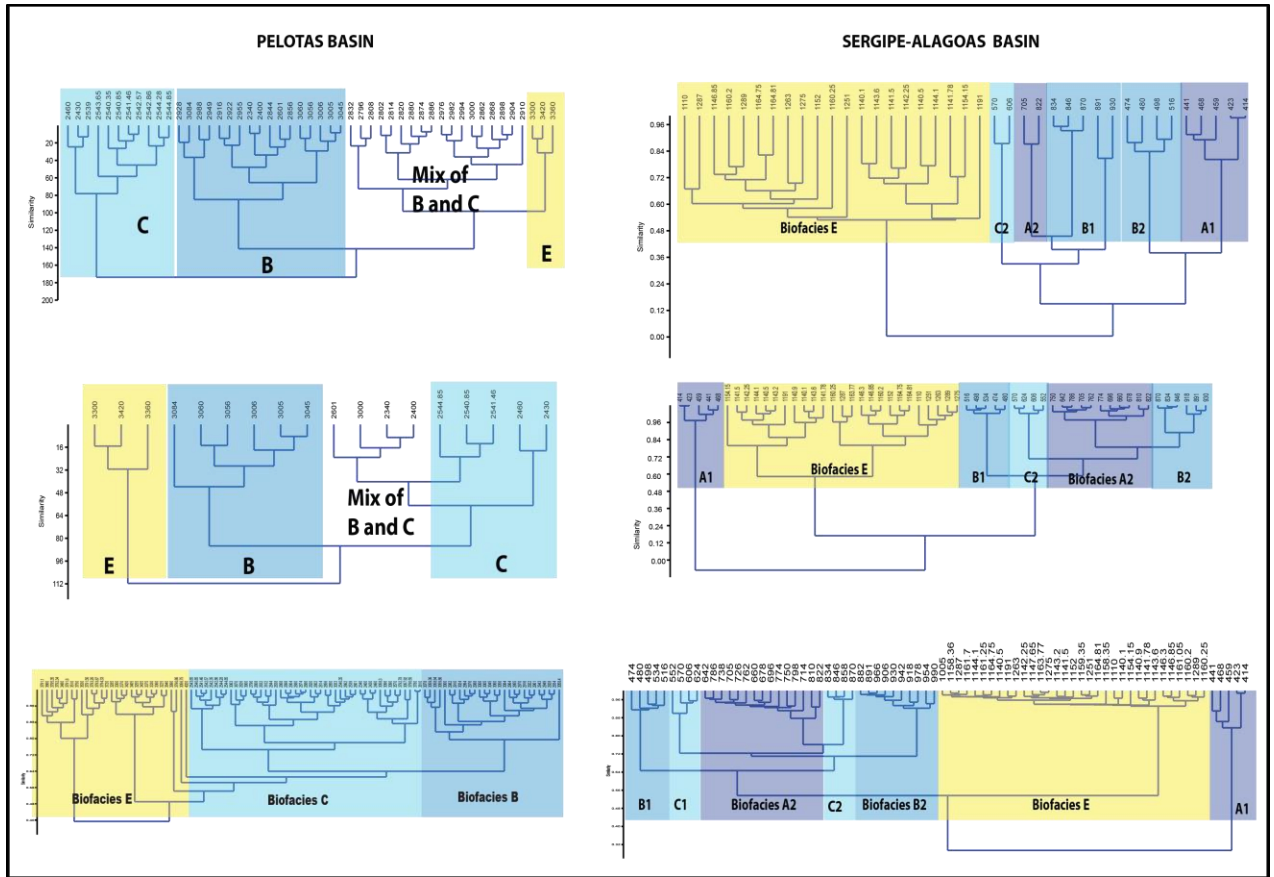


Figure 3.4: Dendrograms of the Q-mode cluster analysis of the Pelotas (left) and Sergipe-Alagoas (right) basins, using samples with number > 35 specimens (top), >100 specimens (middle) and all the samples (bottom). Note that the yellow (agglutinant-rich) and blue (calcareous-rich) contrasts are consistent among all cluster analysis.

The datum for the age versus depth models were based on calcareous nannofossils biostratigraphy, except for the Site 20C where the age model is based on planktic foraminifera. The planktic foraminiferal biozones (*) are from Wade et al. (2011) and the nannofossil biozones (**) from Gradstein et al. (2012).

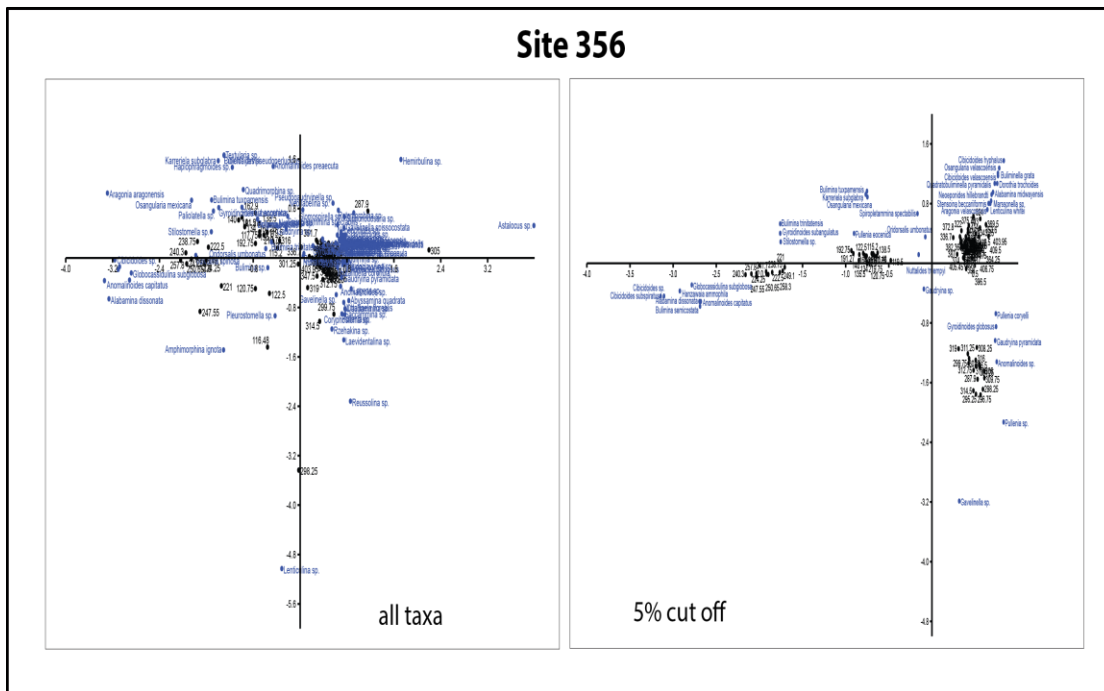


Figure 3.5: Results of two correspondence analyses (CA) for DSDP Site 356 with all taxa (left) and with 5% cut off (right), showing the more pronounced grouping of samples after the cut. Blue = benthic taxa, black = samples depth.

The bathymetric zones follow Van Morkhoven et al. (1986) in agreement with Berggren and Miller (1989):

- Neritic: 0 – 200m
 - inner <30 m
 - middle 30 – 100 m
 - outer 100 – 200 m
- Bathyal: 200 – 2000 m
 - upper 200 – 600 m
 - middle 600 – 1000 m
 - lower 1000 – 2000 m
- Abyssal: >2000 m
 - upper 2000 – 3000 m
 - lower >3000 m (below the CCD)

3.4 – GEOLOGICAL SETTING:

3.4.1 – The Proximal Brazilian Marginal Basins:

The Brazilian marginal basins (Pelotas, Santos, Campos, Mucuri, Bahia-Sul, Sergipe-Alagoas and Pernambuco-Paraíba) have a similar formation and evolution that began with the rifting in the South Atlantic during the break-up of Pangea (Milani et al., 2001, Mohriak, 2003, Zalan, 2004, Torsvik et al., 2009). The tectono-stratigraphic evolution pattern of these basins is quite similar, and can be divided into four stages: pre-rift, rift, restricted marine and open marine. The pre-rift package (upper Jurassic-lower Cretaceous) occurs in the Sergipe-Alagoas basin and southward to the Pelotas Basin. This sequence is generally represented by reddish fluvial sediment deposited in a shallow lacustrine paleoenvironment (Milani et al., 2007). The rift section is recognized as diachronous lacustrine depocenters formed during the Early Cretaceous. These rift lakes contain shale deposits that are important hydrocarbon source rocks. The syn-rift rocks are more abundant in the southern basins (Pelotas and Espírito Santo). During the Aptian, the restricted marine section was deposited that is typically represented by a thick evaporites package (mostly halite and gypsum-anhydrite) and has importance in the Santos, Campos, and Mucuri basins. A thinner succession of evaporites reaches the northern basin of the Sergipe-Alagoas. Evaporite deposition spanned the late Aptian to earliest Albian (Cainelli and Mohriak, 1999, Milani et al., 2001, Mohriak, 2003). Above the salts, a large proto-oceanic gulf accumulated carbonate and siliciclastic deposits with some locally associated magmatism. Such deposits, together with the evaporites, characterize the post-rift section of the eastern Brazilian margin. During the Albian, marine conditions

became established, first represented by carbonates and then by thick siliciclastic sediment, predominantly shales and sandstones representing shallow platform, coastal fans, and slope and basin turbidites. This siliciclastic sequence consists of transgressive-regressive cycles that characterize the Late Cretaceous through the Pleistocene (Asmus and Baisch, 1983, Milani et al., 2007).

During the Cenozoic, the Mucuri Basin experienced an important magmatic event that formed the Abrolhos Volcanic Complex, also known as the Abrolhos coral reef. The Abrolhos carbonate sequence comprises the largest and the richest reef complex of the western South Atlantic (Leão, 1999). The carbonate bank was originally formed on volcanic rocks. The volcanics are intercalated with shales and carbonates. The Ar-Ar ages indicate that the volcanic activity spanned the Paleocene-Eocene (60-40 Ma, Szatmari et al., 2000, Milani et al., 2001, Zalan, 2004).

Salt tectonics has played an important role in the evolution of the Brazilian marginal basins during the Cenozoic (Mohriak et al, 1990, Cainelli and Mohriak, 1999, Milani et al., 2001, Mohriak, 2003, Torsvik et al., 2009). The Campos and Santos basins are by far the most affected by salt mobilization, which generated new depocenters basinwards. The Espirito Santo-Mucuri and Sergipe-Alagoas basins have had less salt tectonic influence, mostly in deep-waters and onshore respectively, while the Pelotas Basin has incipient (northern part) or no significant salt tectonic activity (Cainelli and Mohriak, 1999).

3.4.2 – The Distal DSDP Sites:

3.4.2.1 - DSDP Leg 39 Site 356 – São Paulo Plateau:

Site 356 was drilled at the southeastern edge of São Paulo Plateau on the Brazilian continental margin (28°17.22'S, 41°05.28'W, 3175 m water depth), reaching upper Albian at 741msbf (Perch-Nielsen et al., 1977). Sediments across the Cretaceous/Paleogene boundary were deposited under oxidizing conditions (Supko et al., 1977). The uppermost Maastrichtian to upper Paleocene sequence is relatively pure nannofossil and foraminifer chalk (Supko et al., 1977). During the Eocene, biogenic silica was deposited. Depositional hiatuses span the uppermost Paleocene to lowermost Eocene, and the upper middle Eocene to lower Miocene (Supko et al., 1977).

This site was selected for this study because of the relatively good recovery of the Paleocene, represented by a thick and nearly complete sequence, though with gap spanning the lower Paleocene Zone P1b (Boersma, 1977). Boersma (1977) commented on the excellent preservation of foraminifera in the Danian interval. Paleocene sediments were recovered in Cores 29 to 16. The hiatus of ~5 myr (~57 to 52 Ma) between the latest Paleocene and the earliest Eocene suggest either a break in the accumulation or deposition followed by erosion.

Eocene sediments were recovered in Cores 356-15 to 6. The lower Eocene varies from chalky, foraminifera-rich sediments to radiolarian and diatom-rich sediments containing very few foraminifera (Perch-Nielsen et al., 1977). The lower Eocene silicified chinks (Cores 15 to 10) are overlain by a thin sequence of siliceous calcareous ooze that is associated with high dissolution rate of calcareous sediments in Core 356- 10 (Perch-Nielsen et al., 1977). The middle Eocene sediments vary from chalky,

foraminifer-rich sediments to radiolarian and diatom-rich sediments containing very few foraminifera (Perch-Nielsen et al., 1977).

3.4.2.2 - DSDP Leg 3 Hole 20C – Rio Grande Rise:

This site is located on the Rio Grande Rise (28° 31.47'S and 26° 50.73'W – present water depth 4506m) in the western South Atlantic. A relatively thin and incomplete uppermost Maastrichtian to Paleocene sequence was recovered in Hole 20C (Maxwell et al., 1970). The Cretaceous/Paleogene boundary interval is disturbed by sedimentary processes, possibly sediment reworking (Maxwell et al., 1970). The upper Paleocene to lower Eocene is nearly complete, although the dissolution interval across the Paleocene/Eocene boundary interval (Paleocene Eocene Thermal Maximum, PETM) was not recovered in the cored section. There is also a stratigraphic break between the lower and middle Eocene.

The upper Maastrichtian through the Paleocene consists of very pale brown-pink and pink nannofossil chalky oozes. The lower to middle Eocene unit consists of nannofossil marl oozes and clays in various shades of brown and somewhat enriched in zeolites (Maxwell et al., 1970). This unit may have been deposited near the carbonate compensation depth with the calcium carbonate content varying from 16 to 52 wt%.

3.5 – PALEOCEANOGRAPHIC SETTING OF THE SOUTH ATLANTIC:

Global temperature changes were variable during the upper Cretaceous, including global cooling in the early Maastrichtian and warming some 200-300kyr prior to the end-Cretaceous mass extinction, which has been attributed to Deccan floor basalt volcanism in India (Barrera, 1997; Huber et al., 2002; Cramer et al., 2009; Keller and Abramovich, 2009; Thibault et al., 2010; Thibault and Gardin, 2010). Immediately after the bolide impact that likely caused the mass extinction on the Cretaceous-Paleogene boundary (K/Pg), there was a short interval of global cooling caused by dust or sulfate particles, global wildfires, severe acid rain and acidification of the oceans (Thomas, 2006, Penman et al, 2014). During the early to mid-Paleocene, global temperatures were much warmer than today, but in the late Paleocene (~ 59 Ma) a long-term warming trend began, which culminated with the Early Eocene Climatic Optimum (EECO ~52-50 Ma; Zachos et al., 2001, 2008; Cramer et al., 2009). A number of hyperthermals characterized the early Eocene, beginning with the Paleocene-Eocene Thermal Maximum (PETM, or Eocene Thermal Maximum 1, ETM1) and followed by less severe events ETM2 and ETM3 leading up to the EECO (Zachos et al., 2008; DeConto et al., 2011). Temperatures did not reach freezing even in continental interiors (Zachos et al., 2001, 2005, Thomas et al., 2006) at mid- to high-latitudes, and global deep waters temperatures were 10°-12°C warmer than today (Zachos et al., 2001, 2008). In addition, the ocean circulation was efficient in maintaining the warmer temperatures, with low temperature gradients from high to low latitudes (Thomas et al., 2000, Huber and Sloan, 2001, Cramer et al., 2009, Huber and Caballero, 2011). The continental's configuration was different in the

Paleogene, impacting directly on the ocean circulation and sites of deep water formation. Remarkable changes in the ocean configuration occurred from the Paleocene-Eocene boundary through the Miocene are reflected in significant changes in ocean thermohaline circulation (Bice et al., 2000). In the early Eocene, the North Atlantic was connected to the Arctic by a shallow sea that deepened towards the middle to late Eocene. The exact time of the Drake Passage opening is still controversial, from the late middle Eocene (~41 Ma, Scher and Martin, 2006) to the early Miocene (~20 Ma, Anderson and Delaney, 2005). The opening of the Drake Passage has been reported as playing an important role on the abrupt cooling in the Eocene-Oligocene boundary providing the thermal isolation of Antarctic.

The production of the deep-water is a key factor in the ocean circulation, and there are controversial ideas about where deep waters originated in the Paleogene. One hypothesis is that Warm Saline Bottom Water (WSW) production in the Tethys Seaway flowed southward in the Equatorial Atlantic and/or into the Indian Ocean along the African margin (Kennett and Stott, 1990; Bice et al., 2000). Another hypothesis is deep water forming in the Southern Ocean flowing northwards into the Atlantic and Indian ocean basins (Thomas et al., 2003). Climate modeling shows that the subtropical deep waters (WSW) are not easily produced, however whether a strong WSW component has existed at all, or has existed as either a steady-state or a transient condition remains unknown (Bice, 2000). Thomas (2004) reported a shift in deep water sources from the Southern Ocean to the North Pacific ~65 M, and then reverted back to the Southern Ocean ~40 M, based on neodymium isotopes of fish debris. Possibly a combination of both hypotheses occurred in the Paleogene, with main source from the Southern Ocean

and a smaller or transient contribution from the subtropical Tethys Seaway. The interpreted water masses circulation in the Paleogene Atlantic Ocean is shown in figure 3.6.

The warmer planet scenario changed in the middle Eocene (~49 Ma) when global deep waters and high latitude surface waters cooled. The opening of the Arctic to the world ocean may have been a factor in middle Eocene global cooling (Thomas, 2006; Borrelli et al., 2014). The Middle Eocene Climatic Optimum (~40 Ma) was a short-lived warming during the longer-term middle to late Eocene cooling (Bohaty and Zachos, 2003). The ice free world shifted to small ice on Antarctica by the late Eocene and rapid growth of the Antarctic ice-sheet in the earliest Oligocene (~33.7 Ma; DeConto and Pollard, 2003; Coxall et al., 2005; DeConto et al., 2008; Katz et al., 2011; Borrelli et al., 2014).

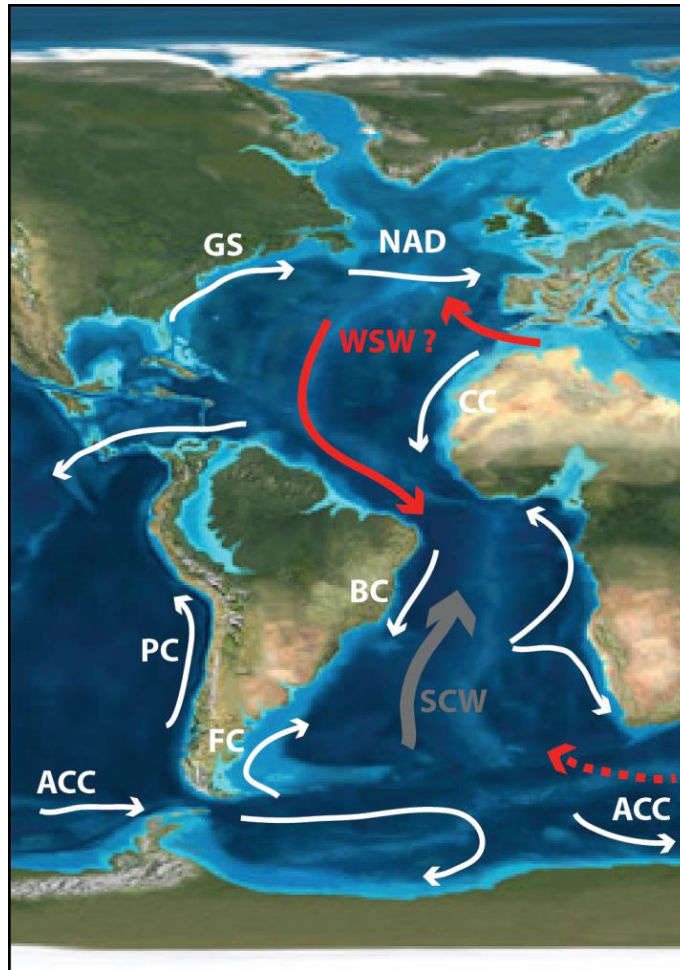


Figure 3.6: Interpretative Atlantic Ocean circulation during the Paleogene. White arrows: surface water currents, red: intermediate water, grey: deep water. GS – Gulf Stream, NAD – North Atlantic Drift, WSW – Warm Saline Water, BC – Brazil Current, FC – Falkland Current, PC – Peru Current, ACC – proto-Antarctic Circumpolar Current, SCW – Southern Component Water, CC – Canary Current. Paleogeographic map from Ron Blakey (<https://www2.nau.edu/>). Surface currents from Bice et al. (2000), WSW from Bice (2000), SCW from Thomas et al. (2003) and Thomas (2004).

3.6 – BENTHIC FORAMINIFERAL BIOFACIES AND PALEOBATHYMETRY:

Five major biofacies (A-E) were determined based on the benthic foraminiferal assemblages and associated parameters, including percentage of planktic foraminifera (% planktics), lithology, and percentage of radiolarians (%rads). The major biofacies groups are not composed of exactly the same taxa at all sites due to basin-to-basin differences (niches). The biofacies are primarily distinguished by the agglutinated/calcareous percentage and the dominant three or four species for each biofacies.

By combining Q-mode cluster analysis and the Correspondence Analysis (CA) it was possible to separate the samples into biofacies and then recognize which taxa were associated with each biofacies. Some taxa are abundant throughout the entire study interval, although they are more abundant in one or two biofacies than the other ones. *Nuttallides truempyi* is the best example because it is the most frequent taxon among our samples (it is present in most of the samples), however it is more abundant at the distal DSDP sites (20C, 356). Therefore, this species contributes more to the biofacies of the deepest sites than the proximal wells.

The biofacies are denoted, as defined below, with letters A to E based on the agglutinated/calcareous percentage. In some locations (wells SEAL-01, SEAL-02, CAM-03, and DSDP sites 20C and 356), the biofacies are repeated in the study interval. To differentiate repeated biofacies, a number is assigned with the biofacies, e.g., Biofacies A1. The stratigraphic oldest interval is assigned the greater number, for example Biofacies A2 is older than A1 in the well SEAL-01 (Figs. 3.7 and 3.8). The biofacies are presented here by basin and with interpreted paleobathymetry.

The siliceous radiolarians appeared as major contributors to the total assemblage during the late Paleocene (BA-01/Biofacies D) and early Eocene (SAN-01/Biofacies A) reaching 40-100%, and there is no foraminifera (planktic or benthic) when the sample contains 100% radiolarians.

Biofacies A – The benthic foraminiferal assemblages included in this biofacies are composed of 100% calcareous taxa. At proximal locations, this biofacies has greater percentages of shallow-water indicator species, e.g. *Amphistegina*, *Elphidium*, *Quinqueloculina*, *Lenticulina*, and *Nodosaria*, which are usually more poorly preserved (yellowish and oxidized tests) due to downslope transport from the continental shelf. At the more distal locations, this biofacies is composed of bathyal benthic foraminiferal species, e.g. *Cibicidoides*, *Hanzawia* and *Nuttallides truempyi*. This biofacies occurs mostly in the Eocene interval in the Sergipe-Alagoas, Mucuri, and Santos basins and at DSDP Sites 356 and 20C.

Biofacies B – The benthic foraminiferal assemblages included in this biofacies have up to 10% agglutinated taxa. For the proximal locations, this biofacies occurs in the Eocene and it is represented by *Paralabamina lunata*, *Hanzawaia ammophila*, *Globobulimina* sp., *Planulina costata*, *Melonis* sp.1, *Gaudryina* sp., and *Gaudryina pyramidata*. In the distal locations it occurs from the Maastrichtian through the late Eocene, where *Gyroidinoides globosus*, *Pullenia coryelli*, *Nuttallides truempyi*, *Gaudryina pyramidata*, and *Gaudryina* sp. represent the Maastrichtian through Paleocene assemblage. *Nuttallides truempyi*, *Globocassidulina subglobosa*, *Cibicidoides grimsdali*, *C. havanensis*, *C. praemundulus*, *C. eocaenus*, *Oridorsalis umbonatus*, *Gaudryina*

pyramidata, and *Gaudryina laevigata* composed the Eocene benthic assemblage of the deepest sections at DSDP Sites 356 and 20C.

Biofacies C – The benthic foraminiferal assemblages included in this biofacies have 11% to 25% agglutinated taxa. This biofacies occurs in the middle to upper Eocene of the proximal locations, and throughout the Paleocene through Eocene of the distal sites. This biofacies contains species that are diagnostic of the lower bathyal paleobathymetric zones based on the presence of *Nuttallides truempyi*, *Osangularia mexicana*, *Osangularia velascoensis*, *Cibicidoides*, *Gyroidinoides*, *Oridorsalis umbonatus*, *Gaudryina pyramidata*, *Gaudryina laevigata*, *Spiroplectammina* sp., *S. spectabilis*, and *Haplophragmoides* sp.

Biofacies D - The benthic foraminiferal assemblages included in this biofacies contain calcareous and agglutinated taxa at about the same abundance. This biofacies is frequently associated with Biofacies E, and occurs from the Maastrichtian through Eocene in the Brazilian marginal basins. Kaminski and Gradstein (2005) described a “slope marls biofacies” that resembles some of the biofacies D over the Paleocene interval.

Biofacies E – The benthic foraminiferal assemblages included in this biofacies are composed primarily of agglutinated taxa, the tubular forms (*Rhizammina*, *Bathysiphon*, *Psammosiphonella*, and *Nothia*) are particularly diagnostic (~20-40% of benthics) associated with coarse-grained coiled taxa (*Haplophragmoides*, *Ammoglobigerina*, *Ammodiscus*, *Recurvoides*, and *Budashevaella*). Biofacies E occurs from the Maastrichtian through the Eocene, but it is much more abundant in the Paleocene interval and occurs exclusively in the Brazilian marginal basins.

It was possible to recognize two major benthic assemblages within the Biofacies E, coarse-grained coiled taxa and tubular forms predominantly compose both of them. The first assemblage is composed exclusively of agglutinated taxa, there are no calcareous benthic or planktic taxa. This agglutinate-only assemblage occurs mostly in the Maastrichtian-Paleocene interval of Pelotas, Campos and Sergipe-Alagoas basins, and it represents the deepest paleo-water depths, probably at or below the calcite compensation depth (CCD). The second assemblage has ~25 % of calcareous taxa and planktic foraminifera (<60% of total assemblage) that shows clear evidence of dissolution (dissolved and corroded calcareous tests). This assemblage also represent very deep water, but above the depth of the CCD. It occurs from the Maastrichtian to the Eocene in the Campos, Santos, Mucuri and Sergipe-Alagoas basins.

This tubular agglutinant-rich biofacies was originally described as a “flysch-type biofacies” by Gradstein and Berggren (1981), and later investigated by Kaminski et al. (1988) and Kaminski and Gradstein (2005). The original flysch-type biofacies was associated with tectonically active basins, although some authors recognized it also on the continental margins basins (Gradstein and Berggren, 1981). Gradstein and Berger (1981) concluded that paleobathymetry per se was not the key factor controlling their presence, although great depth, below the lysocline or CCD creates favorable conditions for the agglutinated assemblage (Kaminski et al, 1988, Koutsoukos, 2000, Kaminski and Gradstein, 2005).

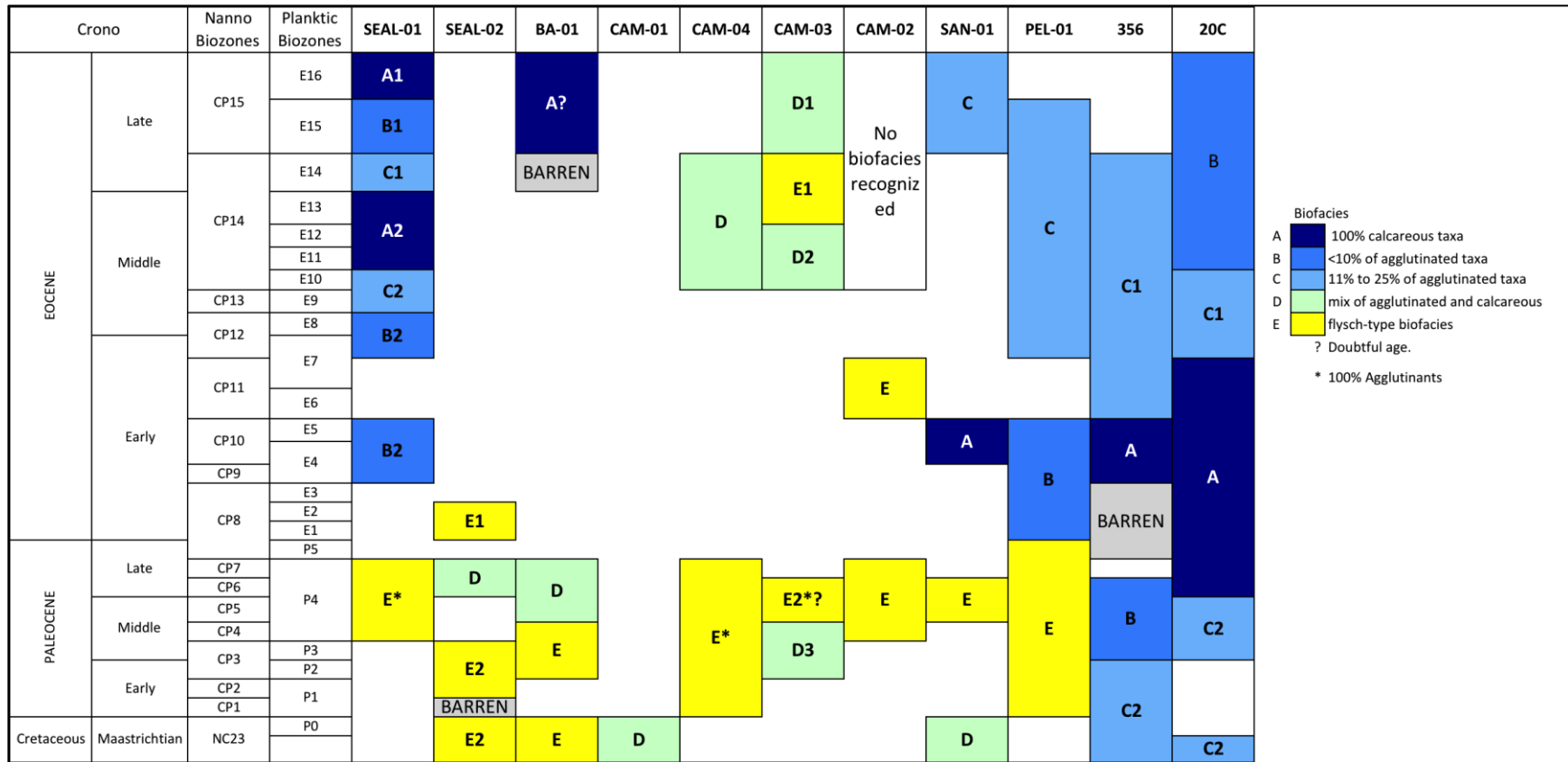


Figure 3.7: Benthic foraminiferal biofacies distributed by age for all wells and sites. The wells are organized northern and shallower (Sergipe-Alagoas) through southern (Pelotas) and deeper (DSDP Sites 356 and 20C). Nannofossil biozones after Gradstein et al. (2012), planktic foraminiferal biozones from Wade et al. (2011).

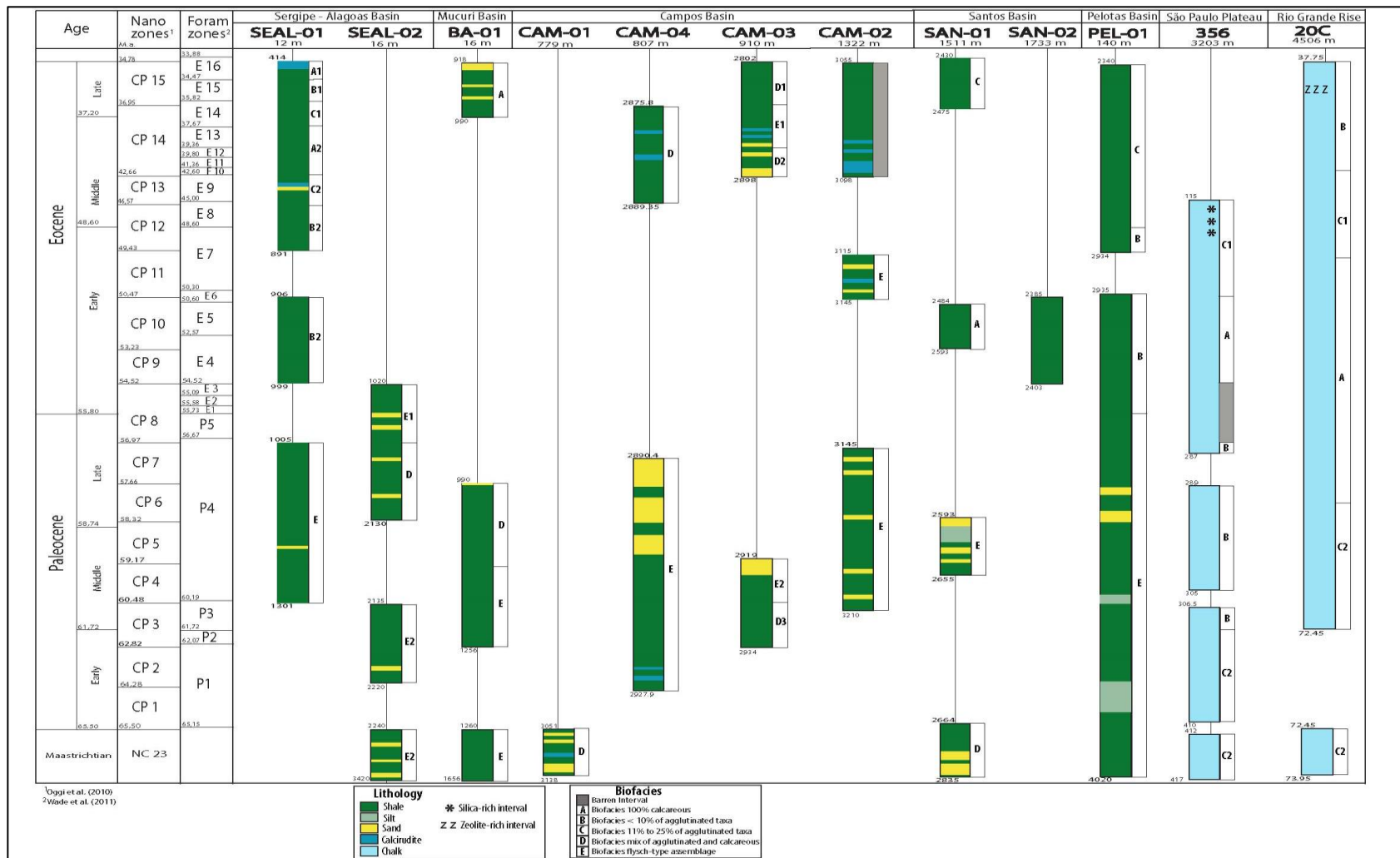


Figure 3.8: Lithology and biofacies of the study locations from the late Maastrichtian through Eocene of the western South Atlantic and Brazilian marginal basins.

In this section, the biofacies are presented by basin, although they are described individually for each site. A paleobathymetric interpretation based on the benthic foraminiferal biofacies is also presented with a tentative paleobathymetric curve.

3.6.1 – Sergipe-Alagoas Basin:

SEAL-01 and SEAL-02 are the wells that represent this basin. The wells are today located in very shallow water depth (12 m and 16 m, respectively), but they are located ~100 km apart (Fig. 3.1). The biofacies were clearly discriminated on the statistics analysis (Figs. 3.9 and 3.10).

The flysch-type biofacies E is very common in this basin, occurring in both wells from the upper Maastrichtian through to the lower Eocene, and usually associated to high sedimentation rates (average ~120m/myr – Figs. 3.11 and 3.12).

The Eocene interval is represented only on SEAL-01 and is predominantly composed by calcareous-rich biofacies A, B and C. There is no linear correlation between the occurrence of the calcareous biofacies and the sedimentation rates, which vary widely from 8 to 96 m/myr (Fig. 3.11).

3.6.1.1 – Well SEAL-01:

Five biofacies were defined based on the CA and Q-mode cluster analysis, for the Paleocene-Eocene interval (Fig. 3.9). The Paleocene biofacies are mostly composed by agglutinated benthics (80-100% of benthics), with no planktics, represented by **Biofacies E**. The most common calcareous taxa are *Globobulimina* sp, *Cibicidoides* sp. and *Gyroidinoides* sp. The agglutinated assemblage is dominated by tubular forms

(*Rhizammina*, *Bathysiphon*, *Psammosiphonella cylindrica*, *P. discreta*, *Nothia* sp., *Nothia latissima*) and coarse-grained taxa (*Ammodiscus*, *Haplophragmoides*). This biofacies occurs in a shale interval with intercalated sandy beds.

The Eocene benthic biofacies are dominated by calcareous taxa (80-100% of benthics), and the diversity of species increases from the lower to upper Eocene. The interval is composed mostly by shale with some layers of sand and calcirudite, especially in the top of the interval (upper Eocene) (Fig. 3.8).

➤ **Biofacies A1**

This biofacies is composed 100% by calcareous taxa and occurs in one distinct interval in the upper Eocene. The interval is composed by an intercalation of calcirudite and shale beds deposited above a thick layer of sandstone (~250m). This benthic foraminiferal assemblage is dominated the large foraminifera *Amphistegina* sp. (80% to 100% of total assemblage) and other calcareous taxa, which are badly preserved, especially in the samples at the base of interval, where *Paralabamina lunata* is also badly preserved with evidence of dissolution. There are no planktic foraminifera recovered in this biofacies at SEAL-01. Ostracodes, echinoid spines, and fragments of corals and bryozoans are also recovered in this interval.

Main taxa: *Amphistegina* sp., *Paralabamina lunata*, *Nodosaria* sp.

Other taxa: *Cibicides* sp., *Lenticulina* sp., *Anomalinoidea* sp., *Melonis* sp.1.

Planktic: 0%.

Paleobathymetric range: middle to outer neritic.

Age range: late Eocene (CP15**).

➤ **2 – Biofacies B1**

Main taxa: *Paralabamina lunata*, *Melonis* sp.1, *Cibicidoides ecoaenus*.

Other taxa: *Amphistegina* sp., *Lenticulina* sp., *Cibicidoides micrus*, *Globobulimina* sp., *Nodosaria* sp.

Planktic: 1-8% of total assemblage.

Paleobathymetric range: outer neritic.

Age range: late Eocene (CP15**).

➤ **Biofacies C1**

Main taxa: *Bulimina alazanensis*, *Karrerulina conversa*, *Gaudryina pyramidata*

Other taxa: *Gaudryina* sp., *Bulimina* sp., *Cibicides* sp., *Lenticulina* sp., *Uvigerina* sp.

Planktic: 5-15% of total assemblage.

Paleobathymetric range: outer neritic to upper bathyal

Age range: late Eocene (CP14**).

➤ **Biofacies A2**

Main taxa: *Globobulimina* sp., *Neoepionides elevatus*, *Globocassidulina subglobosa*

Other taxa: *Planulina costata*, *Anomalinoides* sp., *Cibicidoides* sp., *Nuttallides truempyi*.

Planktic: 50-60% of total assemblage

Paleobathymetric range: upper to middle bathyal.

Age range: middle Eocene (CP14**).

➤ **Biofacies C2**

Main taxa: *Planulina costata*, *Gaudryina pyramidata*, *Bulimina* sp.

Other taxa: *Cibicidoides* sp., *Globocassidulina subglobosa*, *Gyroidinoides* sp., *Lenticulina* sp., *Uvigerina* sp., *Gaudryina* sp.

Planktic: 50-60% of total assemblage

Paleobathymetric range: upper to middle bathyal.

Age range: middle Eocene (CP13/14**).

➤ **Biofacies B2**

Badly preserved tests of *Amphistegina* sp. were found in this biofacies. Tiny reworked planktics and evidence of dissolution on planktic and benthic foraminifera (dissolved and corroded tests) also characterize this biofacies.

Main taxa: *Planulina costata*, *Nuttallides truempyi*, *Cyclamina* sp.

Other taxa: *Gyroidinoides* sp., *Gavelinella* sp., *Gaudryina* sp., *Paralabamina lunata*, *Anomalinoides* sp.

Planktic: 40-60% of total assemblage

Paleobathymetric range: middle to lower bathyal.

Age range: early to middle Eocene (CP9/10** and CP12**, biozone CP11** is missing).

➤ Biofacies E

This benthic foraminiferal biofacies is composed 100% of agglutinated taxa and resembles the flysch-type assemblage (Gradstein and Berggren, 1981, Kaminski and Gradstein, 2005). The agglutinated tubular forms are ~32% of benthics.

Main taxa: *Rhizammina* sp., *Haplophragmoides* sp., *Spiroplectammina navarroana*, *Psammosiphonella cylindrica*.

Other taxa: *Ammodiscus cretaceous*, *Ammoglobigerina* sp., *Cribrostomoides trinitatensis*, *Karrerulina conversa*, *Nothia* sp., *Nothia latissima*, *Recurvoides* sp., *Spiroplectammina* sp., *Trochamminoides* sp.

Planktic: 0-10% (~1% average) of total assemblage

Paleobathymetric range: lower abyssal.

Age range: middle to late Paleocene (CP4 to CP8**, P4/5 to E2*).

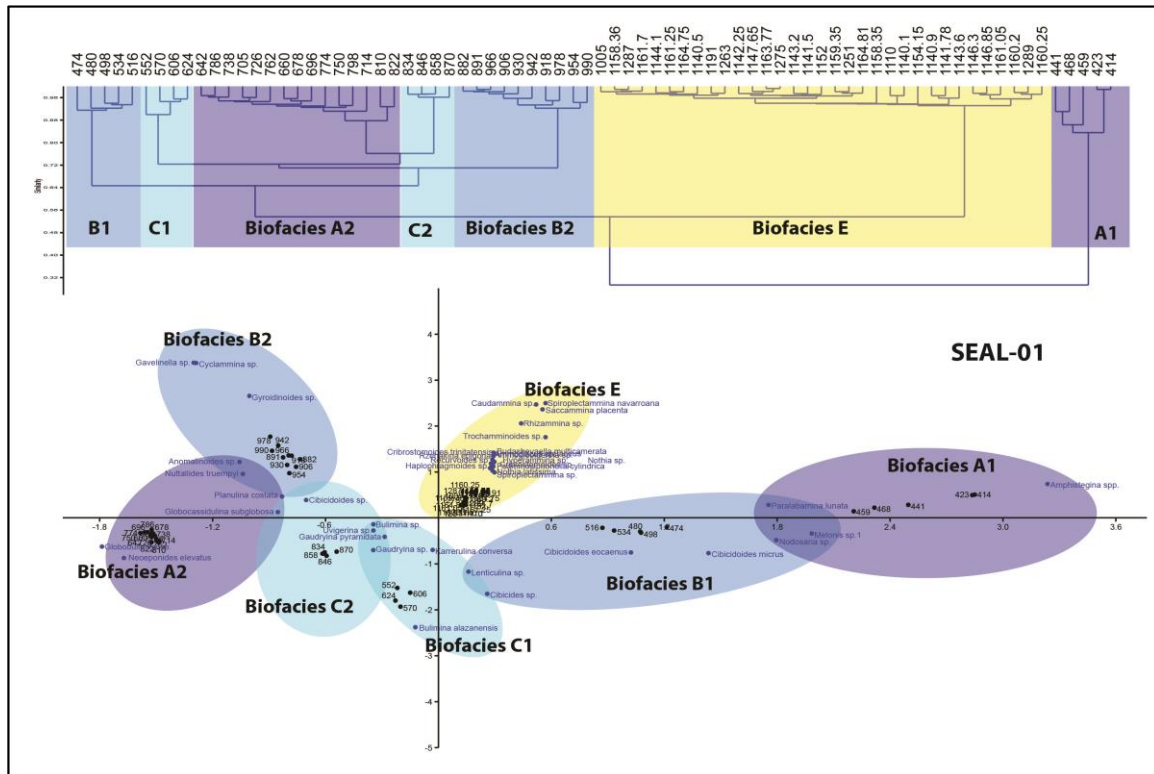


Figure 3.9: Dendrogram classifications of the samples produced by the Q-mode cluster analysis and correspondence analysis showing the seven major biofacies for the well SEAL-01.

3.6.1.2 – Well SEAL-02:

The high percentage of agglutinated taxa is the characteristic feature of the benthic biofacies in this well, although one interval has a balanced agglutinate/calcareous percentage corresponding to Biofacies D. The others biofacies belong to Biofacies E (agglutinated taxa dominates), as explained by combined correspondence analysis and Q-mode cluster analysis (Fig. 3.10). There is an unconformity in the middle Paleocene (missing nannofossil biozones CP4 and CP5) (Fig. 3.8).

➤ **Biofacies E1**

Main taxa: *Haplophragmoides* sp., *Ammoglobigerina* sp., *Nothia robusta*.

Other taxa: *Globobulimina* sp., *Lenticulina* sp., *Globobulimina ovata*, *Cribrostomoides* sp., *Haplophragmoides stomatus*, *Recurvoides* sp., *Psammosiphonella cylindrica*.

Tubular forms 20-30% of benthics.

Planktic: 50-60% of total assemblage.

Paleobathymetric range: lower bathyal.

Age range: early Eocene (E1/E2*, CP8**).

➤ **Biofacies D**

Main taxa: *Haplophragmoides* sp., *Stensioeina beccariiiformis*, *Saccamina placenta*, *Nuttallides truempyi*.

Other taxa: *Gavelinella* sp., *Spiroplectamina* sp., *Globobulimina* sp., *Lenticulina* sp., *Nothia* sp.

Planktic: 40-50% of total assemblage.

Paleobathymetric range: bathyal.

Age range: late Paleocene (CP6/7**).

➤ **Biofacies E2**

This biofacies have *Orthokarstenia* sp. and *Lenticulina* sp. with evidence of transport.

Main taxa: *Psammosphaera irregularis*, *Cribrostomoides trinitatensis*, *Psammosiphonella cylindrica*, *Haplophragmoides* sp.

Other taxa: *Saccamina placenta*, *Nothia* sp., *Recurvoides* sp., *Haplophragmoides stomatus*, *Praebulimina* sp., *Valvulineria* sp., Tubular forms ~20% of benthics.

Planktic: 0-5% total assemblage.
Paleobathymetric range: lower abyssal.
Age range: late Maastrichtian to late Paleocene (NC23 to CP2/3**).

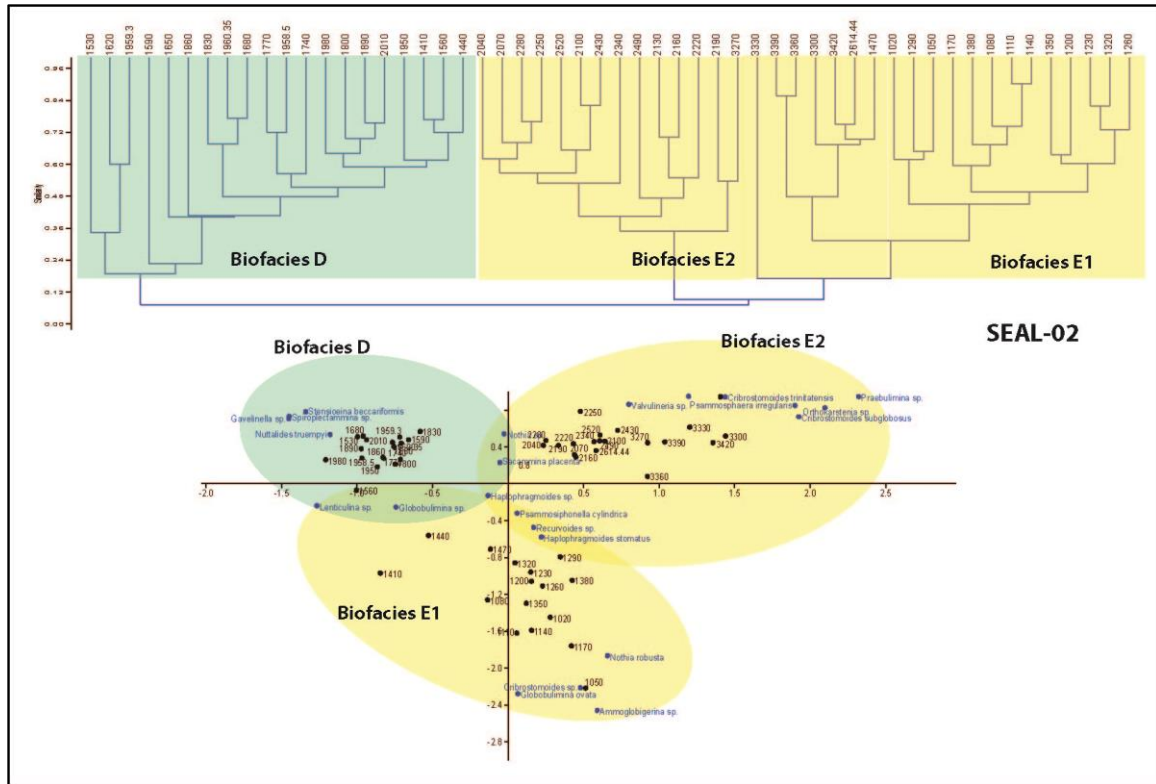


Figure 3.10: Dendrogram classifications of the samples produced by Q-mode cluster analysis and the correspondence analysis showing the three major biofacies of the well SEAL-02.

3.6.1.3 – Paleobathymetry of Sergipe-Alagoas Basin:

The SEAL-01 biofacies sequence shows a progressive shallowing through the Paleocene-Eocene interval (Figs. 3.8, 3.11). We suspect rapid progradation of the margin and shoaling paleobathymetry is the principle cause of this shallowing upwards trend due to the magnitude of the change, from lower abyssal depths in the Paleocene (Biofacies E), to middle-lower bathyal depths in the lower Eocene (Biofacies B), to neritic depths in the upper Eocene (Biofacies A).

Likewise, SEAL-02 records a shallowing upwards sequence through the Paleocene (Fig. 3.12) based on the increase in relative abundance of planktic foraminifera from Biofacies E2 in the Maastrichtian and lower Paleocene (0-5% planktics) to Biofacies E1 in the upper Paleocene (50-60% planktics) as the site shoaled above the CCD. The wells are located 100 km apart, but both locations show a similar bathymetric trend in response to progradation along the margin. SEAL-02 is 10 km away from the present day São Francisco River mouth. There is no Eocene recovered on SEAL-02, either the depositional conditions were not favorable or the entire interval was eroded.

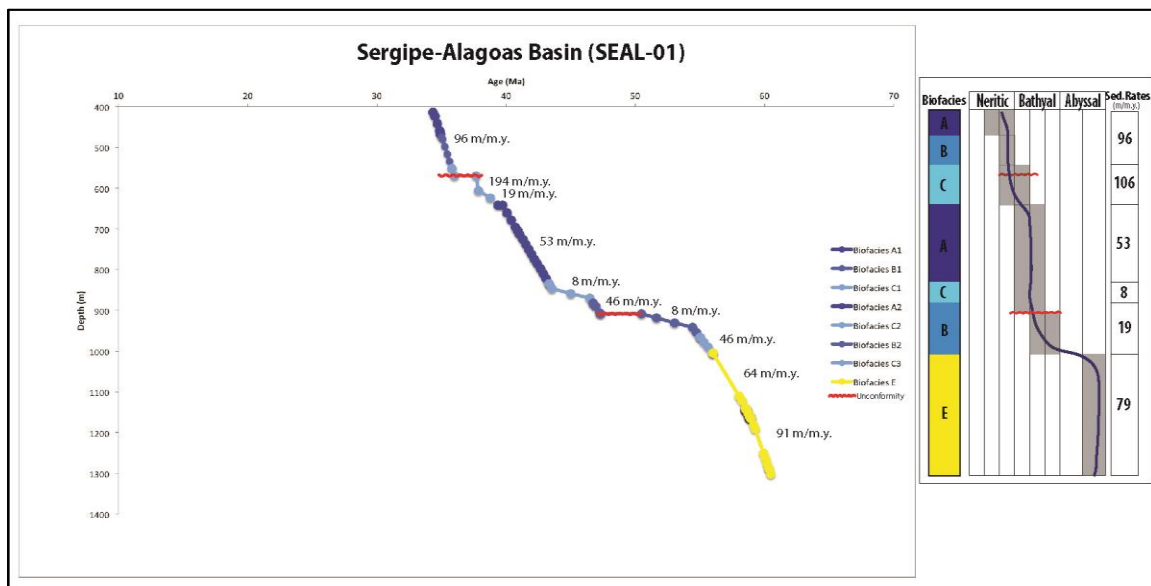


Figure 3.11: Age vs Depth Model of the well SEAL-01 plotted with the benthic foraminiferal biofacies with correlated paleobathymetric range and sedimentation rates.

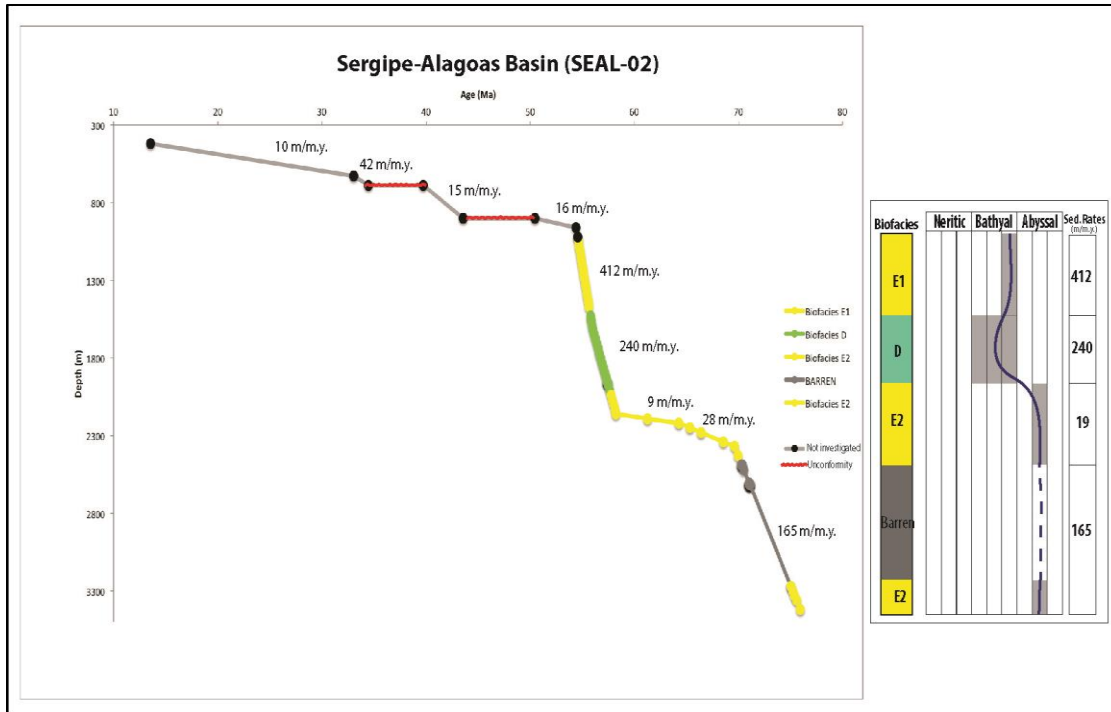


Figure 3.12: Age vs Depth Model of the well SEAL-02 plotted with the benthic foraminiferal biofacies with correlated paleobathymetric range and sedimentation rates.

3.6.2 – Mucuri Basin:

3.6.2.1 – Well BA-01:

The correspondence analysis and the Q-mode cluster analysis discriminated three biofacies for the Paleocene (Fig. 3.13). There may be no Eocene recovered in this well due to a major unconformity where the uppermost Paleocene through the lower Oligocene is missing (missing biozones CP8/9 to CP18). However, there is a nearly 100-m thick interval that the age could not be determined and it could be at least upper Eocene. This interval corresponds to Biofacies A followed by a barren interval. The barren interval coincides with thick layers of sandstone intercalated with thin layers of shale. The Paleocene interval is composed mostly of shale (Fig. 3.8).

➤ **Biofacies A**

This biofacies is characterized by shallow water taxa with evidence of transport (broken, yellowish and oxidized tests). *Quinqueloculina* sp. is poorly preserved.

Main taxa: *Cibicidoides* sp., *Discorbinella betheloti*, *Elphidium* sp. (transported from shallower areas)

Other taxa: *Lenticulina* sp., *Reussolina* sp., *Quinqueloculina* sp., *Pyrgo* sp., *Nodosaria* sp.

Planktic: 0% of total assemblage.

Paleobathymetric range: inner to middle neritic.

Age range: No older than late Eocene, based on the presence of *Elphidium* sp. (first occurrence was in the late Eocene as reported by Loeblich and Tappan, 1988).

➤ **Biofacies D**

This biofacies has a high percentage of radiolarians (60-80% of total assemblage).

This biofacies was deposited in a shale interval.

Main taxa: *Saccamina grzybowski*, *Nuttallides truempyi*, *Stensioeina beccariiiformis*, *Psammosiphonella cylindrica*.

Other taxa: *Cibicidoides velascoensis*, *Gyroidinoides globosus*, *Gyroidinoides* sp., *Saccamina placenta*, *Glomospira* sp., *Trochamminoides* sp.

Planktic: 30-45% of total assemblage.

Paleobathymetric range: middle to lower bathyal.

Age range: middle to late Paleocene (CP5 to CP7**).

➤ **Biofacies E**

Main taxa: *Rhizammina* sp., *Psammosiphonella cylindrica*, *Trochamminodes* sp., *Haplophragmoides* sp.

Other taxa: *Ammodiscus glabratus*, *A. latus*, *A. pennyi*, *Bathysiphon* sp., *Nuttallides truempyi*, *Stensioeina beccariiiformis*, *Cribrostomoides* sp., *Glomospira* sp., *Psammosiphonella discreta*, *Nothia* sp., *Gyroidinoides globosus*, *Caudammina ovula*, *Repmanina* sp., *Saccamina placenta*, and *Spiroplectammina* sp. Tubular forms ~40% of benthics.

Planktic: 35-45% of total assemblage.

Paleobathymetric range: lower bathyal.

Age range: Maastrichtian (NC23**) to early/middle Paleocene (CP3 to CP5**, the nannofossil biozones CP1 and CP2 are missing).

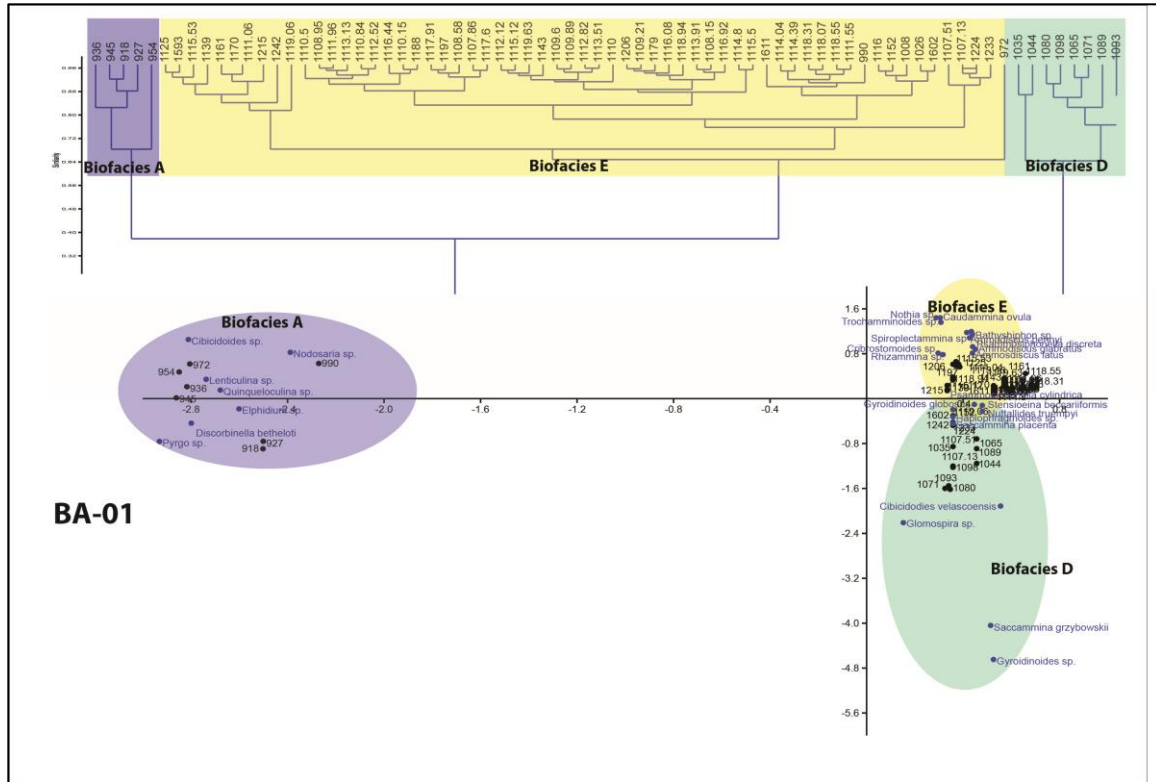


Figure 3.13: Dendrogram classifications of the samples produced by Q-mode cluster analysis and correspondence analysis showing the three major biofacies of the well BA-01.

3.6.2.2 – Paleobathymetry of Mucuri Basin:

The well BA-01 (22 m water depth) is located between the islands of the Abrolhos Coral Reef (Fig. 3.1). There is a major unconformity between the upper Paleocene Biofacies D and upper Eocene Biofacies A associated with abrupt change in the benthic assemblage suggesting a major change of paleobathymetric setting, from at least middle bathyal to neritic. The shoaling upwards trend and unconformity also coincide with a major decrease in sedimentation rates, from an average of ~1743m/myr in the Maastrichtian-Paleocene to 5 m/myr in the upper Eocene (Fig. 3.14). The observed changes in sedimentation rate may be related to the rising of the volcanic islands of

Abrolhos Reef that occurred during the middle/late Paleocene to late Eocene (Szatimati et al., 2000, Zalan, 2004).

The biofacies sequence shows a progressive shallowing up sequence from the upper Maastrichtian through the upper Paleocene. The Maastrichtian-lower Paleocene flysch-type Biofacies E is interpreted as lower bathyal-upper abyssal, followed by Biofacies D in the middle Paleocene composed of calcareous and agglutinated benthic foraminiferal and high percentage of radiolarians (60-80% total assemblage). The Biofacies D interval represents middle to lower bathyal paleodepths. A radiolarian event was recognized in the late Paleocene (~56-57 Ma – Biofacies D) and is restricted to this basin in this period of time.

In the upper Eocene, Biofacies A is composed mostly of shallow water benthic taxa (*Discorbinella*, *Cibicides*, and *Lenticulina*), some of which show evidence of transport (*Quinqueloculina*, *Elphidium*). This interval is interpreted as inner to middle neritic. The absence of planktic foraminifera or calcareous nannofossils precluded a precise age determination for this interval. However the presence of the benthic genus *Elphidium* (shallow water taxon) suggest that this deposition occurred no later than the late Eocene when it first appeared (Loeblich and Tappan, 1988). The shale deposited above Biofacies A was dated as late Oligocene (Fig. 3.7, 3.8).

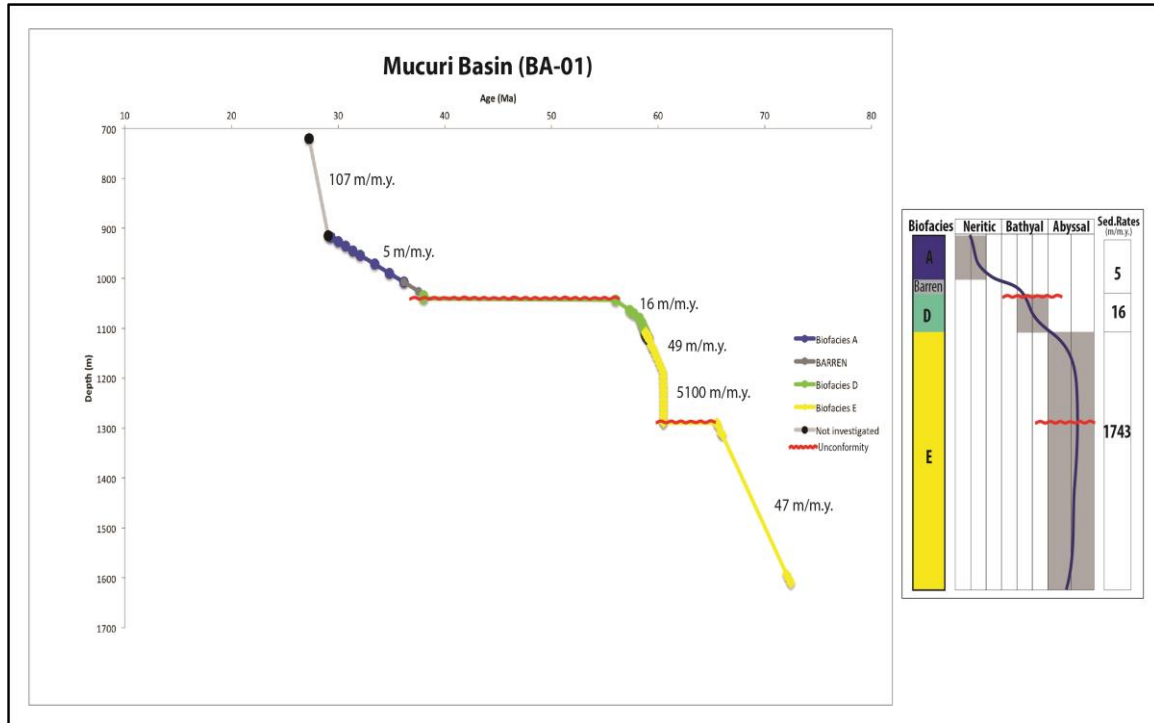


Figure 3.14: Age vs Depth Model of the well BA-01 plotted with the benthic foraminiferal biofacies with correlated paleobathymetric range and sedimentation rates.

3.6.3 – Campos Basin:

Four wells are located in this basin (CAM-01, CAM-02, CAM-03, CAM-04 – Fig. 3.1), covering the Paleocene-Eocene interval. There are several unconformities/depositional gaps that complicate the biofacies identification. These wells have in common the high percentage of the agglutinated benthic foraminiferal taxa, represented by biofacies D and E. Biofacies E occurs mostly in the Paleocene, while Biofacies D occurs more frequently in middle to upper Eocene interval.

3.6.3.1 – Well CAM-01:

There are only four sidewall samples available from this well, which comprises the upper Maastrichtian. Fortunately the samples have a very similar benthic assemblage, so they represent the same biofacies D (mix of calcareous and agglutinated taxa) (Fig. 3.15). The sidewall samples were positioned in shale intervals between thick sand layers.

➤ Biofacies D

Main taxa: *Cibicidoides velascoensis*, *Nuttallides truempyi*, *Bathysiphon* sp., *Budashevaella multicamerata*.

Other taxa: *Stensioeina beccariiformis*, *Gyroidinoides globosus*, *Cribrostomoides trinitatensis*, *Caudammina ovula*, *Ammodiscus glabratus*, *Cibicidoides hyphalus*, *Glomospira charoides*, *G. serpens*, *Rzehakina epigona*, *Recurvoides walteri*, *Gaudryina* sp.

Planktic: ~40% of total assemblage.

Paleobathymetric range: lower bathyal.

Age range: late Maastrichtian (NC23**).

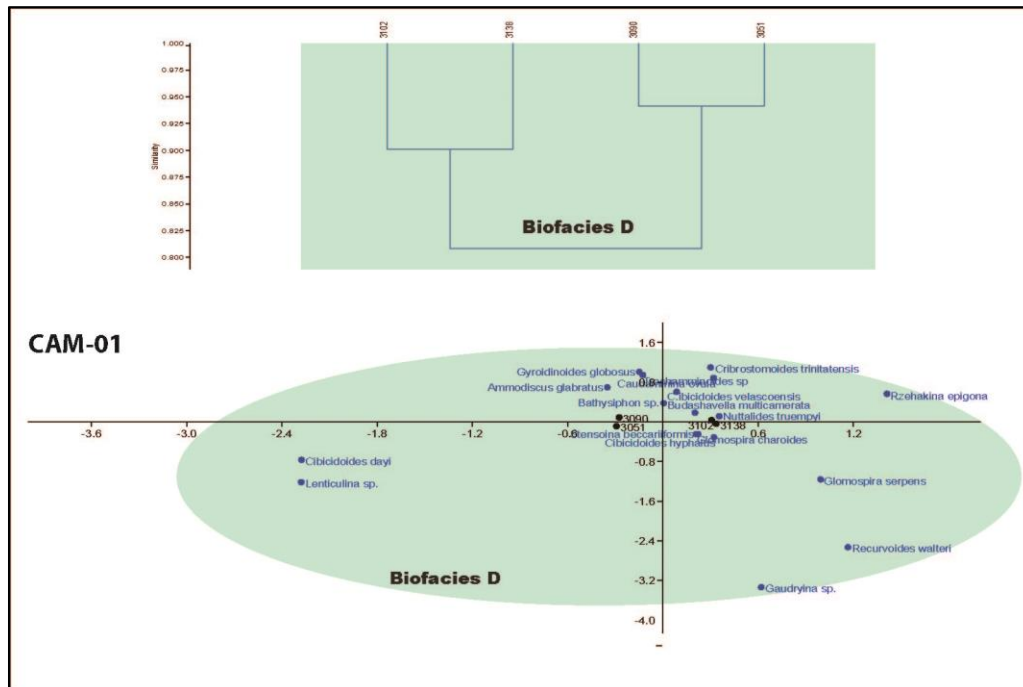


Figure 3.15: Dendrogram classifications of the samples produced by Q-mode cluster analysis and correspondence analysis showing the major biofacies recognized for the well CAM-01.

3.6.3.2 – Well CAM-02:

The six sidewall samples available from this well span the upper Paleocene through the upper Eocene interval with an unconformity from the uppermost Paleocene to lower Eocene (missing nannofossil biozones CP8 to CP10**). The upper, middle and lower Eocene is each represented by a single sample, and the other three samples are from the Paleocene.

Although the very distinct characteristics of each sample, with very low species diversity and poor preservation of the foraminiferal tests, it was possible to recognize one biofacies for the upper Paleocene interval through the lower Eocene (Biofacies E – Fig. 3.16). The middle to upper Eocene interval has 90-100% planktics damaged by dissolution as well as rare benthic calcareous taxa (*Cibicidoides* sp., *Lenticulina* sp.). For this reason, it was not possible to recognize any biofacies for this interval of the Eocene. The entire study interval consists of shale with thin layers of calcirudite and sandstone (Fig. 3.8).

➤ **Biofacies E**

Main taxa: *Bathysiphon* sp., *Haplophragmoides* sp., *Recurvoides* sp.

Other taxa: *Rhizammina* sp., *Glomospira serpens*, *Cribrostomoides subglobosus*, *Karrerulina conversa*, *Trochamminoides* sp., *Subreophax* sp. Tubular forms 35% of benthics.

Planktic: 0%.

Paleobathymetric range: lower abyssal.

Age range: late Paleocene to early Eocene (CP6/7** and CP11**)

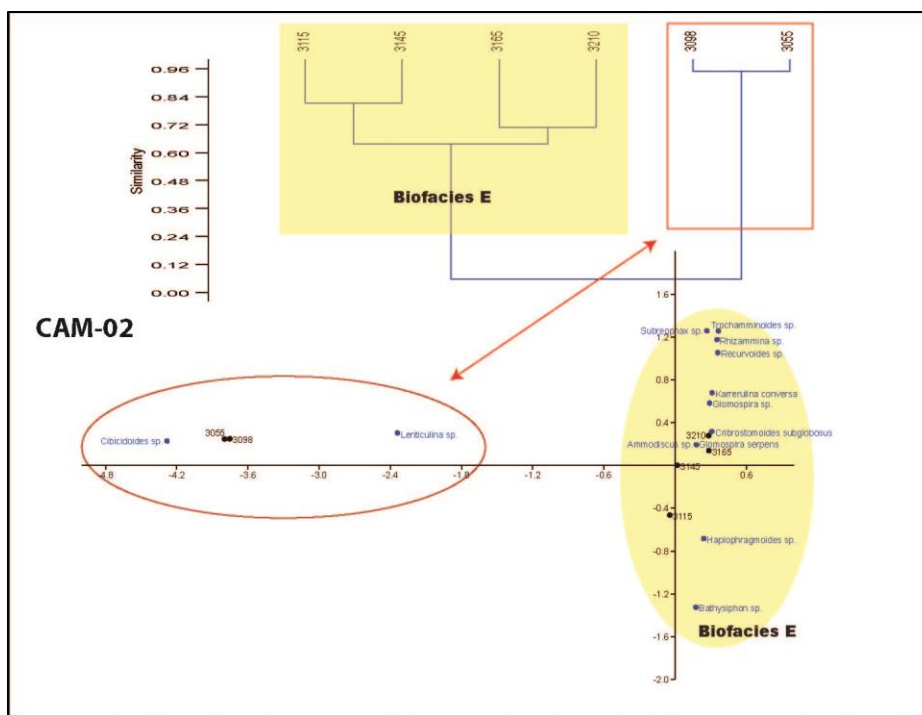


Figure 3.16: Dendrogram classifications of the samples produced by Q-mode cluster analysis and correspondence analysis (CA) showing the major biofacies and the interval with poor recovery of the well CAM-02.

3.6.3.3 – Well CAM-03:

The correspondence analysis and the Q-mode cluster analysis result in two distinct groups corresponding with two major biofacies that occur intercalated in the studied interval (Fig. 3.17). The two major biofacies are D (mix of agglutinants and calcareous taxa) and E (flesch-type assemblage). The biofacies D coincides with increased planktics (>80% of total assemblage). The biofacies E2 contains a true flesch-type benthic assemblage, in which the tubular forms dominate (*Rhizammina*, *Bathysiphon*, *Psammosiphonella discreta*, *P. cylindrica*) associated with the coarse-grain agglutinated taxa (*Haplophragmoides*, *Paratrochamminoides*, *Recurvoides*,

Trochamminoides). The calcareous benthic and planktic foraminifera are poorly preserved, exhibiting clear evidence of dissolution.

The Paleocene-Eocene interval is composed mostly of shale, with layers of calcirudite in the middle Eocene and a thick layer of sandstone in the middle Eocene and middle Paleocene intervals. There is a gap from the upper Paleocene through the lower Eocene, probably missing due to erosional hiatus, a 100-m thick sand layer overlies the Paleocene interval (Fig. 3.8).

➤ **Biofacies D1**

Main taxa: *Cibicidoides havanensis*, *Recurvoides* sp., *Cibicidoides* sp.

Other taxa: *Anomalinoides* sp., *C. eocaenus*, *C. mexicanus*, *Gyroidinoides* sp., *Hanzawaia ammophila*, *Oridorsalis umbonatus*, *Dorothia* sp., *Glomospira* sp., *Psammosiphonella discreta*, *P. cylindrica*, *Recurvoides* sp., *Paratrochamminoides* sp.

Planktic: 80-90% of total assemblage.

Paleobathymetric range: lower bathyal.

Age range: late Eocene (CP15**).

➤ **Biofacies E1**

Main Taxa: *Bathysiphon* sp., *Psammosphaera fusca*, *Rhizammina* sp.

Other taxa: *Cyclamina placenta*, *Haplophragmoides* sp., *H. contortus*, *H. walteri*, *H. porrectus*, *Recurvoides* sp., *R. anormis*, *R. contortus*, *Cribrostomoides subglobosus*, *Kalamopsis grzybowiskii*, *Karrerulina conversa*, *Paratrochamminoides* sp., *Ammodiscus cretaceous*, *A. latus*, *Saccamina placenta*, *Cibicidoides* sp., and *Gyroidindoides* sp.

Tubular forms ~30% of benthics.

Planktic: ~70% of total assemblage.

Paleobathymetric range: lower bathyal/upper abyssal.

Age range: middle Eocene (CP14**).

➤ **Biofacies D2**

Main taxa: *Cibicidoides* sp., *Lenticulina* sp., *Bathysiphon* sp.

Other taxa: *Gyroidindoides* sp., *Globocassidulina subglobosa*, *Dorothia* sp., *Haplophragmoides* sp.

Planktic: ~90% of total assemblage.

Paleobathymetric range: middle to lower bathyal.

Age range: middle Eocene (CP14**).

➤ **Biofacies E2**

Main taxa: *Bathysiphon* sp., *Kalamopsis grzybowskii*, *Psammosiphonella cylindrica*, *Rhizammina* sp.

Other taxa: *Ammodiscus glabratus*, *A. cretaceous*, *A. latus*, *Cribrostomoides subglobosus*, *Cyclammina placenta*, *Glomospira charoides*, *Haplophragmoides* sp., *H. stomatus*, *H. porrectus*, *H. walteri*, *Karrerulina conversa*, *Paratrochamminoides* sp., *Recurvoides* sp., *R. anormis*, *R. contortus*, *Trochamminoides altiformis*, *Spiroplectammina spectabilis*.

Tubular forms 40-60% of benthics.

Planktic: 0%.

Paleobathymetric range: lower abyssal.

Age range: Paleocene (?).

➤ **Biofacies D3**

Main Taxa: *Gyroidinoides* sp., *Nuttallides truempyi*, *Caudammina ovula*

Other taxa: *Alabamina midwayensis*, *Anomalinoides* sp., *Cibicidoides* sp., *Guttulina trigonula*, *Glomospira charoides*, *Eggerella* sp., *Marssonella* sp., *Textularia* sp.

Planktic: 70-80% of total assemblage.

Paleobathymetric range: lower bathyal.

Age range: early Paleocene (P3*, CP3/4**).

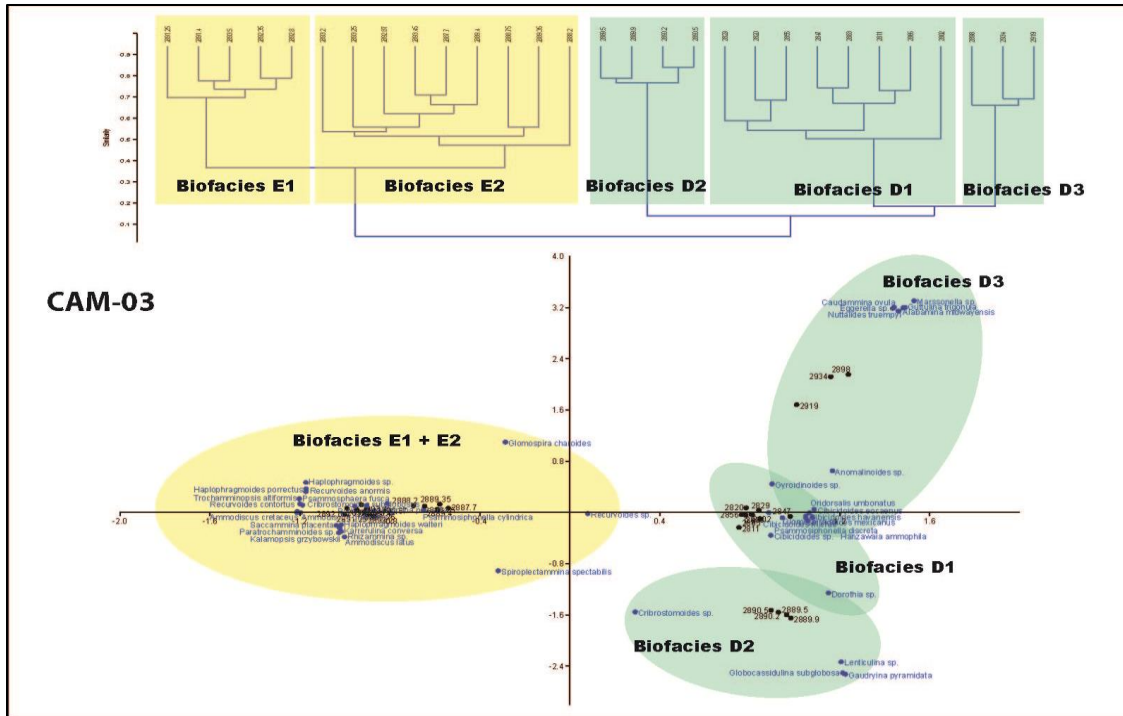


Figure 3.17: Dendrogram classifications of the samples produced by Q-mode cluster analysis and correspondence analysis showing the five major biofacies recognized for the well CAM-03.

3.6.3.4 – Well CAM-04:

The Q-mode cluster and correspondence analyses classified the interval into two biofacies, one for the middle Eocene and other for the Paleocene (Fig. 3.18). The lower Eocene is missing probably related to erosion associated with sandstone deposition. The middle Eocene biofacies was deposited in a shale interval with layers of calcirudite, while the Paleocene is characterized by a sandstone interval with layers of shale. The benthic foraminiferal assemblage for the Paleocene interval corresponds to the flysch-type biofacies and the middle Eocene has a mix of agglutinated and calcareous taxa. The planktic and calcareous benthic foraminifera are poorly preserved, especially in the Biofacies E interval. Planktic and calcareous benthic foraminifera exhibit evidence of dissolution in the Biofacies D interval.

➤ **Biofacies D**

Main taxa: *Cibicidoides eocaenus*, *Globocassidulina subglobosa*, *Dorothia* sp., *Gaudryina* sp., *Gaudryina pyramidata*.

Other taxa: *Cibicidoides* sp., *Gyroidinoides* sp., *Hanzawaia ammophila*, *Oridorsalis umbonatus*, *Eggerella* sp.

Planktic: ~80% of total assemblage (very poorly preserved).

Paleobathymetric range: middle bathyal.

Age range: middle Eocene (CP13/14**).

➤ **Biofacies E**

Main taxa: *Rhizammina* sp., *Psammosiphonella cylindrica*, *Kalamopsis grzybowski*, *Bathysiphon* sp. Tubular forms ~60% of benthics.

Other taxa: *Ammodiscus latus*, *A. glabratus*, *Cribrostomoides trinitatensis*, *Glomospira charoides*, *Haplophragmoides* sp., *Saccamina placenta*, *Cibicidoides velascoensis*, *Karrerulina conversa*, *Stensioeina beccariiiformis*, *Nuttallides truempyi*, *Gyroidinoides globosus*, *Nothia* sp., *Recurvoides* sp.,

Planktic: 0%.

Paleobathymetric range: lower abyssal.

Age range: Paleocene (CP1/7**).

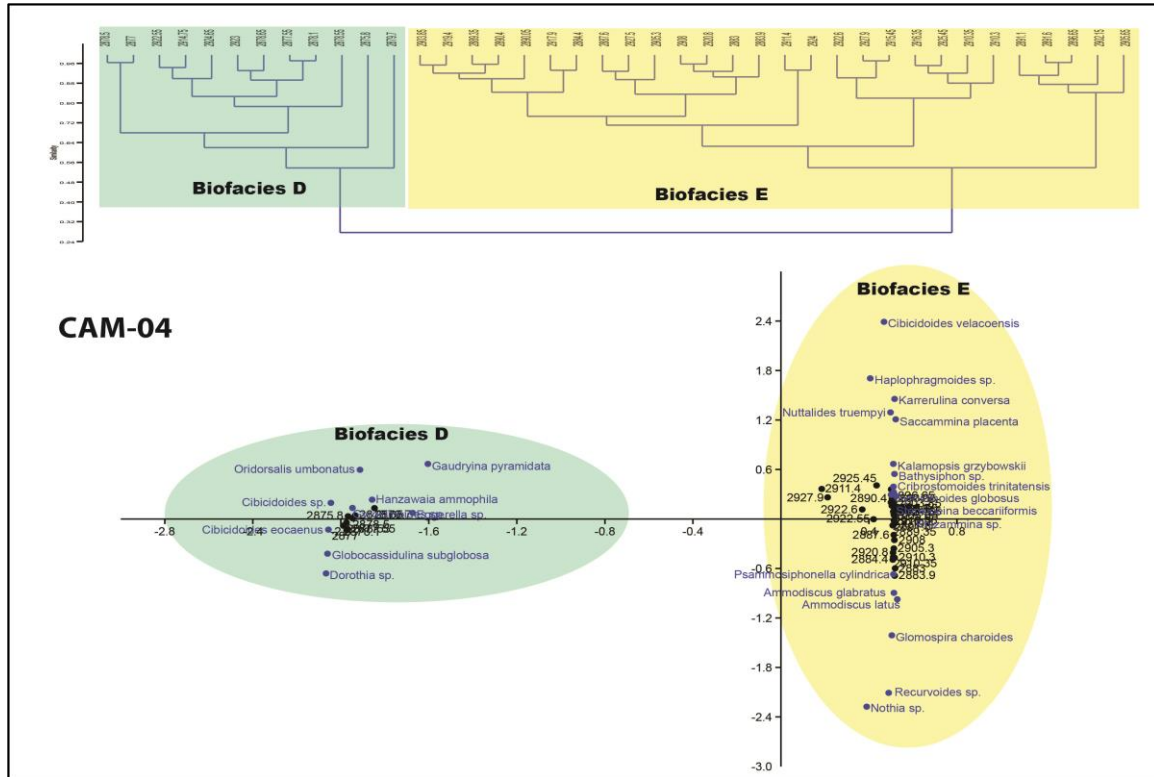


Figure 3.18: Dendrogram classifications of the samples produced by Q-mode cluster analysis and correspondence analysis showing the two major biofacies recognized for the well CAM-04.

3.6.3.4 – Paleobathymetry of Campos Basin:

There were four major depositional sequences identified in the Paleocene-Eocene interval of the Campos Basin: lower Paleocene (biozones CP1 to CP3), lower to upper Paleocene (biozones CP4 to CP6), middle Eocene (biozones CP12 to CP13) and middle to upper Eocene (nanno biozones CP14 to CP15) (Becker et al., 2000). The lower Eocene is poorly represented among the wells of this basin (CAM-01, CAM-02, CAM-03, CAM-04 – Fig. 3.8). This near-absence of lower Eocene deposits may be related to tectonic reactivation in the source area (Serra do Mar Mountains) inland that increased mass wasting and the downslope transport in the area (Almeida and Carneiro, 1998,

Modica and Brush, 2004). Becker et al. (2000) reported an unconformity between the middle Eocene and Paleocene.

The age model for the wells CAM-01, CAM-02, CAM-03 and CAM-04 shows a relatively low sedimentation rate (0.26 to 13m/myr) for the upper Maastrichtian to the middle Eocene (Figs. 3.19 to 3.22). The upper Eocene had a significantly increase in sedimentation rate (12 to 35 m/myr). The low sedimentation rate (when compared with other Brazilian marginal basins) could be one of the factors that contributed to the establishment of the flysch-type biofacies. The tubular forms are mainly suspension-feeders and have been reported as inhabit tranquil bathyal and abyssal regions with low organic matter flux (Jones and Charnock, 1985, Kaminski and Gradstein, 2005).

Biofacies E occurs mainly in Paleocene of the Brazilian marginal basins with a paleobathymetric range from lower abyssal through lower bathyal zones. These depths represented by Biofacies E were close to, or below the CCD. Relatively high sea-level in the Paleocene was suggested by sedimentological and stratigraphic evidences by Becker et al. (2000). These authors interpreted the early Cenozoic depositional sequences as cover for the Cretaceous bottom sea irregularities. The thickness of the Paleogene cover varies across the basin, and it was basically controlled by salt tectonics and turbidite deposition. High sea level may have contributed to an elevated CCD during the Paleocene and early Eocene. Biofacies D occurred more frequently in the middle to upper Eocene interval and represents shoaling of the basin to lower to middle bathyal paleobathymetric zones.

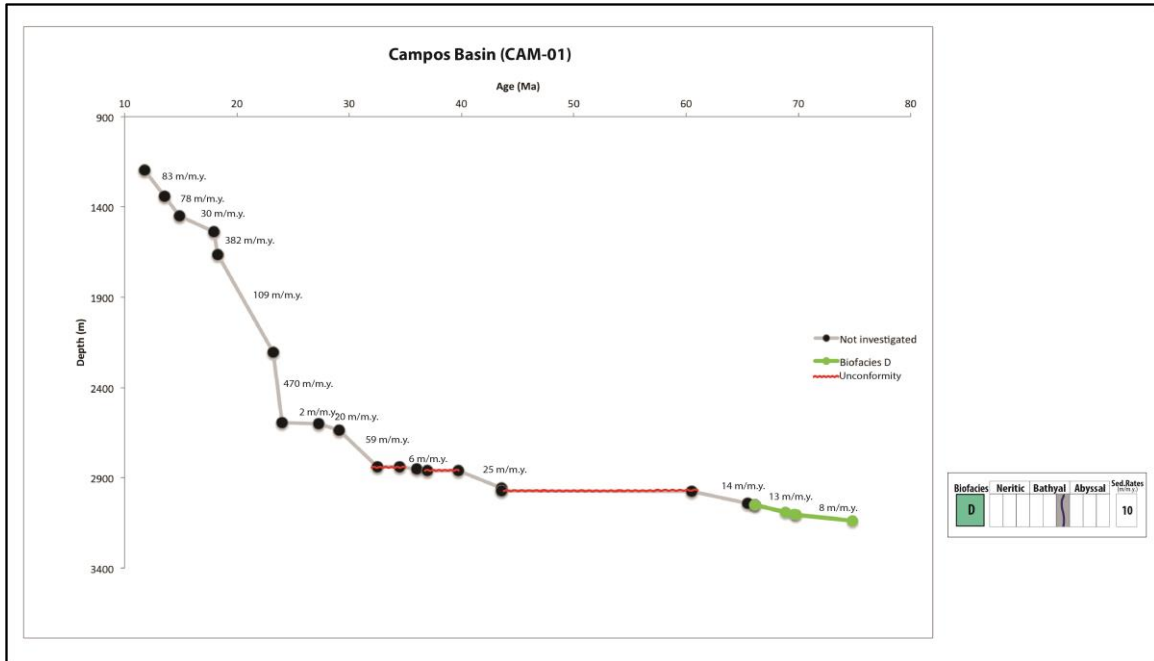


Figure 3.19: Age vs Depth Model of the well CAM-01 plotted with the benthic foraminiferal biofacies with correlated paleobathymetric range and sedimentation rates.

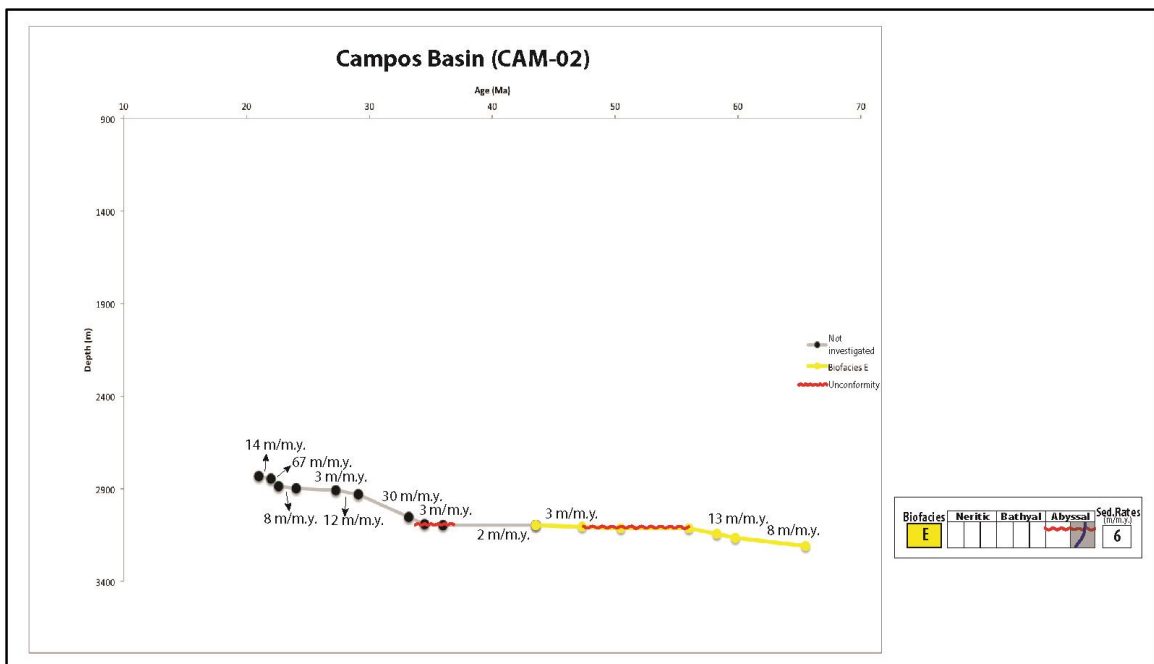


Figure 3.20: Age vs Depth Model of the well CAM-02 plotted with the benthic foraminiferal biofacies with correlated paleobathymetric range and sedimentation rates.

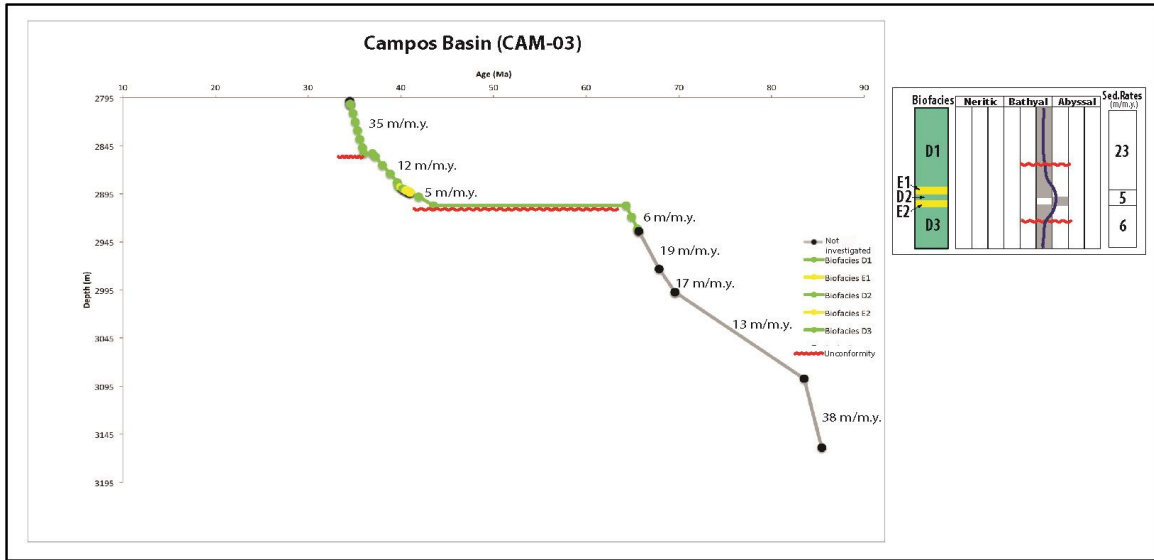


Figure 3.21: Age vs Depth Model of the well CAM-03 plotted with the benthic foraminiferal biofacies with correlated paleobathymetric range and sedimentation rates.

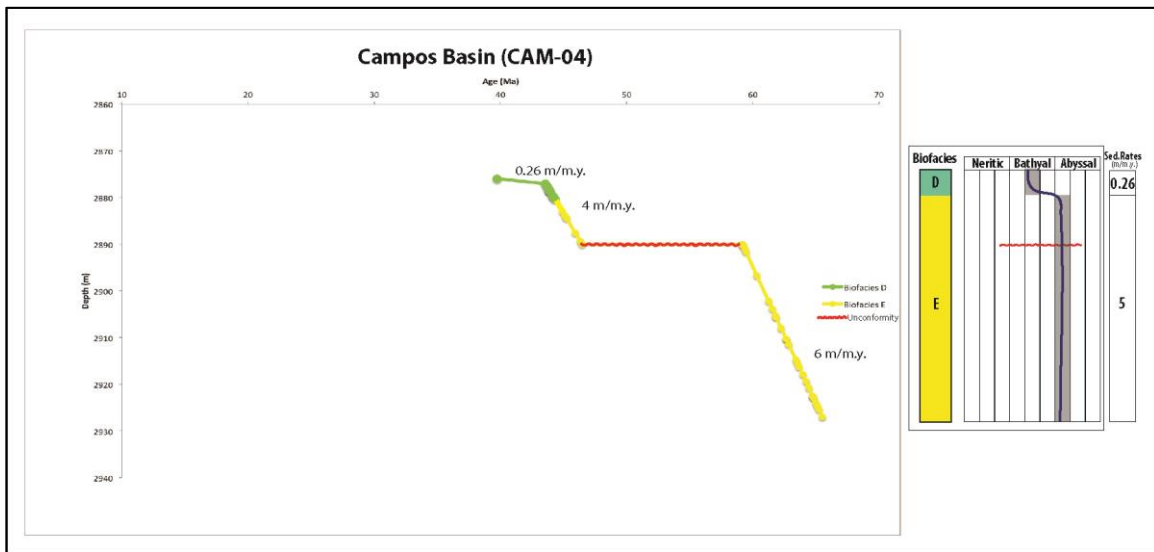


Figure 3.22: Age vs Depth Model of the well CAM-04 plotted with the benthic foraminiferal biofacies with correlated paleobathymetric range and sedimentation rates.

3.6.4 – Santos Basin:

3.6.4.1 – Well SAN-01:

The Santos Basin is represented by two wells (SAN-01 and SAN-02) that are ~500km apart (Fig. 3.1). Biofacies were recognized in only one of them, SAN-01, due to the poor preservation of the benthic and planktic foraminifera in SAN-02.

The Paleocene-Eocene interval recovered from this well has at least three major unconformities associated with the turbidite deposition on the slope: lower to middle Paleocene (nannofossil biozones CP1 to CP4), upper Paleocene to lower Eocene (nannofossil biozones CP6 to CP9) and middle to upper Eocene (nannofossil biozones CP11 to CP14) (Fig. 3.8). Despite the presence of these depositional gaps, it was possible to recognize four distinct biofacies of benthic foraminifera based on the Q-mode cluster and correspondence analysis (Fig. 3.23). The biofacies are distinct for each time slice from the Maastrichtian through the upper Eocene.

➤ **Biofacies C**

Main taxa: *Nuttallides truempyi*, *Oridorsalis umbonatus*, *Globocassidulina subglobosa*.

Other taxa: *Osangularia mexicana*, *Cibicidoides* sp., *Dorothia beloides*, *Eggerelina brevis*, *Hanzawaia ammophila*.

Planktics: 50% of total assemblage.

Paleobathymetric range: lower bathyal.

Age range: late Eocene (CP15**).

➤ **Biofacies A**

Main taxa: *Hanzawaia ammophila*, *Stainforthia* sp., *Pullenia* sp.

Other taxa: *Nuttallides truempyi*, *Gavelinella* sp., *Globobulimina* sp., *Oridorsalis umbonatus* and radiolarians (40-100% of total assemblage).

Planktics: 50-60% of total assemblage.

Paleobathymetric range: middle to lower bathyal.

Age range: early Eocene (CP10**).

➤ **Biofacies E**

This biofacies is dominated by agglutinated taxa, however a mix of agglutinants and calcareous benthic foraminifera is present in some samples. The agglutinated taxa have a greater percentage of tubular forms (*Rhizammina*, *Bathysiphon*, *Psammosiphonella cylindrica*) reaching 70% of benthics in some samples, the average is ~40%.

Main taxa: *Psammosiphonella cylindrica*, *Rhizammina* sp., *Spiroplectammina jarvisi*.

Other taxa: *A. glabratus*, *A. latus*, *Haplophragmoides* sp., *Karrerulina conversa*, *Psammosphaera fusca*, *Haplophragmoides suborbicularis*, *Cribrostomoides trinitatensis*, *Nuttallides truempyi*, *Gavelinella* sp., *G. globosus*, *Cibicidoides pseudoperlucidus*, *Anomalinoidea capitatus*.

Planktics: 40-50% of total assemblage, although they are poorly preserved.

Paleobathymetric range: lower bathyal to upper abyssal.

Age range: late Paleocene (P4*, CP5/6**).

➤ **Biofacies D**

This biofacies is mostly composed by calcareous taxa, although some samples have a contribution of agglutinated taxa (30-40% of benthics). The agglutinated taxa have a significant percentage of tubular forms (20-30% of agglutinants).

Main taxa: *Psammosiphonella cylindrica*, *Globobulimina* sp., *Gyroidinoides globosus*

Other taxa: *Stensioeina beccariiiformis*, *Gavelinella* sp., *Bulimina* sp., *Ammodiscus pennyi*, *Caudammina excelsa*, *Haplophragmoides eggeri*, *Bathysiphon* sp., *Nuttallides truempyi*.

Planktics: 45-60% of total assemblage.

Paleobathymetric range: middle to lower bathyal.

Age range: late Maastrichtian (NC23**).

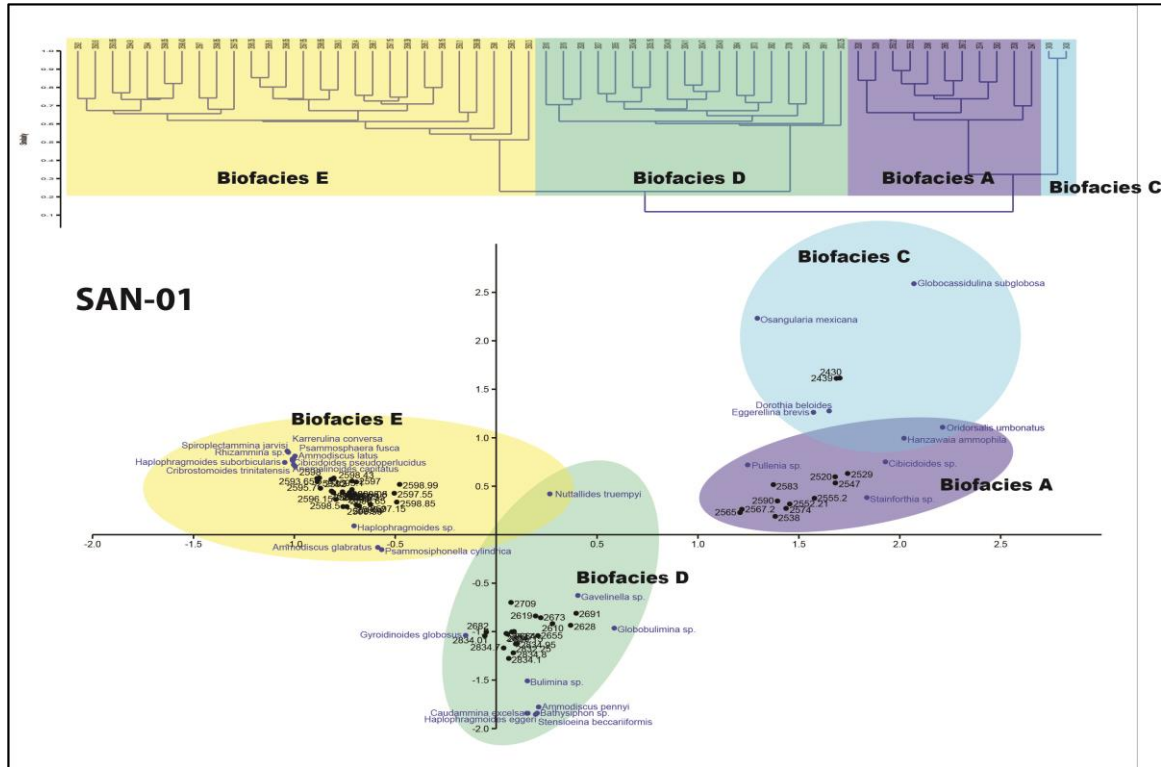


Figure 3.23: Dendrogram classifications of the samples produced by Q-mode cluster analysis and correspondence analysis showing the four major biofacies recognized for the well SAN-01.

3.6.4.2 – Well SAN-02:

The well SAN-02 recovered the lower Eocene interval (CP9/10**) and there was not possible to recognize any benthic foraminiferal biofacies. The interval is mostly dominated by radiolarians (60% to 100% of total assemblage) and the rare planktic and calcareous benthic foraminifera recovered were totally damaged by dissolution. The agglutinants are very rare and are not diagnostic of any biofacies (*Saccammina*, *Caudammina*, *Haplophragmoides*).

3.6.4.3 – Paleobathymetry of Santos Basin:

The biofacies recognized at SAN-01 represented a sequence from the middle to lower bathyal in the upper Maastrichtian (Biofacies D), to lower bathyal to upper abyssal in the upper Paleocene (Biofacies E), middle to lower bathyal in the lower Eocene (Biofacies A) and lower bathyal in the upper Eocene (Biofacies C) (Fig. 3.24). The Paleocene interval is very thin, corresponding to ~40-m thick silt-sand layer. Biofacies E (upper Paleocene) occurs in the transition from a ~34-m thick silt interval to a coarse sandy interval (Fig. 3.8).

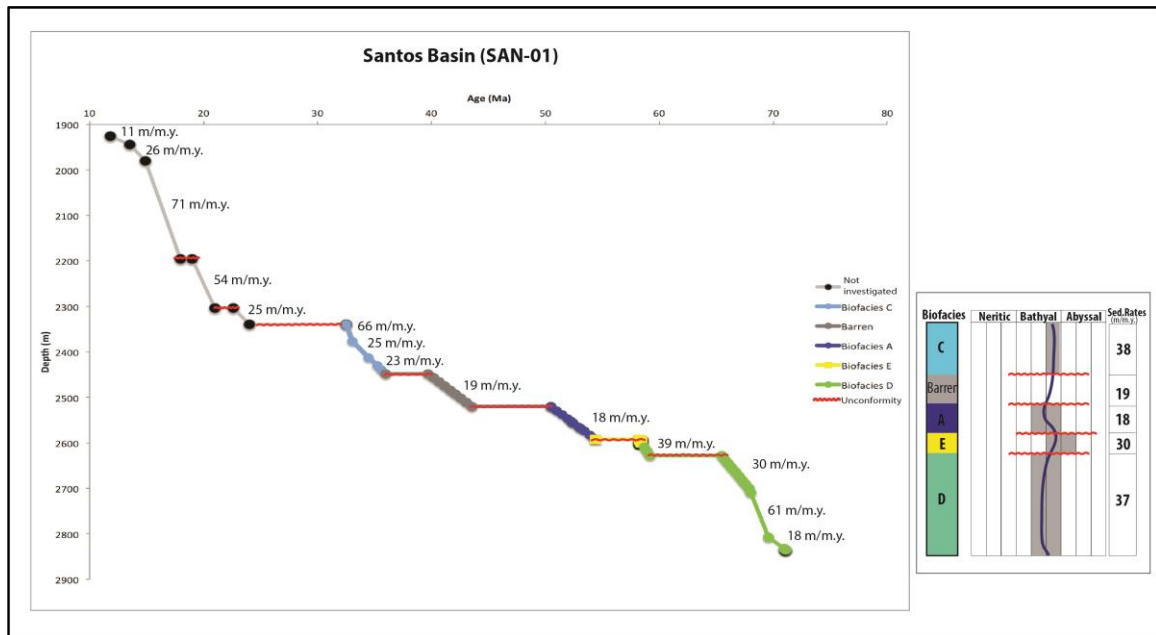


Figure 3.24: Age vs Depth Model of the well SAN-01 plotted with the benthic foraminiferal biofacies with correlated paleobathymetric range and sedimentation rates.

3.6.5 – Pelotas Basin:

3.6.5.1 – Well PEL-01:

The Pelotas Basin is represented by the well PEL-01, and the samples cover the Maastrichtian through the upper Eocene (biozones NC23 to CP15). There is only one major unconformity in the lower Eocene (missing biozone CP11). This location has one of the best preservation of the benthic foraminifera among the industry wells examined in this study.

The three biofacies classified by the Q-mode cluster and correspondence analysis (Fig. 3.25) could be differentiated into distinct paleoecological settings, evolving from more turbulent bottom water with turbidity currents during the Paleocene to a more stable slope where hemipelagic deposition dominated for most of the Eocene. The flysch-type biofacies dominates the lower part of the interval. This environment changed to an environment where calcareous taxa are part of the assemblage and tubular taxa such as *Bathysiphon* sp. disappeared.

➤ **Biofacies C**

Main Taxa: *Anomalinoides garzaensis*, *Bulimina alazanensis*, *Gaudryina pyramidata*, *Cibicidoides eoceanus*, *C. praemundulus*.

Other taxa: *Anomalinoides* sp., *Bulimina* sp., *Bulimina midwayensis*, *B. alazanensis*, *Neoeponides elevatus*, *N. byramensis*, *Globobulimina* sp., *Nuttallinella* sp.1, *Planulina costata*, *Praebulimina* sp., *Siphonina* sp., *Uvigerina* sp., *Cribrostomoides* sp., *Clavulinoides* sp., *Gaudryina* sp., *Haplophragmoides* sp., *Reticulphragmium acutidorsatum*, *R. amplectens*.

Planktic: 0-10% of total assemblage (planktics very tiny or poorly preserved on this biofacies interval)

Paleobathymetric range: middle bathyal.

Age range: early Eocene (E6* - CP11/12**) through late Eocene (E15* - CP15**).

➤ **Biofacies B**

Main taxa: *Cibicidoides eocaenus*, *Paralabamina lunata*, *Hanzawaia ammophila*.

Other taxa: *Alabamina dissonata*, *Cibicidoides sp.*, *Gyroidinoides subangulatus*, *Nuttallides truempyi*, *Pullenia sp.*, *Gaudryina sp.*, *Anomalinoides sp.*, *Globobulimina sp.*, *Spiroplectammina sp.*

Planktic: 0 to 25% (very tiny planktics when they occur).

Paleobathymetric range: middle to lower bathyal.

Age range: late Paleocene (P5* – CP8**) through early Eocene (E6/7* – CP11/12**).

➤ **Biofacies E**

Main taxa: *Bathysiphon sp.*, *Haplophragmoides sp.*, *Gaudryina pyramidata*, *Cyclammina placenta*.

Other taxa: *Bolivinopsis spectabilis*, *Budashevaella multicamerata*, *Cribrostomoides subglobosus*, *Gaudryina sp.*, *G. laevigata*, *Hormosina sp.*, *Marssonella sp.*, *Marssonella trochoides*, *Psammosiphonella cylindrica*, *Saccammina placenta*. Tubular forms 10 to 25% of benthics.

Planktic: 0%.

Paleobathymetric range: lower abyssal.

Age range: Maastrichtian (P0* - NC23**) through late Paleocene (P4/P5* - CP7/8**).

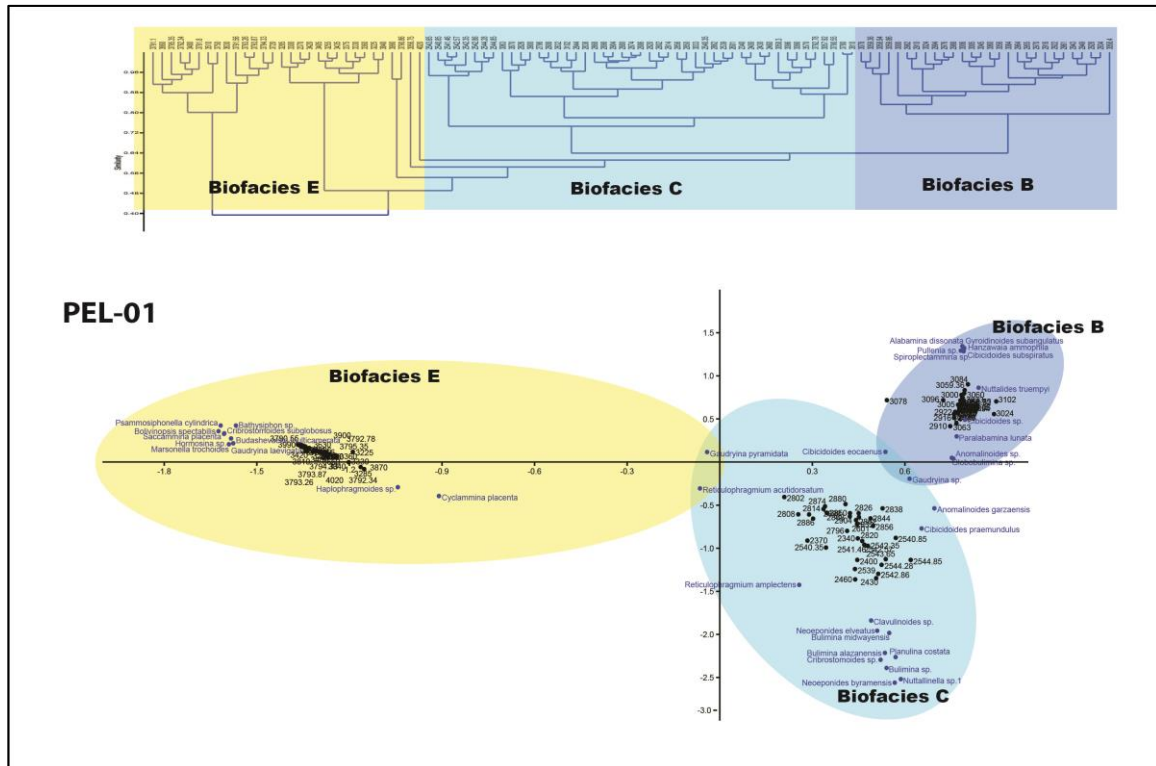


Figure 3.25: Dendrogram classifications of the samples produced by Q-mode cluster analysis and correspondence analysis showing the three major biofacies recognized for the well PEL-01

3.6.5.2 – Paleobathymetry of Pelotas Basin:

The age vs depth model demonstrates that this location experienced nearly continuous sedimentation with alternating intervals of higher and lower sedimentation rates (Fig. 3.26). Correa (2004) reported an average of 53m/myr sedimentation rate for the Maastrichtian through the upper Eocene. The Maastrichtian-Paleocene interval is dominated by the Biofacies E, with abyssal paleodepths. During the Eocene, the bottom water conditions changed as the basin shoaled, creating a more favorable environment for calcareous benthic taxa. Biofacies B characterizes the lower Eocene with paleodepth of middle to lower bathyal. Biofacies C dominates the middle and upper Eocene with middle bathyal paleodepths. Overall, the basin records a shallowing upwards trend, as observed in the other marginal basins, due primarily to the progradation of the continental margin and shoaling of the slope during the Paleocene-Eocene.

The planktic foraminifera are rare to absent throughout the entire interval, with percentages up to 25%. The preservation is bad and very tiny specimens are the most common suggesting depths below the foraminiferal lysocline (Berger, 1970, 1973, Berger et al., 1982, Kucera et al., 1997, Waškowska-Oliwa, 2005).

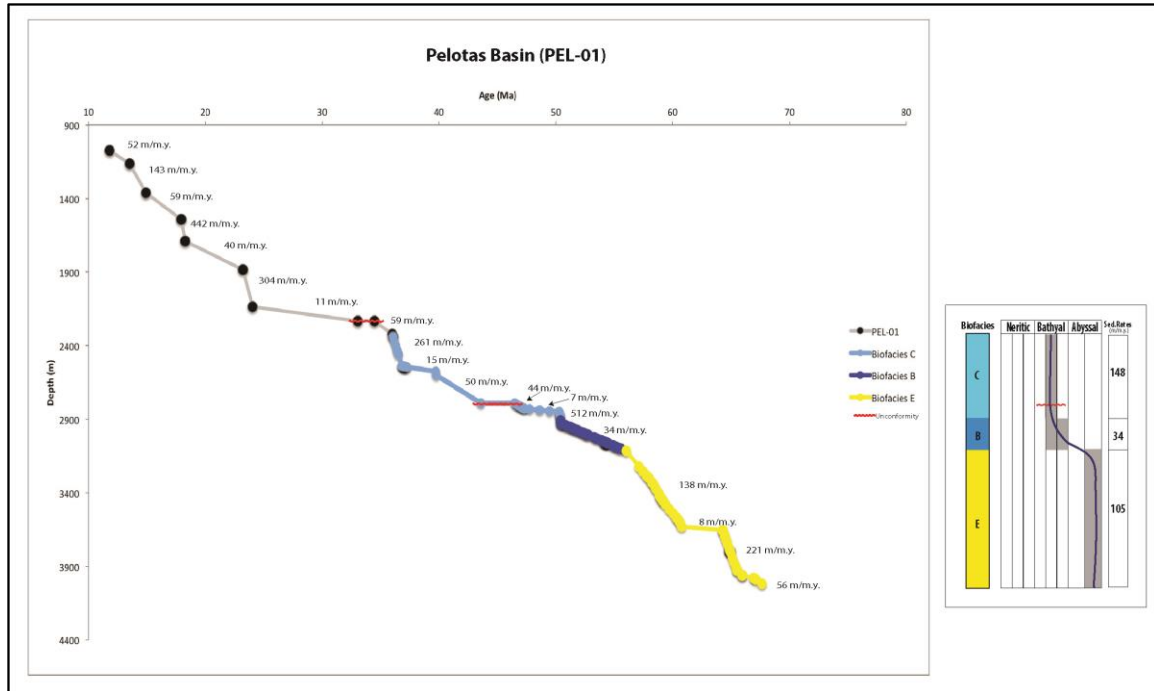


Figure 3.26: Age vs Depth Model of the well PEL-01 plotted with the benthic foraminiferal biofacies with correlated paleobathymetric range and sedimentation rates.

3.6.6 – Abyssal Basin:

DSDP Sites 356, on the São Paulo Plateau, and Site 20C on the Brazil Basin abyssal plain represent the most distal locations included in this study and provide a contrast with the deep-water settings along the Brazilian continental margin. The Paleocene-Eocene was recorded at both locations, although the Site 20C covers from upper Maastrichtian through the upper Eocene. The preservation of the microfossils and continuity of these cores provides a valuable comparison with the Brazilian marginal basins, which were highly affected by turbidites, downslope debris flows and dissolution.

3.6.6.1 – Site 356 – São Paulo Plateau:

The Q-mode cluster analysis associated with the correspondence analysis classified four major calcareous-rich biofacies for this site. (Fig. 3.27). The radiolarians were included due to increased frequency in the middle Eocene interval. The Paleocene – Eocene interval is mostly composed of chalk with enrichment in silica in the middle Eocene. A barren interval corresponds to the lower Eocene (E3*, CP8**) (Figs. 3.7, 3.8).

➤ **Biofacies C1**

This biofacies occurs in the continuous record from the lower through middle Eocene and occurs in the silica-rich interval, especially in the middle Eocene. The benthic foraminiferal assemblage is mostly composed by calcareous taxa, although some agglutinated taxa are represented. The radiolarians are very expressive in this biofacies, reaching 60% in some samples (average 30-40% of total assemblage).

Main taxa: *Nuttallides truempyi*, *Osangularia mexicana*, *Gyrodinoides subangulatus*, *Stilostomella* sp., *Gaudryina* sp.

Other taxa: *Oridorsalis umbonatus*, *Bulimina tuxpamensis*, *B. trinitatensis*, *Karreruela subglabra*, *Spiroplectammina spectabilis*, *Haplophragmoides* sp., *Pullenia eocenica*.

Planktic: 93-99% of total assemblage.

Paleobathymetric range: lower bathyal to upper abyssal.

Age range: early (E6*, CP11**) to middle Eocene (E12*, CP14**).

➤ **Biofacies A**

This biofacies occurs above the barren Paleocene/Eocene boundary interval and is characterized by a benthic foraminiferal assemblage composition that is 100% calcareous taxa, along with radiolarians around 10% of total assemblage.

Main taxa: *Cibicidoides subspiratus*, *Globocassidulina subglobosa*, *Hanzawaia ammophila*.

Other taxa: *Alabamina dissonata*, *Anomalinoides capitatus*, *B. semicostata*, *B. trinitatensis*, *Cibicidoides* sp., *Gyroidinoides* sp., *G. subangulatus*, *Oridorsalis umbonatus*, *Stilostomella* sp., *Nuttallides truempyi*.

Planktic: 80-98% of total assemblage.

Paleobathymetric range: lower bathyal.

Age range: early Eocene (E4/5*, CP9/10**).

➤ **Biofacies B**

This biofacies has the lowest species richness compared with other biofacies at this site and occurs below the barren Paleocene/Eocene boundary interval.

Main taxa: *Gyroidinoides globosus*, *Pullenia coryelli*, *Anomalinoides* sp.

Other taxa: *Gavelinella* sp., *Osangularia* sp., *Pullenia* sp., *Gaudryina* sp., *Gaudryina pyramidata*, *Nuttallides truempyi*.

Planktic: 50-80% of total assemblage.

Paleobathymetric range: middle to lower bathyal

Age range: middle (P3*, CP3/4**) to late Paleocene (P4*, CP5/6**).

➤ **Biofacies C2**

This biofacies occurs from the upper Maastrichtian through the upper Paleocene, and correlates with the 'Velasco-type' assemblage described by Berggren and Aubert (1975). This biofacies comprises the pre-PETM benthic foraminiferal assemblage.

Main taxa: *Nuttallides truempyi*, *Stensioeina beccariiformis*, *Neoeponides hillebrandti*, *Gaudryina pyramidata*

Other taxa: *Alabamina midwayensis*, *Aragonia velascoensis*, *Anomalinoides* sp., *Bulimina* sp., *B. trinitatensis*, *Buliminella grata*, *Cibicidoides hyphalus*, *C. velascoensis*, *Gavelinella* sp., *Guttulina trigonula*, *Gyroidinoides*, *G. globosus*, *Lenticulina whitei*, *Osangularia velascoensis*, *Oridorsalis umbonatus*, *Oridorsalis* sp., *Pullenia coryelli*, *Quadratobuliminella pyramidalis*, *Pyramidina* sp., *Dorothia trochoides*, *Clavulinoides* sp., *Marssonella*, *Spiroplectammina spectabilis*.

Planktic: 70-90% of total assemblage.

Paleobathymetric range: middle to lower bathyal.

Age range: late Maastrichtian (NC23**) through late Paleocene (P3*, CP3**)

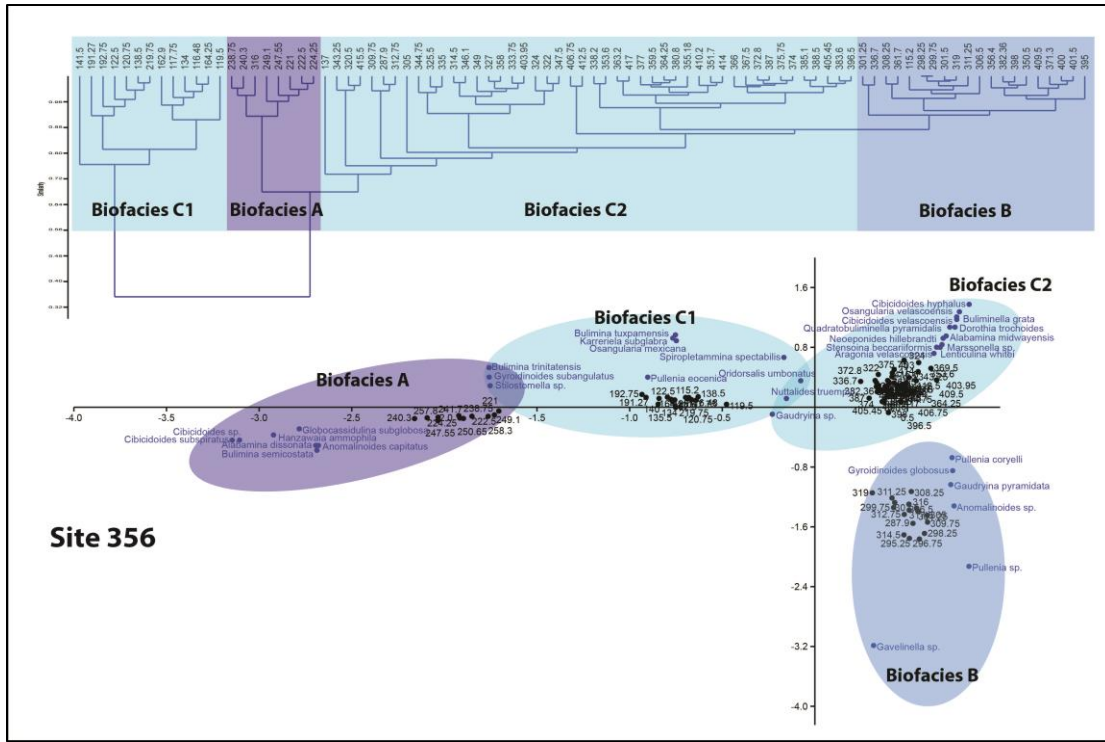


Figure 3.27: Dendrogram classifications of the samples produced by Q-mode cluster analysis and correspondence analysis showing the four major biofacies recognized for the Site 356.

3.6.6.2 – Site 20C – Brazilian Basin:

The Q-mode cluster analysis and the correspondence analysis discriminates four major biofacies that represent an intercalation between biofacies A, B and C through the upper Maastrichtian-Eocene interval (Fig. 3.28). This interval is composed of chalk and calcareous ooze with some zeolite-rich layers on the middle Eocene. Biofacies C2 correlates with the Velasco-type assemblage described by Berggren and Aubert (1975).

➤ Biofacies B

Main taxa: *Nuttallides truempyi*, *Globocassidulina subglobosa*, *Cibicidoides grimsdalei*, *Cibicidoides havanensis*, *Oridorsalis umbonatus*.

Other taxa: *Cibicidoides eocaenus*, *C. praemundulus*, *Alabamina dissonata*, *Aragonia aragonensis*, *Bolivina huneri*, *Buliminella grata*, *Plectofrondicularia lirata*, *Siphonodosaria* sp., *Stilostomella aculeata*, *S. spinosa*, *Gaudryina pyramidata*, *G. laevigata*, *Dorothia* sp.

Planktic: <20% of total assemblage

Paleobathymetric range: lower bathyal to upper abyssal.

Age range: middle to late Eocene (E10* to E16*).

➤ **Biofacies C1**

Main taxa: *Nuttallides truempyi*, *Oridorsalis umbonatus*, *Gaudryina pyramidata*, *Globocassidulina subglobosa*.

Other taxa: *Alabamina dissonata*, *Anomalinoides welleri*, *Aragonia aragonensis*, *Bulimina semicostata*, *Bulimina tuxpamensis*, *Cibicidoides eocaenus*, *Cibicidoides grimsdalei*, *C. havanensis*, *C. micrus*, *C. mexicanus*, *Gyroidinoides beisseli*, *G. subangulatus*, *Hanzawaia ammophila*, *Karreriella cubensis*, *Gaudryina laevigata*.

Planktic: 60-80% of total assemblage.

Paleobathymetric range: lower bathyal.

Age range: early to middle Eocene (E7* to E10*).

➤ **Biofacies A**

Main taxa: *Nuttallides truempyi*, *Anomalinoides praeacuta*, *Oridorsalis umbonatus*.

Other taxa: *Abyssamina poagi*, *A. quadrata*, *Alabamina midwayensis*, *Anomalinoides capitatus*, *Aragonia velascoensis*, *Nodosaria velascoensis*.

Planktic: ~70% of total assemblage.

Paleobathymetric range: lower bathyal.

Age range: late Paleocene to early Eocene (P4* to E7*).

➤ **Biofacies C2**

Main taxa: *Nuttallides truempyi*, *Gyroidinoides globosus*, *Stensioeina beccariiiformis*, *Oridorsalis umbonatus*.

Other taxa: *Neoeponides hillebrandti*, *Cibicidoides hyphalus*, *Anomalinoides praeacuta*, *Aragonia velascoensis*, *Buliminella grata*, *Cibicidoides velascoensis*, *Pullenia coryelli*, *Dorothia trochoides*, *Gaudryina pyramidata*, *G. laevigata*, *Tritaxia* sp., *Spiroplectammia* sp., *Osangularia velascoensis*.

Planktic: ~70% of total assemblage.

Paleobathymetric range: middle to lower bathyal.

Age range: late Maastrichtian to late Paleocene (NC23** to P4*).

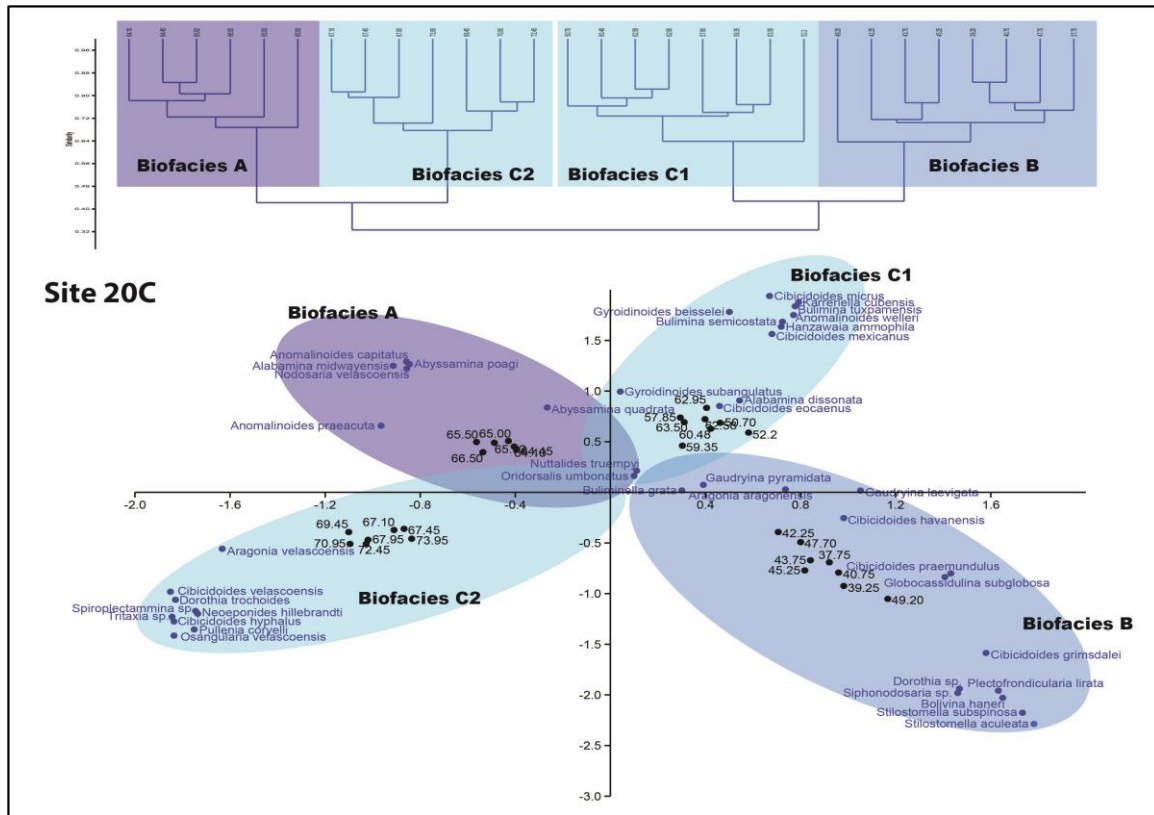


Figure 3.28: Dendrogram classifications of the samples produced by Q-mode cluster analysis and correspondence analysis showing the four major biofacies recognized for the Site 20C.

3.6.6.3 – Paleobathymetry:

The agglutinated taxa that dominated biofacies D and E on the Brazilian margin are absent in this area, probably related to the fact that the siliciclastic input could not reach this distal area with lower sedimentation rates (Figs. 3.29 and 3.30). The paleobathymetric range of both sites varies from the lower to middle bathyal in the Paleocene to abyssal to lower bathyal in the upper Eocene. The calcareous dominated biofacies (A, B and C) occur along the two sites from the upper Maastrichtian through the upper Eocene.

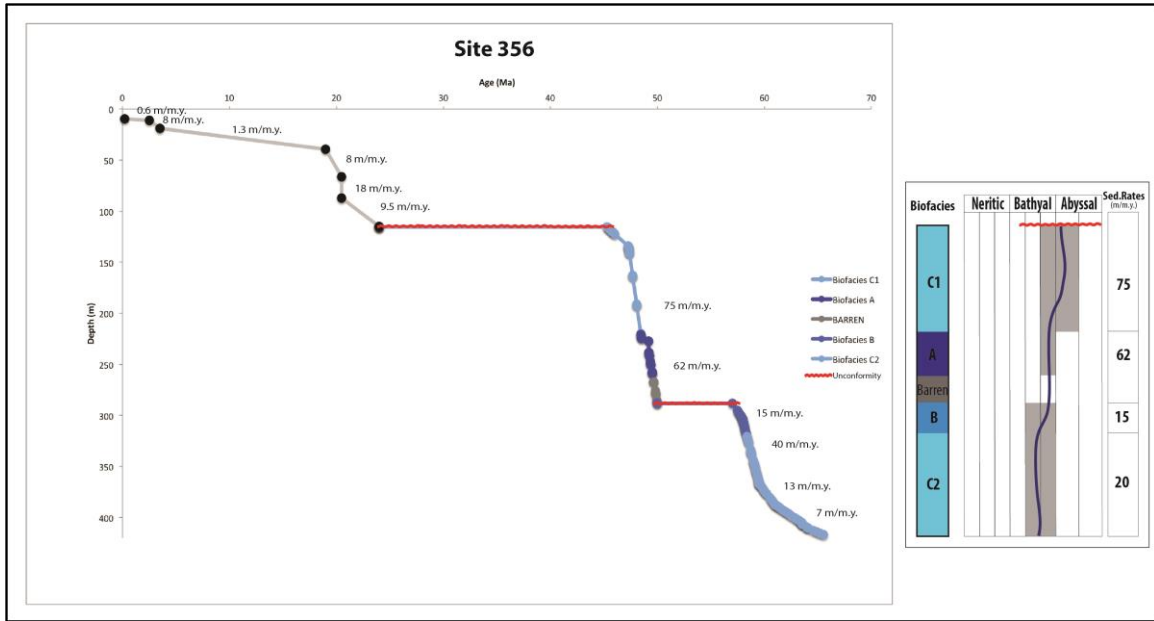


Figure 3.29: Age vs Depth Model of the DSDP Site 356 plotted with the benthic foraminiferal biofacies with correlated paleobathymetric range and sedimentation rates.

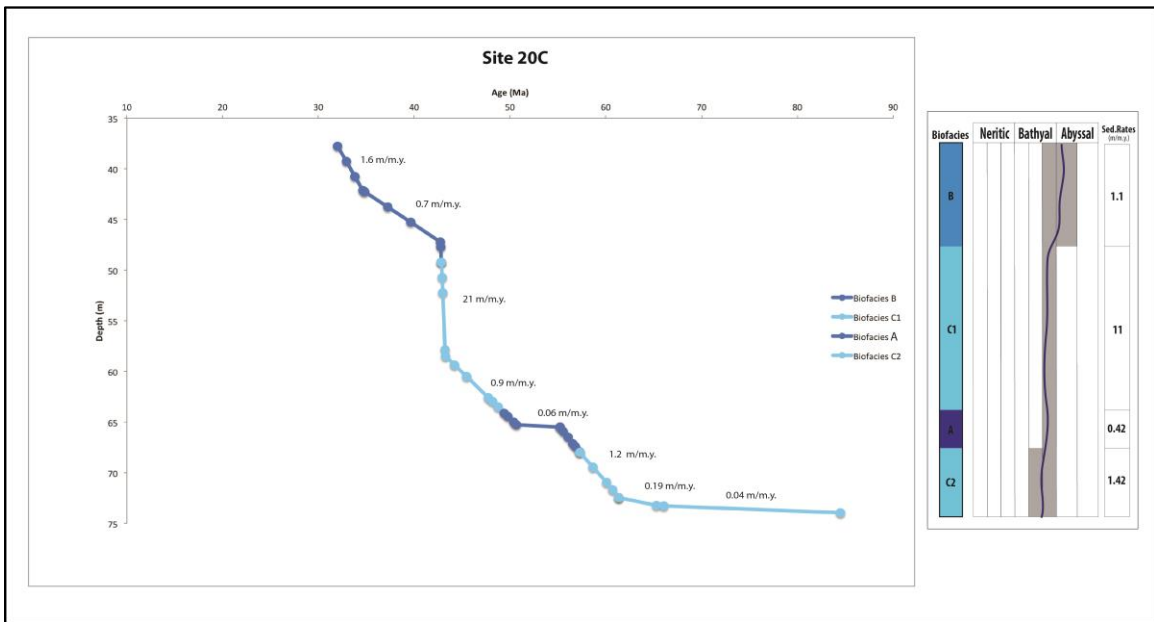


Figure 3.30: Age vs Depth Model of the DSDP Site 20C plotted with the benthic foraminiferal biofacies with correlated paleobathymetric range and sedimentation rates.

3.7 –BIOFACIES DISTRIBUTION IN THE WESTERN SOUTH ATLANTIC:

The benthic foraminiferal biofacies defined above by basin is now integrated and its distribution is presented here. The biofacies distribution maps shows how the biofacies were distributed and evolved from the late Maastrichtian through the late Eocene in the western South Atlantic.

The benthic foraminiferal biofacies reflect the environmental conditions in which the benthic foraminiferal assemblages lived. Late Maastrichtian sea-level was higher than present (Miller et al., 2005, Kominz et al., 2008), and during this time the western South Atlantic was mainly inhabited by three benthic foraminiferal biofacies: Biofacies D and E occurred exclusively on the Brazilian continental margin, and Biofacies C characterized the distal DSDP sites (Fig. 3.31).

The northern and southern basins (Sergipe-Alagoas, Mucuri and Pelotas) were dominated by the Biofacies E, although the presence of 35-45% planktic foraminifera in the Mururi Basin assemblages suggest that this location was above the CCD during the Maastrichtian, while the Sergipe-Alagoas and Pelotas basins with 0% planktics were below the CCD. This flysch-type assemblage had occurred since the late Coniacian in the Sergipe-Alagoas, as reported by Koutsoukos (2000). The Campos and Santos basins were populated by the Biofacies D during the Maastrichtian and early Paleocene. There may be a weak correlation between the type of biofacies and the sedimentation rate. For example, there is a tendency for Biofacies E to be associated with higher sedimentation rates, except in the Campos Basin (Fig. 3.31), while Biofacies D is associated with the decrease in the sedimentation rates in Campos and Santos basins. In the distal sites 356 and 20C,

calcareous taxa dominate the Maastrichtian assemblages (*Nuttallides truempyi*, *Stensioeina beccariiformis*, *Neoeponides hillebrandti*) in association with *Gaudryina pyramidata* and *Gaudryina* sp. (Biofacies C).

In the early and middle Paleocene, sea level fell (Kominz et al., 2008) and this condition was possibly favorable to the establishment of agglutinated-dominated Biofacies E across all of the marginal basins, while calcareous taxa dominated at the distal sites (Biofacies B and C) (Fig. 3.32). As observed in the upper Maastrichtian, Biofacies E is generally associated with higher sedimentation rates (Fig. 3.32), except in the Campos Basin, which shows the lowest sedimentation rates among the Brazilian marginal basins. Biofacies B occupied the region of DSDP Site 356, while Biofacies C characterizes Site 20C in the lower and middle Paleocene. Both biofacies contain a Velasco-type calcareous assemblage (e.g., *Nuttallides truempyi*, *Stensioeina beccariiformis*, *Pullenia coryelli*, *Cibicidoides hyphalus*, *C. velascoensis*, *Osangularia velascoensis* and *Gyroidinoides globosus*, Berggren and Aubert, 1975), differing only in the agglutinated foraminiferal content (*Gaudryina* sp., *G. laevigata*, *G. pyramidata*, *Karriella cubensis*).

The period between the late Maastrichtian through middle Paleocene appears to have relatively stable environmental conditions, without abrupt or large changes in the benthic foraminiferal biofacies of the western South Atlantic region. The relative continuity of high sea level was possibly the main reason for this relative environmental stability. The dominance of epifaunal benthic foraminifera suggests generally oligotrophic conditions during this time in the western South Atlantic.

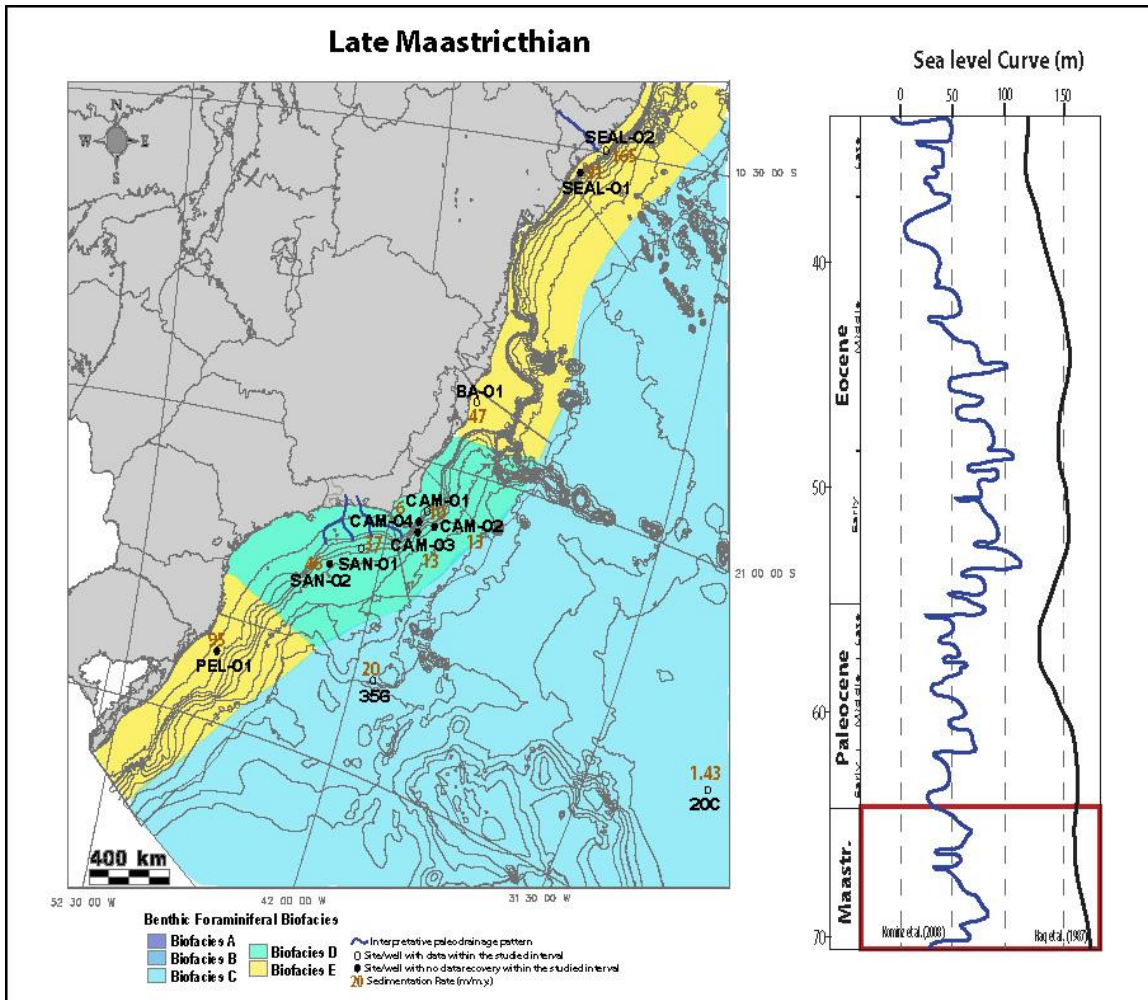


Figure 3.31: Benthic foraminiferal biofacies distribution in the late Maastrichtian of the western South Atlantic.

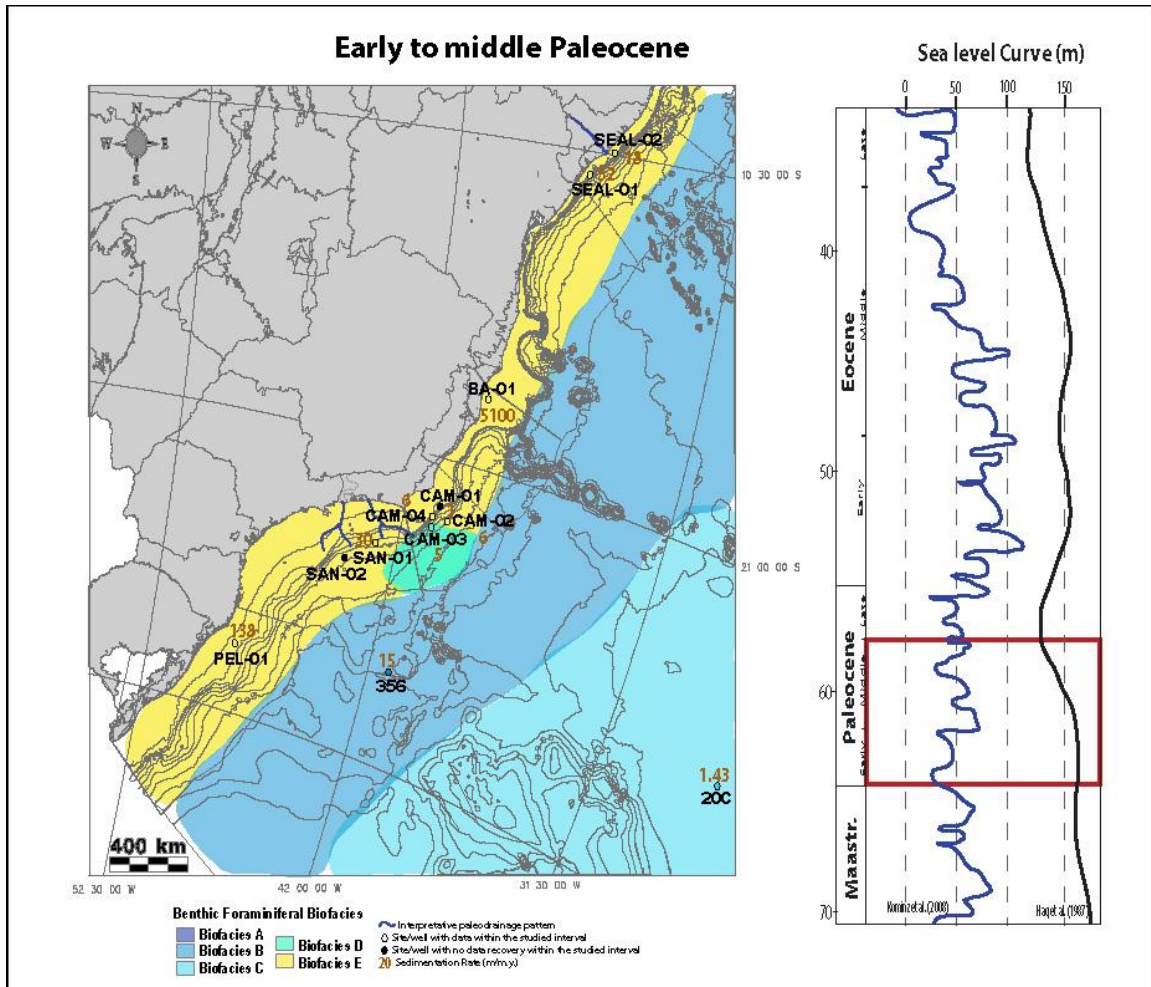


Figure 3.32: Benthic foraminiferal biofacies distribution in the early to middle Paleocene of the western South Atlantic.

The late Paleocene was a time of Biofacies E dominance in the southern Brazilian marginal basins (Pelotas, Campos and Santos, Fig. 3.33). The occurrence and expansion of the Biofacies E could be associated to the interplay of two main factors in the late Paleocene: the Serra do Mar uplift and a sea level fall. The Serra do Mar Mountains uplift occurred from the Late Cretaceous to the Paleocene (Almeida and Carneiro, 1998, Cobbold et al, 2001, Modica and Brush, 2004). Erosion of the mountains introduced a large volume of clastic sediment to the Santos and Pelotas basins. This erosional process

was carried out by the Paraíba do Sul drainage system that was fairly well developed in the late Paleocene (Cobbold et al, 2001, Modica and Brush, 2004). In addition, a global eustatic sea level fall (Haq et al., 1998, Kominz et al., 2008) exposed outer shelf sediments of the marginal basins that were redeposited basinward. This erosional event caused canyon cutting as recognized in seismic data from the Campos, Santos and Sergipe-Alagoas basins (Cainelli, 1992, Becker et al., 2000, Cobbold et al., 2001, Modica and Brush, 2004).

Biofacies D occurred in the Mucuri Basin and in one of the wells of the Sergipe-Alagoas Basin during the late Paleocene (Fig. 3.33). In the Sergipe-Alagoas Basin, each well exhibits a distinct biofacies, SEAL-01 has Biofacies E in the upper Paleocene, while 100 km away SEAL-02 has Biofacies D. The main reason for this distinct character of the biofacies may be related to the presence of the São Francisco River since the Campanian (Koutsoukos, personal comm. 2015); SEAL-02 is located closer to the mouth of this river. The terrigenous input from the São Francisco River is enriched in refractory organic matter that serves as food for the benthic foraminiferal community (Jorissen et al., 1995, Gooday and Rathburn, 1999). In addition, the increase in organic matter flux to the seafloor due to higher productivity along the Brazilian margin could have increased the CO₂ due to degradation of both terrestrial and marine organic matter that possibly caused the CCD to shoal (Berger, 1970). At the distal sites, there is no change in biofacies for Site 356 (Biofacies B, Figs. 3.31 and 3.32), but Site 20C changed from Biofacies C in the lower-middle Paleocene to Biofacies A in the upper Paleocene, probably due to the continued subsidence of the oceanic crust.

Fluctuations of the sea level in the Eocene, especially in the late Paleocene/early Eocene transition, could be the main reason for the development of several erosional unconformities, particularly in the Campos, Santos and Sergipe-Alagoas basins (Fig. 3.8).

The major benthic extinction event (BEE) coincided with the Paleocene-Eocene boundary and the Paleocene-Eocene Thermal Maximum (e.g., Tjalsma and Lohmann, 1983, Thomas, 1990, 1998, 2003, 2007, Thomas and Shackleton, 1996, Thomas et al., 2000, Alegret and Thomas, 2001, Kaiho, 2006, Luciani et al., 2007, Takeda and Kaiho, 2007, Stassen et al., 2012). The BEE was recognized in the Brazilian marginal basins and at the DSDP Sites. The detailed discussion is found in the Chapter 2. In general, the BEE affected the calcareous taxa more than the agglutinant; calcareous taxa are more abundant at the distal Sites 356 and 20C than the Brazilian margin during the late Paleocene. The Paleocene-Eocene boundary also coincides with the abrupt change of agglutinant-dominance in the Paleocene to calcareous-dominant in the Eocene of the Brazilian marginal basins (Fig. 3.34). This abrupt change of biofacies is closely related to the large input of sediments that forced the margin to prograde and the basins to shoal (Cainelli, 1992, Becker et al., 2000, Cobbold et al., 2001, Modica and Brush, 2004).

The Brazilian margin progradation is discussed in more detailed in the Chapter 4 after the establishment of the paleobathymetric model for the Brazilian marginal basins.

During the early Eocene, biofacies A and B dominated in most of the basins as the margin prograded and the slope shoaled. At this time, the sediment supply generally decreased and the shallower basins were no longer favorable for the agglutinant assemblage to inhabit the Brazilian marginal basins. Biofacies E was restricted to the deep Campos Basin and one of the wells of Sergipe-Alagoas Basin (SEAL-02) (Fig.

3.34). Biofacies A occurs in the early Eocene of the Santos Basin and at DSDP sites 356 and 20C suggesting a relatively uniform widespread deep-sea environment.

Campos Basin had a very different depositional history than the Santos and Pelotas basins during the Eocene due to a relatively low sediment supply during the Paleocene and Eocene. Seismic interpretations from Cobbold et al. (2001) and Modica and Brush (2004) indicated that the Paraíba do Sul River shifted its drainage system from the Santos to the Campos basin in the late Eocene/Oligocene, at which time the margin prograded. However, the presence of Biofacies D in the middle to upper Eocene suggest that the fluvial influence could have begun in the middle Eocene, possibly as a transition from Santos to Campos basins.

Calcareous biofacies dominated all basins in the middle and upper Eocene, with the exception of the Campos Basin where Biofacies D and E persisted through the Eocene (Fig. 3.35). Progradation and shoaling in the Sergipe-Alagoas and Mucuri basins established neritic conditions represented by the Biofacies A (*Elphidium*, *Amphistegina*, *Nodosaria*, *Discorbinella berheloti*, *Cibicides*, *Paralabamina lunata*) by the late Eocene. By contrast, Pelotas and Santos basins and Site 356 were colonized by the Biofacies C, interpreted as bathyal/upper abyssal assemblages. The Site 20C was populated by Biofacies B interpreted as lower bathyal/upper abyssal assemblage.

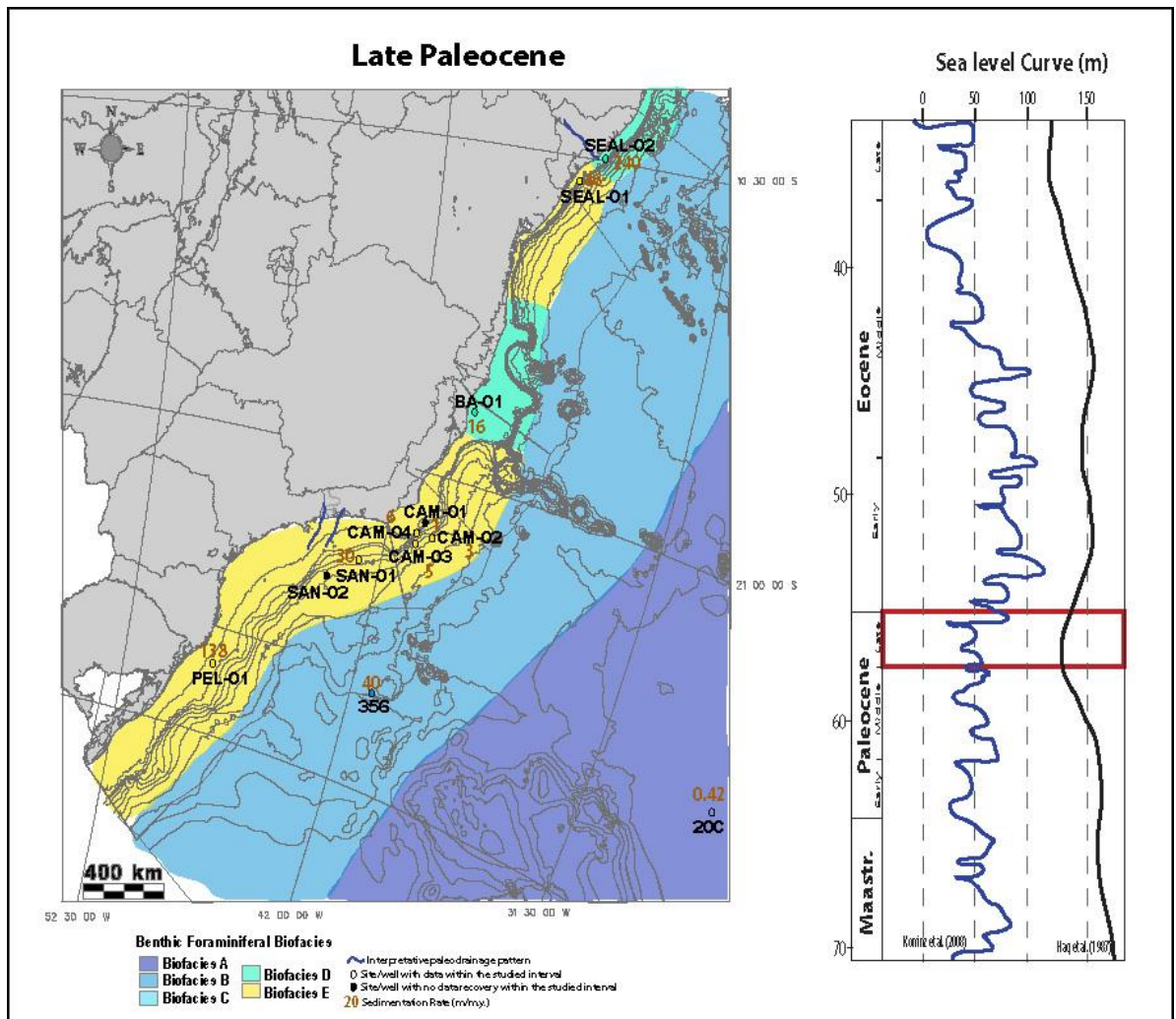


Figure 3.33: Benthic foraminiferal biofacies distribution in the late Paleocene of the western South Atlantic.

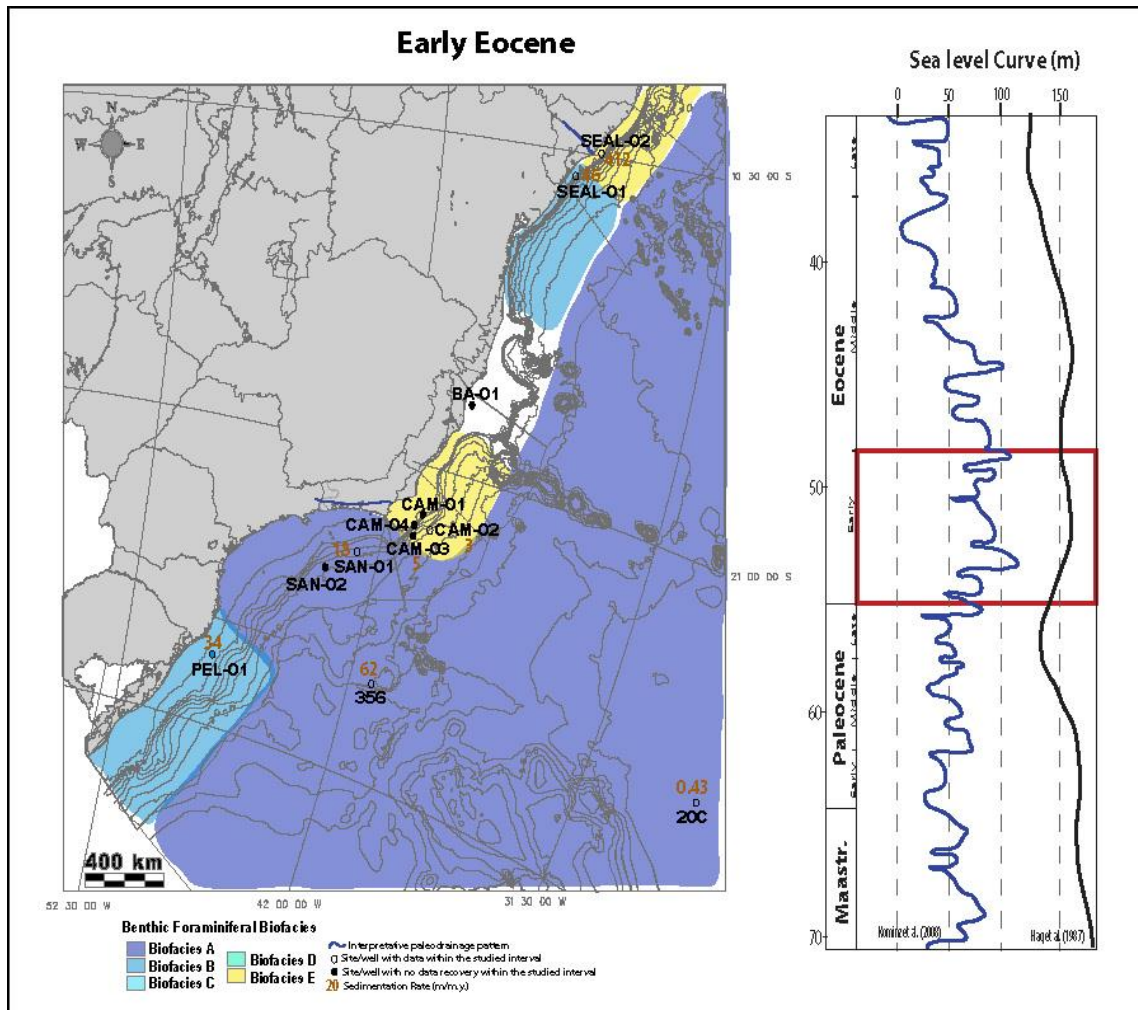


Figure 3.34: Benthic foraminiferal biofacies distribution in the early Eocene of the western South Atlantic.

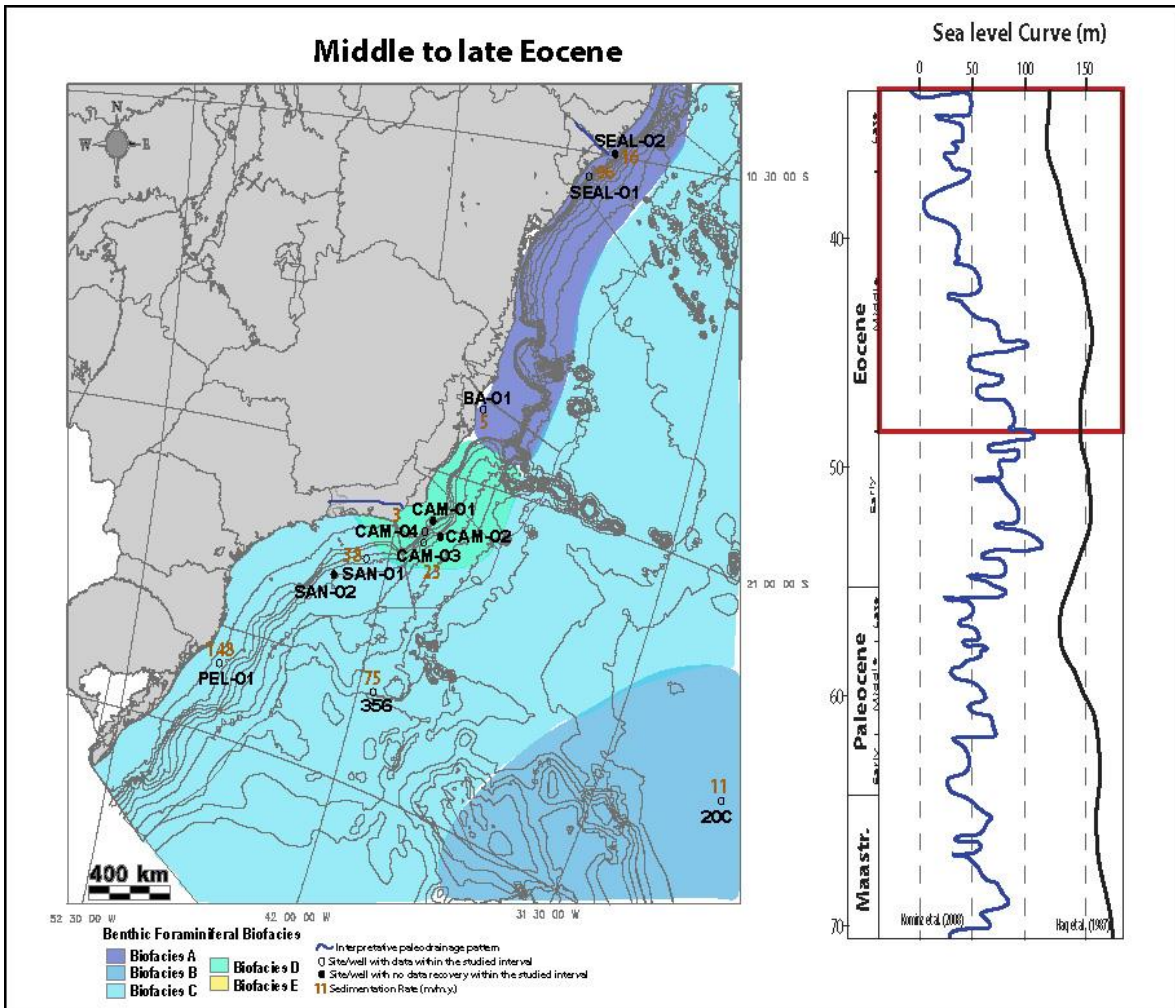


Figure 3.35: Benthic foraminiferal biofacies distribution in the middle to late Eocene of the western South Atlantic.

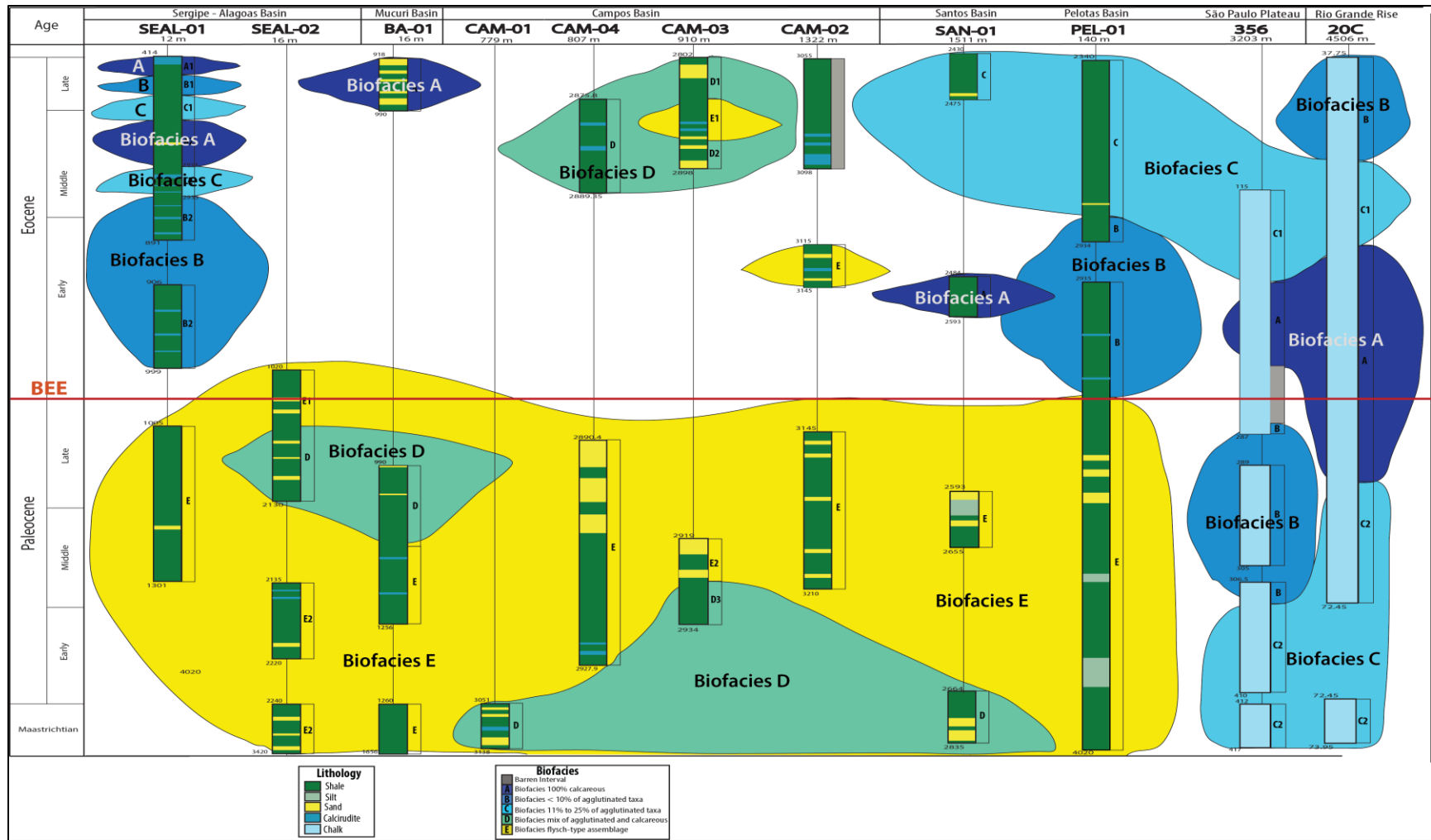


Figure 3.36: Benthic foraminiferal biofacies distribution in the Paleogene of the western South Atlantic. Brazilian marginal wells are displayed from northern (SEAL-01) to southern (PEL-01) and the distal DSDP Sites 356 and 20C. BEE: Benthic Extinction Event.

3.8 –THE FLYSCH-TYPE BIOFACIES E – DISTRIBUTION AND SIGNIFICANCE:

Biofacies E is interpreted as a flysch-type biofacies and it is extremely widespread in the Maastrichtian-Paleocene of the Brazilian marginal basins (Fig. 3.36). The flysch-type benthic foraminiferal biofacies has been previously reported in the Cretaceous-Paleogene of numerous locations (Table 3.2). The term flysch-type assemblage was first introduced by Bouwer (1965) referring to benthic foraminiferal assemblages dominated by single-chambered and uniserial, multi-chambered agglutinated taxa. This assemblage was first associated with flysch facies of the Alpine-Carpathian belt, but later found in turbidite sequences with high terrigenous input (Gradstein and Berggren, 1981, Wrinkler, 1984).

The agglutinated-rich biofacies occurs across a wide range of water depth and its distribution is more likely related to variations in other depth-related environmental factors rather than to depth alone. These environmental factors include the organic flux to the seafloor, lysocline and CCD depths, the nature of substrate, deep water oxygen levels, and the presence of contour or turbidity currents (Kaminski and Gradstein, 2005). The dominance of agglutinated foraminifera below the CCD depends on their ability to secrete organic, rather than calcareous cement, as a consequence the location of the CCD has a decisive influence on the relative abundance of agglutinated foraminiferal assemblages (Goody, 1990).

The influx of terrigenous sediments probably had a significant impact on the benthic community in our study area (Alegret and Thomas, 2001). Downslope

gravitational processes delivered clastic sediment from the outer continental shelf to the slope and rise increasing the availability of siliciclastic grains for use by agglutinated benthic foraminifera (Kaminski et al., 1988). The uplift of the Serra do Mar Mountains associated with local tectonic reactivations related to the opening of the South Atlantic from Cretaceous through Paleogene time provided an abundant terrigenous sediment supply to the marginal basins, especially the Santos and Pelotas basins (Almeida and Carneiro, 1998, Modica and Brush, 2004).

Continental slopes experience elevated productivity and can have strong gradients in organic flux, which can also be influenced by the presence of oxygen minimum zones (OMZ) and deep boundary currents. Hess and Kuhnt (1996) investigated a possible analogue to the flysch-type assemblage from the South China Sea, and demonstrated that the flysch-type assemblage is composed of taxa with organic cement survive and flourish on low-energy, fine-grained and organic-rich terrigenous substrates formed under stratified water masses, with moderate to high C_{org} and lower $CaCO_3$ productivity. Kaminski and Gradstein (2005) concluded that this ecological condition frequently occurs in relatively small, silled basins such as the South China Sea where an OMZ develops in mid-water settings. The deep-sea agglutinated assemblage appears to be strongly related to the organic carbon flux (Hess and Kuhnt, 1996, Kaminski and Gradstein, 2005).

In the western South Atlantic, the flysch-type biofacies is represented by two types of Biofacies E: one associated with calcareous taxa and planktic percentages 40% to 60%, and the other with very low planktic percentages (0% to 10%) and no calcareous

benthic taxa (Table 3.3). These two types of Biofacies E result in distinct environmental interpretations, and consequently paleobathymetric zones.

The Biofacies E with rare to very low planktic foraminifera and calcareous benthic taxa is interpreted as lower abyssal, deposited in a carbonate free environment, below the calcite compensation depth (CCD). This interpretation is supported by a lithofacies of shale with sandy intervals, interpreted to be distal turbidites. This type of Biofacies E occurs in shale intervals the Pelotas, Campos, and Sergipe-Alagoas, suggesting that these basins were located in very deep-waters (>3000 m) during the Maastrichtian and Paleocene, and into the lower Eocene of the Campos Basin.

The second type of Biofacies E is interpreted as lower bathyal to upper abyssal and occurs in the Paleocene of the Sergipe-Alagoas, Santos, and Mucuri basins, and Paleocene through upper Eocene of the Campos Basin. This type of Biofacies E occurs associated with calcareous taxa typical of the Velasco-type assemblage in the Paleocene (*Nuttallides truempyi*, *Stensioeina beccariiformis*, *Gyroidinoides globosus*, *Osangularia velascoensis*, *Cibicidoides hyphalus*, *C. velascoensis*; Berggren and Aubert, 1975), and with taxa typical of the Barbados-type assemblage in the Eocene (*Cibicidoides eocaenus*, *Nuttallides truempyi*, *Osangularia mexicana*, *Hanzawaia ammophila*, *Planulina costata*, *Globocassidulina subblogosa*; Wood et al., 1985, Van Markoven et al., 1986, Berggren and Miller, 1989, Bolli et al., 1994).

Table 3.2: Flysch-type assemblages reported from numerous locations in the Cretaceous – Paleogene interval.

Age	Paleodepth	Location	Assemblage	Source
Late Cretaceous-Paleogene	Abyssal (below CCD)	several	<i>Rhabdammina</i> -fauna	Brower (1965)
Paleocene-middle Eocene	Bathyal	Lodo Fm - Central CA	<i>Bathysiphon</i> , <i>Haplophragmoides</i> , <i>Trochammina</i> , <i>Ammodiscus pennyi</i> , <i>Silicosignoлина</i> , <i>Rhabdammina</i> , <i>Miliolids</i> and <i>Lagenids</i>	Israelsky (1951)
upper Cretaceous	Abyssal	Indian Ocean (Site 260) and Argo Abyssal Plain (Site 261)	upper Cretaceous: <i>Haplophragmoides</i> , <i>Recurvoides</i> , <i>Paratrochamminoides</i> , <i>Haplophragmium</i> , <i>Bolivinopsis</i> , <i>Pseudobolivina</i> , <i>Trochammina</i> , <i>Karrieriella</i> , <i>Plectina</i> , <i>Dorothia</i> , <i>Plectrocurvoides</i> , <i>Verneulina</i> , <i>Uvigerinammina</i> , <i>Ammodiscus</i> , <i>Glomospira</i> , <i>Glomospirella</i> , <i>Saccammina</i> , <i>Pelosina</i> , <i>Hyperammina</i>	Krashennikov (1974)
Cretaceous (Albian to Maastrichtian)	Site 356 - middle bathyal (500 to 1500m) Albian and lower bathyal (1500 to 2500m) for the Santonian to Maastrichtian) Site 357 - middle to lower bathyal in the Santonian and lower bathyal in the Campanian and Maastrichtian	sites 355, 356, 357, 358 (western South Atlantic)	Agglutinated species dissolution resistant: <i>Haplophragmoides</i> , <i>Paratrochamminoides</i> , <i>Recurvoides</i> and <i>Saccammina</i> , <i>Ammodiscus</i> , <i>Glomospira</i> , <i>Hyperammina</i> . Non-resistant: <i>Tritaxia aspera</i> , <i>Dorothia oxycona</i> , <i>D. bulletta</i> , <i>Gaudryina laevigata</i> , <i>G. franki</i> , <i>Spiroplectammina dentata</i> .	Sliter (1977)
upper Cretaceous-lowe Eocene	Abyssal (below CCD)	Site 328 (Falkland Outer Basin)	<i>Ammodiscus cretaceous</i> , <i>Glomospira charoides</i> , <i>G. gordialis</i> , <i>Rzehakina epigona</i> , <i>Haplophragmoides</i> sp., <i>H. excavata</i> , <i>Nodelum velascoense</i> , <i>Bathysiphon</i> sp., <i>Saccammina complanata</i> , <i>Hormosina ovulum</i> , <i>Uvigerinammina</i> sp., <i>Paratrochamminoides</i> sp.	Tjalsma (1977)
late Paleocene-early Eocene	Bathyal	Site 112 (North Atlantic)	<i>Cyclammina</i> , <i>Glomospira</i> , <i>Ammodiscus</i> , <i>Bolivinopsis</i> , <i>Rhabdammina</i> , <i>Cribrostomoides</i> , <i>Haplophragmoides</i> + <i>Osangularia pteromphalia</i> <i>Oridorsalis ecuadorensis</i> , <i>Nuttallides truempyi</i> , <i>Cibicidoides</i> sp., siphonodosariids and stilostomellids	Berggren (1972)
Maastrichtian-Paleogene	wide range (200-4000m)	Labrador and North Seas	Locus typicus - Alpine-Carpatian flysch belt (dominated by single chambered and uniserial taxa): <i>Rhabdammina</i> , <i>Bathysiphon</i> , <i>Ammodiscus</i> , <i>Lituotuba</i> , <i>Reophax</i> , <i>Hormosina</i> , <i>Rzehakina</i> . <i>Biserial and multiserial</i> (<i>Spiroplectammina</i> , <i>Texturalia</i> , <i>Gaudryina</i> , <i>Dorothia</i> , <i>Gaudryina</i>) and more complex trochoids (<i>Trochammina</i> , <i>Recurvoides</i> , <i>Trochamminoides</i> , <i>Cribrostomoides</i> , <i>Haplophragmoides</i> , <i>Cyclammina</i>) are generally less common	Gradstein & Berggren (1981)
Maastrichtian-Paleogene	2500-3500m	Pacific and Atlantic Oceans	Type A - robust and relatively coarse-grained taxa, high diversity (compared with B): <i>Rhizammina</i> , <i>Bathysiphon/Rhabdammina</i> , <i>Ammodiscus</i> , <i>Glomospira</i> , <i>Hormosina</i> , <i>Reophax</i> , <i>Kalamopsis</i> , <i>Rzehakina</i> , <i>Haplophragmoides</i> , <i>Trochamminoides</i> , <i>Recurvoides</i> , <i>Paratrochamminoides</i> , <i>Cyclammina</i> , <i>Trochammina</i> , <i>Spiroplectammina</i> , <i>Dorothia</i> .	
Middle to late Cretaceous	~ 4000m	Indo-Pacific and Atlantic Oceans	Type B - small size and thin, smooth wall benthic aggl taxa: <i>Hyperammina</i> , <i>Saccammina</i> , <i>Pitulina</i> , <i>Glomospira</i> , <i>Glomospirella</i> , <i>Hormosina</i> , <i>Haplophragmoides</i> , <i>Paratrochamminoides</i> , <i>Recurvoides</i> , <i>Haplophragmium</i> , <i>Trochammina</i> , <i>Praecystammina</i> , <i>Labrospira</i> , <i>Plectrocurvoides</i> , <i>Bolivinopsis</i> , <i>Pseudobolivina</i> , <i>Uvigerinammina</i> , <i>Dorothia</i> , <i>Verneulina</i> , <i>Plectina</i> .	
Late Maastrichtian to Eocene	bathyal to abyssal	Gumigei-Schlieren flysch	Turbiditic sequences - calcareous (P+B) foraminifera with debris of algae, bryozoans, etc. <i>Rhabdammina</i> -type assemblage not well developed and less individualized, repopulation on the finest pelitic interval (mud clouds). In turbiditic shales a poorer association of "diluted" calcareous and arenaceous agglutinated faunas was reported, indicating their reworked nature. Hemipelagic sequences - generally carbonate-free with well developed <i>Rhabdammina</i> -type assemblage that compare with Cretaceous-Paleogene abyssal assemblages below CCD	Wrinkler (1984)
Late Paleocene	bathyal-abyssal	North Sea	Flysch-type assemblage : tubular forms dominates, <i>Trochammina</i> , <i>Haplophragmoides</i> , <i>Spiroplectammina</i> . Calcareous are absence or rare. Radiolarians in some samples. Jones (1988) split the tubular forms into 4 groups correlated to modern genera.	Jones (1988)

CONTINUED

Age	Paleodepth	Location	Assemblage	Source
Maastrichtian to lower Eocene	upper to lower bathyal	Trinidad (Guayaguayare and Lizard Spring Fm)	Guayaguayare Fm: dominated by simple, coarse grained species of asterozooids, saccamminids and hormosinids (<i>Dendrophyra</i> ex. Gr. <i>Excelsa</i> , <i>Rzehakina epigona</i> , <i>Saccamina complanata</i> , <i>Hormosina trinitatis</i> , <i>Karrerella conversa</i> , <i>Ammobaculites</i> sp., <i>Spirolectammina spectabilis</i> , <i>Rhizammina gryzbowski</i> , <i>Gaudryina</i> ex. gr. <i>cretacea</i> . Lizard Spring Fm: dominated by asterozooids. Four major assemblages: 1) <i>Dendrophyra</i> ex. gr. <i>excelsa</i> , <i>Rzehakina epigona</i> , <i>Spirolectammina spectabilis</i> , <i>Saccamina placenta</i> , <i>Bathysiphon</i> . 2) <i>Ammosphaeroidina pseudopauiculata</i> , <i>Rhizammina indivisa</i> , <i>Recurvoides gerochi</i> , <i>Rzehakina epigona</i> . 3) low diversity of aggl., consisting of robust and coarse forms: <i>Clavulinoides globulifera</i> , <i>Dorothia retusa</i> , <i>Phenacophragma beckmanni</i> , <i>Haplophragmoides</i> ex. gr. <i>suborbicularis</i> .	Kaminski et al (1988)
Upper Aptian to Albian and upper Coniacian to Maastrichtian	deep-neritic to upper bathyal	Sergipe Basin (NE South Atlantic)	<i>Bathysiphon</i> , <i>Dendrophyra</i> , <i>Hyperammina</i> , <i>Rhabdammina</i> , <i>Rhizammina</i> , and <i>Kalamopsis</i> associated with <i>Ammodiscus</i> , <i>Glomospira</i> , <i>Glomospirella</i> , <i>Psammospira</i> , <i>Saccamina</i> , <i>Rzehakina</i> , <i>Silicisigmoilina</i> , <i>Spirolocammina</i> , <i>Hormosina</i> , and <i>Caudammina</i>	Koutsoukos (2000)
late Paleocene to early Eocene	outer neritic to middle bathyal (flysch-type cosmopolitan nature) reveal close similarities to Palaeogene faunas of Haltenbanken, offshore Mid-Norway, Viking Graben (North Sea), and Alpine and Carpathian flysch occurrences	Barent Sea	FB3: dominant species are <i>Budashevaella multicamerata</i> and <i>Recurvoides</i> aff. <i>turbinatus</i> . Common and typical taxa include: <i>Verneuilinoides</i> aff. <i>propinqua</i> , <i>Recurvoides contortus</i> and <i>Cribrostomoides</i> aff. <i>globosus</i> . FB4: The quantitatively most important taxa include: <i>Bathysiphon</i> sp. 2, <i>Spirolectammina spectabilis</i> , <i>Haplophragmoides walteri</i> , <i>Recurvoides</i> sp. 1, and <i>Ammosphaeroidina pseudopauiculata</i> . Tubular species occur commonly, and are referred mostly to <i>Rhizammina</i> , <i>Bathysiphon</i> , and <i>Hyperammina</i> with open nomenclature.	Nagy et al (2000)
Paleogene	below 4000m	Iberian Abyssal Plain and Celebes Sea	Abyssal biofacies: restricted to below 4km. Eocene common taxa <i>Reticulophragmium amplexans</i> , <i>Haplophragmoides walteri</i> is an important abyssal species over the Paleogene. • Tubular forms dominates the assemblage (very small, finely branched such as <i>Rhizammina</i> , <i>Bathysiphon</i> , <i>Hyperammina kenmilleri</i>)	
Cretaceous to Paleogene	upper to lower bathyal (usually influenced by contour currents)	North Atlantic and eastern Atlantic Oceans	Flysch-type biofacies: intercalated with turbiditic flysch sequences. Tubular forms dominates (<i>Bathysiphon</i> , <i>Nothia</i> , <i>Rhabdammina</i> , <i>Rhizammina</i>). Some coarse-grained taxa <i>Ammobaculites</i> , <i>Psammospira</i> , <i>Saccamina</i> and thin-walled tubular <i>Psammospira</i> . <i>Rzehakina</i> , <i>Ammodiscus</i> , <i>Paratrochamminoids</i> , <i>Trochamminoids</i> , <i>Hyperammina</i> , <i>Hormosina</i> , <i>Saccamina placenta</i> .	
upper Cretaceous to Paleogene	deep-water limestones	Western Tethys	Scaglia-type biofacies: small-sized aggl. forms. <i>Paratrochamminoids</i> , <i>Cystammina</i> . Rich in calcareous cemented taxa: <i>Remesella varians</i> , <i>Karrerella chapotensis</i> , and <i>Spirolectammina israeli</i> .	Kaminski & Gradstein (2005)
Paleogene	1000-2000m		Slope Marls biofacies: mixed low-latitude calcareous-aggl. assemblages (Calc, Aggl and Planktic). Presence of calcareous cemented species belonging to the genera <i>Clavulinoides</i> , <i>Dorothia</i> , <i>Gaudryina</i> , <i>Marssonella</i> , <i>Popovia</i> , and <i>Arenobulimina</i> . Redeposited assemblages in turbidites includes <i>Nothia excelsa</i> , <i>Clavulinoides</i> , <i>Popovia</i> , <i>Rzehakina</i> , <i>Recurvoides</i> , <i>Ammosphaeroidina</i> , <i>Haplophragmoides</i> , <i>Trochammina</i> , <i>Conotrochammina</i> . <i>Dorothia</i> , <i>Marssonella</i> and <i>Arenobulimina</i> could be present too. Occurs associated to the calcareous assemblage dominated by <i>S. beccariiiformis</i> .	

The Biofacies E that occurs below the CCD is similar to the abyssal agglutinated assemblage described from the Indian Ocean (Krasheninnikov, 1974), Falkland Outer Basin (Site 328, Tjalsma, 1977), Pacific and Atlantic oceans (Gradstein and Berggren, 1981), North Sea (Jones, 1988), and Iberian Abyssal Plain and Celebes Sea (Kuhnt and Urquhart, 2001, Kaminski and Gradstein, 2005). These locations have in common the

great percentage of tubular forms (*Bathysiphon*, *Rhizammina*, *Nothia*, *Psammosiphonella*) associated with other agglutinated taxa (*Haplophragmoides*, *Recurvoides*, *Ammodiscus*, *Bolivinopsis*, *Saccammina*, *Trochammina*, *Trochamminoides*, *Rzehakina*, *Spiroplectammina*, *Glomospira*).

In summary, Biofacies E represents a deep-water biofacies deposited near or below the CCD and it is typical of siliciclastic settings, such as deep tectonically active basins and lower continental slopes and rises. In addition, the 100% agglutinated Biofacies E has stratigraphic importance as cosmopolitan deep water agglutinated foraminifera (DWAF) with organic cement (*Bathysiphon*, *Recurvoides*, *Ammodiscus*, *Glomospira*, *Rhizammina*) that allows correlation of sedimentary sequences deposited below the CCD, where planktic foraminifera or calcareous nannofossils are not preserved (Gradstein and Berggren, 1981, Kunht and Urquhart, 2001, Kaminski and Gradstein, 2005).

Table 3.3: The two types of Biofacies E recognized in the Maastrichtian-Paleogene of the Brazilian marginal basins.

Biofacies	Age	Lithology	Paleobathymetric range	Key Taxa	Planktics (%)	Basins
E	Maastrichtian to upper Eocene	shale intervals with medium to coarse sand layers (>5m of thickness)	lower bathyal to upper abyssal	<i>Rhizammina</i> , <i>Bathysiphon</i> , <i>Psammosiphonella cylindrica</i> , <i>Haplophragmoides</i> , <i>Trochamminoides</i> , <i>Ammodiscus</i> + calcareous taxa (Velasco-type assemblage in the Paleocene, and Barbados-type assemblage in the Eocene)	40 -60	Sergipe-Alagoas, Mucuri, Campos, and Santos
	Maastrichtian to upper Paleocene		lower abyssal (below CCD)	<i>Rhizammina</i> , <i>Bathysiphon</i> , <i>Psammosiphonella cylindrica</i> , <i>Haplophragmoides</i> , <i>Trochamminoides</i> , <i>Ammodiscus</i> , <i>Recurvoides</i>	0 - 10	Pelotas, Campos, Sergipe-Alagoas

3.9 – SUMMARY AND CONCLUSIONS:

The Maastrichtian to Eocene benthic foraminiferal biofacies recognized in the Brazilian marginal basins and DSDP Sites 20C and 356 reflects the environmental changes associated with progradation of the continental margin, as well as sea level and climatic fluctuations. Relatively lower sea level and generally cooler conditions in the Paleocene gave way to rising sea level and global warmth culminating with the Early Eocene Climatic Optimum before a long-term cooling trend during the middle and late Eocene. These general trends climate and sea level are recorded in the evolution of the Maastrichtian-Eocene benthic foraminiferal biofacies of the Brazilian marginal basins. The following observations are summarized in Figure 3.37.

In general, two distinct biofacies regions are recognized. The proximal region is represented by the Brazilian marginal basins, from north to south: Sergipe-Alagoas, Mucuri, Santos, and Pelotas basins (Fig. 3.37). DSDP Sites 356 and 20C were in deeper paleo-water depths and more distal to the continental margin of Brazil, and the locations did not receive siliciclastic input. Both regions experienced environmental change as recorded by the benthic foraminiferal biofacies, which can be divided into three major intervals: the Maastrichtian to late Paleocene, early Eocene, and the middle to late Eocene.

The Maastrichtian to middle Paleocene interval is represented by Biofacies E in the Sergipe-Alagoas, Mucuri, and Pelotas basins, Biofacies D in the Campos and Santos basins, and the Biofacies C at DSDP Sites 356 and 20C. The sedimentation rates decreased drastically from proximal to distal regions. Campos Basin is the only basin

with low sedimentation rates (~6 m/myr) as compared to the Santos (30 m/myr) and Pelotas (105 m/myr) basins. The sea level highstand during this time was associated with the uplift of the Serra do Mar. The increased delivery of siliclastic sediments and terrestrial organic matter in the marginal basins may be primary reason for the establishment of the flysch-type benthic assemblage in the Paleocene.

During the late Paleocene, sea level fell and Biofacies E extended into the most proximal and intermediate regions of the Sergipe-Alagoas, Mucuri, Campos, Santos, and Pelotas basins. The uplift and subsequent erosional processes that acted on the Serra do Mar Mountains were responsible for a marked increase in the siliclastic input in Campos, Santos, and Pelotas basins, causing the margin to prograde (Almeida and Carneiro, 1998, Cobbold et al., 2001, Modica and Brush, 2004). The Santos Basin was by far the most affected by the large volume of terrigenous material arriving in the Paleocene from the Paraíba do Sul drainage system (Cobbold et al, 2001, Modica and Brush, 2004). The combination of relatively low sea-level and the uplift of the Serra do Mar in the late Paleocene provided the source for the coarse-grain agglutinated flysch-type Biofacies E. In addition, Biofacies E had a distinctive character in the Campos and Sergipe-Alagoas basins, by being composed exclusively of agglutinated taxa. This feature suggests that Biofacies E was established under carbonate unsaturated water, below the CCD along the marginal basins (Gradstein and Berggren, 1981, Kaminski et al., 1988, Kaminski et al., 1989, Kuhnt et al., 1989, Kuhnt and Collins, 1996).

The distal Sites 356 and 20C were dominated by Biofacies C and B, and C and A, respectively, during the late Maastrichtian through the late Paleocene. The Paleocene/Eocene boundary is marked by the global benthic extinction event (BEE)

(Thomas, 1990, 1998, 2003, 2007, Tjalsma and Lohmann, 1983, Zachos et al., 1993, 2001, 2005, Thomas et al., 2000, Lourens et al., 2005, Stassen et al., 2012a, b). The BEE is recognized at Sites 20C and 356 and in the marginal basins affecting preferentially the calcareous taxa (extinction ~35% and 16%, respectively), although at other locations agglutinat taxa were also strongly affected (Thomas, 1998). In the proximal and intermediate basins, Biofacies E dominated. The early Eocene seems to have been a special period in the western South Atlantic following the Paleocene-Eocene Maximum Thermal and BEE (~56 Ma). The benthic foraminiferal assemblage showed a progressive recovery, observed as a new origination of new species, especially in the deepest sites. The origination rates differs from the proximal (marginal basins) to distal (DSDP sites) regions, accounting ~25% and 47% respectively.

Biofacies E was restricted to the Sergipe-Alagoas and Campos basins following the Paleocene/Eocene boundary, likely related to fluvial siliciclastic input (São Francisco and Paraíba do Sul rivers, respectively). Pelotas Basin was at middle to lower bathyal depths as interpreted from the Biofacies B. Santos Basin and DSDP Sites 356 and 20C were populated by the Biofacies A suggesting an expansion of a more typical deep-sea environment into the Santos Basin, which was at middle to lower bathyal depths during the early Eocene.

The middle to late Eocene was dominated by typical, calcareous dominated deep-sea biofacies in the Pelotas and Santos basins, and at DSDP Sites 356 and 20C, as intermediate/distal regions. Only in the Campos Basin the agglutinated taxa persisted (Biofacies D and E). The disappearance of Biofacies E in the middle to late Eocene was coeval with the decrease in siliciclastic input from the Serra do Mar Mountains. The

fluvial sediments are restricted to the deeply incised Paraíba do Sul River, reported to have been well established in the late Eocene/Oligocene interval (Cobbold et al, 2001, Modica and Brush, 2004). The more proximal Mucuri and Sergipe-Alagoas basins were at middle to upper bathyal water depths and contain a distinct Biofacies A dominated by shallow water calcareous taxa. Mucuri Basin was greatly influenced by the Abrolhos volcanism in the middle to late Eocene.

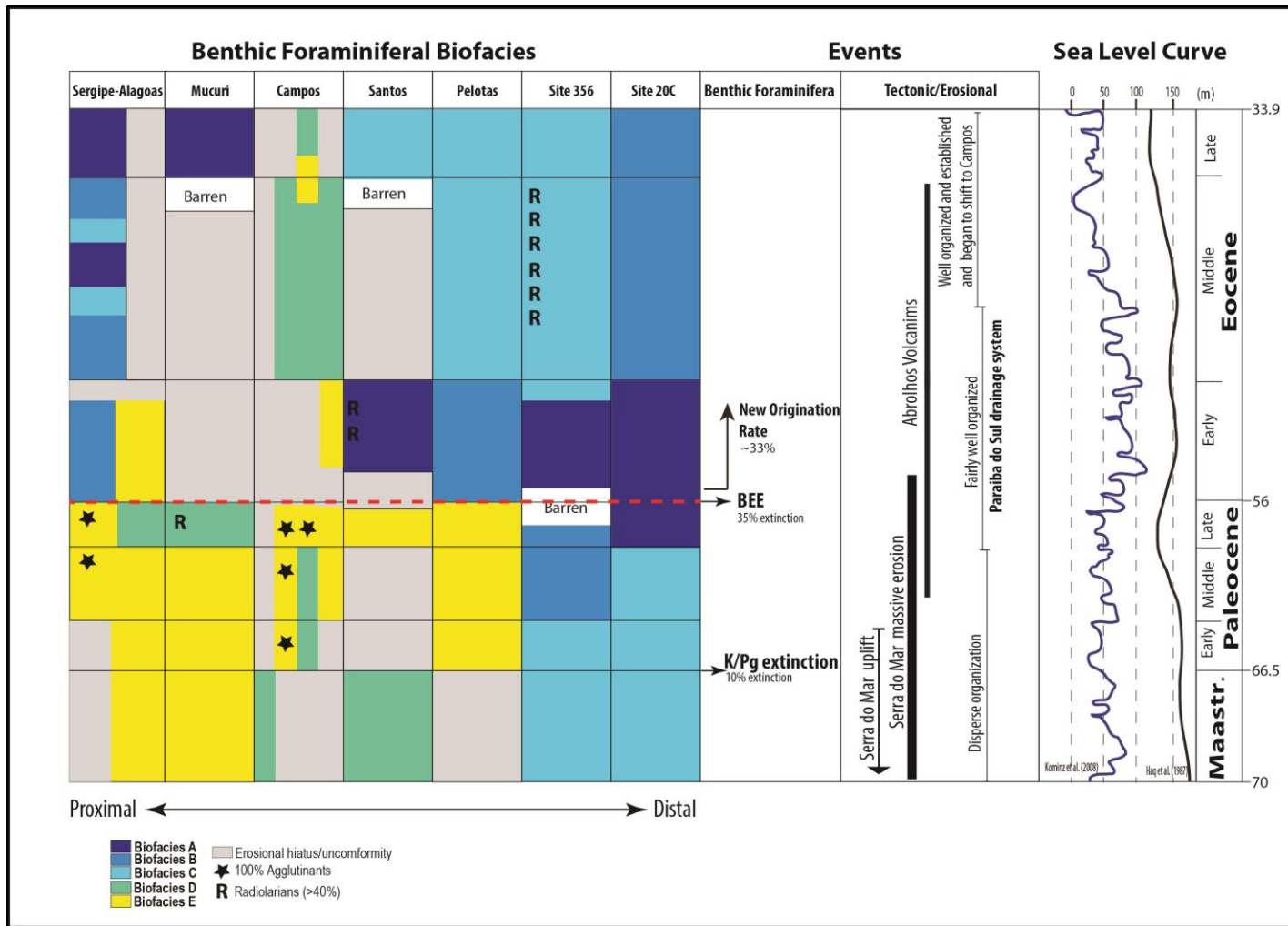


Figure 3.37: Benthic foraminifera biofacies correlation with sea level and events from the Maastrichtian through the Eocene of the western South Atlantic.

CHAPTER 4

A PALEOBATHYMETRIC MODEL AND THE EVOLUTION OF THE BRAZILIAN MARGINAL BASINS DURING THE LATE MAASTRICHTIAN – EOCENE BASED ON BENTHIC FORAMINIFERAL BIOFACIES

DE MELLO, RENATA MOURA ^{1,2,*}, LECKIE, R. MARK ¹

¹ Department of Geosciences, University of Massachusetts, 611 N. Pleasant St., Amherst, MA 01003, USA

² PETROBRAS Research and Development Center, Av. Horacio de Macedo 950, Ilha do Fundão, Rio de Janeiro, RJ 21941-915, Brazil

* Correspondence author: renatamouramello@yahoo.com.br.

4.1 – ABSTRACT:

A paleobathymetric and paleoenvironmental model is established based on benthic foraminiferal biofacies from five marginal basins of the eastern Brazilian continental margin. The model tracks the evolution of the margin as it built seaward and transitioned from abyssal (2000-3000 m) to bathyal (<2000 m) and neritic (<200 m) depositional environments during the Maastrichtian to late Eocene. It is a powerful predictive tool for reconstructing depositional systems in deep-water and for correlation in tectonically disturbed and complex hydrocarbon basins. The biofacies were established using Q-mode Cluster Analysis combined with Correspondence Analysis. The biofacies were primarily distinguished by the agglutinated/calcareous percentage and the dominant three or four species for each biofacies. Five major biofacies are recognized: Biofacies A (100% calcareous benthic taxa, inner neritic to upper bathyal), Biofacies B (up to 10% agglutinated taxa, outer neritic to lower bathyal), Biofacies C (11-25% agglutinated taxa,

outer neritic to lower bathyal), Biofacies D (a mix of agglutinated and calcareous taxa, middle to lower bathyal), and Biofacies E (dominated by agglutinated benthic taxa, lower bathyal to abyssal). The Maastrichtian – Paleocene interval was dominated by Biofacies E, also known as a flysch-type assemblage, and secondarily by Biofacies D. Sea level fluctuations contributed to downslope transport of siliciclastic material and terrestrial organic matter, while surface water productivity supplied marine organic matter and contributed to the shallow the calcite compensation depth (CCD) along the continental margin resulting in dissolution of planktic and calcareous benthic taxa, respectively, and the alternation between biofacies E and D. An abrupt change in biofacies across the Paleocene/Eocene boundary is observed in all the Brazilian marginal basins, with the exception of the Campos Basin. The Eocene interval is characterized by calcareous-dominated biofacies A, B and C in the Sergipe-Alagoas, Mucuri, Santos and Pelotas basins due to progradation of the margin and shoaling of the slope allowing for better preservation of carbonate. Biofacies D and E continued to dominate the Campos Basin during the Eocene due to its distal location relative to major centers of deposition and its continued deep-water setting. Major progradation of the Campos Basin segment of the margin occurred during the Oligocene and Miocene.

4.2 – INTRODUCTION:

Benthic foraminiferal assemblages have been used as paleobathymetric tools for oil industry exploration since the pioneer work of Cushman and Natland in the 1920's and 1930's (Cushman, 1927, Natland, 1933), followed by those of Parker, Phelger, Bandy, and others in the late 1940's, 1950's, and 1960's (e.g., Parker, 1948, 1954, Phelger, 1960, Phelger et al., 1953, Bandy, 1953, 1956, Upshaw and Stehli, 1962, Stehli and Creath, 1964, Walton, 1964, Bandy and Chierici, 1966). Traditionally, the paleobathymetric studies were based on comparing fossil species or genera with the bathymetric range of the modern taxa or homeomorphs of ancient genera (Sliter, 1975, Sliter and Baker, 1972, Gibson and Buzas, 1973, Anderson, 1975, Sliter, 1975, Poag, 1981, Van Morkhoven et al., 1986, Culver, 1988, Jones, 1988, Berggren and Miller, 1989). However, this methodology is based on the correlation between modern and fossil species, which can be progressively more difficult when applying to older intervals (Sikora and Olsson, 1991). In addition to this traditional paleobathymetry proxy based on benthic foraminiferal bathymetric ranges, other non-taxonomic methods including calculation of planktic/benthic ratios (planktic percentages) and benthic diversity indices, both of which have been shown to have a positive correlation with water depth (Buzas and Gibson, 1969, Murray, 1976, Gibson, 1989, Van der Zwaan, et al., 1990, Leckie and Olson, 2003).

The depth distributions of benthic foraminifera can be highly variable in distinct geographic regions. However, a predictable sequence of benthic foraminiferal assemblages with increasing depth can be reconstructed (Parker, 1954, Sliter and Baker,

1972, Murray, 1976, Poag, 1981, Nyong and Olsson, 1983/84, Olsson and Nyong, 1984, Pekar and Kominz, 2001, Leckie and Olson, 2003). For example, Olsson and Nyong (1984) proposed a paleobathymetric model of the coastal plain of Maryland and New Jersey for the Campanian-lower Maastrichtian. Applying Walter's Law to the analysis of foraminiferal biofacies, these authors demonstrated that the biofacies occurring laterally downdip are repeated vertically in section as relative sea level changed from deeper to shallower facies, or vice versa. The main idea of the paleoslope model is based on the benthic foraminiferal assemblages in terms of succeeding populations along a paleoslope direction, which should reflect a biofacies sequence integrated with other criteria (e.g., species diversity, planktic percentages, and comparison of morphologic trends in fossil genera with modern homeomorphs) (Nyong and Olsson, 1984).

The paleoslope model of Olsson and Nyong (1984) and Nyong and Olsson (1984) based on benthic foraminiferal biofacies from shelf to abyssal environments enhances the accuracy of estimating paleobathymetry. A potential paleobathymetric model using benthic foraminiferal biofacies would be a powerful predictive tool to aid oil exploration in deep-waters (Jones, 1988). Benthic foraminiferal biofacies previously had not been used to develop a paleobathymetric model for the Brazilian marginal basins. The biofacies established for the Brazilian marginal basins were delimited using statistical method Q-mode Cluster Analysis combined with Correspondence Analysis (Olsson and Nyong, 1983, Nyong and Olsson, 1983/84, Liu et al., 1997).

The challenge in developing a paleobathymetric model in this study was three fold. First, some of the foraminiferal assemblage data are based on well cuttings rather than core or sidewall samples, which mask the true character of *in situ* samples

unaffected by downhole mixing. Second, submarine slides and erosion, as well as turbidites and downslope transport are common in most of the Brazilian marginal basins so that the sections are not always complete and downslope reworking of assemblages can complicate the record. These factors represent a challenge for correlation of the sections between basins. Lastly, the five marginal basins are represented by too few wells each in order to conduct a paleoslope analysis similar to the studies done along the U.S. coastal plain and continental margin. Despite these challenges, a robust biofacies analysis was generated for the Brazilian basins and clear paleobathymetric trends have emerged from the data that reveal the evolution of the Brazilian margin during the Paleogene. Fillon (2003, 2005, 2009) highlighted the importance of the micropaleontological data applied in integrated reservoir investigations. This application usually has a strong positive impact on the petroleum industry, particularly in deep-water environments where well-to-well correlations are difficult to access, as is the case of the deep-water oil fields in the Brazilian marginal basins.

4.3 – MATERIALS AND METHODS:

The samples from the Brazilian marginal basins represent a variety of sources: core samples, cuttings and sidewall samples. These samples are from oil industry wells from the Brazilian Petroleum Company (Petrobras S.A.). Core samples were obtained from discrete cored intervals in industry wells. Cutting samples are drilled rock fragments that are transported up the well bore by the drilling mudstream. Sidewall core samples are

obtained by percussion sidewall coring systems that shoot hollow cylindrical bullets into the borehole wall.

The majority of the analyzed samples are core samples, cuttings and sidewall samples were selected from intercalated intervals where the coring was not continuous.

The industry wells are located in five Brazilian marginal basins (Sergipe-Alagoas, Mucuri, Campos, Santos and Pelotas) (Fig. 4.1). The locations were selected based on their stratigraphic continuity over the Paleocene-Eocene interval, although some locations also recovered the upper Maastrichtian interval (Table 4.1).

The samples were processed at the Biostratigraphy and Paleoecology Department at Petrobras Research Center, Rio de Janeiro, Brazil. The DSDP core samples consisted of unconsolidated sediment, they were washed the over 63 μm sieves and dried. The core/cutting samples of the petroleum wells were crushed and soaked in solution of hydrogen peroxide washed over a 63 μm sieves and dried, as standard procedure of the company. The Brazilian marginal basins samples are from the industry and were provided in slides, picked. The picking follows the procedure of the company where approximately 300 tests are picked (planktics and benthics). For the DSDP sites, all the benthics were picked of each sample (volume 10cc) and the planktics counted using the splitter. For detailed discussion on the samples processing, see Materials and Methods in Chapter 3.

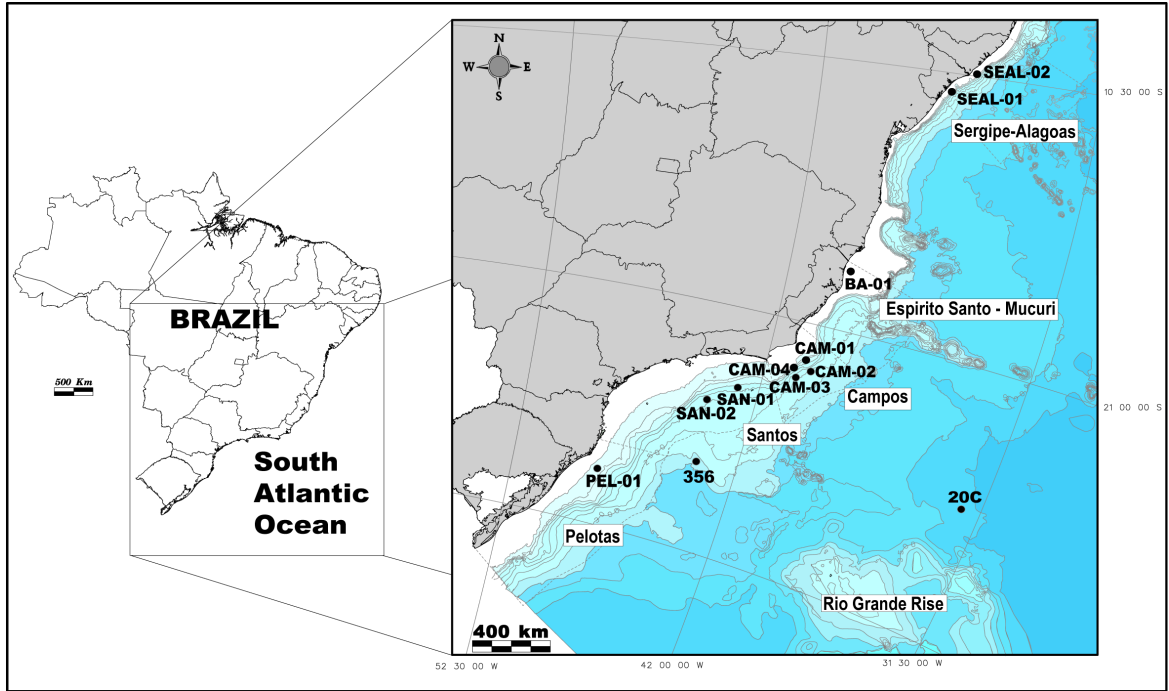


Figure 4.1: Present bathymetric map of the study area including the five Brazilian marginal basins (Sergipe-Alagoas, Mucuri, Campos, Santos, and Pelotas) and the DSDP Sites 20C and 356.

Table 4.1: Present geographic locations and age interval of samples in this study.

Well/Site	Location	Present water depth (m)	Samples	Sample type	Age
20C	Rio Grande Rise	4506	28	core	Paleocene-Eocene
356	São Paulo Pupperau - Santos Basin	3203	107	core	Paleocene-Eocene
PEL-01	Pelotas Basin	151	15	core	middle to upper Eocene
			40	cuttings	lower Eocene
			8	core	lower Eocene
			28	cuttings	upper Paleocene
			14	core	lower Paleocene
			9	cuttings	upper Maastrichtian
SAN-01	Santos Basin	1515	13	cuttings	upper Eocene
			14	sidewall	lower Eocene
			16	core	upper Paleocene-lower Eocene
			11	cuttings	upper Maastrichtian
SAN-02	Santos Basin	1733	12	core	upper Maastrichtian
			48	core	lower Eocene
CAM-01	Campos Basin	791	4	core	upper Maastrichtian
CAM-02	Campos Basin	1336	6	sidewall	Paleocene-Eocene
			11	cuttings	upper Eocene
			22	core	lower to middle Eocene
CAM-03	Campos Basin	923	3	cuttings	upper Maastrichtian to lower Paleocene
			42	core	Paleocene-Eocene
CAM-04	Campos Basin	820	16	cuttings	upper Eocene
			46	core	Paleocene
			31	cuttings	upper Maastrichtian to lower/middle Paleocene
SEAL-01	Sergipe-Alagoas Basin	27	44	cuttings	Eocene
			30	core	Paleocene
SEAL-02	Sergipe-Alagoas Basin	24	30	cuttings	upper Paleocene-lower Eocene
			18	core	Paleocene
			16	cuttings	upper Maastrichtian

4.4 – GEOLOGICAL SETTING:

Five marginal basins were studied along the eastern Brazilian margin: Sergipe-Alagoas, Mucuri, Campos, Santos, and Pelotas (Fig. 4.1). These sedimentary basins were formed during the continental rift phase of the African and South American plates, as a result of the fragmentation of the Gondwana supercontinent (Asmus and Baisch, 1983, Milani et al., 2007). As a consequence, the general tectonic and sedimentary evolution of the Brazilian marginal basins is quite similar, despite regional differences related to sediment supply and salt tectonics. Cainelli and Mohriak (1999) established the depositional megasequences as the mutual evolution of the basins: pre-rift, continental, transitional and marine.

The pre-rift megasequence represents the intracratonic phase of the Gondwana Supercontinent, preceeding the South American Rift and occurs only in the Paleozoic of the Sergipe-Alagoas Basin. The continental megasequence corresponds to the main rift caused by the divergent motion of the African and South American tectonic plates in the Late Jurassic/Early Cretaceous. The early syn-rift phases occur as thick packages of siliciclastic rocks registered between Espírito Santo and Sergipe-Alagoas basins, while tholeiitic basalts were extruded in the Santos and Campos basins. This volcanic event, dated from 130 to 120 Ma, is time-equivalent to the large Serra Geral basalt extrusion in the neighboring intracratonic Paraná Basin (Zalán et al., 1990). This megasequence contains the organic-rich lacustrine deposits, the main hydrocarbon source rock in the Campos Basin (Mohriak et al., 1990, Milani et al., 2001, Zalán, 2004). Coquinas (accumulations of pelecypod shells) developed along the flanks and crests of rift internal

highs, away from the input source of terrigenous sediments and, besides fractured basalts, they are the only producing hydrocarbon reservoirs of the rift phase in the Campos Basin while sandstones and conglomerates are the only producing reservoirs in the Sergipe-Alagoas Basin. The termination of the rift phase is diachronous along the Brazilian margin, ending in the southern segments by the early/middle Aptian, whereas in the northeastern segments, it may extend up to middle/late Albian times (Cainelli and Mohriak, 1999).

The transitional megasequence is the passage from the continental megasequence to the drift-phase of the marine megasequence. This transition phase marks the end of the stretching and rifting of the continental crust with the late Aptian siliciclastic deposition and ends with the evaporites spanning in age from the late Aptian to very early Albian (Cainelli and Mohriak, 1999, Zalan, 2004). Salt tectonics played an important role in the evolution of the Brazilian marginal basins (Mohriak et al, 1990, Cainelli and Mohriak, 1999, Milani et al., 2001, Mohriak, 2003). The Campos and Santos basins are by far the most affected by salt mobilization, where it generated new depocenters basinwards. The Espirito Santo, Mucuri and Sergipe-Alagoas basins have reduced salt tectonics influence, mostly in deep-waters and onshore, respectively, while the Pelotas Basin has incipient (northern part) or lacks deformation by salt tectonics (Cainelli and Mohriak, 1999).

The marine megasequence starts gradually with minor sub-regional unconformities (Cainelli and Mohriak, 1999). The progressive displacement of the mid-ocean ridge by Brazil and Africa caused the cooling and contraction of the lithosphere, resulting in increasing thermal subsidence seaward (Cainelli and Mohriak, 1999, Mohriak, 2003, Zalán, 2004). This megasequence is divided into restricted marine

supersequence (shallow water carbonate) and open marine supersequence (siliciclastic). The restricted marine supersequence is also subdivided in neritic, hemipelagic and deepening sequences (Cainelli and Mohriak, 1999). The neritic sequence is characterized by high energy, shallow water carbonates deposited in a ramp/platform setting and ending with the drowning of the platform in the late Albian coinciding in time with an anoxic event that affected the entire South Atlantic (Mohriak et al, 1990, Koutsoukos, 1999, 2000, Cainelli and Mohriak, 1999). This neritic sequence is constituted mainly by calcarenites and dolomites deposited in warm and dry weather on shallow neritic settings with hypersaline water and oxygenated bottom (Koutsoukos and Dias-Brito, 1987).

The hemipelagic and deepening sequences, that followed the neritic sequence, represent the demise of the shallow water carbonates that culminated with the deposition of organic-rich black shales of the Cenomanian/Turonian anoxic event. This sequence is formed mainly by calcilutites interbedded with marls and shales (Cainelli and Mohriak, 1999).

The open marine supersequence is the truly oceanic phase of the marginal basins, marked by relative environmental stability in lower bathyal to abyssal paleodepths (Cainelli and Mohriak, 1999, Zalán, 2004). Upper-Cretaceous and Tertiary sand-rich turbidites of the Open Marine Megasequence are presently responsible for most of the hydrocarbon production and reserves in the offshore basins (Cainelli and Mohriak, 1999, Zalán, 2004).

During the Cenozoic, the Mucuri Basin experienced an important magmatic event that formed the Abrolhos Volcanic Complex, also known as the Abrolhos coral reef. The Abrolhos carbonates comprise the largest and the richest reef complex of the western

South Atlantic (Leão, 1999). The carbonate bank was originally formed on volcanic rocks. The volcanics are intercalated with shales and carbonates. The Ar-Ar ages indicate that the volcanic activity spanned the Paleocene-Eocene (60-40 Ma, Szatmari et al., 2000, Milani et al., 2001, Zalan, 2004).

This study is focused on the upper Maastrichtian through upper Eocene interval of the Brazilian marginal basins that belongs to the open marine supersequence as defined by Cainelli and Mohriak (1999). The thicknesses of the depositional sequences are highly variable (Table 4.2). The Maastrichtian sequence is thinner in the Campos Basin (65m) and increases toward north (Mucuri ~450m and Sergipe-Alagoas ~ 600m) and south (Santos ~180m, Pelotas ~306m). The same pattern is followed in the Paleocene and Eocene intervals (see table 4.2). The Campos Basin has the thinnest Maastrichtian-Eocene sequence of the eastern Brazil marginal basins. It is separated from the Santos Basin to the south by the Cabo Frio High, and from the Mucuri Basin to the north by the Vitoria High (Asmus and Baisch, 1983).

Table 4.2: Thicknesses of the sequences for the Brazilian marginal basins (thickness in meters).

		Sergipe-Alagoas	Mucuri	Campos	Santos	Pelotas
EOCENE	upper	237		30	6	306
	middle	266		35	70	288
	lower	420		22	72	278
PALEOCENE	upper	180		7	120	258
	middle	130	220	30	200	156
	lower	60		24	158	210
MAASTR.		600	450	65	200	306
TOTAL		1893	670	213	826	1802

4.5 – PALEOCEANOGRAPHIC SETTING OF THE SOUTH ATLANTIC:

Global temperature changes were variable during the upper Cretaceous, including global cooling in the early Maastrichtian and warming some 200-300kyr prior to the end-Cretaceous mass extinction, which has been attributed to Deccan floor basalt volcanism in India (Barrera, 1997; Huber et al., 2002; Cramer et al., 2009; Keller and Abramovich, 2009; Thibault et al., 2010; Thibault and Gardin, 2010). Immediately after the bolide impact that likely caused the mass extinction on the Cretaceous-Paleogene boundary (K/Pg), there was a short interval of global cooling caused by dust or sulfate particles, global wildfires, severe acid rain and acidification of the oceans (Thomas, 2006, Penman et al, 2014). During the early to mid-Paleocene, global temperatures were much warmer than today, but in the late Paleocene (~ 59 Ma) a long-term warming trend began, which culminated with the Early Eocene Climatic Optimum (EECO ~52-50 Ma; Zachos et al., 2001, 2008; Cramer et al., 2009). A number of hyperthermals characterized the early Eocene, beginning with the Paleocene-Eocene Thermal Maximum (PETM, or Eocene Thermal Maximum 1, ETM1) and followed by less severe events ETM2 and ETM3 leading up to the EECO (Zachos et al., 2008; DeConto et al., 2011). Temperatures did not reach freezing even in continental interiors (Zachos et al., 2001, 2005, Thomas et al., 2006) at mid- to high-latitudes, and global deep waters temperatures were 10°-12°C warmer than today (Zachos et al., 2001, 2008). In addition, the ocean circulation was efficient in maintaining the warmer temperatures, with low temperature gradients from high to low latitudes (Thomas et al., 2000, Huber and Sloan, 2001, Cramer et al., 2009, Huber and Caballero, 2011). The continental's configuration was different in the

Paleogene, impacting directly on the ocean circulation and sites of deep water formation. Remarkable changes in the ocean configuration occurred from the Paleocene-Eocene boundary through the Miocene are reflected in significant changes in ocean thermohaline circulation (Bice et al., 2000). In the early Eocene, the North Atlantic was connected to the Arctic by a shallow sea that deepened towards the middle to late Eocene. The exact time of the Drake Passage opening is still controversial, from the late middle Eocene (~41 Ma, Scher and Martin, 2006) to the early Miocene (~20 Ma, Anderson and Delaney, 2005). The opening of the Drake Passage has been reported as playing an important role on the abrupt cooling in the Eocene-Oligocene boundary providing the thermal isolation of Antarctic.

The production of the deep-water is a key factor in the ocean circulation, and there are controversial ideas about where deep waters originated in the Paleogene. One hypothesis is that Warm Saline Bottom Water (WSW) production in the Tethys Seaway flowed southward in the Equatorial Atlantic and/or into the Indian Ocean along the African margin (Kennett and Stott, 1990; Bice et al., 2000). Another hypothesis is deep water forming in the Southern Ocean flowing northwards into the Atlantic and Indian ocean basins (Thomas et al., 2003). Climate modeling shows that the subtropical deep waters (WSW) are not easily produced, however whether a strong WSW component has existed at all, or has existed as either a steady-state or a transient condition remains unknown (Bice, 2000). Thomas (2004) reported a shift in deep water sources from the Southern Ocean to the North Pacific ~65 M, and then reverted back to the Southern Ocean ~40 M, based on neodymium isotopes of fish debris. Possibly a combination of both hypotheses occurred in the Paleogene, with main source from the Southern Ocean

and a smaller or transient contribution from the subtropical Tethys Seaway. The interpreted water masses circulation in the Paleogene Atlantic Ocean is shown in figure 3.6.

The warmer planet scenario changed in the middle Eocene (~49 Ma) when global deep waters and high latitude surface waters cooled. The opening of the Arctic to the world ocean may have been a factor in middle Eocene global cooling (Thomas, 2006; Borrelli et al., 2014). The Middle Eocene Climatic Optimum (~40 Ma) was a short-lived warming during the longer-term middle to late Eocene cooling (Bohaty and Zachos, 2003). The ice free world shifted to small ice on Antarctica by the late Eocene and rapid growth of the Antarctic ice-sheet in the earliest Oligocene (~33.7 Ma; DeConto and Pollard, 2003; Coxall et al., 2005; DeConto et al., 2008; Katz et al., 2011; Borrelli et al., 2014).

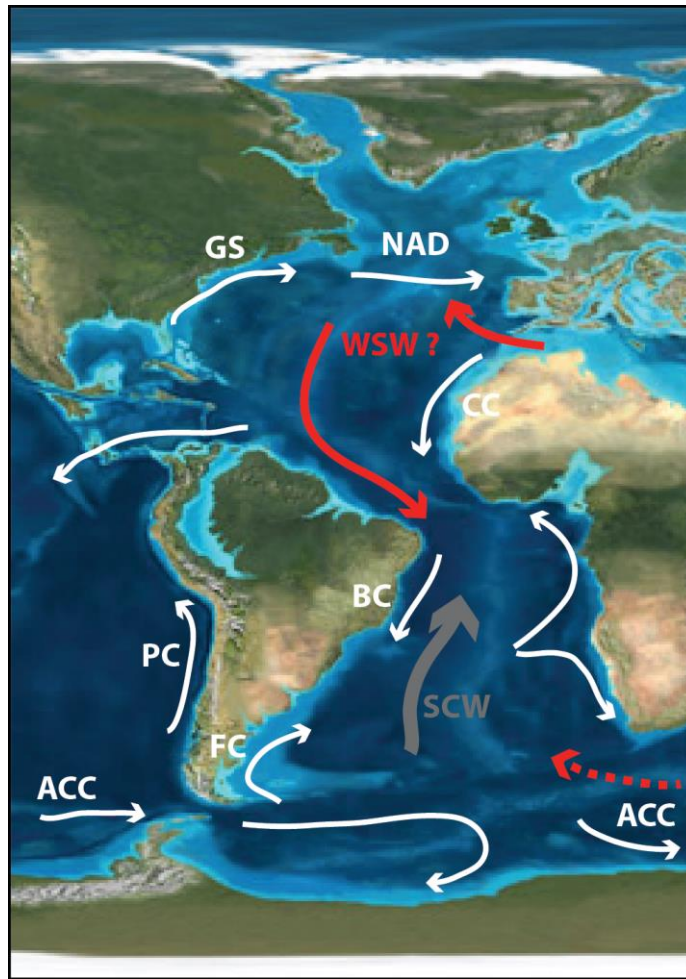


Figure 4.2: Interpretative Atlantic Ocean circulation during the Paleogene. White arrows: surface water currents, red: intermediate water, grey: deep water. GS – Gulf Stream, NAD – North Atlantic Drift, WSW – Warm Saline Water, BC – Brazil Current, FC – Falkland Current, PC – Peru Current, ACC – proto-Antarctic Circumpolar Current, SCW – Southern Component Water, CC – Canary Current. Paleoceanographic map from Ron Blakey (<https://www2.nau.edu/>). Surface currents from Bice et al. (2000), WSW from Bice (2000), SCW from Thomas et al. (2003) and Thomas (2004).

4.6 – BENTHIC FORAMINIFERAL BIOFACIES:

Five major benthic foraminiferal biofacies were defined based on the benthic foraminiferal assemblage and associated parameters, including percentage of planktic foraminifera (% planktics), lithology, and percentage of radiolarians (% rads). The biofacies were determined using a combination of Q-mode cluster and Correspondence

Analysis (CA). This combination of statistical methods provides not only the biofacies but also which taxa are more related to a specific biofacies (see Chapter 2).

The major biofacies groups are not composed of exactly the same taxa due to basin-to-basin differences (niches). The biofacies are primarily distinguished by the agglutinated/calcareous benthic percentage and the dominant three or four species for each biofacies. The detailed biofacies characterization is in Chapter 3. Here we present a summary of the biofacies recognized in the nine wells analyzed from the Brazilian marginal basins (Fig. 4.3).

The bathymetric zones were based on the zonation applied by Van Morkhoven et al. (1986) and Berggren and Miller (1989), as following:

Neritic: 0 – 200 m
 inner <30 m
 middle 30 – 100 m
 outer 100 – 200 m
Bathyal: 200 – 2000 m
 upper 200 – 600 m
 middle 600 – 1000 m
 lower 1000 – 2000 m
Abyssal: >2000m
 upper 2000 – 3000 m
 lower >3000 m

➤ **Biofacies A**

The benthic foraminiferal assemblages included in this biofacies are composed of 100% calcareous taxa. At the more proximal basins (Sergipe-Alagoas and Mucuri), this biofacies has greater percentages of shallower species, e.g. *Amphistegina*, *Elphidium*, *Quinqueloculina*, *Lenticulina*, *Nodosaria*, which are usually more poorly preserved (yellowish and oxidized tests) due to transport from the continental shelf, associated with

Paralabamina lunata, *Neoeponides elevatus*, *Planulina costata*, *Globocassidulina subglobosa* and *Globobulimina* spp. At the more distal basin (Santos), this biofacies is composed of bathyal benthic foraminiferal species, e.g. *Cibicidoides* sp., *Hanzawaia ammophila*, *Nuttallides truempyi*, *Pullenia* sp., *Gavelinella* sp. and *Oridorsalis umbonatus*. This biofacies occurs mostly in the Eocene interval in the Sergipe-Alagoas, Mucuri and Santos basins. Planktic percentages vary from 0% to 60%.

➤ **Biofacies B**

The benthic foraminiferal assemblages included in this biofacies have up to 10% agglutinated taxa. This biofacies was recognized in Sergipe-Alagoas and Pelotas basins. The calcareous taxa include *Cibicidoides eocaenus*, *Hanzawaia ammophila*, *Melonis* sp.1, *Paralabamina lunata*, *Lenticulina* sp., *Globobulimina* sp. and *Anomalinoidea* sp. The agglutinated taxa are *Gaudryina* sp., *Cyclammina* sp. and *Spiroplectammina* sp.

This biofacies occurs in the lower to middle Eocene of the Sergipe-Alagoas Basin and in the lower Eocene for the Pelotas Basin. Planktic percentages vary from 0% to 60%.

➤ **Biofacies C**

The benthic foraminiferal assemblages included in this biofacies have 11% to 25% agglutinated taxa in its composition. This biofacies occurs in the middle to upper Eocene of the Sergipe-Alagoas, Santos, and Campos basins.

This biofacies contains species that are diagnostic of the lower bathyal paleobathymetric zones based on the presence of *Nuttallides truempyi*, *Osangularia mexicana*, *Osangularia velascoensis*, *Cibicidoides*, *Gyroidinoidea*, and *Oridorsalis umbonatus*. Planktic percentages vary from 0% to 60%.

➤ **Biofacies D**

The benthic foraminiferal assemblages included in this biofacies contain a more equal balance of calcareous and agglutinated benthic taxa. This biofacies always occur in association with Biofacies E, and occurs from the Maastrichtian through the upper Eocene in all the marginal basins. The diagnostic agglutinate taxa include *Bathysiphon* sp., *Rhizammina* sp., *Recurvoides* sp., *Gaudryina* sp., *Dorothia* sp., *Trochamminoides* sp., *Ammoglobigerina* sp., *Marssonella* sp. and *Haplophragmoides* sp. The calcareous taxa are represented by *Stensioeina beccariiformis*, *Nuttallides truempyi*, *Gyroidinoides globosus*, and *Gavelinella* sp. in the Paleocene and *Nuttallides truempyi*, *Gyroidinoides* sp., *Globocassidulina subglobosa*, *Cibicidoides havanensis*, and *C. eocaenus* in the Eocene. Planktic percentages vary from 30% to 90%.

➤ **Biofacies E**

The benthic foraminiferal assemblages included in this biofacies are composed primarily of agglutinated taxa; the tubular forms (*Rhizammina*, *Bathysiphon*, *Psammosiphonella*, *Nothia*) are particularly diagnostic (~20-40% of benthics) associated with *Haplophragmoides*, *Ammoglobigerina*, *Ammodiscus*, *Recurvoides*, *Budashevaella multicamerata*. Biofacies E occurs from the Maastrichtian through the Eocene in all marginal basins, but it is much more diagnostic of the Paleocene interval. Planktic percentages vary from 0% to 60%.

It was possible to recognize two sub-groups within Biofacies E, coarse-grained coiled taxa and tubular forms predominantly compose both of them. The first sub-group is composed exclusively of agglutinated taxa, with extremely rare or no calcareous benthic or planktic taxa. This sub-group of Biofacies E occurs mostly in the

Maastrichtian-Paleocene of Pelotas, Campos and Sergipe-Alagoas basins. The other subgroup of Biofacies E has a minor content of calcareous taxa (~30% of benthics) and planktic foraminifera (<60% of total assemblage), which show clear evidence of dissolution. This assemblage occurs from the Maastrichtian through the Paleocene of the Mucuri Basin, and in the middle Paleocene to lowermost Eocene of the Santos Basin, and in the upper Eocene of the Campos Basin

This tubular agglutinated-rich biofacies was originally denominated as flysch-type biofacies by Gradstein and Berggren (1981) and later investigated by Kaminski et al. (1988) and Kaminski and Gradstein (2005). The flysch-type biofacies was originally described as associated with tectonically active or restricted basins poor in carbonate, although some authors recognized it also siliciclastic continental margins basins. They also conclude that paleobathymetry is not a key factor controlling their presence, although great depths, below the lysocline and/or CCD may create favorable conditions for the agglutinated assemblages (Kaminski et al, 1988, Koutsoukos, 2000, Kunht and Urquhart, 2001, Kaminski and Gradstein, 2005). The flysch-type agglutinated benthic foraminiferal assemblages characterize deep-water turbidites in all of the major deep-water petroleum basins, many of them situated along passive margins, e.g., Brazil (Mesquita, 1998, Koutsoukos, 2000), North Sea and Labrador Sea (Gradstein et al., 1983, Jones, 1999) and the northern Gulf of Mexico basin (Fillon, 2003, 2005).

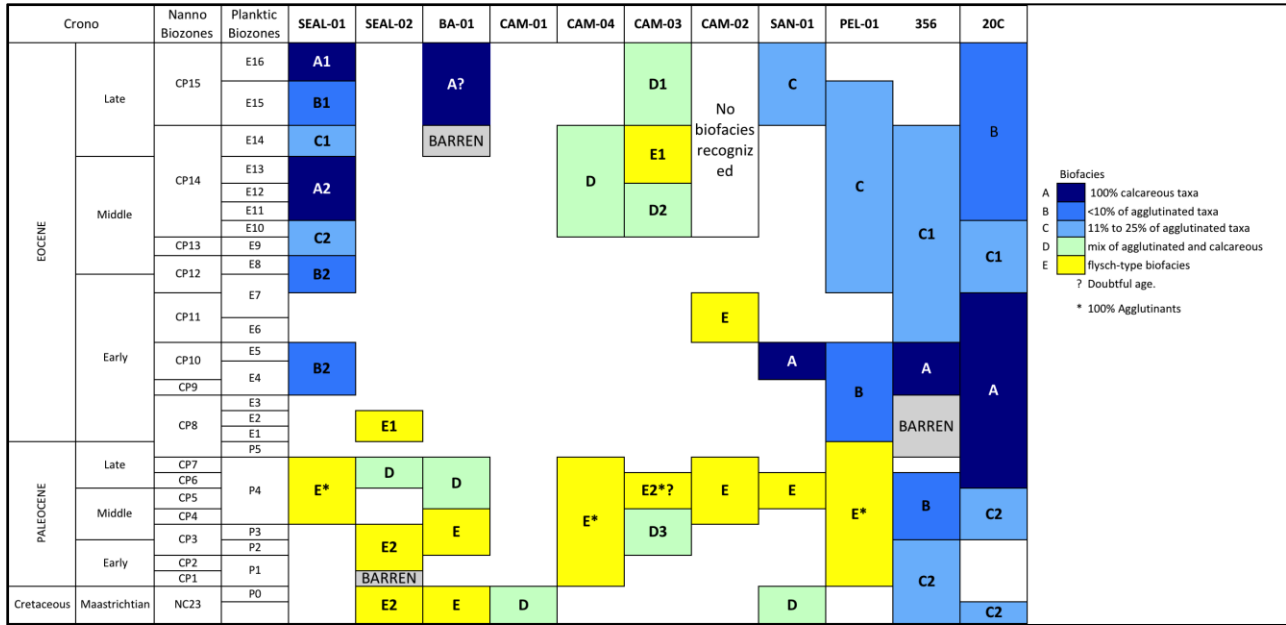


Figure 4.3: Benthic foraminiferal biofacies distributed by age for all wells and sites. Note the implied presence of hiatuses in the studied marginal basins wells and deep-sea sites. Nannofossil biozones from Ogg et al. (2010), planktic foraminiferal biozones from Wade et al. (2011).

4.7 – THE PALEOBATHYMETRIC MODEL:

A paleobathymetric model for the Brazilian marginal basins was developed based mainly on the benthic foraminiferal biofacies, which provide valuable information on the sedimentary processes involved in their deposition, as well as paleoenvironmental information that improves reservoir investigations (Fillon, 2003). Studies of modern taxa distributions reveal the close relationship between benthic foraminifera and environmental factors, including bottom water oxygen levels and redox conditions in the sediments, food availability related to terrigenous input, surface water productivity, and seasonality, fluctuations in the carbonate compensation depth (CCD), substrate conditions, and bottom current strength (Corliss, 1985, 1991, Jorissen et al., 1995,

Loubere, 1996, Thomas and Gooday, 1996, Gooday and Rathburn, 1999, Schonfeld, 2002, Sen Gupta, 2003, Jorissen et al., 2007). In addition, physical parameters of the bottom sediment also influence the benthic foraminiferal distribution, e.g., grain-size and mineralogy (Fillon, 2003, Schroder-Adams, 2008).

Benthic foraminiferal biofacies and lithology were integrated for the paleobathymetric model. The paleobathymetry is inferred from the biofacies analysis that resulted in the following stratigraphic sequence: Biofacies A (inner neritic to upper bathyal), Biofacies B (outer neritic to lower bathyal), Biofacies C (outer neritic to lower bathyal), Biofacies D (middle to lower bathyal), and Biofacies E (lower bathyal to abyssal). There is overlap in the paleobathymetric zones due to the lateral differentiation among the marginal basins.

The biofacies are listed below with foraminiferal taxa and lithofacies as a tentative means to understand biofacies-lithology relationships on the paleobathymetric and paleoenvironmental model for the Brazilian marginal basins.

Biofacies A:

- High percentage of reworked shallow water taxa (*Elphidium*, *Amphistegina*, *Quinqueloculina*).
- Calcareous taxa (*Hanzawaia ammophila*, *Planulina costata*, *Cibicidoides eocaenus*, *Nodosaria* sp., *Lenticulina* sp.).
- Epifaunal species that tolerate downslope transport.
- Moderate to high energy of the bottom currents.
- Medium to coarse sand with shale layers or shale with layers of fine sand.
- Inner neritic to upper bathyal paleobathymetric zones.
- Occur in the Sergipe-Alagoas, Mucuri, and Santos basins.
- Lower to upper Eocene interval.

Biofacies B:

- Moderate reworking of shallow water taxa (*Amphistegina*, *Lenticulina*).
- Calcareous taxa dominate (*Cibicidoides eocaenus*, *C. praemundulus*, *Paralabamina lunata*, *Hanzawaia ammophila*, *Melonis* sp. 1, *Globobulimina* sp., *Nuttallides truempyi*) with minor agglutinate component (*Gaudryina* sp., *G. pyramidata*, *Cyclamina placenta*).
- Shale with brownish calcilutite layers (< 5-m thickness).
- Outer neritic to lower bathyal paleobathymetric zones.
- Occur in the Pelotas and Sergipe-Alagoas basins.
- Lower to upper Eocene interval.

Biofacies C:

- Reworking of shallow water taxa is less frequent (*Lenticulina*).
- Moderate to low evidence of dissolution on planktic and benthic tests.
- Calcareous taxa (*Cibicidoides praemundulus*, *Cibicidoides* sp., *Lenticulina* sp., *Bulimina* sp., *Globocassidulina subglobosa*, *Globobulimina* sp., *Anomalinoides garzaensis*, *Neoeponides elevatus*, *Nuttallides truempyi*) are more abundant than the agglutinants (*Gaudryina* sp., *G. pyramidata*, *Eggerellina* sp., *Dorothia* sp.).
- Dark gray shale interval with layers of calcilutite.
- Outer neritic to lower bathyal.
- Occurs in the Pelotas, Santos, and Sergipe-Alagoas basins.
- Middle to upper Eocene.

Biofacies D:

- Reworking of shallow water taxa is very rare.
- Always associated to the Biofacies E.
- Moderate evidence of dissolution on planktic and benthic tests
- Calcareous and agglutinated taxa in equal amounts (*Rhizammina*, *Bathysiphon*, *Psammosiphonella cylindrica*, *Haplophragmoides*, *Trochamminoides*, *Ammodiscus*, *Recurvoides*, *Nuttallides truempyi*, *Cibicidoides*, *Gyroidinoides globosus*, *Stensioeina beccariiformis*).
- Shale (gray to dark gray) intervals with thin layers of fine sand (< 5-m thickness).
- Upper Maastrichtian to upper Eocene.
- Occur in the Sergipe-Alagoas, Mucuri, Campos, and Santos basins.
- Middle to lower bathyal.

Biofacies E:

- Flysch-type agglutinated taxa dominate (*Haplophragmoides*, *Trochamminoides*, *Ammodiscus*, *Recurvoides*), especially the tubular forms (*Rhizammina*, *Bathysiphon*, *Psammosiphonella cylindrica*, *Nothia*).
- When present, calcareous taxa are represented by the Velasco-type assemblage (*Nuttallides truempyi*, *Stensioeina beccariiiformis*, *Cibicidoides velascoensis*, *C. hyphalus*, *Osangularia velascoensis*, *Gyroidinoides globosus*) in the Paleocene (Berggren and Aubert, 1975), and the Barbados-type assemblage (*Cibicidoides eocaenus*, *Osangularia mexicana*, *Nuttallides truempyi*, *Bulimina trinitatensis*) in the Eocene (Wood et al., 1985, Bolli et al., 1994).
- Epifaunal species dominate with great number of suspension feeders that indicates a relatively tranquil benthic environment with pulses of downslope currents (turbidites – sandy intervals).
- Shallow water taxa transported to deeper sections, very commonly associated with sand intervals
- Reworked and dissolved planktic foraminifera when present.
- Moderate to high evidence of dissolution of planktic and calcareous benthic tests.
- Shale intervals (hemipelagic sedimentation) interbedded with thick sand layers (>5m).
- Lower bathyal to abyssal.
- Occurs in all marginal basins, but is more developed and abundant in the Campos Basin.
- Upper Maastrichtian to upper Eocene, peak in the Paleocene.

The integration of lithofacies and the benthic foraminiferal biofacies (Table 4.3, Figs. 3 and 4) is summarized in figure 4.5. Our model shows an abrupt change in biofacies across the Paleocene/Eocene boundary for the Brazilian marginal basins (Figs. 4.4). The biofacies distribution could be correlated to depositional sequences:

1. Outer shelf to the shelf break: Biofacies A, B and C,
2. Shelf break to the continental slope: Biofacies B, C, D, and E,
3. Deep continental slope to abyssal plain: Biofacies D and E.

The Maastrichtian to Paleocene interval is mainly composed by Biofacies D and E, where the agglutinate taxa formed at least 50% of the benthic community. Biofacies E

is much more abundant than Biofacies D within Maastrichtian-Paleocene interval. This interval also has a greater sand interval associated with Biofacies E. The establishment of Biofacies D and E was favored by the eustatic sea level changes in the same interval (Coffey and Read, 2004, Kominz et al., 2008). A late Paleocene sea level fall (e.g., Miller et al., 2005, Kominz et al., 2008) may have provided more siliciclastic input to the deeper sections, which are the main source of grains used by the agglutinated benthic foraminifera to build their tests.

The calcareous-dominant biofacies A, B and C occur exclusively in the Eocene interval in the Sergipe-Alagoas, Mucuri, Santos, and Pelotas basins. The Sergipe-Alagoas Basin sequence of the biofacies recorded a clear shallowing upwards sequence in response to the prograding shelf edge. By the late Eocene, the Sergipe-Alagoas Basin had shoaled to neritic depths.

The absence of the calcareous-rich biofacies in the Campos Basin has a close relationship with the evolution of the Paraíba do Sul drainage system and the uplift of the Serra do Mar. The Serra do Mar uplift occurred from the Late Cretaceous to the Paleocene (Almeida and Carneiro, 1998, Cobbold et al, 2001, Modica and Brush, 2004). This uplift was followed by a massive erosional event that sculpted the mountains introducing large volumes of siliciclastic into Santos and Pelotas basins, as demonstrated by high sedimentation rates during this time (65m/myr and 120m/myr, respectively). These erosional processes were delimited by the Paraíba do Sul drainage system that was fairly well developed in the upper Paleocene and initially flowed into Santos Basin and progressively shifted to Campos Basin in the upper Eocene/Oligocene (Cobbold et al, 2001, Modica and Brush, 2004). This shifting of the drainage system is observed in the

Age versus Depth Model of CAM-01 (Fig. 4.6), which documents the low sedimentation rates in the Maastrichtian (8-14m/myr) increasing progressively in the upper Eocene (20-59m/myr) and Oligocene (109-470m/myr). The Oligocene interval is one of the most important oil plays in the Campos Basin (Milani et al., 2001). In the Santos Basin, a large volume of sediments supplied by the Serra do Mar erosional processes were deposited in the Campanian/Maastrichtian interval (Cainelli and Mohriak, 1999), supported by the high sedimentation rates during the Maastrichtian/Paleocene (30-61m/myr, Fig. 4.6). The Pelotas Basin received an increasing volume of sediments from the paleo-Rio de la Plata.

Table 4.3: Biofacies characteristics associated with the lithofacies in the Brazilian marginal basins.

Biofacies	Age	Lithology	Paleobathymetric range	Key Taxa	Planktics (%)	Radiolarian (%)	Basins
A	middle to upper Eocene	medium to coarse sand with shale layers	Inner to outer Neritic	<i>Elphidium</i> , <i>Amphistegina</i> , <i>Lenticulina</i> , <i>Cibicides</i>	0 - 45		Mucuri and Sergipe-Alagoas
	lower to upper Eocene	shale with thin layers of fine sand	upper to middle bathyal	<i>Cibicidoides</i> , <i>Hanzawaia ammophila</i> , <i>Planulina costata</i> , <i>Lenticulina</i> , <i>Nodosaria</i>	50 - 60	40 - 100*	Santos* and Sergipe-Alagoas
B	upper Eocene	shale with layers of calcilutite	outer neritic	<i>Amphistegina</i> , <i>Lenticulina</i> , <i>Paralabammina lunata</i> , <i>Cibicidoides eocaenus</i> , <i>Melonis sp.1</i>	0 - 25		Sergipe-Alagoas
	lower Eocene	shale with layers of calcilutite	middle to lower bathyal	<i>Planulina costata</i> , <i>Hanzawaia ammophila</i> , <i>Nuttallides truempyi</i> , <i>Gaudryina sp.</i> , <i>Cyclammina sp.</i> , <i>Paralabammina lunata</i> , <i>Cibicidoides eocaenus</i>	0 - 60		Sergipe-Alagoas, Pelotas
C	lower to upper Eocene	shale with layers of calcilutite	outer neritic to lower bathyal	<i>Cibicidoides sp.</i> , <i>C. praemundulus</i> , <i>Lenticulina sp.</i> , <i>Bulimina sp.</i> , <i>Gaudryina sp.</i> , <i>G. pyramidata</i> , <i>Globocassidulina subglobosa</i> ,	0 - 60		Santos, Pelotas and Sergipe-Alagoas
D	Maastrichtian to upper Eocene (peak in the Paleocene)	shale intervals (gray to dark gray) with thin layers of fine grain sand (<5m of thickness)	middle to lower bathyal	<i>Rhizammina</i> , <i>Bathysiphon</i> , <i>Psammosiphonella cylindrica</i> , <i>Haplophragmoides</i> , <i>Trochamminoides</i> , <i>Ammodiscus</i> , <i>Recurvoides</i> , <i>Nuttallides truempyi</i> , <i>Cibicidoides</i> , <i>Gyroidinoides</i>	40 - 90	60 - 80*	Sergipe-Alagoas, Mucuri*, Campos, and Santos
E	Maastrichtian to upper Eocene	shale intervals with medium to coarse sand layers (>5m of thickness)	lower bathyal to abyssal	<i>Rhizammina</i> , <i>Bathysiphon</i> , <i>Psammosiphonella cylindrica</i> , <i>Haplophragmoides</i> , <i>Trochamminoides</i> , <i>Ammodiscus</i> + calcareous taxa (Velasco-type assemblage in the Paleocene, and Barbados-type assemblage in the Eocene)	40 - 60		Sergipe-Alagoas, Mucuri, Campos, and Santos
	Maastrichtian to upper Paleocene		upper/middle bathyal to abyssal	<i>Rhizammina</i> , <i>Bathysiphon</i> , <i>Psammosiphonella cylindrica</i> , <i>Haplophragmoides</i> , <i>Trochamminoides</i> , <i>Ammodiscus</i> , <i>Recurvoides</i>	0		Pelotas, Campos, Sergipe-Alagoas

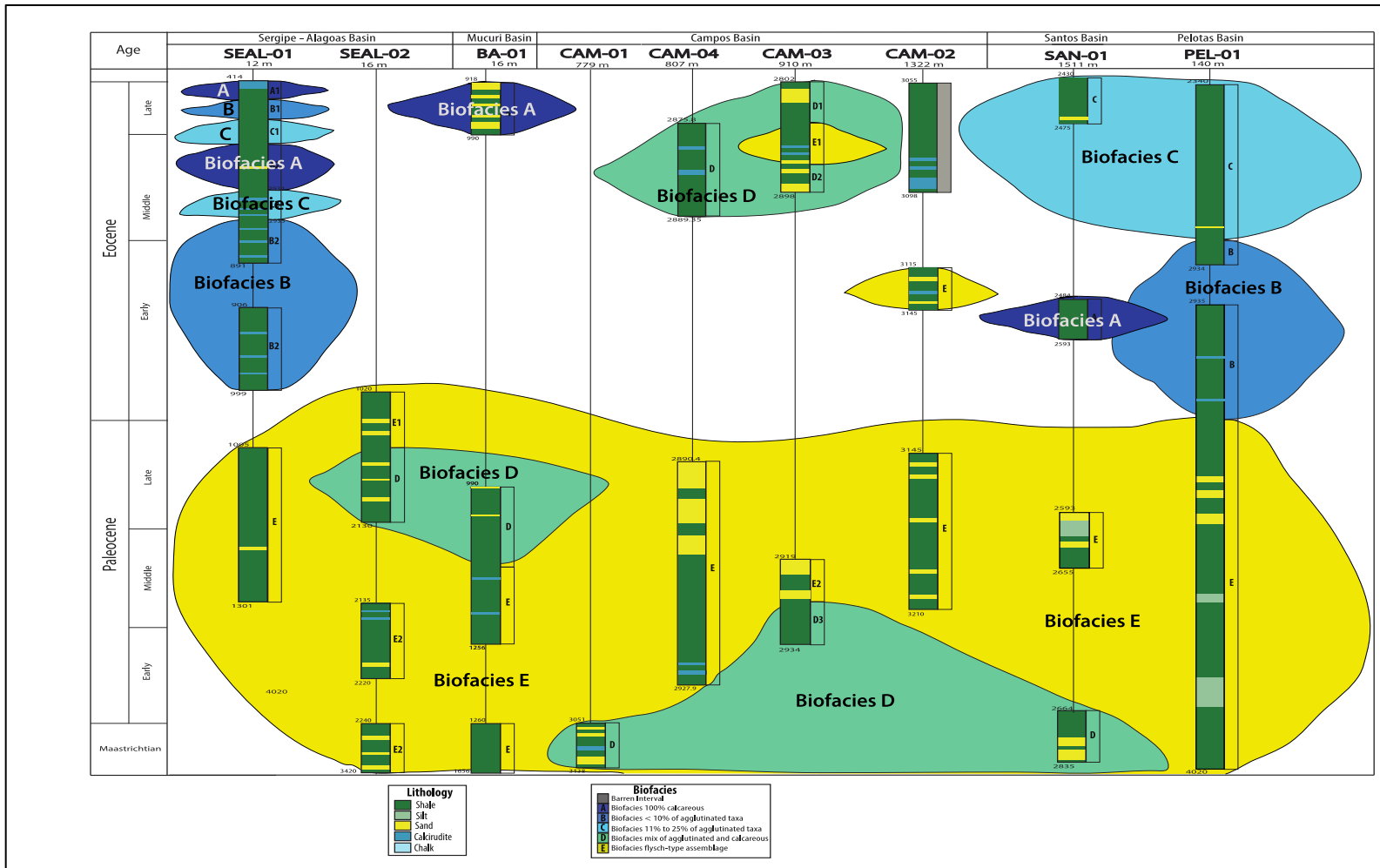


Figure 4.4: Biofacies distribution in the Maastrichtian through upper Eocene interval for the Brazilian marginal basin.

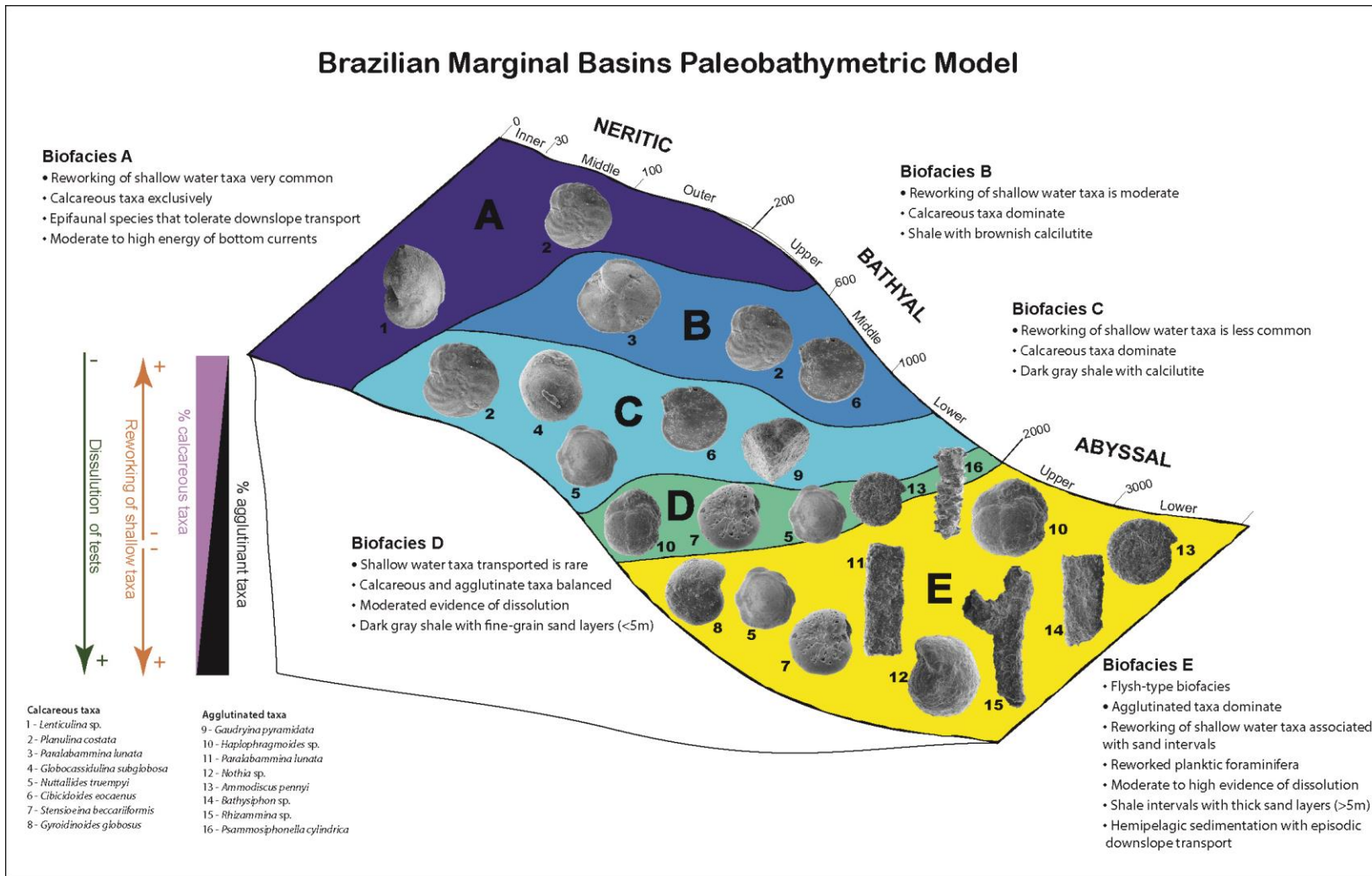


Figure 4.5: The paleobathymetric and paleoenvironmental model for the Brazilian marginal basins based on benthic foraminiferal biofacies

4.8 – PALEOENVIRONMENT:

The biofacies reflect the environmental conditions in the marginal basins across the Maastrichtian-Eocene interval. The deep-water was dominated by the flysch-type Biofacies E associated with Biofacies D (Figs. 4.3 and 4.4). Biofacies E is defined by the high content of agglutinate taxa, although some calcareous taxa occur in the same interval. However, in the Paleocene, this biofacies was composed almost exclusively of agglutinated taxa in one well of the Sergipe-Alagoas Basin, two wells of the Campos Basin, and in the Pelotas Basin with very low planktic percentages (0% to 10%). This feature suggests either a relatively shallow carbonate compensation depth (CCD) along the continental margin during this time, and/or that these three basins were at lower abyssal paleodepths (>3000 m).

In general, the epifaunal calcareous taxa (*Nuttallides truempyi*, *Cibicidoides velascoensis*, *Osangularia velascoensis*, *Stensioeina beccariiformis*, *Gyroidinoides globosus*) and epifaunal tubular agglutinated suspension feeders (*Rhizammina*, *Bathysiphon*, *Nothia*, *Psammosiphonella*) dominate Biofacies E and D in the Maastrichtian – Paleocene interval. The dominance of tubular forms (*Rhizammina*, *Bathysiphon*, *Nothia*, *Psammosiphonella*) in Biofacies E reflects an oligotrophic hemipelagic environment with relatively low organic matter influx (Jones and Charnock, 1985, Kaminski and Gradstein, 2005). In the marginal basins, the tranquil bathyal/abyssal realms were episodically disturbed by downslope transport as suggested by the occurrence of shallow water taxa concentrated in some layers associated with sand deposition (Fillon, 2003, 2009).

Similar environmental conditions persisted up the slope into bathyal and neritic realms. The Biofacies A, B and C are also dominated by epifaunal species of *Cibicidoides*, *Gyroidinoides*, *Hanzawaia*, *Planulina*. However, some seasonal input of marine organic matter based on the presence of *Globocassidulina subglobosa*, which has been reported as an opportunistic taxon that responds to seasonal pulses of high-quality organic matter (Gooday, 1988, Alegret et al., 2009, d'Haenens et al., 2012).

4.9 – DISCUSSION:

The paleobathymetric and paleoenvironmental model developed here, based on benthic foraminiferal biofacies, provides a valuable tool for interpreting the depositional history of the Brazilian marginal basins. The depositional history of the five basins analyzed records the seaward growth of the Brazilian continental margin during the Paleogene (Fig. 4.7). Flysch-type assemblages (Biofacies E) have previously been reported associated with deep-water turbidite sequences (Gradstein and Berggren, 1981, Wrinkler, 1984, Mesquita, 1998, Koutsoukos, 2000, Kaminski and Gradstein, 2005). Biofacies E (tubular agglutinated dominated) is a diagnostic feature in the Maastrichtian-Paleocene interval of all marginal basins, and continued through the upper Eocene only in the Campos Basin (Figs. 4.4). The Eocene interval is dominated by calcareous biofacies (A, B and C) in all other basins (Sergipe-Alagoas, Mucuri, Santos, and Pelotas).

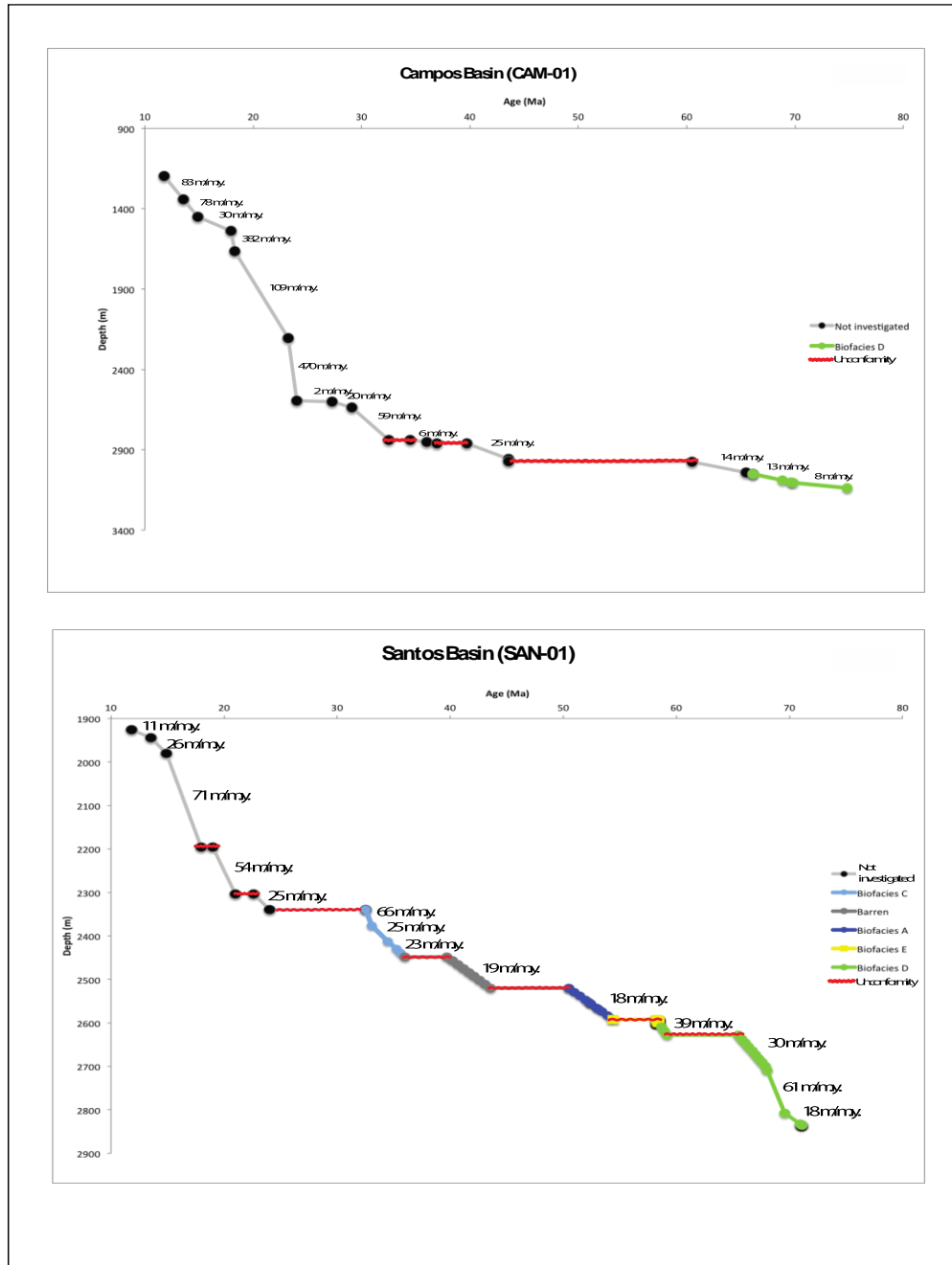


Figure 4.6: Age vs. depth models of Campos (CAM-01) and Santos (SAN-01) basins, with sedimentation rates and benthic foraminiferal biofacies. The age-depth model was based on nanofossils datums from PETROBRAS.

The uplift of the Serra do Mar Mountains associated with its erosion strongly influenced the complex fill history of the Santos Basin (Almeida and Carneiro, 1998, Modica and Brush, 2004). This large clastic influx forced massive shelf progradation and development of deep-water fan systems despite globally high sea level (Cobbold et al., 2001, Modica and Brush, 2004). The Pelotas Basin was also influenced by massive clastic input from the erosion of the Paraná flood basalts and sediment delivery via the paleo-Rio de al Plata (Fig. 4.8). At the same time, the Mucuri and Sergipe-Alagoas basins had major fluvial sediment supply provided by the paleo-Doce River and São Francisco River, respectively (Fig. 4.8).

The Campos Basin seems to have a distinct depositional history, mainly characterized by very low sedimentation rates at least until the Oligocene (generally <15 m/myr), and by being occupied exclusively by deep-water benthic foraminiferal biofacies D and E, where the agglutinate taxa constitute at least 50% of the assemblage, in the Maastrichtian through upper Eocene (Figs. 4.4). The main reason of this distinction could be due to the position of Campos Basin in relation to major fluvial systems and depositional centers during the Paleocene and Eocene. As a distal basin, the sediment supply occurred as turbidite pulses during lowstands (medium to coarse grain sand intervals) or as deep-sea fans in periods of sea-level highstand (fine to very fine grain sand intervals) (Covault and Graham, 2010). The relatively narrow shelf in the Campos Basin facilitated growth of the deep-sea fans during high sea level periods (Covault and Graham, 2010).

Sergipe-Alagoas and Mucuri basins are the most proximal areas, where the calcareous biofacies A, B and C dominated (Figs. 4.1, 4.4, 4.8). Calcareous biofacies also

dominated the Eocene of the Santos and Pelotas basins, although they were deeper (bathyal) and less influenced by reworked neritic input.

The Brazilian passive margin was actively prograding during the Paleocene and Eocene as reflected by the stratigraphic changes in the benthic foraminiferal biofacies and patterns of sediment accumulation. At the same time, changes in the sea level may have contributed to a series of unconformities within the study interval due to sediment starvation on the slope during transgression, or submarine canyon erosion or mass wasting on the slope during highstands and lowstands. In addition, salt tectonics associated with terrestrial influx during lowstands in the Campos and Santos basins was responsible for the erosional unconformities, especially in the Eocene. The Abrolhos Volcanic Complex was the major cause of the big erosional unconformity in the Mucuri Basin during the Eocene.

PALEOGENE PROGRADATION OF THE BRAZILIAN CONTINENTAL MARGIN

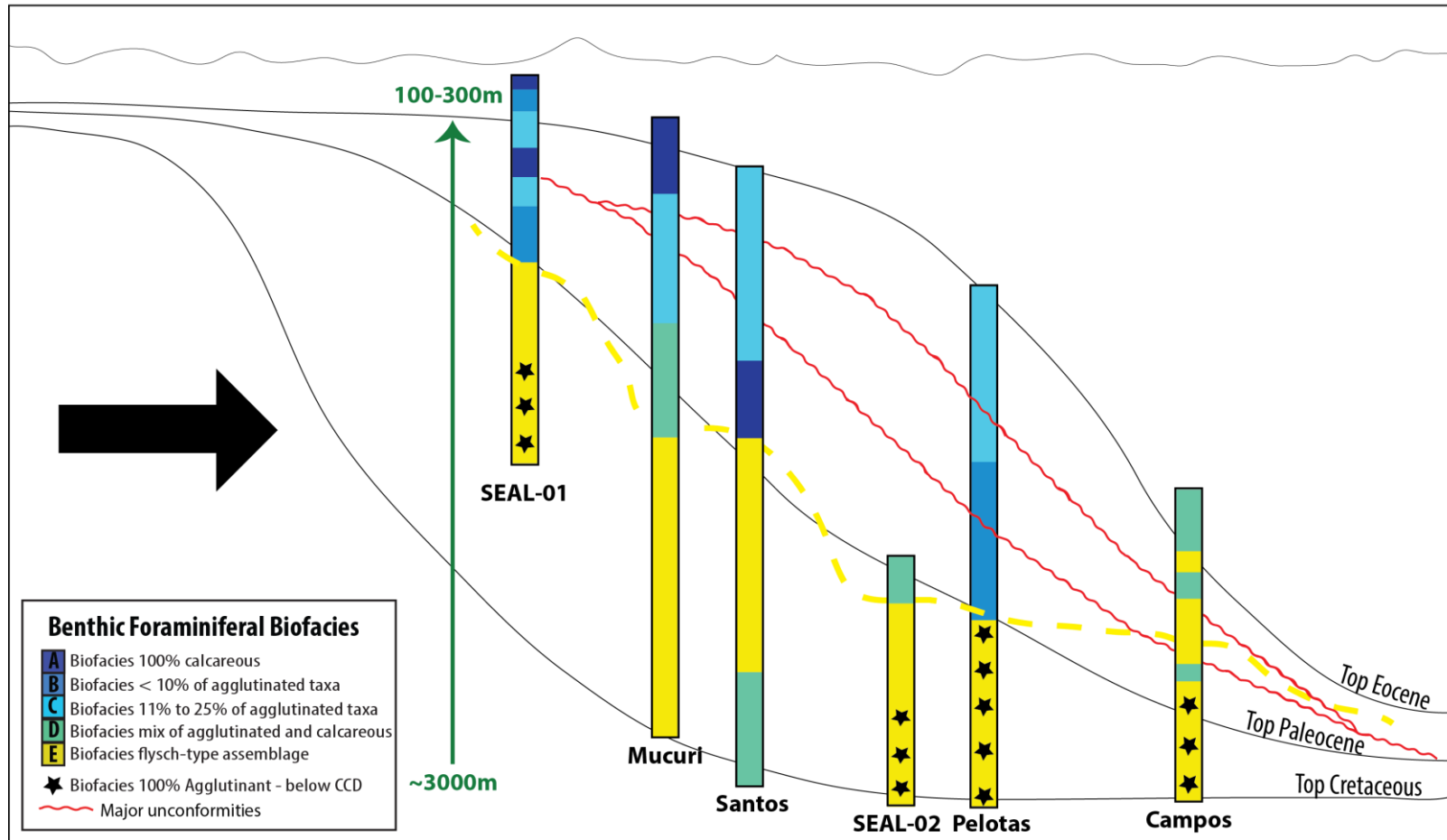


Figure 4.7: Brazilian continental margin progradation in the Paleogene based on benthic foraminiferal biofacies and the relative position of the marginal basins included in this study.

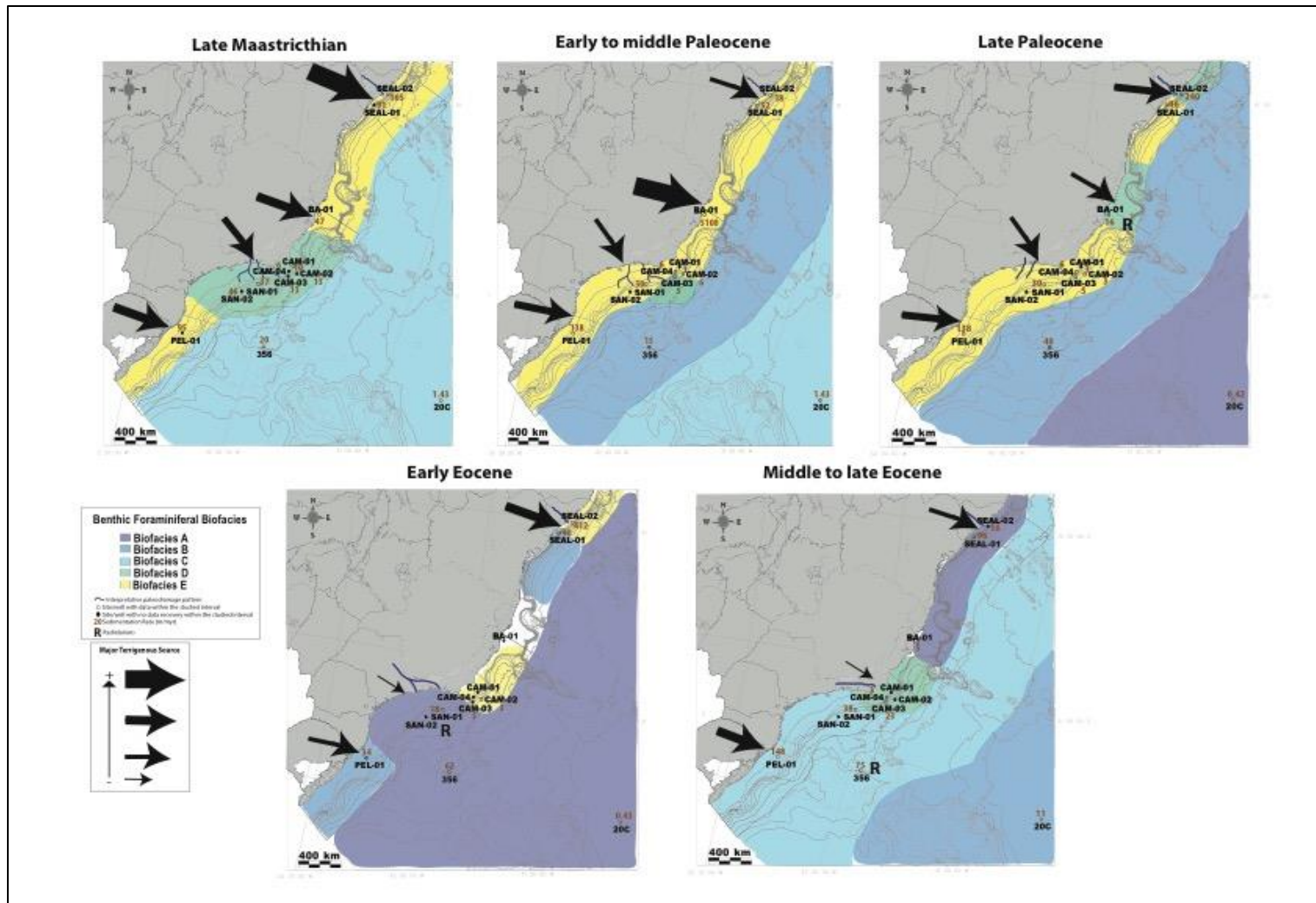


Figure 4.8: Sediment supply for the Brazilian marginal basins and the benthic foraminiferal biofacies. Width of the arrows shows relative sediment supply.

4.10 – LYSOCLINE AND CCD ALONG THE BRAZILIAN MARGIN:

The preservation of the tests of calcareous benthic and planktic foraminifera has long been used to evaluate carbonate dissolution through time (Kennett, 1966, Berger, 1967, 1970a, b, Berger and Soutar, 1970, Moore et al., 1973, Thiede, 1973, Sliter, 1975, Berger et al., 1982, Chen et al., 1988, Opdyke and Wilkinson, 1993, Lee et al., 2000, Lyle et al., 2008, Pälike et al., 2012).

The distribution of the marine carbonate is primarily controlled by the carbonate (or calcite) saturation of ocean water (Berger, 1967, 1970a, b). The carbonate compensation depth (CCD) is the level in the ocean below which calcium carbonate cannot be preserved due to undersaturation of the deep-waters, the lysocline is above the CCD and represents the level of rapid increase in dissolution rate (Berger, 1970a).

Cenozoic CCD fluctuations in the major ocean basins are generally well understood (e.g., Berger, 1967, 1970a, b, Berger and Soutar, 1970, Van Andel, 1975, Van Andel et al., 1977, Berger et al., 1982, Chen et al., 1988, Zachos et al., 2004, Lyle et al., 2008, Pälike et al., 2012), but the behavior of the lysocline and CCD along continental margins is less well known (e.g., Moore et al., 1973, Thiede, 1973, Cullen and Curry, 1997).

A proposed model of the relationship between the CCD and lysocline by Berger (1970a, b, fig. 4.9) states that the accumulation rate of calcite in the sediments is determined by the interaction of three factors: rate of carbonate supply from the surface ocean (i.e., flux rate of calcareous plankton), depth of the lysocline, and the gradient of increase in dissolution rate with depth below the lysocline. This model suggests that the

CCD shoals along the continental margins (Fig. 4.9) as observed in the Panama Basin (Swift and Wenkam, 1978) and in the Tropical Atlantic (Site 927, Cullen and Curry, 1997). Berger (1970a, b) attributes the shallowing of the CCD near the continent to an increase in the carbon dioxide (CO₂) content of sediments due to oxidation and degradation of higher amounts of marine organic matter produced in the surface waters of the continental margins and/or from input of terrestrial organic matter from the continent. Therefore, carbonate dissolution and consequently the position of the CCD on a siliciclastic continental margin possesses its own characteristic pattern of carbonate preservation that differs from open ocean regions (Berger, 1970a, b, Thiede, 1973).

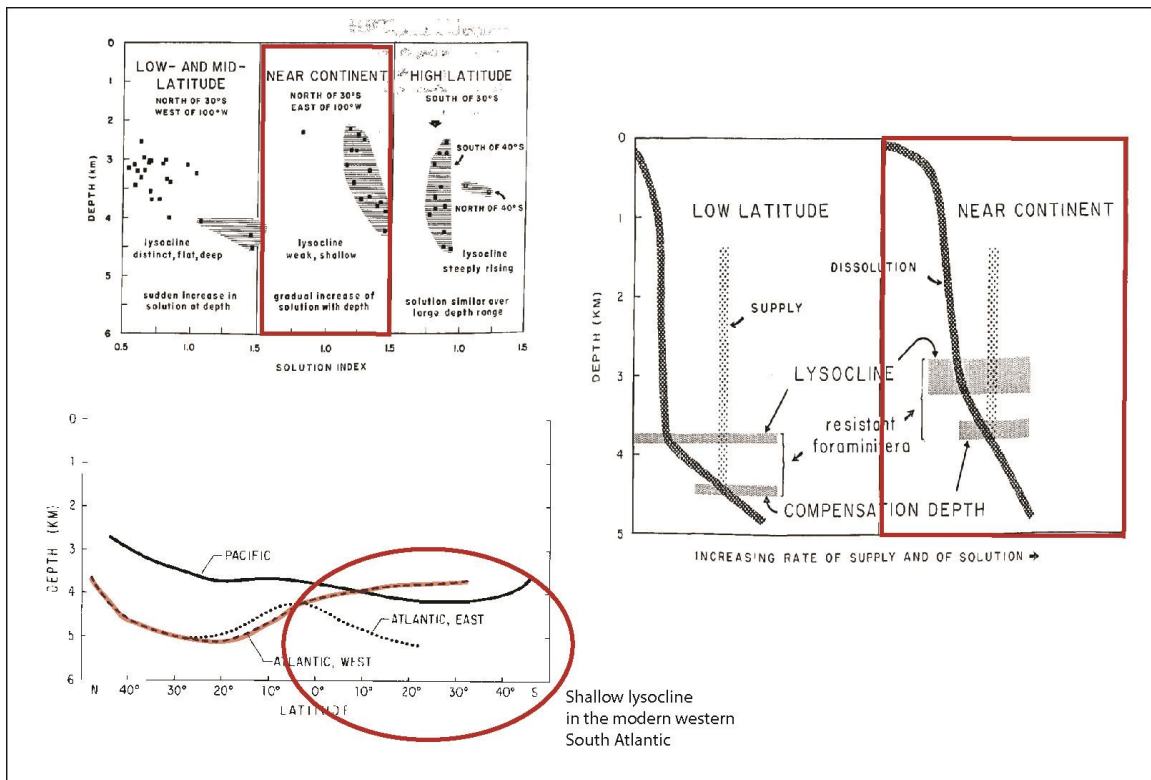


Figure 4.9: Berger (1970a, b) proposed model of the relationship between the lysocline and the CCD in the southeast Pacific. The red lines highlight the model for near the continent where the lysocline and CCD shoal along the margin.

Evidence for shallowing of the CCD along the Brazilian continental margin is recorded by the benthic foraminiferal biofacies compared with the two distal DSDP sites from the western South Atlantic (Sites 20C and 356). Biofacies E is composed of 100% agglutinated taxa and with low percentage of planktic foraminifera (0-10%) and is interpreted as lower abyssal paleodepths, below the CCD, during the Paleocene (Gradstein and Berggren, 1981, Kaminski et al., 1988, Kaminski et al., 1989, Kuhnt et al., 1989, Kuhnt and Collins, 1996, Kaminski and Gradstein, 2005). This was observed in Sergipe-Alagoas, Campos, and Pelotas basins. The Pelotas and Sergipe-Alagoas basins show a similar pattern in the benthic assemblages from agglutinate-dominant to calcareous-dominant as documented by Kennett (1966) for the Ross Sea, Antarctica, where the CCD is very shallow near the continent (Fig. 4.10), although low temperatures (0° to -2° C) and high salinities (34.75 to 35.00 ‰) associated with high concentrations of carbon dioxide of the bottom water also contributed to the solution of the calcium carbonate in the Ross Sea. Biofacies D (mix of agglutinated and calcareous benthic taxa) always occurs in association with Biofacies E and can be interpreted as a transitional assemblage between agglutinate- to calcareous-dominated, as seen in the intermediate assemblage of Ross Sea, Antarctica (Kennett, 1966). Progradation of the Brazilian margin during the Paleogene resulted in shoaling of the seafloor above the CCD in most of the marginal basins by Eocene time. However, the Campos Basin remained more distal and deeper than the other basins during the Paleocene-Eocene interval and was mostly dominated by agglutinated taxa until the Oligocene, when the margin prograded and the basin rapidly shoaled and a shallow water carbonate environment became established (BouDagher-Fadel et al., 2010).

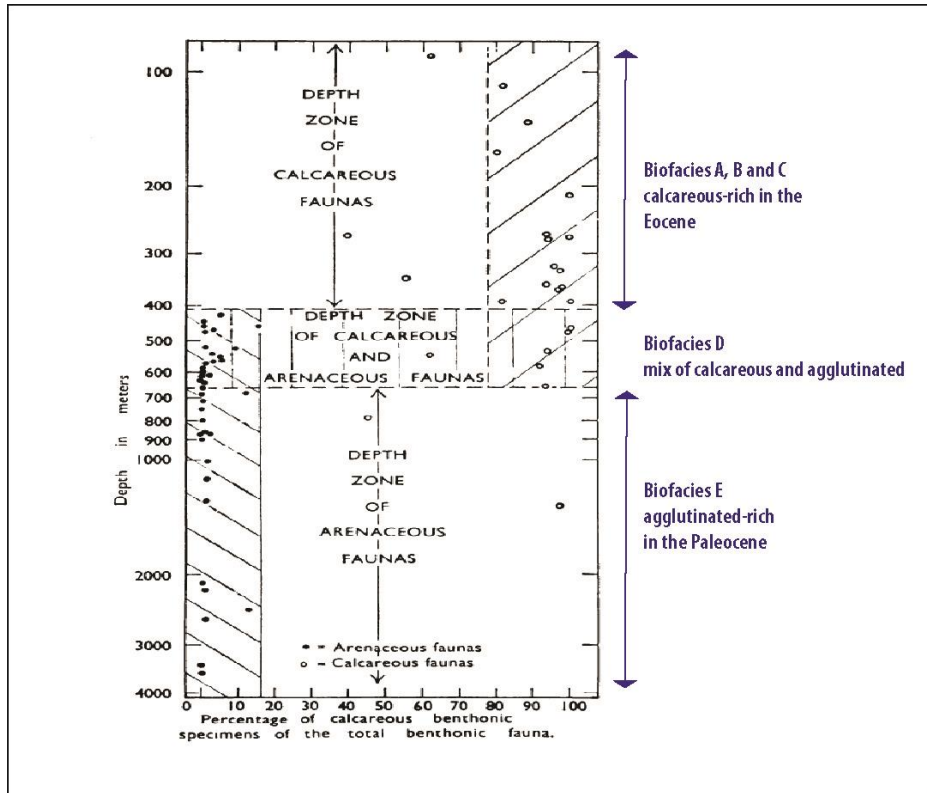


Figure 4.10: Benthic foraminiferal biofacies comparison with the benthic assemblage of the Ross Sea, Antarctica, related to the position of the CCD (modified from Kennett, 1966).

In the Eocene, the CCD was globally shallower as demonstrated for the equatorial Pacific (Pälike et al., 2012) and the Walvis Ridge in the southeast Atlantic (Fig. 4.11, Zachos, et al., 2004), however we observed an abrupt change from agglutinated-dominance in the Paleocene to calcareous-dominance in the Eocene of the Brazilian marginal basins. This occurred due to the massive sediments input that forced a progressive progradation of the continental margin off eastern Brazil. The paleodepth of the basins changed from abyssal/lower bathyal in the Paleocene to middle bathyal/neritic in the Eocene. The shallowing of the basins was favorable to the establishment of the calcareous benthic assemblage in the Eocene (Biofacies A, B and C) (Fig. 4.12).

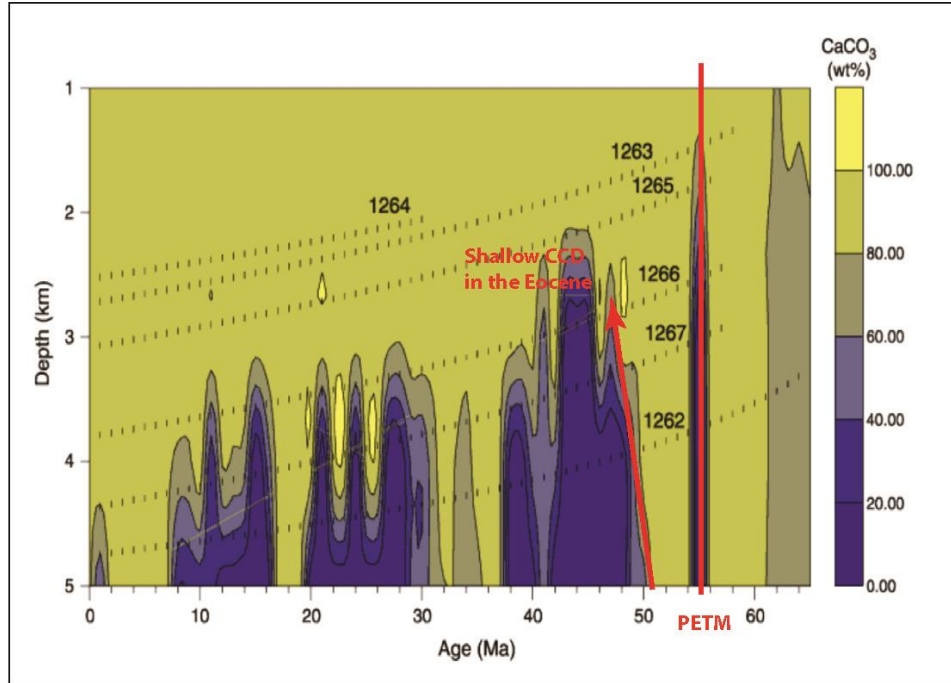


Figure 4.11: CaCO₃ (wt%) of the Walvis Ridge showing the shallow lysocline and CCD at the PETM and during the Eocene (modified from Zachos et al., 2004).

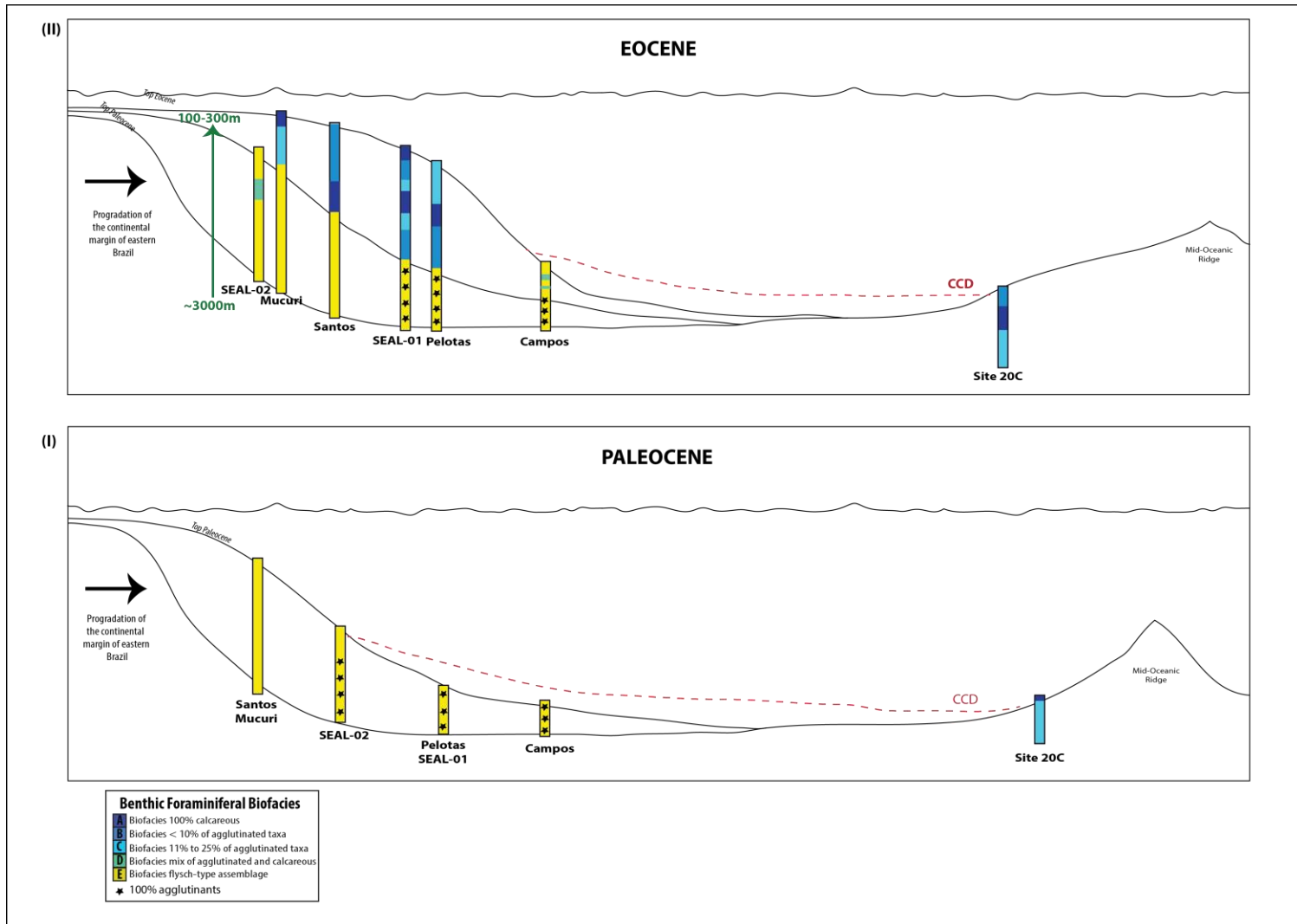


Figure 4.12: Sketch with the position of representative wells of the Brazilian marginal basins showing the change in agglutinant-dominated Biofacies E (I) to calcareous-dominated Biofacies A, B and C (II) and fluctuation of the CCD during the Paleogene..

4.11 – COMPARISON WITH THE NORTHERN GULF OF MEXICO:

The evolution of the Brazilian passive margin during the Paleogene is similar to the progradation of the southern U.S. continental margin along the northwestern Gulf of Mexico during the same time interval (e.g., Wilcox Formation). In both regions, the basins were located in deep-waters in the Paleocene and progressively built out relatively quickly. The Paleocene through Eocene had major pulses of terrigenous input with drainage focused at large deltaic systems in the northern Gulf of Mexico (Galloway et al., 2000, McDonnell et al., 2008, Power et al., 2013), and in the Santos, Pelotas, Mucuri and Sergipe-Alagoas basins on the Brazilian margin (Cainelli and Mohriak, 1998, Cobbold et al., 2001, Modica and Brush, 2004, Zalán, 2004). By late Eocene time, the slope had shoaled to neritic depths in the Sergipe-Alagoas and Mucuri basins (Figs. 4.13 and 4.14). In addition, the salt tectonics created minibasins that influenced the slope deposition in the Gulf of Mexico and Santos, Pelotas, and Campos basins (Mohriak, 1990, Cainelli and Mohriak, 1998, McDonnell et al., 2008, Mohriak, 2003) (Fig. 4.15).

In summary, the Brazilian margin and the northwestern margin of the Gulf of Mexico basin had similar history of Paleogene progradation. In both regions, a great volume of sediment supply forced the continental margin to shoal. The deep-water oil fields are associated with turbidites, slope fans, and basin-floor fan systems in both regions (Mohriak, 1990, Milani et al., 2001, McDonnell et al., 2003, Zalán, 2004, Lewis et al., 2007, Power et al., 2013).

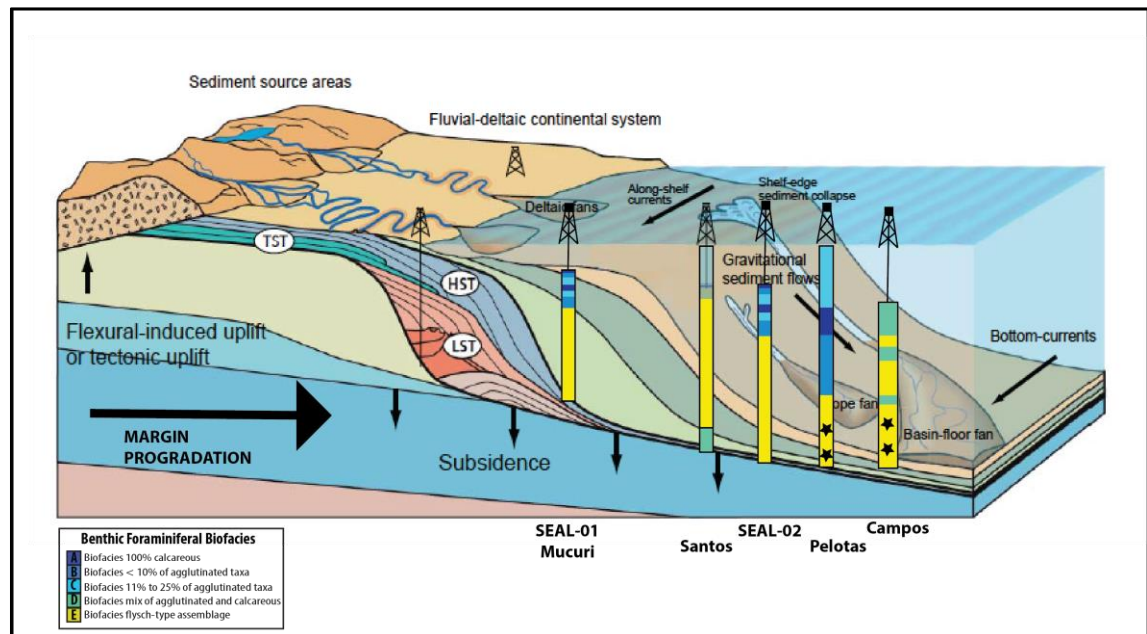


Figure 4.13: Brazilian continental margin model progradation. Modified from Contreras (2011).

The agglutinated benthic foraminiferal assemblage, the so-called flysch-type assemblage (Gradstein and Berggren, 1981), dominates the deep-water turbidite systems in both regions. The flysch-type assemblage distinguishes deep-water turbidites in the major petroleum basins located along progradational passive margins, e.g., eastern Brazil margin (Mesquita, 1998, Koutsoukos, 2000, Viviers and Ferreira, 2006, Costa and Viviers, 2012), northern Gulf of Mexico basin (Fillon, 2003, 2009), North Sea, and Labrador Sea (Gradstein and Berggren, 1981, Jones, 1988, Kaminski et al., 1989).

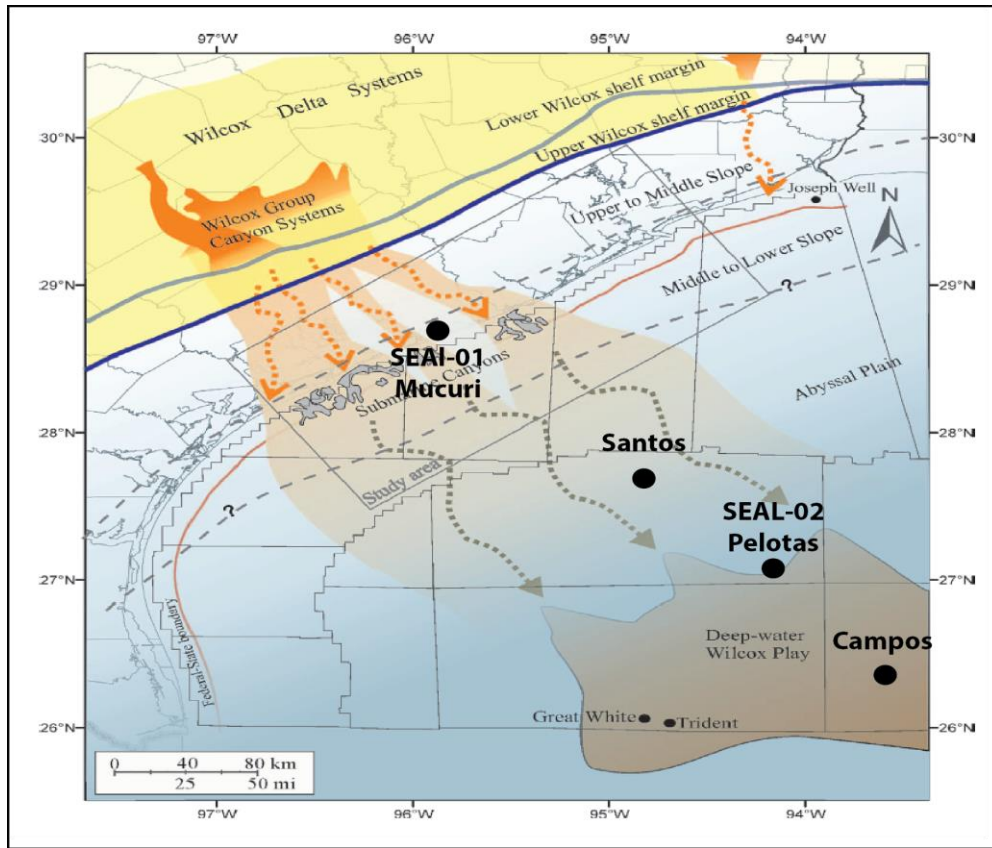


Figure 4.14: Schematic paleoceanographic map for the upper Paleocene-lower Eocene Wilcox Formation in the Gulf of Mexico that compares with the Brazilian continental margin progradation. Black dots are the hypothetical positions of the Brazilian marginal basins relative to the major sources of siliciclastic sediment. Modified from McDonnell et al. (2008).

4.12 – CONCLUSIONS:

Most of the petroleum exploration in the Brazilian marginal basins is offshore. Seismic data, and exploration and production wells provide vital information about the depositional history of the oil fields. A paleobathymetric and paleoenvironmental model based on the distribution of Maastrichtian-Eocene benthic foraminiferal biofacies will improve considerably the interpretation of the depositional history of hydrocarbon basins and reservoir geometry. Benthic foraminiferal biofacies also provide a means of correlation within tectonically complex

basins. The model integrates benthic foraminiferal biofacies distribution with the lithofacies. Five biofacies are recognized: Biofacies A (inner neritic to upper bathyal), Biofacies B (outer neritic to lower bathyal), Biofacies C (outer neritic to lower bathyal), Biofacies D (middle to lower bathyal), and Biofacies E (lower bathyal to abyssal). There is some overlap in the paleobathymetric zones due to the lateral differentiation among the marginal basins.

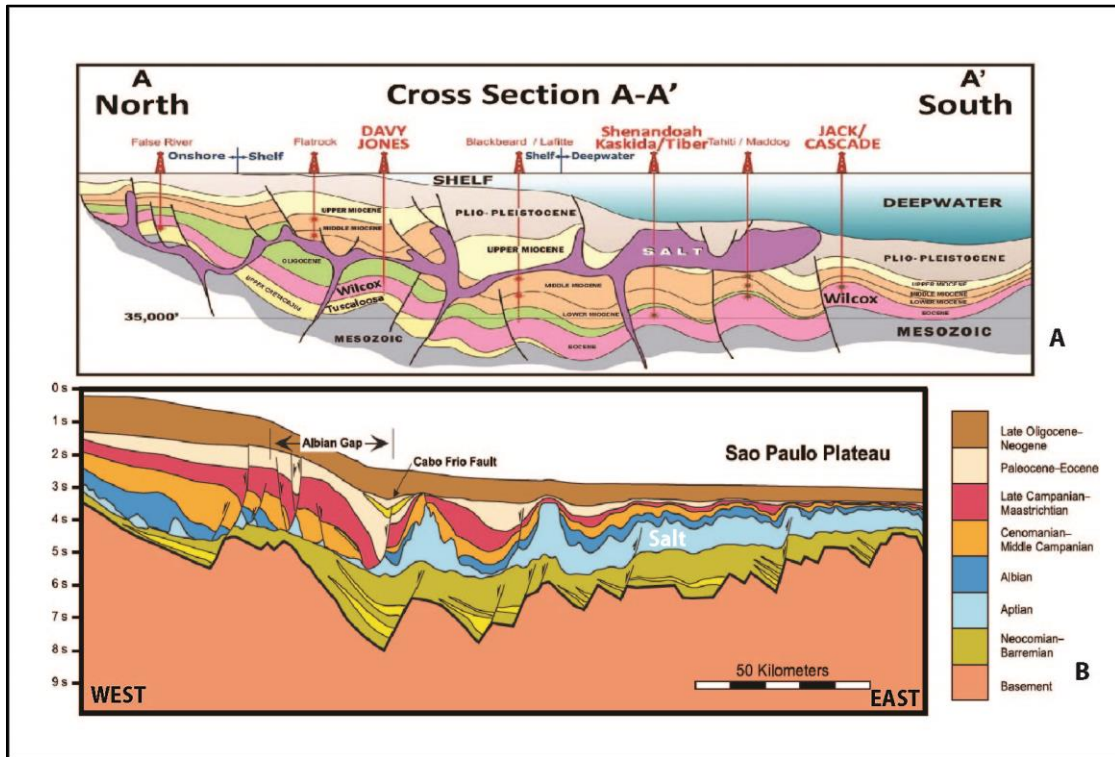


Figure 4.15: Interpreted seismic section of Gulf of Mexico (A) and Santos Basin (B) showing the influence of salt tectonics influencing the deposition in both regions. Modified from McMoran Exploration Company (2009) and Modica and Brush (2004), A and B respectively.

The Maastrichtian – Paleocene interval was dominated by Biofacies E and Biofacies D. There is an abrupt change in biofacies across the Paleocene/Eocene boundary in the Brazilian marginal basins. The dominance of the flysch-type Biofacies E in the Maastrichtian-Paleocene interval is associated with deposition along the lower slope and continental rise near or below

the depth of the CCD. The position of the lysocline and CCD were shallower along the Brazilian margin than in the adjacent distal western South Atlantic due to the degradation of marine and terrestrial organic matter from seasonal productivity and riverine input along the continental margin. The change to calcareous-dominated biofacies during the Eocene records progradation of the shelf edge and shoaling of the continental slope to bathyal depths above the CCD. The Sergipe-Alagoas and Mucuri basins reached neritic depths by the late Eocene.

We observed major unconformities in the lower to middle Eocene of the Brazilian marginal basins. These erosional unconformities are likely related to the salt tectonics, as well as terrigenous influx associated to changes in the sea level. The erosional unconformities in the Mucuri Basin are associated to the rising of the Abrolhos Volcanic Complex during the Paleocene-middle Eocene interval.

The Eocene interval was dominated by the biofacies A, B and C, however these biofacies do not occur in the Campos Basin, which continued to be dominated by Biofacies D and E. The absence of the calcareous-rich biofacies in the Campos Basin is related to the distal position of this basin relative to major sources of sediment. The proximal basins (Sergipe-Alagoas, Mucuri, Santos, and Pelotas) had greater sediment supply that provided the margin progradation, while the distal Campos Basin continued to be in a deep-water setting through the Eocene and was relatively starved of sediment until the Oligocene.

CHAPTER 5

SUMMARY AND CONCLUSIONS

Here I provide an overview of conclusions presented in the previous chapters dealing with the upper Maastrichtian-Eocene benthic foraminiferal biofacies in the western South Atlantic and Brazilian marginal basins. My dissertation research has effectively used benthic foraminiferal biofacies in a unique way to create a paleobathymetric and paleoenvironmental model for the reconstructing the latest Cretaceous and Paleogene geologic evolution of the eastern Brazil continental margin, as well as providing new insights into the Benthic Extinct Event (BEE) across the Paleocene/Eocene boundary and the nature of the CCD and lysocline along a siliclastic margin. Results of this study provide critical ground-truth data in the upper Maastrichtian-Eocene interval for the offshore petroleum exploration in the Brazilian marginal basins. Here are my primary conclusions:

1. Approximately 330 benthic foraminiferal taxa, 180 of calcareous, and 150 of agglutinated taxa are described from the Maastrichtian to upper Eocene of the five Brazilian marginal basins and two distal DSDP sites. These taxa span lower abyssal to neritic paleodepths, and provide the basis of the assemblages analyzed in this study.
2. The Benthic Extinction Event (BEE), and associated with the Paleocene Eocene Thermal Maximum (PETM), was recognized in the Brazilian marginal basins

and at the DSDP sites. The extinction was more severe in the calcareous taxa and is less pronounced in the marginal basins (~16% extinction) where agglutinated dominated than at distal, deeper water DSDP sites (~35%). In the marginal basins, the extinction coincides with an abrupt change of the benthic assemblage from agglutinate-dominated in the Paleocene to calcareous-dominated in the Eocene. This abrupt change occurred due to the relatively rapid margin progradation and shoaling of the continental margin from abyssal to lower bathyal or middle bathyal paleodepths, and eventually neritic paleodepths in the Sergipe-Alagoas and Mucuri basins.

3. In the early Eocene, origination of new calcareous species emerged in the Brazilian margins and at the DSDP sites. However, the origination rate is higher at the distal DSDP sites (47%) compared with the marginal basins (25%).
4. Q-mode cluster analysis of the benthic foraminiferal census data from each well or site, coupled with correspondence analysis, revealed five primary biofacies.

Biofacies A is composed 100% of calcareous taxa and is more frequent in the Eocene. **Biofacies B** has up to 10% agglutinated taxa and occurs from the middle Paleocene to upper Eocene. **Biofacies C** has 11% to 25% agglutinated taxa in its composition and is recorded from the upper Maastrichtian to upper Eocene.

Biofacies D contains a more balanced percentage of calcareous and agglutinated taxa and always occurs associated with Biofacies E in the marginal basins.

Biofacies E is dominated by agglutinated taxa, especially tubular forms (*Bathysiphon*, *Nothia*, *Rhizammina*, *Psammosiphonella*). This biofacies correlates with the so-called “fysch-type” biofacies of Berggren and Gradstein

(1981) and it occurs exclusively in the marginal basins from the Maastrichtian to the upper Eocene, although it is characteristic of the Paleocene interval.

5. The five biofacies integrated with lithofacies of the Brazilian margin provided the essential information to establish the paleobathymetric and paleoenvironmental model of the eastern Brazilian continental margin. The model tracks the evolution of the margin as it built seaward and transitioned from abyssal (2000-3000 m) to bathyal (<2000 m) and neritic (<200 m) depositional environments during the Maastrichtian – late Eocene. It is a powerful predictive tool for reconstructing depositional systems in deep-water and for correlation in tectonically disturbed and complex hydrocarbon basins.
6. Changes in relative sea level, including a sea level fall in the late Paleocene followed by sea level rise in the early Eocene, as well as changes in the position of the CCD along the lower slope and rise of the Brazilian margin also affected the development of foraminiferal biofacies in the Brazilian marginal basins. The distal DSDP sites were never below the CCD during the Maastrichtian-Eocene and were dominated by calcareous benthic biofacies.
7. The dominance of the Biofacies E (flysch-type benthic assemblage) in the Paleocene along the Brazilian continental margin suggests that the CCD shoaled in this interval. The shoaling of the CCD in the Paleocene of the Brazilian continental margin confirms the hypothesis of Berger (1970) stating the CCD shoals along the continental margin. Berger (1970) hypothesis is also supported by the increase in the terrestrial input of major rivers in the Brazilian margin that provided terrestrial organic matter into the ocean. The degradation and oxidation

of the terrestrial organic matter increased the CO₂ content causing more corrosive waters and, consequently shoaling the CCD along the margin.

8. The evolution of the Brazilian passive margin during the Paleogene is similar to the progradation of the southern U.S. continental margin along the northwestern Gulf of Mexico during the same time interval (e.g., upper Paleocene-lower Eocene Wilcox Formation). In both regions, the basins were located in deep-waters in the Paleocene and progressively built out relatively quickly. Uplift and increased terrigenous supply was the major cause of the margin progradation along both of these margins. The deep-water oil fields are associated with turbidites, slope fans, and basin-floor fan systems in both regions. The agglutinated benthic foraminiferal assemblage dominates the deep-water turbidite systems in both regions, so-called flysch-type assemblage. The flysch-type Biofacies E can be used to distinguish deep-water turbidites in basins along progradational passive margins.

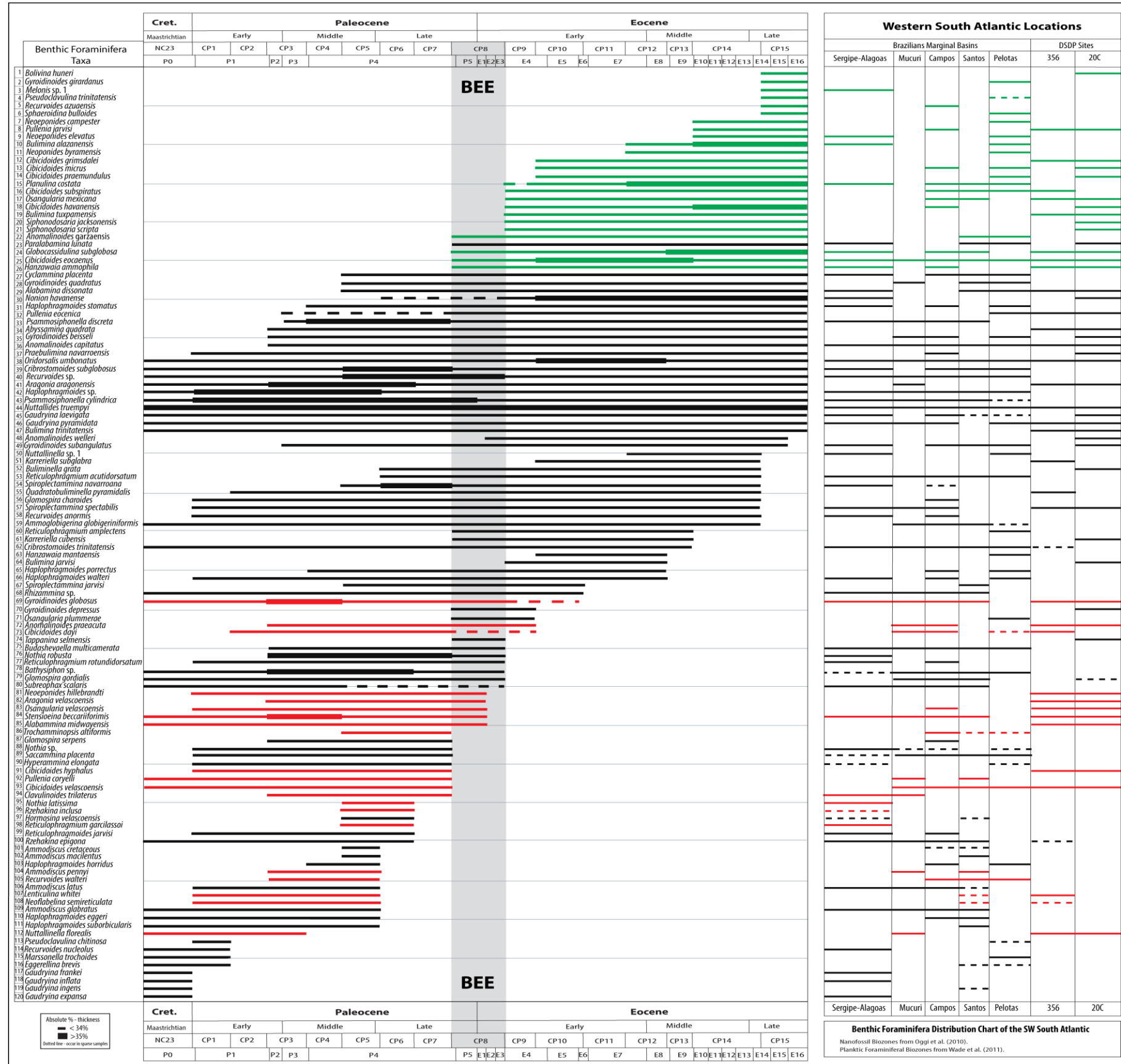
APPENDICES

APPENDIX I

STRATIGRAPHIC DISTRIBUTION CHART OF THE BENTHIC FORAMINIFERA

Red – benthic foraminifera taxa extinct after the PETM in the Brazilian marginal basins.

Green – new benthic foraminiferal taxa that appeared after the PETM in the Brazilian marginal basins.



APPENDIX II

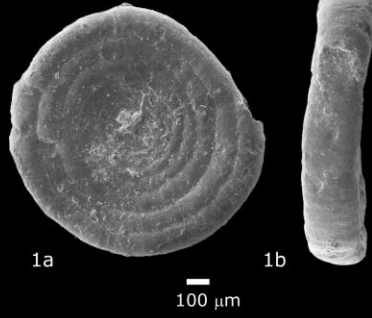
PLATES OF THE BENTHIC FORAMINIFERA

PLATE I

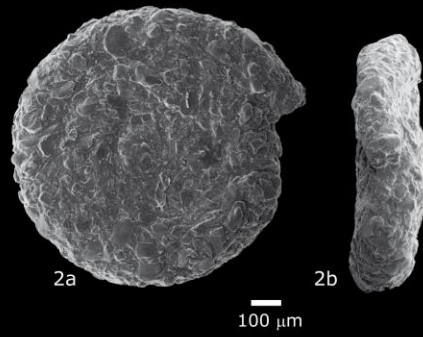
- 1a,b – *Ammodiscus cretaceous* (Reuss,1845) #2599,39 m – SAN-01, Santos Basin, late Paleocene, pg. 66.
- 2a,b – *Ammodiscus pennyi* Cushman & Jarvis (1928) #2628 m – SAN-01, Santos Basin, late Paleocene, pg. 68.
- 3 – *Glomospira charoides* Jones & Parker (1860) #3102 m – CAM-01, Campos Basin, Maastrichtian, pg. 69.
- 4 – *Bathysiphon* sp. #1960,35 m – SEAL-02, Sergipe-Alagoas Basin, late Paleocene, pg. 70.
- 5 – *Psammosiphonella cylindrica* Glaessner (1937) #2891,10 m – CAM-04, Campos Basin, middle Paleocene, pg. 70.
- 6 – *Psammosiphonella discreta* Brady (1881) #2597,15 m – SAN-01, Santos Basin, middle Paleocene, pg. 71.
- 7 – *Nothia latissima* Grzybowski (1898) #1164,75m – SEAL-01, Sergipe-Alagoas Basin, late Paleocene, pg.72.
- 8 – *Nothia robusta* Grzybowski (1898) #1200 m – SEAL-02, Sergipe-Alagoas Basin, early Eocene, pg. 72.
- 9a,b – *Rhizammina* sp. #1141,78 m – SEAL-01, Sergipe-Alagoas Basin, late Paleocene, pg. 73.

PLATE I

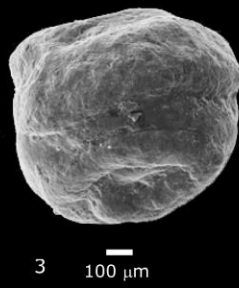
Ammodiscus cretaceous



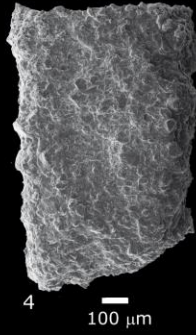
Ammodiscus pennyi



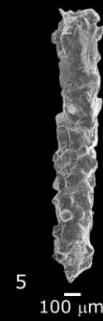
Glomospira charoides



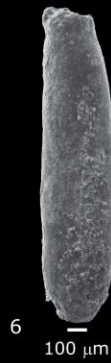
Bathysiphon sp.



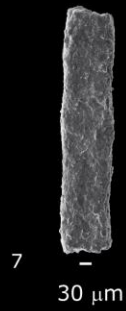
Psammosiphonella cylindrica



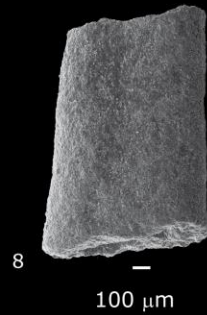
Psammosiphonella discreta



Nothia latissima



Nothia robusta



Rizhammina sp.

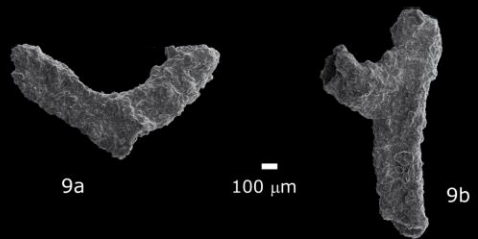
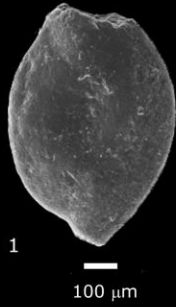


PLATE II

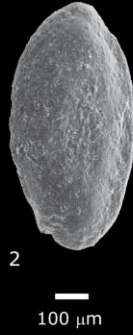
- 1 – *Rzehakina epigona* Rzehak (1895) #2832,25 m – SAN-01, Santos Basin, late Maastrichtian, pg. 74.
- 2 – *Rzehakina inclusa* Grzybowski (1901) #1140,50 m – SEAL-01, Sergipe-Alagoas Basin, late Paleocene, pg. 74.
- 3 – *Subreophax scalaris* Grzybowski (1896) #2834,70 m – SAN-01, Santos Basin, late Maastrichtian, pg. 75.
- 4 – *Hormosina velascoensis* Cushman (1926) #1146,85 m – SEAL-01, Sergipe-Alagoas Basin, middle Paleocene, pg. 75.
- 5 – *Cribrostomoides subglobosus* Cushman (1910) # 3420, 00 m – SEAL-02, Sergipe-Alagoas Basin, late Maastrichtian, pg. 75.
- 6 – *Cribrostomoides trinitatis* Cushman & Jarvis (1928) #3300,00 m – SEAL-02, Sergipe-Alagoas Basin, late Maastrichtian, pg. 75.
- 7a,b – *Budashevaella multicamerata* Voloshinova (1961) #1251,00 m – SEAL-01, Sergipe-Alagoas Basin, middle Paleocene, pg. 80.

PLATE II

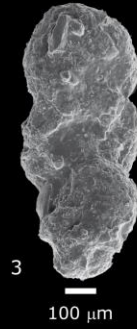
Rzehakina epigona



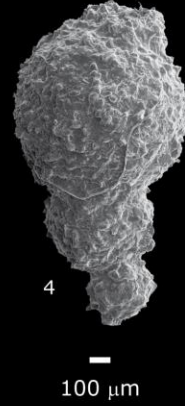
Rzehakina inclusa



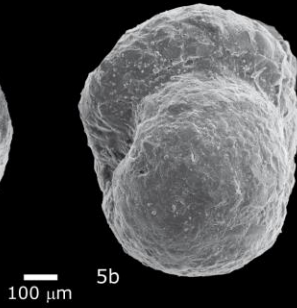
Subreophax scalaris



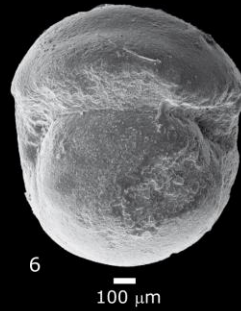
Hormosina velascoensis



Cribrostomoides subglobosus



Cribrostomoides trinitatis



Budahsevaella multicamerata

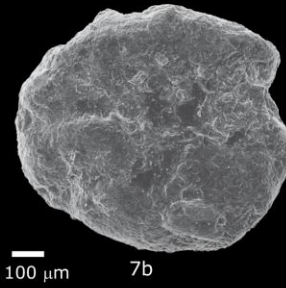
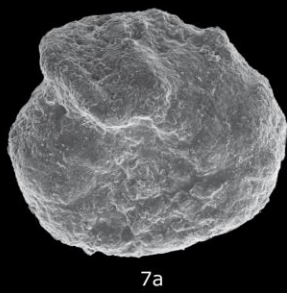


PLATE III

1a,b – *Haplophragmoides eggeri* Cushman (1926) #2834,01 m – SAN-01, Santos Basin, late Maastrichtian, pg. 77.

2 – *Haplophragmoides horridus* Grzybowski (1901) #3420,00 m – PEL-01, Pelotas Basin, late Paleocene, pg. 77.

3a,b – *Haplophragmoides porrectus* Maslakova (1955) #3420,00 m - PEL-01, Pelotas Basin, late Paleocene, pg. 77.

4a,b – *Haplophragmoides stomatus* Grzybowski (1898) emend Kaminski & Geroch (1993) #3300,00 m – SEAL-02, Sergipe-Alagoas Basin, late Maastrichtian, pg. 78.

5 – *Haplophragmoides suborbicularis* Grzybowski (1896) emend Kaminski & Geroch (1993) #2832,25 m – SAN-01, Santos Basin, late Maastrichtian, pg. 78.

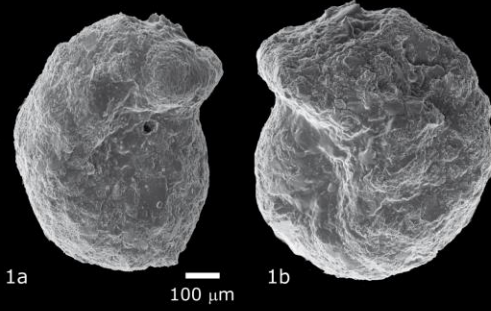
6 – *Haplophragmoides walteri* Grzybowski (1898) # 3420,00 m – PEL-01, Pelotas Basin, late Paleocene, pg. 79.

7 – *Recurvoides anormis* Mjatluk (1970) #1140,10 m – SEAL-01, Sergipe-Alagoas Basin, late Paleocene, pg. 80.

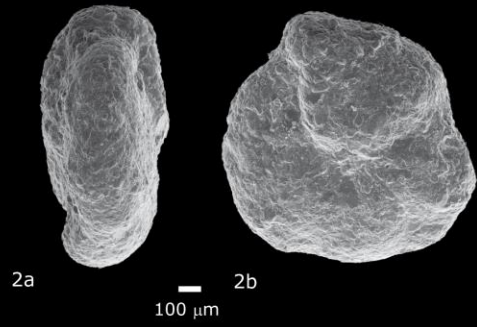
8a,b – *Recurvoides azuaensis* Bermudez (1949) #2811,00 m – CAM-03, Campos Basin, late Eocene, pg. 80.

PLATE III

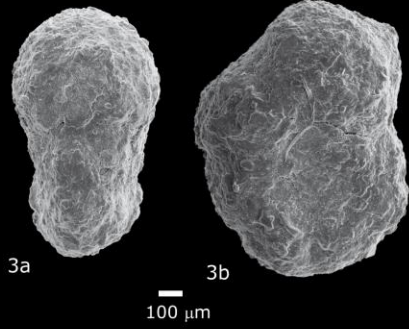
Haplophragmoides eggeri



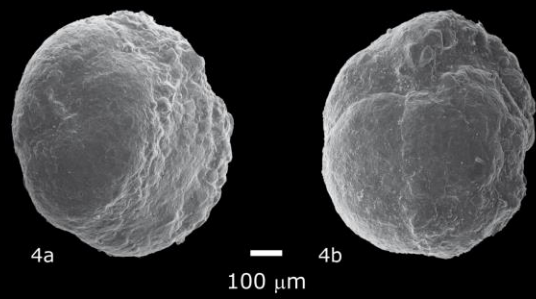
Haplophragmoides horridus



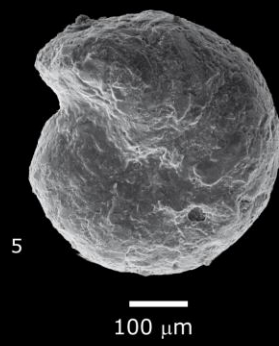
Haplophragmoides porrectus



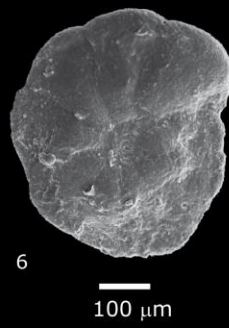
Haplophragmoides stomatus



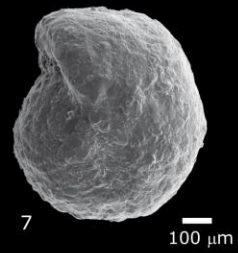
Haplophragmoides suborbicularis



Haplophragmoides walteri



Recurvoides anormis



Recurvoides azuaensis

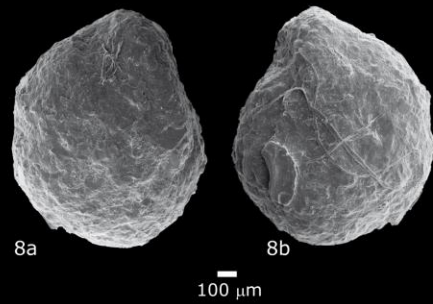


PLATE IV

1a,b – *Reticulophragmium acutidorsatum* Hantken (1868) #2802,00 m – PEL-01, Pelotas Basin, middle Eocene, pg. 82.

2 – *Reticulophragmium amplexans* Grzybowski (1898) #2850,00 m - PEL-01, Pelotas Basin, middle Eocene, pg. 83.

3a,b – *Reticulophragmium garcilassoi* Frizzell (1943) #1251,00 m – SEAL-01, Sergipe-Alagoas Basin, middle Paleocene, pg. 83.

4a,b – *Reticulophragmium rotundidorsatum* Hantken (1875) #1140,50m – SEAL-01, Sergipe-Alagoas Basin, late Paleocene, pg. 84.

5 – *Reticulophragmoides jarvisi* Thalmann (1932) #1140,10 m – SEAL-01, Sergipe-Alagoas Basin, late Paleocene, pg. 84.

6a,b – *Cyclammia placenta* Reuss (1851) #1080,00 m – SEAL-02, Sergipe-Alagoas Basin, early Eocene, pg. 85.

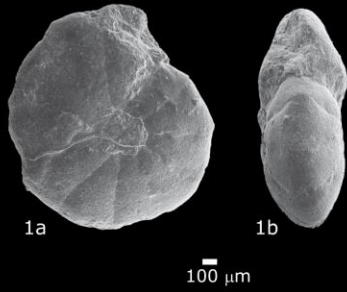
7a,b – *Spiroplectamina jarvisi* Cushman (1939) #2597,15 m – SAN-01, Santos Basin, late Paleocene, pg. 86.

8 – *Spiroplectamina navarroana* Cushman (1932) emend Gradstein & Kaminski (1989) #1141,50 m – SEAL-01, Sergipe-Alagoas Basin, late Paleocene, pg. 86.

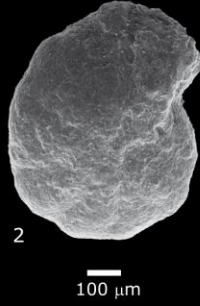
9a,b – *Ammoglobigerina globigeriniformis* Parker & Jones (1865) #2883,90 m – CAM-04, Campos Basin, middle Eocene, pg. 87.

PLATE IV

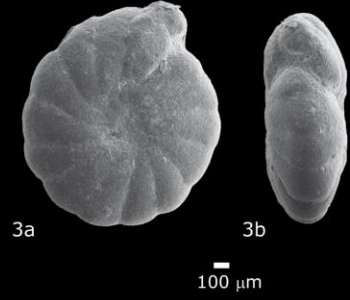
Reticulophragmium acutidorsatum



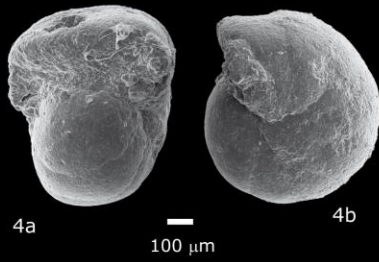
Reticulophragmium amplexens



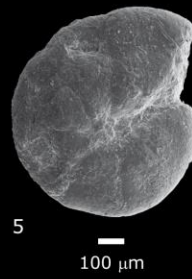
Reticulophragmium garcilasso



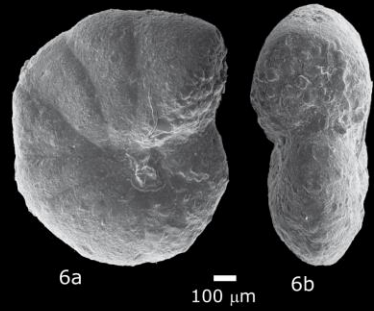
Reticulophragmium rotundidorsatum



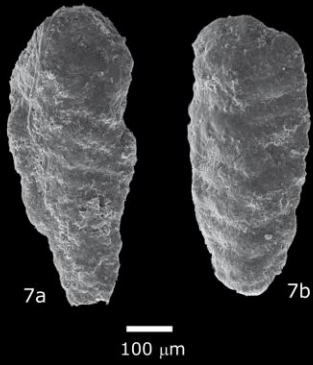
Reticulophragmoides jarvisi



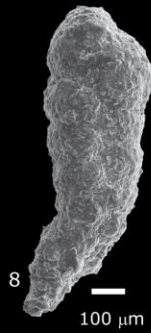
Cyclamina placenta



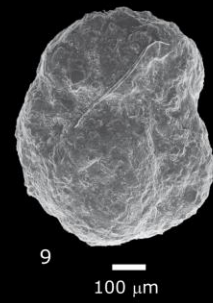
Spiroplectammina jarvisi



Spiroplectammina navarroana



Trochamminopsis altiformis



Ammoglobigerina globigeriniformis

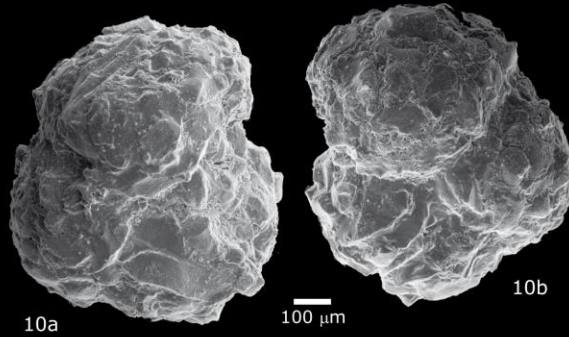
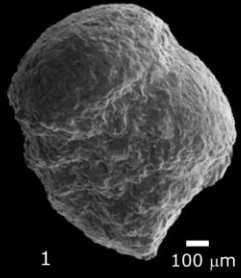


PLATE V

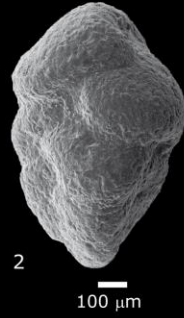
- 1 – *Gaudryina expansa* Israelsky (1951) #3420,00 m – SEAL-02, Sergipe-Alagoas Basin, late Maastrichtian, pg. 89.
- 2 – *Gaudryina frankei* Brotzen (1936) #3300,00 m – SEAL-02, Sergipe-Alagoas Basin, late Maastrichtian, pg. 89.
- 3 – *Gaudryina inflata* Israelsky (1951) #3420,00 m – SEAL-02, Sergipe-Alagoas Basin, late Maastrichtian, pg. 89.
- 4 – *Gaudryina ingens* Voloshinova (1972) #2832,25 m – SAN-01, Santos Basin, late Maastrichtian, pg. 90.
- 5 – *Gaudryina laevigata* Franke (1914) #3300,00 m – SEAL-02, Sergipe-Alagoas Basin, late Maastrichtian, pg. 90.
- 6 – *Gaudryina pyramidata* Cushman (1926) #3300,00 m – PEL-01, Pelotas Basin, late Maastrichtian, pg. 91.
- 7 – *Marssonella trochoides* Marsson (1878) #3960,00 m – PEL-01, Pelotas Basin, late Paleocene, pg. 91.
- 8 – *Karriella cubensis* Cushman & Bermudez (1937) #57,85 m – Site 20C, middle Eocene, pg. 92.
- 9 – *Pseudoclavulina chitinosa* Cushman & Jarvis (1932) #3690,00 m – PEL-01, Pelotas Basin, late Paleocene, pg. 93.
- 10 – *Clavulinoides trilaterus* Cushman (1926) #1141,78 m – SEAL-01, Sergipe-Alagoas Basin, middle Paleocene, pg. 93.
- 11 – *Karriella subglabra* Gumbel (1868) #115,20 m – Site 356, early Eocene, pg. 92.

PLATE V

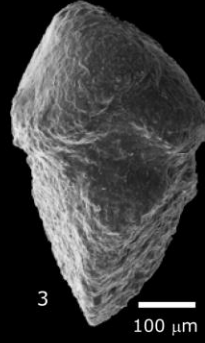
Gaudryina expansa



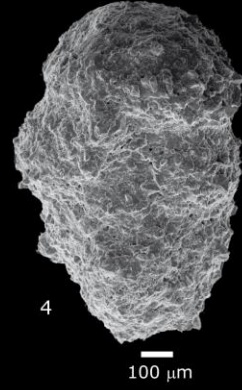
Gaudryina frankei



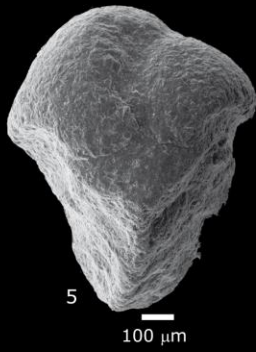
Gaudryina inflata



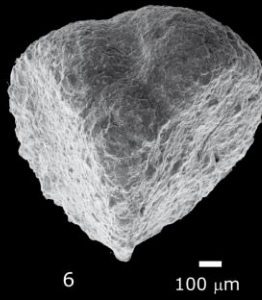
Gaudryina ingens



Gaudryina laevigata



Gaudryina pyramidata



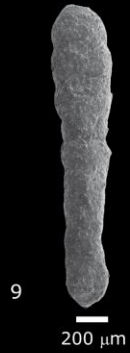
Marssonella trochoides



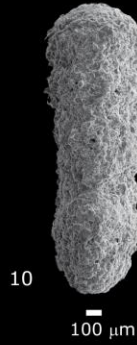
Karriella cubensis



Pseudoclavulina chitinsa



Clavulinoides trilaterus



Karriella subglabra

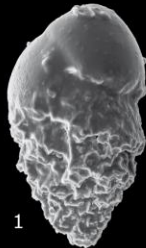


PLATE VI

- 1 – *Bolivina huneri* Howe (1939) #37,75 m – Site 20C, middle Eocene, pg. 94.
- 2 – *Tappanina selmensis* Cushman (1933) #65,00 m – Site 20C, early Eocene, pg. 94.
- 3 – *Aragonia aragonensis* Nuttall (1930) #42,25 m – Site 20C, middle Eocene, pg. 95.
- 4 – *Aragonia velascoensis* Cushman (1925) #69,45 m – Site 20C, late Paleocene, pg. 95.
- 5 – *Globocassidulina subglobosa* Brady (1881) #37,75 m – Site 20C, middle Eocene, pg. 96.
- 6 – *Bulimina alazanensis* Cushman (1927) #2400,00 m – PEL-01, Pelotas Basin, middle Eocene, pg. 96.
- 7 – *Bulimina jarvisi* Cushman & Parker (1936) #57,85 m – Site 20C, middle Eocene, pg. 97.
- 8 – *Praebulimina navarroensis* Cushman & Parker (1935) #2539,00 m – PEL-01, Pelotas Basin, middle Eocene, pg. 96.
- 9 – *Bulimina trinitatensis* Cushman & Jarvis (1928) #69,45 m – Site 20C, late Paleocene, pg. 98.
- 10 – *Buliminella grata* Parker & Bermudez (1937) #42,25 m – Site 20C, middle Eocene, pg. 99.
- 11 – *Quadratobuliminella pyramidalis* de Klasz (1953) #135,50 m – Site 356, Paleocene, pg. 99.
- 12 – *Siphonodosaria jacksonensis* Cushman & Applin (1926) #37,75 m – Site 20C, middle Eocene, pg. 100.
- 13 – *Siphonodosaria scripta* d'Orbigny (1846) #37,75 m – Site 20C, middle Eocene, pg. 100.

PLATE VI

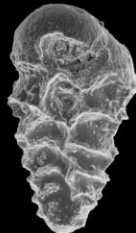
Bolivina huneri



1

20 μm

Tappania selmensis



2

20 μm

Aragonia aragonensis



3

20 μm

Aragonia velascoensis



4

20 μm

Globocassidulina subglobosa



5

20 μm

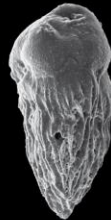
Bulimina alazanensis



6

100 μm

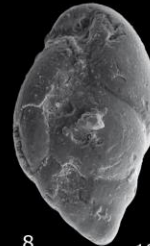
Bulimina jarvisi



7

30 μm

Praebulimina navarroensis



8

100 μm

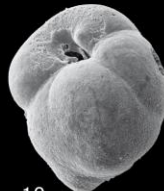
Bulimina trinitatis



9

20 μm

Buliminella grata



10

20 μm

Quadratobuliminella pyramidalis



11

20 μm

Siphonodosaria jacksonensis



12

100 μm

Siphonodosaria scripta



13

100 μm

PLATE VII

1a,b,c – 2a,b, b – *Neoeponides byramensis* Cushman (1922) 1a,b,c - #2400,00 m – PEL-01, Pelotas Basin, late Eocene, 2a,b,c - #2539,00 m – PEL-01, Pelotas Basin, middle Eocene, pg. 101.

3a,b,c – *Neoeponides campester* Palmer & Bermudez (1941) #2820,00 m – PEL-01, Pelotas Basin, middle Eocene, pg. 101.

4 a,b,c – *Neoeponides elevatus* Plummer (1926) #2400,00 m – PEL-01, Pelotas Basin, late Eocene, pg. 102.

5 a,b,c – *Neoeponides hillebrandti* Fisher (1962) #3096 m – PEL-01, Pelotas Basin, late Paleocene, pg. 103.

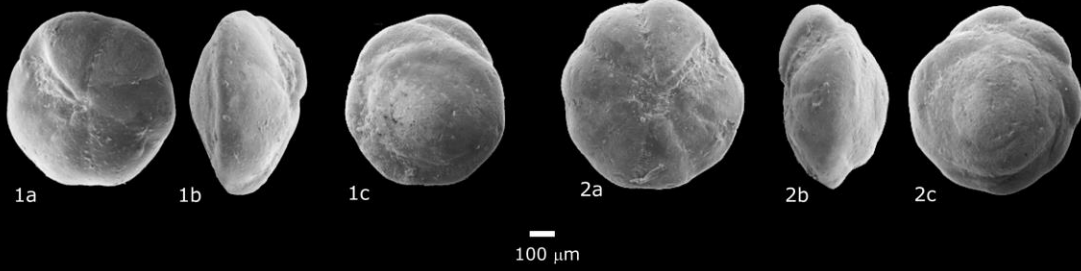
6 – *Sphaeroidina bulloides* d'Orbigny (1826) #2340 m – PEL-01, Pelotas Basin, late Eocene, pg. 103.

7 a,b,c – *Planulina costata* Hantken (1875) #2542,86 m – PEL-01, Pelotas Basin, middle Eocene, pg. 109.

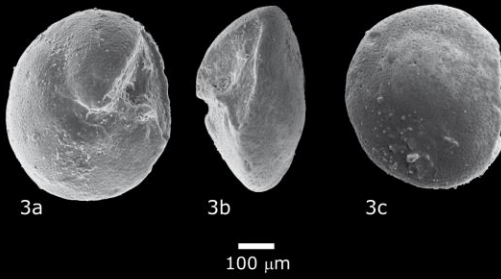
8a,b – *Nonion havanense* Cushman & Bermudez (1937) #67,45 m – Site 20C, late Paleocene, pg. 111.

PLATE VII

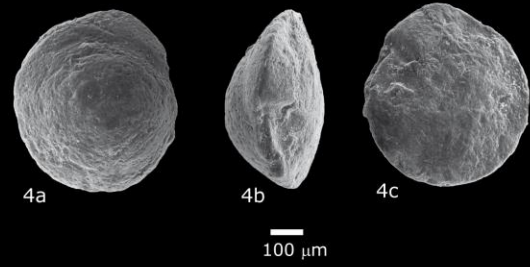
Neoeponides byramensis



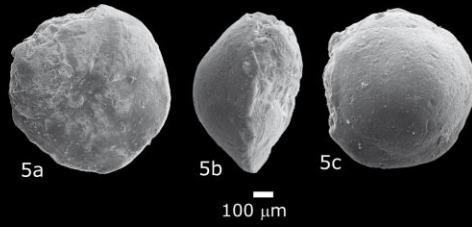
Neoeponides campester



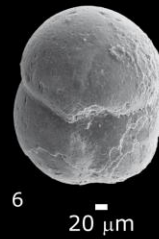
Neoeponides elevatus



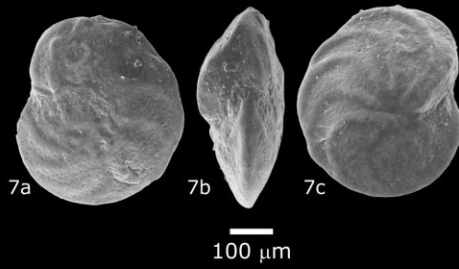
Neoeponides hillebrandti



Sphaeroidina bulloides



Planulina costata



Nonion havanense



PLATE VIII

- 1a,b,c – *Cibicidoides dayi* White (1928) #361,70 m – Site 356, late Paleocene, pg. 104.
- 2a,b,c – *Cibicidoides grimsdalei* Nuttall (1930) #47,70 m – Site 20C, middle Eocene, pg. 105.
- 3a,b,c – 4a,b,c – *Cibicidoides eocaenus* Gümbel (1868) 3a,b,c - #2910 m – PEL-01, Pelotas Basin, early Eocene, 4a,b,c - #2878,55 m – CAM-04, Campos Basin, middle Eocene, pg. 104.
- 5a,b,c – *Cibicidoides havanensis* Cushman & Bermudez (1937) #47,70 m – Site 20C, middle Eocene, pg. 106.
- 6a,b,c – *Cibicidoides micrus* Bermudez (1949) #2802 m – CAM-03, Campos Basin, late Eocene, pg. 107.
- 7a,b,c – *Cibicidoides praemundulus* Berggren & Miller (1986) #39,72 m – Site 20C, middle Eocene, pg. 107.
- 8a,b,c – *Cibicidoides subspiratus* Nuttall (1930) #224,30 m – Site 20C, early Eocene, pg. 108.

PLATE VIII

Cibicoides dayi



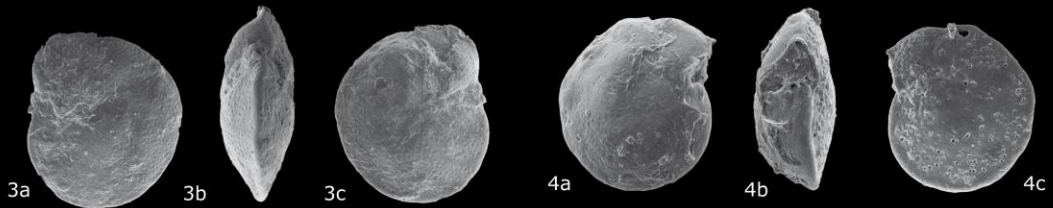
100 μ m

Cibicoides grimsdalei



100 μ m

Cibicoides eoacaenus



100 μ m

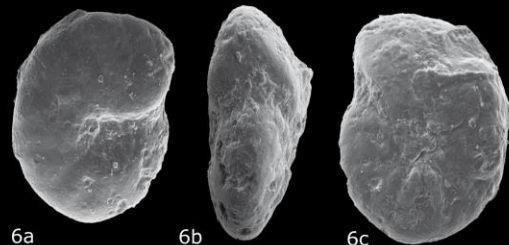
100 μ m

Cibicoides havanensis



100 μ m

Cibicoides micrus



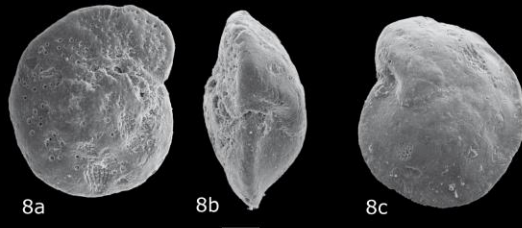
100 μ m

Cibicoides preamundulus



100 μ m

Cibicoides subspiratus



100 μ m

PLATE IX

1a,b,c – *Cibicidoides velascoensis* Cushman (1925) #366 m – Site 356, late Paleocene, pg. 108.

2a,b,c – *Nuttallinella florealis* White (1928) #1112,52 m – BAS-01, Mucuri Basin, early Paleocene, pg. 110.

3a,b,c – 4a,b,c – *Nuttallides truempyi* Nuttall (1930) 3a,b,c - #2964 m – PEL-01, Pelotas Basin, early Eocene, #40,75 m – Site 20C, middle Eocene, pg. 109.

5a,b,c – *Nuttallinella sp. 1* #2601 m - PEL-01, Pelotas Basin, middle Eocene, pg. 111.

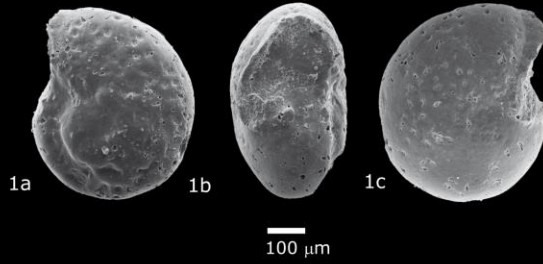
6a,b,c – *Pullenia coryelli* White (1929) #2682 m – SAN-01, Santos Basin, late Maastrichtian, pg. 112.

7a,b – *Pullenia eocenica* Cushman & Siegfus (1939) #47,70 m – Site 20C, middle Eocene, pg. 113.

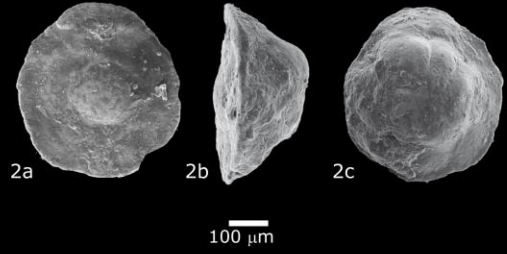
8a,b – *Pullenia jarvisi* Cushman (1936) #2808 m – PEL-01, Pelotas Basin, middle Eocene, pg. 114.

PLATE IX

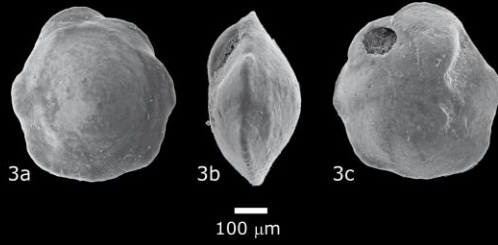
Cibicoides velascoensis



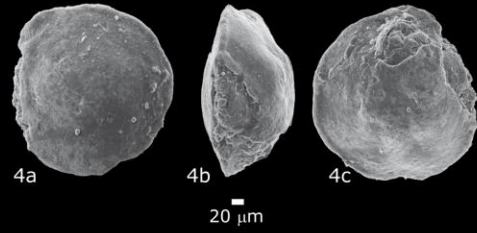
Nuttallinella florealis



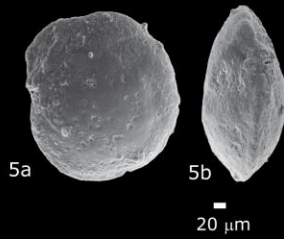
Nuttallides truempyi - type 1



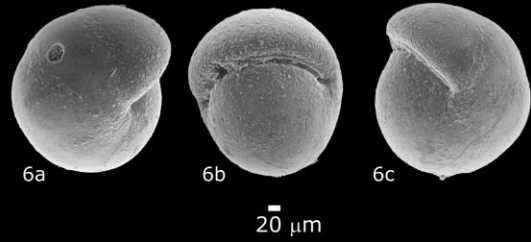
Nuttallides truempyi - type 2



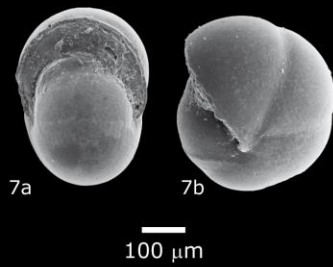
Nuttallinella sp.1



Pullenia coryelli



Pullenia eocenica



Pullenia jarvisi

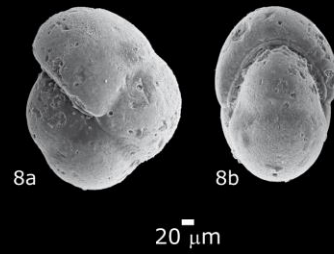


PLATE X

1a,b,c – *Melonis* sp. 1 #474 m – SEAL-01, Sergipe-Alagoas Basin, late Eocene, pg. 112.

2a,b – *Abyssamina quadrata* Schnitker & Tjalsma (1980) #59,35 m – Site 20C, early Eocene, pg. 114.

3a,b – *Alabamina dissonata* Cushman & Renz (1948) #64,10 m – Site 20C, early Eocene, pg. 115.

4a,b – *Alabamina midwayensis* Brotzen (1948) #42,25 m – Site 20C, middle Eocene, pg. 115.

5a,b – *Osangularia mexicana* Cole (1927) #224,30 m – Site 356, early Eocene, pg. 116.

6a,b,c – *Osangularia plummerae* Brotzen (1948) #3058,40 m – PEL-01, Pelotas Basin, early Eocene, pg. 116.

7 – *Osangularia velascoensis* Cushman (1925) #72,45 m – Site 20C, late Paleocene, pg. 117.

8a,b,c – *Oridorsalis umbonatus* Reuss (1851) #219,80 m – Site 356, early Eocene, pg. 117.

PLATE X

Melonis sp.1



100 μm

Abyssamina quadrata



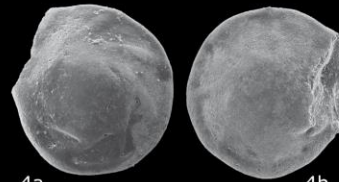
20 μm

Alabamina dissonata



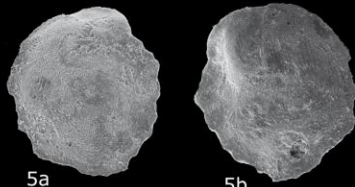
100 μm

Alabamina midwayensis



100 μm

Osangularia mexicana



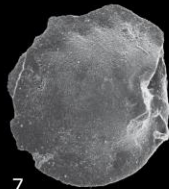
100 μm

Osangularia plummerae



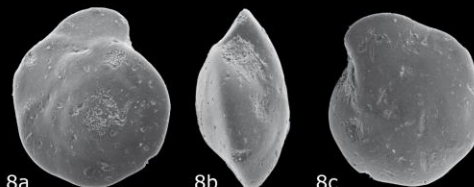
100 μm

Osangularia velascoensis



100 μm

Oridorsalis umbonatus



100 μm

PLATE XI

1a,b – *Anomalinoides capitatus* Gümbel (1868) #2598,85 m – SAN-01, Santos Basin, late Paleocene, pg. 118.

2a,b,c – *Anomalinoides garzaensis* Cushman & Siegfus (1939) #2400 m – PEL-01, Pelotas Basin, late Eocene, pg. 119.

3a,b,c – *Anomalinoides praecuta* Vasilenko (1950) #64,10 m – Site 20C, early Eocene, pg. 120.

4a,b – *Anomalinoides welleri* Plummer (1926) #57,85 m – Site 20C, middle Eocene, pg. 120.

5a,b,c – *Stensioeina beccariiformis* White (1928) #1602 m – BA-01, Mucuri Basin, late Maastrichtian, pg. 124.

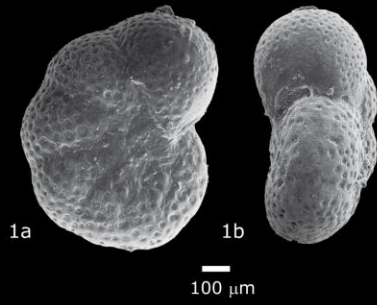
6a,b,c – *Paralabamina lunata* Brotzen (1948) #474 m – SEAL-01, Sergipe-Alagoas Basin, late Eocene, pg. 126.

7a,b,c – *Hanzawaia ammophila* Gümbel (1868) #57,85 m – Site 20C, middle Eocene, pg. 125.

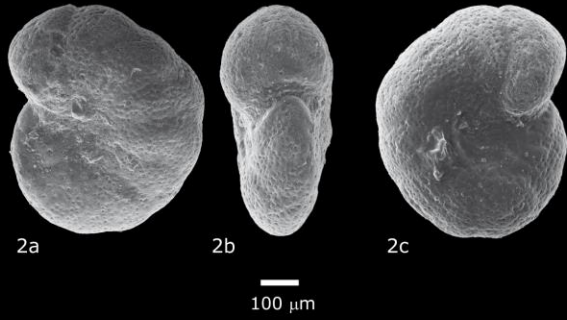
8a,b,c – *Hanzawaia mantaensis* Galloway & Morrey (1929) #2928 m – PEL-01, Pelotas Basin, early Eocene, pg. 126.

PLATE XI

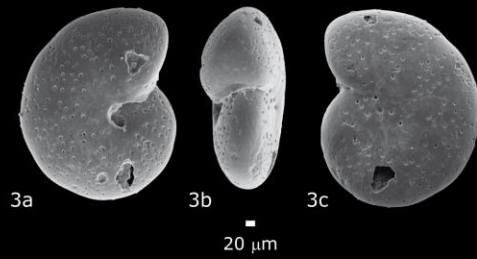
Anomalinoides capitatus



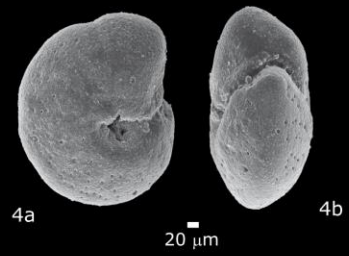
Anomalinoides garzaensis



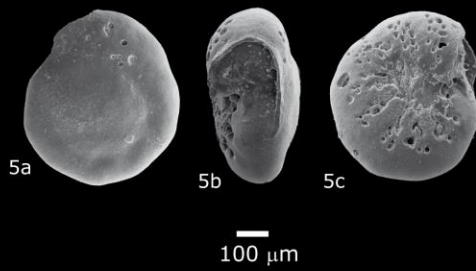
Anomalinoides praecuta



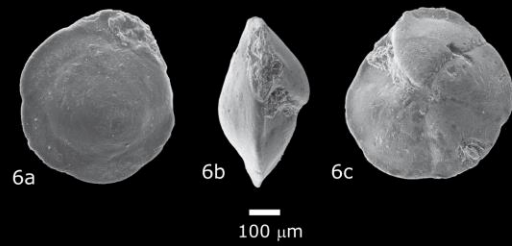
Anomalinoides welleri



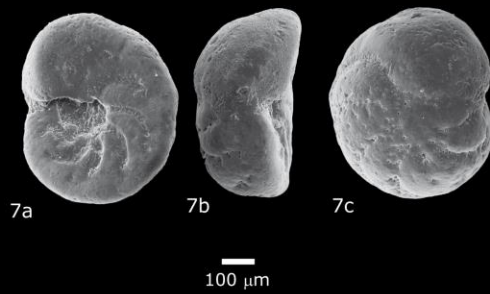
Stensioeina beccariiformis



Paralabamina lunata



Hanzawaia ammophila



Hanzawaia mantaensis

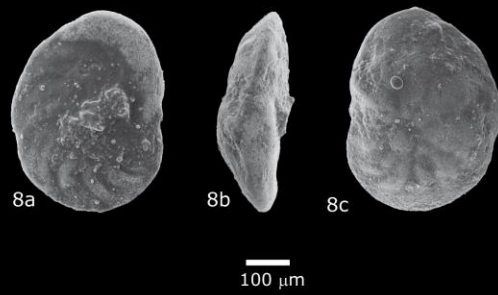


PLATE XII

1a,b,c – *Gyroidinoides beisseli* White (1928) emend Alegret & Thomas (2001) #3096 m – PEL-01, Pelotas Basin, late Paleocene, pg. 121.

2 – *Gyroidinoides depressus* Alth (1850) #59,35 m – Site 20C, early Eocene, pg. 121.

3a,b,c – *Gyroidinoides girardanus* Reuss (1851) #2340 m – PEL-01, Pelotas Basin, late Eocene, pg. 122.

4a,b – *Gyroidinoides globosus* Hagenow (1842) emend Alegret & Thomas (2001) #2682 m – SAN-01, Santos Basin, late Paleocene, pg. 122.

5a,b,c – *Gyroidinoides quadratus* Cushman & Church (1929) #2664 m – SAN-01, Santos Basin, late Paleocene, pg. 123.

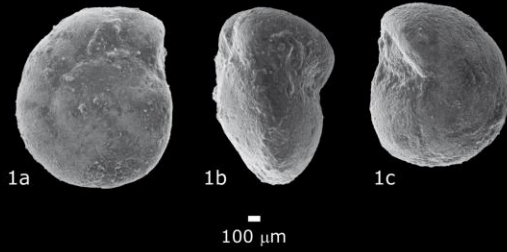
6a,b,c – *Gyroidinoides subangulatus* Plummer (1926) #2340 m – PEL-01, Pelotas Basin, late Eocene, pg. 123.

7 – *Lenticulina whitei* Tjalsma & Lohmann (1983) #2598,05 m – SAN-01, Santos Basin, late Paleocene, pg. 127.

8 – *Neoflabelina semireticulata* Cushman & Jarvis (1928) #2597,65 m – SAN-01, Santos Basin, late Paleocene, pg. 127.

PLATE XII

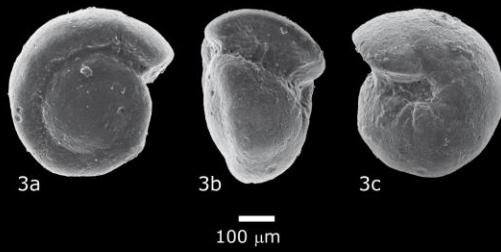
Gyroidinoides beisseli



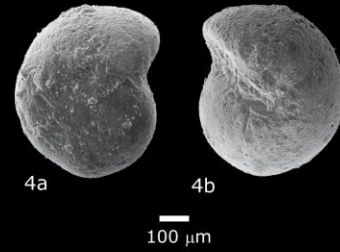
Gyroidinoides depressus



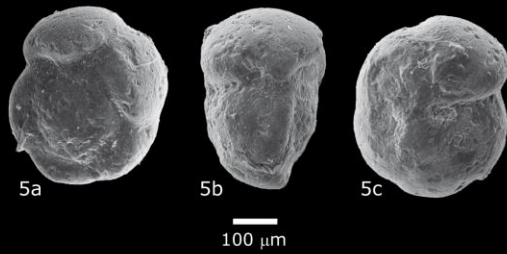
Gyroidinoides girardanus



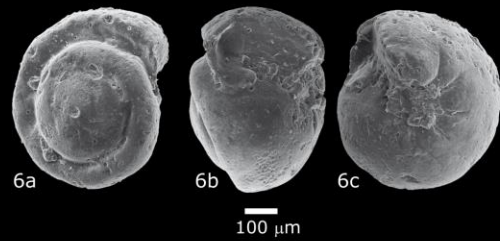
Gyroidinoides globosus



Gyroidinoides quadratus



Gyroidinoides subangulatus



Lenticulina whitei



Neoflabellina semireticulata



APPENDIX III

ABSOLUTE PERCENTAGE OF THE BENTHIC FORAMINIFERA

Well – CAM-01

Depth (m)	Age (Ma)	<i>Anomalinoidea sp.</i>	<i>Anomalinoidea garzaensis</i>	<i>Bulimina sp.</i>	<i>Cibicides sp.</i>	<i>Cibicides dayi</i>	<i>Cibicides velascoensis</i>	<i>Cibicideshyphalus</i>	<i>Fissurina sp.</i>	<i>Globocassidulina sp.</i>	<i>Gyrogonoides sp.</i>	<i>Hemiorbulina sp.</i>	<i>Lagena tenuistriata</i>	<i>Lenticulina sp.</i>	<i>Nuttalides truempyi</i>	<i>Pullenia sp.</i>	<i>Quadriformina sp.</i>	<i>Reusoolina sp.</i>	<i>Stensioeina beccariformis</i>	<i>Sphaeroidina sp.</i>	<i>Ammodiscus glabratus</i>	<i>Ammosphaeroidina pseudopauciloculata</i>	<i>Bathysiphon sp.</i>	<i>Budashavella multicamerata</i>	<i>Caudamina ovula</i>	<i>Cribrostomoides trinitatensis</i>	<i>Gaudryina sp.</i>	<i>Glomospira charoides</i>	<i>Glomospira serpens</i>	<i>Recurvoides walteri</i>	<i>Rzehakina epigona</i>	<i>Textularia sp.</i>
3051.00	66.12	3.51	1.75	0.00	8.77	7.02	8.77	1.75	1.75	3.51	7.02	3.51	1.75	12.28	14.04	0.00	0.00	0.00	3.51	0.00	3.51	0.00	5.26	1.75	1.75	1.75	1.75	0.00	0.00	3.51	1.75	0.00
3090.00	68.81	4.08	2.04	0.00	8.16	6.12	4.08	4.08	2.04	6.12	10.20	2.04	2.04	10.20	14.29	0.00	0.00	0.00	4.08	0.00	2.04	0.00	8.16	0.00	0.00	4.08	0.00	0.00	2.04	2.04	2.04	0.00
3102.00	69.64	2.08	0.00	4.17	16.67	0.00	12.50	8.33	0.00	0.00	6.25	0.00	0.00	0.00	4.17	0.00	4.17	4.17	6.25	0.00	4.17	0.00	2.08	0.00	2.08	0.00	2.08	6.25	6.25	4.17	4.17	0.00
3138.00	74.80	1.96	0.00	5.88	23.53	0.00	7.84	7.84	0.00	0.00	5.88	0.00	0.00	0.00	5.88	1.96	1.96	1.96	7.84	1.96	0.00	3.92	0.00	0.00	0.00	0.00	1.96	7.84	3.92	5.88	0.00	1.96

Well CAM-02

Depth (m)	Age (Ma)	<i>Cibicides sp.</i>	<i>Lenticulina sp.</i>	<i>Ammodiscus sp.</i>	<i>Bathysiphon sp.</i>	<i>Cribrostomoides subglobosus</i>	<i>Glomospira sp.</i>	<i>Glomospira serpens</i>	<i>Haplophragmoides sp.</i>	<i>Karrerulina conversa</i>	<i>Karrerulina conversa</i>	<i>Recurvoides sp.</i>	<i>Rhizammina sp.</i>	<i>Trochamminoides sp.</i>	<i>Subreophax sp.</i>
3055.00	33.21	0.00	0.00	0.00	0.00	0.00	0.00	0.00	0.00	0.00	0.00	0.00	0.00	0.00	0.00
3098.00	36.00	0.00	0.00	0.00	0.00	0.00	0.00	0.00	0.00	0.00	0.00	0.00	0.00	0.00	0.00
3115.00	50.47	6.67	0.00	0.00	60.00	0.00	0.00	0.00	26.67	0.00	0.00	0.00	0.00	0.00	0.00
3145.00	58.26	0.00	8.33	8.33	41.67	0.00	0.00	8.33	0.00	0.00	0.00	16.67	0.00	0.00	8.33
3165.00	59.78	0.00	0.00	0.00	33.00	15.38	0.00	0.00	0.00	0.00	0.00	30.77	15.38	0.00	0.00
3210.00	65.50	0.00	0.00	5.26	15.79	5.26	10.53	5.26	10.53	5.26	5.26	5.26	21.05	15.79	0.00

Table with 33 columns and 2000+ rows. Columns include Depth (m), MWD, and various MWD parameters (M1-M32). Each row contains numerical data for these parameters, representing well log data.

BIBLIOGRAPHY

- Alegret L., Molina E., and Thomas E. 2001. **Benthic foraminifera at the Cretaceous/Tertiary boundary around the Gulf of Mexico.** *Geology*, 29 (10): 891-894.
- Alegret, L. and Ortiz, S. 2006. **Global extinction event in benthic foraminifera across the Paleocene/Eocene boundary at the Dababiya Stratotype section.** *Micropaleontology*, v.52 (5): 433-447.
- Alegret, L. and Thomas, E. 2007. **Deep-sea environments across the Cretaceous/Paleogene boundary in the eastern South Atlantic Ocean (ODP Leg 208, Walvis Ridge).** *Marine Micropaleontology*, 64:1-17.
- Alegret, L., and Thomas, E. 2005. **Cretaceous/Paleogene boundary bathyal paleo-environments in the central North Pacific (DSDP Site 465), the Northwestern Atlantic (ODP Site 1049), the Gulf of Mexico and the Tethys: The benthic foraminiferal record.** *Palaeogeography, Palaeoclimatology, Palaeoecology*, 224(1), 53-82.
- Alegret, L., and Thomas, E. 2005. **Cretaceous/Paleogene boundary bathyal paleo-environments in the central North Pacific (DSDP Site 465), the Northwestern Atlantic (ODP Site 1049), the Gulf of Mexico and the Tethys: The benthic foraminiferal record.** *Palaeogeography, Palaeoclimatology, Palaeoecology*, 224(1), 53-82.
- Alegret, L., and Thomas, E. 2013. **Benthic foraminifera across the Cretaceous/Paleogene boundary in the Southern Ocean (ODP Site 690): Diversity, food and carbonate saturation.** *Marine Micropaleontology*, 105, 40-51.
- Alegret, L., Ortiz, S., and Molina, E. 2009. **Extinction and recovery of benthic foraminifera across the Paleocene–Eocene Thermal Maximum at the Alamedilla section (Southern Spain).** *Palaeogeography, Palaeoclimatology, Palaeoecology*, 279(3), 186-200.
- Almeida, F. F. M., and Carneiro, C. D. R. 1998. **Origem e evolução da Serra do Mar.** *Brazilian Journal of Geology*, 28(2), 135-150.
- Anderson, J.B. 1975. **Ecology and Distribution of Foraminifera in the Weddell Sea of Antarctica.** *Micropaleontology*, 21 (1): 69-96.
- Anderson, L. D., and Delaney, M. L. 2005. **Use of multiproxy records on the Agulhas Ridge, Southern Ocean (Ocean Drilling Project Leg 177, Site 1090) to investigate sub-Antarctic hydrography from the Oligocene to the early Miocene.** *Paleoceanography*, 20(3).
- Asmus, H.E. and Baisch, P.R. 1983. **Geological Evolution of the Brazilian Continental Margin.** *Episodes*, 4:3-9.
- Asmus, H.E. and Ponte, F.C. 1973. **The Brazilian marginal basins.** In: Nairn, A.E.M. and Stehli, F.G. (eds.). *The Ocean Basins and Margins*, v.1, The South Atlantic, p. 87-133, New York, Plenum Press.
- Bandy, O. L. 1953. **Ecology and paleoecology of some California foraminifera. Part I. The frequency distribution of recent foraminifera off California.** *Journal of Paleontology*, 161-182.
- Bandy, O. L. 1956. **Ecology of foraminifera in northeastern Gulf of Mexico.** *US Geol. Surv., Prof. Pap*, 274, 179-204.
- Bandy, O. L., and Arnal, R. E. 1960. **Concepts of foraminiferal paleoecology.** *AAPG bulletin* 44.12: 1921-1932.
- Bandy, O. L., and Chierici, M. A. 1966. **Depth-temperature evaluation of selected California and Mediterranean bathyal foraminifera.** *Marine Geology* 4 (4): 259-271.
- Becker, M.R., Rodrigues, E.B., Viviers, M.C., Rodrigues, R., Antunes, R.L. and Andrade, S.B. 2000. **Sedimentologia e Estratigrafia dos Reservatórios Paleocenos e Eocenos em Águas Profundas do Sul da Bacia de Campos.** *Relatório Interno*, CENPES, PETROBRAS.
- Berger, W. H. 1967. **Foraminiferal ooze: solution at depths.** *Science*, 156(3773), 383-385.
- Berger, W. H. 1970a. **Planktonic foraminifera: selective solution and the lysocline.** *Marine Geology*, 8(2), 111-138.
- Berger, W. H. 1970b. **Biogenous deep-sea sediments: fractionation by deep-sea circulation.** *Geological Society of America Bulletin*, 81(5), 1385-1402.
- Berger, W. H. 1973. **Deep-sea carbonates, Pleistocene dissolution cycles.** *The Journal of Foraminiferal Research*, 3(4), 187-195.
- Berger, W. H., and Soutar, A. 1970. **Preservation of plankton shells in an anaerobic basin off California.** *Geological Society of America Bulletin*, 81(1), 275-282.
- Berger, W. H., Bonneau, M. C., and Parker, F. L. 1982. **Foraminifera on the deep-sea floor-lysocline and dissolution rate.** *Oceanologica Acta*, 5(2), 249-258.
- Berggren, W. A. 1972. **A Cenozoic time-scale—some implications for regional geology and paleobiogeography.** *Lethaia* 5(2): 195-215.
- Berggren, W. A., and Miller, K. G. 1989. **Cenozoic bathyal and abyssal calcareous benthic foraminiferal zonation.** *Micropaleontology*, 308-320.

- Berggren, W.A., Aubert, J. 1975. **Paleocene benthonic foraminiferal biostratigraphy, paleobiogeography and paleoecology of Atlantic-Tethyan regions: Midway-type fauna.** *Paleogeography, Paleoclimatology, Paleoecology*, 18:73-192.
- Bice, K. L., Scotese, C. R., Seidov, D., and Barron, E. J. 2000. **Quantifying the role of geographic change in Cenozoic ocean heat transport using uncoupled atmosphere and ocean models.** *Palaeogeography, Palaeoclimatology, Palaeoecology*, 161(3), 295-310.
- Boersma, A. 1977. **Eocene to early Miocene benthic foraminifera DSDP Leg 39, South Atlantic.** *DSDP Initial Reports* vol.3.
- Bohaty, S. M. and Zachos, J.C.. 2003. **A significant Southern Ocean warming event in the late middle Eocene.** *Geology*. v. 31, p. 1017-1020.
- Bolli, H. M., Beckmann, J. P., and Saunders, J. B. 1994. **Benthic foraminiferal biostratigraphy of the south Caribbean region,** Cambridge University Press, Cambridge, 1-408.
- Borrelli, C., Cramer, B. S., and Katz, M. E. 2014. **Bipolar Atlantic deepwater circulation in the middle-late Eocene: Effects of Southern Ocean gateway openings.** *Paleoceanography*, 29(4), 308-327.
- BouDagher-Fadel, M. K., Price, G. D., and Koutsoukos, E. A. 2010. **Foraminiferal biostratigraphy and paleoenvironments of the Oligocene-Miocene carbonate succession in Campos Basin, southeastern Brazil.** *Stratigraphy*, 7(4), 283-299.
- Brouwer, J. 1965. **Agglutinated Foraminiferal Faunas from some turbiditic sequences. I.** *KONINKLIJKE NEDERLANDSE AKADEMIE VAN WETESCHAPPEN-PROCEEDINGS SERIES B-PHYSICAL SCIENCES*, 68(5), 309.
- Bubik, M., Kaminski, M.A. (Eds.), *Proceedings of the Sixth International Workshop on Agglutinated Foraminifera: Grzybowski Foundation Special Publication*, 8, pp. 317–349.
- Buzas, M. A. 1979. Quantitative biofacies analysis. *Foraminiferal Ecology and Paleoecology*, SEPM Short Course no. 6, Houston, TX.
- Buzas, M. A., and Gibson, T. G. 1969. **Species diversity: benthonic foraminifera in western North Atlantic.** *Science*, 163(3862), 72-75.
- Cainelli, C. 1992. **Sequence stratigraphy, canyons, and gravity mass-flow deposits in the Piaçabuçu Formation, Sergipe-Alagoas basin, Brazil.** PhD dissertation, University of Texas, Austin.
- Cainelli, C., and Mohriak, W. U. 1999. **Some remarks on the evolution of sedimentary basins along the Eastern Brazilian continental margin.** *Episodes-Newsmagazine of the International Union of Geological Sciences*, 22(3), 206-216.
- Chen, C. T. A., Feely, R. A., and Gendron, J. F. 1988. **Lysocline, calcium carbonate compensation depth and calcareous sediments in the North Pacific Ocean.** *Pacific Science*, 42(3-4), 237-252.
- Cobbold, P. R., Meisling, K. E., and Mount, V. S. 2001. **Reactivation of an obliquely rifted margin, Campos and Santos basins, southeastern Brazil.** *AAPG bulletin*, 85(11), 1925-1944.
- Coffey, B. P., and Read, J. F. 2004. **Mixed carbonate–siliciclastic sequence stratigraphy of a Paleogene transition zone continental shelf, southeastern USA.** *Sedimentary Geology*, 166(1), 21-57.
- Cole, W.S. and Gillespie, R. 1930. **Some small foraminifera from the Meson formation of Mexico.** Harris Company.
- Corliss, B. H. 1985. **Microhabitats of benthic foraminifera within deep-sea sediments.** *Nature*, 23 : 435-438.
- Corliss, B. H. 1991. **Morphology and microhabitat preferences of benthic foraminifera from the northwest Atlantic Ocean.** *Marine Micropaleontology*, 17(3), 195-236.
- Corliss, B.H. and Honjo, S. 1981. **Dissolution of deep-sea benthonic foraminifera.** *Micropaleontology*, 27(4): 356-378.
- Costa, D.S. and Viviers, M.C. 2012. **Characterization of agglutinated benthic foraminifera biofacies in Upper Cretaceous sediments of the Brazilian equatorial margin.** In: Alegret, Ortiz and Kaminski (eds.), 2012. Ninth International Workshop on Agglutinated Foraminifera, Abstract Volume, Grzybowski Foundation.
- Covault, J. A., and Graham, S. A. 2010. **Submarine fans at all sea-level stands: tectono-morphologic and climatic controls on terrigenous sediment delivery to the deep sea.** *Geology*, 38(10), 939-942.
- Coxall, H. K., Wilson, P. A., Pälike, H., Lear, C. H., and Backman, J. 2005. **Rapid stepwise onset of Antarctic glaciation and deeper calcite compensation in the Pacific Ocean.** *Nature*, 433(7021), 53-57.
- Cramer, B. S., Toggweiler, J. R., Wright, J. D., Katz, M. E., and Miller, K. G. 2009. **Ocean overturning since the Late Cretaceous: Inferences from a new benthic foraminiferal isotope compilation.** *Paleoceanography*, 24(4).

- Cullen, J. L., and Curry, W. B. 1997. **Variations in planktonic foraminifer faunas and carbonate preservation at site 927: evidence for changing surface water conditions in the Western Tropical Atlantic Ocean during the middle Pleistocene.** In *Proceedings of the Ocean Drilling Program. Scientific results* (Vol. 154, pp. 207-228). Ocean Drilling Program.
- Culver, S. J. 1988. **New foraminiferal depth zonation of the northwestern Gulf of Mexico.** *Palaios*, 69-85.
- Cushman, J. A. 1927. **New and interesting foraminifera from Mexico and Texas.** *Contributions from the Cushman Laboratory for Foraminiferal Research*, 3(2): 111-117.
- Cushman, J.A. 1945. **A foraminiferal fauna from the Twiggs clay of Georgia,** *Contributions from the Cushman Laboratory for Foraminiferal Research*, 21: 1-11.
- d'Haenens, S., Bornemman, A., Röhl, U. and Speijer, R.P. 2010. **Detection and characterization of early Eocene hyperthermal using benthic foraminiferal associations and stable isotopes at DSDP Site 401, Bay of Biscay, North East Atlantic.** *Geophysical Research Abstracts*, vol.12.
- d'Haenens, S., Bornemman, A., Stassen, P., and Speijer, R.P. 2012. **Multiple early Eocene benthic foraminiferal assemblage and $\delta^{13}\text{C}$ fluctuations at DSDP Site 401 (Bay of Biscay – NE Atlantic).** *Marine Micropaleontology*, 88-89:15-35.
- Dailey, D. H. 1983. **Late Cretaceous and Paleocene benthic foraminifers from Deep-Sea Drilling Project Site 516, Rio Grande Rise, western South Atlantic.** *Initial Reports of the Deep Sea Drilling Project*, 72(DEC), 757-782.
- DeConto, R. M., Galeotti, S., Pagani, M., Tracy, D., Schaefer, K., Zhang, T., Pollard, D and Beerling, D. J. 2012. **Past extreme warming events linked to massive carbon release from thawing permafrost.** *Nature*, 484(7392), 87-91.
- DeConto, R. M., Pollard, D., Wilson, P. A., Pälike, H., Lear, C. H., and Pagani, M. 2008. **Thresholds for Cenozoic bipolar glaciation.** *Nature*, 455(7213), 652-656.
- Douglas, R. G., and Woodruff, F. 1981. *Deep sea benthic foraminifera.* Wiley-Interscience.
- Fillon, R. H. 2003. **Foraminiferal litho-biofacies of linked delta-fan deposystems in the northern Gulf of Mexico: Paleontologic and lithologic characteristics.** In *Shelf Margin Deltas and Linked Down Slope Petroleum Systems: Global Significance and Future Exploration Potential: SEPM Foundation, Gulf Coast Section, 23 rd Annual Bob F. Perkins Research Conference* (pp. 725-764).
- Fillon, R. H. 2009. **Linked micropaleontology and lithology of Cenozoic deep water sediments: Application of multiple overlapping foraminiferal lithobiofacies to cuttings based analysis of reservoir properties.** *Geological problem solving with microfossils: Society for Sedimentary Geology Special Publication*, 93, 323-336.
- Fillon, R. H., Lawless, P. N., and Waterman, A. S. 2005. **Paleocene-Eocene Deposystems and Evolution of the Gulf of Mexico Basin Petroleum System.** *Gulf Coast Association of Geological Societies Transactions*, 55: 195-222.
- Finlay, H.J. and Marwick, J. 1940. **The division of the Upper Cretaceous and Tertiary in New Zealand.** *Royal Society of New Zealand.*
- Fluegeman Jr, R. H., Berggren, W. A., and Briskin, M. 1990. **Paleocene benthonic foraminiferal biostratigraphy of the eastern Gulf Coastal Plain.** *Micropaleontology*, 56-64.
- Galloway, J.J. 1933. **A manual of Foraminifera:** Bloomington, Principia Press, 483 p.
- Gibson, T. G. 1989. **Planktonic benthonic foraminiferal ratios: modern patterns and Tertiary applicability.** *Marine Micropaleontology*, 15(1), 29-52.
- Gibson, T. G., and Buzas, M. A. 1973. **Species diversity: patterns in modern and Miocene foraminifera of the eastern margin of North America.** *Geological Society of America Bulletin*, 84(1), 217-238.
- Gooday, A. J. 1988. **A response by benthic foraminifera to the deposition of phytodetritus in the deep sea.** *Nature*, 332(6159), 70-73.
- Gooday, A.J. 1990. **Recent deep-sea agglutinated foraminifera: a brief review.** Hemleben, C. et al. (eds), *Paleoecology, Biostratigraphy, Paleoceanography and Taxonomy of Agglutinated Foraminifera*, 271-304, Kluwer Academic Publishers.
- Gooday, A.J. 1993. **Deep-sea benthic foraminiferal species which exploit phytodetritus: Characteristic features and controls on distribution.** *Marine Micropaleontology*, 22: 187-205.
- Gooday, A. J., 1996. **Epifaunal and shallow infaunal foraminiferal communities at three abyssal NE Atlantic sites subject to differing phytodetritus input regimes.** *Deep-Sea Research*, 43: 1395-1421.

- Gooday, A. J. 2003. **Benthic foraminifera (Protista) as tools in deep-water palaeoceanography: environmental influences on faunal characteristics.** *Advances in marine biology*, 46, 1-90.
- Gooday, A. J., and Rathburn, A. E. 1999. **Temporal variability in living deep-sea benthic foraminifera: A review.** *Earth-Science Reviews*, 46(1), 187-212.
- Gradstein, F. M., and Berggren, W. A. 1981. **Flysch-type agglutinated foraminifera and the Maestrichtian to Paleogene history of the Labrador and North Seas.** *Marine Micropaleontology*, 6(3), 211-268.
- Gradstein, F. M., Ogg, J. G., Schmitz, M., and Ogg, G. (Eds.). 2012. *The Geologic Time Scale 2012 2-Volume Set* (Vol. 2). Elsevier.
- Gradstein, F.M. and Kaminski, M.A. 1989. **Taxonomy and biostratigraphy of new and emended species of Cenozoic deep-water agglutinated foraminifera from the Labrador and North Seas.** *Micropaleontology*, 35, p. 83, pl. 9, figs. 1a-12.
- Hammer, Ø. and Harper, D.A.T. 2006. *Paleontological Data Analysis*. Blackwell.
- Hancock, H.J.L., Dickens, G.R., Thomas, E., and Blake, K.L. 2006. **Reappraisal of early Paleogene CCD curves: foraminiferal assemblages and stable carbon isotopes across the carbonate facies of Perth Abyssal Plain.** *International Journal of Earth Sciences*, 96 (5):925-946.
- Haq, B. U., Hardenbol, J., and Vail, P. R. 1987. Chronology of fluctuating sea levels since the Triassic. *Science*, 235(4793), 1156-1167.
- Heinz, P., Kitazato, H., Schmiedl, G., and Hemleben, C. 2001. **Response of deep-sea benthic foraminifera from the Mediterranean Sea to simulated phytoplankton pulses under laboratory conditions.** *The Journal of Foraminiferal Research*, 31(3), 210-227.
- Heron-Allen, E. 1915. **IX—A short Statement upon the Theory, and the Phenomena of Purpose and Intelligence exhibited by the Protozoa, as illustrated by Selection and Behaviour in the Foraminifera.** *Journal of the Royal Microscopical Society* 35 (6): 547-557.
- Hess, S., and Kuhnt, W. 1996. **Deep-sea benthic foraminiferal recolonization of the 1991 Mt. Pinatubo ash layer in the South China Sea.** *Marine Micropaleontology*, 28(2), 171-197.
- Higgins, J. A., and Schrag, D. P. 2006. **Beyond methane: towards a theory for the Paleocene–Eocene thermal maximum.** *Earth and Planetary Science Letters*, 245(3), 523-537.
- Hoenisch, B., Ridgwell, A., Schmidt, D. N., Thomas, E., Gibbs, S. J., Sluijs, A., ... and Williams, B. 2012. **The Geological Record of Ocean Acidification: Supporting Online Material.**
- Holbourn, A., Henderson, A. S., and MacLeod, N. 2013. **Atlas of benthic foraminifera.** John Wiley and Sons.
- Huber, M., and Caballero, R. 2011. **The early Eocene equable climate problem revisited.** *Climate of the Past*, 7(2), 603-633.
- Huber, M., and Sloan, L. C. 2001. **Heat transport, deep waters, and thermal gradients: Coupled simulation of an Eocene greenhouse climate.** *Geophys. Res. Lett.*, 28(18), 3481-3484.
- Israelsky, M. C. 1951. **Foraminifera of the Lodo Formation, central California, General introduction and Part 1, arenaceous foraminifera.** *U. S. Geological Survey Professional Paper*, 240-A: 1-29.
- Jones, G.D. 1988. **A paleoecological model of Late Paleocene “flysch-type” agglutinated foraminifera using the paleoslope transect approach, Viking Graben, North Sea.** *Abh. Geol. B-A.*, 41: 143-153.
- Jones, R. W. 1994. **The Challenger Foraminifera.** *Oxford University Press*, Oxford, 1-149.
- Jones, R. W., and Charnock, M. A. 1985. **Morphogroups of agglutinating foraminifera. Their life positions and feeding habits and potential applicability in (paleo) ecological studies.** *Revue de Paléobiologie*, 4(2), 311-320.
- Jorissen, F.J., Fontanier, C., and Thomas, E. 2007. **Paleoceanographical proxies based on deep-sea benthic foraminiferal assemblage characteristics.** In: Hillaire-Marcel, C., de Vernal, A. (Eds.), *Proxies in Late Cenozoic Paleoclimatology* (Pt. 2): Biological tracers and biomarkers. Elsevier, Amsterdam.
- Jorissen, F.J., Stigter, H.C., and Widmark, J.G.V., 1995. **A conceptual model explaining benthic foraminiferal microhabitats.** *Marine Micropaleontology*, 26, 3–15.
- Kaiho, K. 1998. **Phylogeny of deep-sea calcareous trochospiral benthic foraminifera: evolution and diversification.** *Micropaleontology*, 44 (3): 291-311.
- Kaiho, K., Takeda, K., Petrizzo, M. R., and Zachos, J. C. 2006. Anomalous shifts in tropical Pacific planktonic and benthic foraminiferal test size during the Paleocene–Eocene thermal maximum. *Palaeogeography, Palaeoclimatology, Palaeoecology*, 237(2), 456-464.
- Kaminski, M. A., Gradstein, F. M., and Berggren, W. A. 1989. Paleogene benthic foraminifer biostratigraphy and paleoecology at Site 647, southern Labrador Sea. In *Proceedings of the Ocean Drilling Program: Scientific Results* (Vol. 105, pp. 705-730).

- Kaminski, M. A., Gradstein, F. M., Berggren, W. A., Geroch, S., and Beckmann, J. P. 1988. **Agglutinated foraminiferal assemblages from Trinidad: Taxonomy, Stratigraphy, and Paleobathymetry.** In Gradstein, F. M. and Rögl, F., (eds.), Second International Workshop on Agglutinated Foraminifera, Vienna 1986, *Abhandlungen der Geologischen Bundesanstalt*, 41: 155-228.
- Kaminski, M. A., Kuhnt, W., and Radley, J. D. 1996. **Palaeocene–Eocene deep water agglutinated foraminifera from the Numidian Flysch (Rif, Northern Morocco): Their significance for the palaeoceanography of the Gibraltar gateway.** *Journal of Micropalaeontology*, 15(1), 1-19.
- Kaminski, M.A. and Gradstein, F.M. 2005. **Atlas of Paleogene Cosmopolitan Deep-Water Agglutinated Foraminifera.** *Grzybowski Foundation Special Publication* n.10.
- Katz, M. E., and Miller, K. G. 1991. **Early Paleogene benthic foraminiferal assemblages and stable isotopes in the Southern Ocean.** In *Proc. Ocean Drill. Program Sci. Results* (Vol. 114, pp. 481-512).
- Katz, M. E., Cramer, B. S., Toggweiler, J. R., Esmay, G., Liu, C., Miller, K. G., Rosenthal, Y., Wade, B.S. and Wright, J. D. 2011. **Impact of Antarctic Circumpolar Current development on late Paleogene ocean structure.** *Science*, 332(6033), 1076-1079.
- Katz, M. E., Pak, D. K., Dickens, G. R., and Miller, K. G. 1999. **The source and fate of massive carbon input during the latest Paleocene thermal maximum.** *Science*, 286 (5444), 1531-1533.
- Katz, M.E., Cramer, B.S., Mountain, G.S., Katz, S., and Miller, K.G. 2001. **Uncorking the bottle: What triggered the Paleocene/Eocene thermal maximum methane release?** *Paleoceanography*, 16 (6): 549-562.
- Kelly, D.C., Nielsen, T.M.J., McCarren, H.K., Zachos, J.C., and Röhl, U. 2010. **Spatiotemporal patterns of carbonate sedimentation in the South Atlantic: Implications for carbon cycling during the Paleocene-Eocene Thermal Maximum.** *Palaeogeography, Palaeoclimatology, Palaeoecology*, 293:30-40.
- Kennett, J. P. 1966. **Foraminiferal evidence of a shallow calcium carbonate solution boundary, Ross Sea, Antarctica.** *Science*, 153(3732), 191-193.
- Kennett, J.P. and Stott, L.D. 1990. **Proteus and proto-oceanus: ancestral Paleogene oceans as revealed from Antarctic stable isotopic results; ODP leg 113.** In *Proceedings of the Ocean Drilling, Scientific Results*, vol.113, p. 865 – 880.
- Kitazato, H., Shirayama, Y., Nakatsuka, T., Fujiwara, S., Shimanaga, M., Kato, Y., ... and Suzuki, K. 2000. **Seasonal phytodetritus deposition and responses of bathyal benthic foraminiferal populations in Sagami Bay, Japan: preliminary results from “Project Sagami 1996–1999”.** *Marine Micropaleontology*, 40(3), 135-149.
- Klitgaard, K. D., and Sejrup, H. P. **Modern benthic foraminiferal biofacies across the northern North Sea.** *Sarsia* 81.2 (1996): 97-106.
- Kominz, M. A., Browning, J. V., Miller, K. G., Sugarman, P. J., Mizintseva, S., and Scotese, C. R. 2008. Late Cretaceous to Miocene sea-level estimates from the New Jersey and Delaware coastal plain coreholes: An error analysis. *Basin Research*, 20(2), 211-226.
- Koutsoukos, E. A. 1992. **Late Aptian to Maastrichtian foraminiferal biogeography and palaeoceanography of the Sergipe Basin, Brazil.** *Palaeogeography, palaeoclimatology, palaeoecology*, 92(3), 295-324.
- Koutsoukos, E. A. 2000. **“Flysch-type” foraminiferal assemblages in the Cretaceous of northeastern Brazil.** In *Proceedings of the Fifth International Workshop on Agglutinated Foraminifera*, *Grzybowski Foundation Special Publication* (Vol. 7, pp. 243-260).
- Koutsoukos, E. A. M. 1998. **Upper Cretaceous palaeogeography of the Sergipe Basin, NE Brazil: area of the Divina Pastora and Mosqueiro lows.** *Zentralblatt für geologie und Paläontologie, Teil I*.
- Koutsoukos, E. A. M., and Dias-Brito, D. 1987. **Paleobatimetria da margem continental do Brasil durante o Albiano.** *Revista Brasileira de geociências*, 17(2), 86-91.
- Koutsoukos, E. A., and Hart, M. B. 1990. **Cretaceous foraminiferal morphogroup distribution patterns, palaeocommunities and trophic structures: a case study from the Sergipe Basin, Brazil.** *Transactions of the Royal Society of Edinburgh: Earth Sciences*, 81(03), 221-246.
- Koutsoukos, E. A., Leary, P. N., and Hart, M. B. 1990. **Latest Cenomanian—earliest Turonian low-oxygen tolerant benthic foraminifera: a case-study from the Sergipe basin (NE Brazil) and the western Anglo-Paris basin (southern England).** *Palaeogeography, Palaeoclimatology, Palaeoecology*, 77(2), 145-177.

- Krasheninnikov, V. A. 1974. **Upper Cretaceous benthonic agglutinated foraminifera, Leg 27 of the Deep Sea Drilling Project.** In Veevers, J. J., Heirtzler, J. R. et al., (eds.), *Initial Reports of the Deep Sea Drilling Project*, 27: 531-662.
- Kucera, M., Malmgren, B. A., and Sturesson, U. 1997. **Foraminiferal dissolution at shallow depths of the Walvis Ridge and Rio Grande Rise during the latest Cretaceous: Inferences for deep-water circulation in the South Atlantic.** *Palaeogeography, Palaeoclimatology, Palaeoecology*, 129(3), 195-212.
- Kuhnt, W. 1987. *Biostratigraphie und Paläoenvironment der externen Kreidesequenzen des westlichen Rif und Betikum: e. Ansatz zur Rekonstruktion der Kreidepaläogeographie des Gibraltarbogens* (Doctoral dissertation).
- Kuhnt, W., and Collins, E. S. 1996. Cretaceous to Paleogene benthic foraminifera from the Iberia Abyssal Plain. In: *Proceedings of the ODP Scientific Results* (pp. 203-216). National Science Foundation.
- Kuhnt, W., and Urquhart, E. 2001. **Tethyan flysch-type benthic foraminiferal assemblages in the North Atlantic: Cretaceous to Palaeogene deep water agglutinated foraminifera from the Iberia Abyssal Plain (ODP Leg 173).** *Revue de micropaléontologie*, 44(1), 27-58.
- Kuhnt, W., Kaminski, M. A., and Moullade, M. 1989. **Late Cretaceous deep-water agglutinated foraminiferal assemblages from the North Atlantic and its marginal seas.** *Geologische Rundschau*, 78(3), 1121-1140.
- Leckie, R. M. and Olson, H.C. 2003. **Foraminifera as proxies for sea-level change on siliciclastic margins.** In: *Micropaleontologic Proxies for Sea-level Change and Stratigraphic discontinuities. SEPM Special Publication*, 75: 5-19.
- Lee, G. H., Park, S. C., and Kim, D. C. 2000. **Fluctuations of the calcite compensation depth (CCD) in the East Sea (Sea of Japan).** *Geo-Marine Letters*, 20(1), 20-26.
- Legendre, P., and Legendre, L. 1998. *Numerical Ecology*, Volume 24, (Developments in Environmental Modelling).
- Lipps, J. H., and Valentine, J. W. 1970. **The role of foraminifera in the trophic structure of marine communities.** *Lethaia* 3 (3): 279-286.
- Liu, C., Browning, J. V., Miller, K. G., and Olsson, R. K. 1997. **Paleocene benthic foraminiferal biofacies and sequence stratigraphy, Island Beach borehole, New Jersey.** In *Proceedings of the Ocean Drilling Program. Scientific results* (Vol. 156, pp. 267-275). Ocean Drilling Program.
- Loeblich, A. R. and Tappan, H. 1955. **Revision of some Recent foraminiferal genera.** Smithsonian Institution, Miscellaneous Collections, 128: 1-37.
- Loeblich, A. R. and Tappan, H. 1964. **Sarcodina-chiefly "Thecamoebians" and Foraminiferida.** In Moore, R.C. (ed.), *Treatise on Invertebrate Paleontology, Part C, Protista 2* (2 volumes.), University of Kansas Press, 1-900.
- Loeblich, A. R. and Tappan, H. 1986. **Some new and revised genera and families of hyaline calcareous Foraminiferida (Protozoa).** *Transactions of the American Microscopical Society*, 105: 239-265.
- Loeblich, A. R. and Tappan, H. 1987/1988. **Foraminiferal Genera and their Classification.** Van Nostrand Reinhold Co., New York.
- Loeblich, A. R. and Tappan, H. 1994. **Foraminifera of the Sahul Shelf and Timor Sea.** Cushman Foundation for Foraminiferal Research, Special Publication, 31: 1-661.
- Lohmann, G. P. 1978. **Abyssal benthonic foraminifera as hydrographic indicators in the western South Atlantic Ocean.** *The Journal of Foraminiferal Research*, 8(1), 6-34.
- Loubere, P. 1996. **The surface ocean productivity and bottom water oxygen signals in deep water benthic foraminiferal assemblages.** *Marine Micropaleontology*, 28(3), 247-261.
- Lourens, L. J., Sluijs, A., Kroon, D., Zachos, J. C., Thomas, E., Röhl, U., ... and Raffi, I. 2005. **Astronomical pacing of late Palaeocene to early Eocene global warming events.** *Nature*, 435(7045), 1083-1087.
- Luciani, V., Giusberti, L., Agnini, C., Backman, J., Fornaciari, E., and Rio, D. 2007. **The Paleocene–Eocene Thermal Maximum as recorded by Tethyan planktonic foraminifera in the Forada section (northern Italy).** *Marine Micropaleontology*, 64(3), 189-214.
- Lyle, M., Barron, J., Bralower, T. J., Huber, M., Olivarez Lyle, A., Ravelo, A. C., Rea, D.K. and Wilson, P. A. 2008. **Pacific Ocean and Cenozoic evolution of climate.** *Reviews of Geophysics*, 46(2).

- Maxwell, A. E. *et al*, 1970, **Initial Reports of the Deep Sea Drilling Project, Volume III**. Washington (U.S. Government Printing Office).
- McCarren, H., Thomas, E., Hasegawa, T., Röhl, U., and Zachos, J. C. 2008. **Depth dependency of the Paleocene-Eocene carbon isotope excursion: Paired benthic and terrestrial biomarker records** (Ocean Drilling Program Leg 208, Walvis Ridge). *Geochemistry, Geophysics, Geosystems*, 9(10).
- Mesquita, A. 1998. **High-resolution biostratigraphy and paleoecology of early Miocene foraminiferal assemblages from turbidite reservoirs in the Campos Basin** (abstract): American Association of Petroleum Geologists. *Bulletin*, 82, 1943.
- Milani, E. J., Brandão, J. A. S. L., Zalán, P. V., and Gamboa, L. A. P. 2000. **Petróleo na margem continental brasileira: geologia, exploração, resultados e perspectivas**. *Brazilian Journal of Geophysics*, 18(3), 351-396.
- Milani, E.J., Rangel, H.D, Bueno, G.V., Stica, J.M., Winter, W.R., Caixeta, J.M. and Pessoa-Neto, O.C. 2007. **Bacias Sedimentares Brasileiras - Cartas Estratigráficas**, *Boletim de Geociencias da Petrobras*, v.15, n.2.
- Miller, K. G., Fairbanks, R. G., and Mountain, G. S. 1987. **Tertiary oxygen isotope synthesis, sea level history, and continental margin erosion**. *Paleoceanography*, (2), 1-19.
- Miller, K. G., Gradstein, F. M., and Berggren, W. A. 1982. **Late Cretaceous to early Tertiary agglutinated benthic foraminifera in the Labrador Sea**. *Micropaleontology*, 1-30.
- Miller, K. G., Kominz, M. A., Browning, J. V., Wright, J. D., Mountain, G. S., Katz, M. E., ... and Pekar, S. F. 2005. **The Phanerozoic record of global sea-level change**. *Science*, 310(5752), 1293-1298.
- Miller, K.G. and Katz, M. E. 1987. **Oligocene to Miocene benthic foraminiferal and abyssal circulation changes in the north Atlantic**. *Micropaleontology*, 33(2): 97-149.
- Modica, C. J., and Brush, E. R. 2004. **Postrift sequence stratigraphy, paleogeography, and fill history of the deep-water Santos Basin, offshore southeast Brazil**. *AAPG bulletin*, 88(7), 923-945.
- Mohriak, W. U. 2003. **Bacias sedimentares da margem continental Brasileira**. *Geologia, Tectônica e Recursos Minerais do Brasil*, 87-165.
- Mohriak, W. U., Mello, M. R., Dewey, J. F., and Maxwell, J. R. 1990. **Petroleum geology of the Campos Basin, offshore Brazil**. *Geological Society, London, Special Publications*, 50(1), 119-141.
- Moore Jr, T. C., Heath, G. R., & Kowsmann, R. O. (1973). Biogenic sediments of the Panama Basin. *The Journal of Geology*, 458-472.
- Muller-Merz, E. and Oberhansli, H., 1991. **Eocene bathyal and abyssal benthic foraminifera from a South Atlantic transect at 20° 30° S**. *Palaeogeography, Palaeoclimatology, Palaeoecology*, 83:117-171.
- Murray, J. W. 2001. **The niche of benthic foraminifera, critical thresholds and proxies**. *Marine Micropaleontology*, 41(1), 1-7.
- Murray, J. W. 2006. *Ecology and applications of benthic foraminifera*. Cambridge University Press.
- Murray, J. W. 2007. **Biodiversity of living benthic foraminifera: How many species are there?**. *Marine Micropaleontology*, 64(3), 163-176.
- Murray, J. W. 2014. *Ecology and palaeoecology of benthic foraminifera*. Routledge.
- Murray, J.W. 1976. **A method of determining proximity of marginal seas to an ocean**. *Marine Geology*, 22: 103-119.
- Nagy, J., Kaminski, M. A., Kuhnt, W., and Bremer, M. A. 2001. **Agglutinated foraminifera from neritic to bathyal facies in the Palaeogene of Spitsbergen and the Barents Sea**. In: Hart, M.B., Kaminski, M.A., and Smart, C.W. (eds) 2000. Proceedings of the Fifth International Workshop on Agglutinated Foraminifera. Grzybowski Foundation Special Publication, 7, 333-361.
- Natland, M. L. 1933. *The temperature and depth-distribution of some Recent and fossil Foraminifera in the southern California region*. University of California Press.
- Natland, M. L., Eduardo, G. P., Cañon, A., and Ernst, M. 1974. **A system of stages for correlation of Magallanes Basin sediments**. *Geological Society of America Memoirs*, 139, 1-126.
- Nomura, R. 1991. **Paleoceanography of Upper Maestrichtian to Eocene benthic foraminiferal assemblages at sites 752, 753 and 754, Eastern Indian Ocean**. In: *Proc. ODP, Sci. Res* (Vol. 121, pp. 3-29).
- Nomura, R., and Takata, H. 2005. **Data report: Paleocene/Eocene benthic foraminifera, ODP Leg 199 Sites 1215, 1220, and 1221, equatorial central Pacific Ocean**. In: P. A. Wilson, M. Lyle, and J. V. Firth (Eds.), *Proceeding of Ocean Drilling Program, Scientific Results* (Vol. 199, pp. 1-34).
- Nyong, E.E., and Olsson, R.K., 1983/84, **A paleoslope model of Campanian to lower Maestrichtian foraminifera in the North Atlantic Basin and adjacent continental margin**: *Marine Micropaleontology*, v. 8, p. 437-477.

- Olsson, R.K. and Nyong, E. 1984. **A paleoslope model for Campanian-Lower Maastrichtian foraminifera of New Jersey and Delaware.** *Journal of Foraminiferal Research*, 14 (1): 50-68.
- Opdyke, B. N., and Wilkinson, B. H. (1993). Carbonate mineral saturation state and cratonic limestone accumulation. *American Journal of Science*, 293, 217-217.
- Ortiz, N. 1995. **Differential patterns of benthic foraminiferal extinctions near the Paleocene/Eocene boundary in the North Atlantic and the western Tethys.** *Marine Micropaleontology*, 26(1), 341-359.
- Ortiz, S. and Thomas, E. 2006. **Lower-middle Eocene benthic foraminifera from the Fortuna Section (Betic Cordillera, southeastern Spain).** *Micropaleontology*, 52 (2): 97-150.
- Pak, D.K. and Miller, K.G. 1992. **Paleocene to Eocene benthic foraminiferal isotopes and assemblages: Implications for deepwater circulation.** *Paleoceanography*, 7 (4): 405-422.
- Pälike, H., Lyle, M. W., Nishi, H., Raffi, I., Ridgwell, A., Gamage, K., ... and Sawada, K. 2012. **A Cenozoic record of the equatorial Pacific carbonate compensation depth.** *Nature*, 488(7413), 609-614.
- Parker, F. L. 1948. *Foraminifera of the continental shelf from the Gulf of Maine to Maryland.* Museum of Comparative Zoology.
- Parker, F. L. 1954. **Distribution of the Foraminifera in the northeastern Gulf of Mexico,** *Bulletin of The Museum of Comparative Zoology*, 111(10): 451-588.
- Parker, W. C., and Arnold, A. J. 1999. **Quantitative methods of data analysis in foraminiferal ecology.** In *Modern foraminifera* (pp. 71-89). Springer Netherlands.
- Pawlowski, J., 2000. **Introduction to the molecular systematics of foraminifera.** *Micropaleontology*, 46 (Supplement no.1), 1-12.
- Pawlowski, J., Holzmann, M. and Tyska, J. 2013. **New supraordinal classification of Foraminifera: molecules meet morphology.** *Marine Micropaleontology*, 100: 1-10.
- Pawlowski, J., Holzmann, M., Berney, C., Fahrni, J., Gooday, A. J., Cedhagen, T. ... and Bowser, S. S. 2003. **The evolution of early Foraminifera.** *Proceedings of the National Academy of Sciences*, 100(20), 11494-11498.
- Pearson, P. N. 2012. **Oxygen isotopes in foraminifera: Overview and historical review.** *Paleontological Society Papers* 18: 1-38.
- Pekar, S.F. and Kominz, M.A. 2001. **Two-dimensional paleoslope modeling: a new method for estimating water depths on benthic foraminiferal biofacies and paleoshelf margins.** *Journal of Sedimentary Research*, 71 (4): 608-620.
- Penman, D. E., Hönisch, B., Zeebe, R. E., Thomas, E., & Zachos, J. C. 2014. **Rapid and sustained surface ocean acidification during the Paleocene-Eocene Thermal Maximum.** *Paleoceanography*, 29(5), 357-369.
- Perch-Nielsen et al., 1977. **Site 356: São Paulo Plateau.** In: Supko, P. R., Perch-Nielsen, K. et al., 1977. Initial Reports of the Deep Sea Drilling Project, Volume 39: Washington (U.S. Government Printing Office), pp. 1099-1132.
- Phleger, F. B. 1960. *Ecology and distribution of recent foraminifera.* The Johns Hopkins Press, Baltimore, pp. 297.
- Phleger, F. B., Parker, F. L., and Peirson, J. F. 1953. *North Atlantic Foraminifera.* Elanders Boktryckeri Aktiebolag.
- Poag, C.W., 1981. *Ecologic Atlas of Benthic Foraminifera of the Gulf of Mexico:* Woods Hole, Massachusetts, Marine Science International, 174 p.
- Scheibner, C., and Speijer, R. P. 2008a. **Late Paleocene–early Eocene Tethyan carbonate platform evolution—a response to long- and short-term paleoclimatic change.** *Earth-Science Reviews*, 90(3), 71-102.
- Scheibner, C., and Speijer, R. P. 2008b. **Decline of coral reefs during late Paleocene to early Eocene global warming.** *EEarth*, 3(1), 19-26.
- Scher, H. D., and Martin, E. E. 2006. **Timing and climatic consequences of the opening of Drake Passage.** *Science*, 312(5772), 428-430.
- Schmitz, B., Speijer, R. P., and Aubry, M. P. 1996. Latest Paleocene benthic extinction event on the southern Tethyan shelf (Egypt): Foraminiferal stable isotopic ($\delta^{13}\text{C}$, $\delta^{18}\text{O}$) records. *Geology*, 24(4), 347-350.
- Schonfeld, J. 2002. A new benthic foraminiferal proxy for near-bottom current velocities in the Gulf of Cadiz, northeastern Atlantic Ocean Deep-Sea Research I, 49, 1853-1875.
- Schönfeld, J. 2002. **Recent benthic foraminiferal assemblages in deep high-energy environments from the Gulf of Cadiz (Spain).** *Marine Micropaleontology*, 44(3), 141-162.
- Sen Gupta, B. K. 2000. *Modern Foraminifera.* Kluwer Academic Publishers, 345 pp.

- Sender, S., Kaminski, M.A., and Jones, R. 2008. **Oligocene Deep-Water Agglutinated Foraminifera from the Congo Fan, Offshore Angola: Palaeoenvironments and Assemblage distributions.** In: Kaminski, M.A. and Coccioni, R. (eds.), 2008. *Proceedings of the Seventh International Workshop on Agglutinated Foraminifera*. Grzybowski Foundation Special Publication, 13, 107-156.
- Sikora, P.J., and Olsson, R.K., 1991, **A paleoslope model of late Albian to early Turonian foraminifera of the western Atlantic margin and North Atlantic basin.** *Marine Micropaleontology*, v. 18, p. 25–72.
- Sliter, W. V. 1975. **Foraminiferal life and residue assemblages from Cretaceous slope deposits.** *Geological Society of America Bulletin*, 86(7), 897-906.
- Sliter, W.V. 1977. **Cretaceous benthic foraminifers from the western South Atlantic Leg 39, DSDP. Initial Reports.**
- Sliter, W.V. and Baker, R. 1972. **Cretaceous bathymetric distribution of benthic foraminifera.** *Journal of Foraminiferal Research*, 2 (4): 167-183.
- Speijer, R., Scheibner, C., Stassen, P., and Morsi, A. M. M. 2012. **Response of marine ecosystems to deep-time global warming: A synthesis of biotic patterns across the Paleocene-Eocene thermal maximum (PETM).** *Austrian Journal of Earth Sciences*, 105(1), 6-16.
- Speijer, R., Schmitz, B., Aubry, M. P., and Charisi, S. D. 1995. **The latest Paleocene benthic extinction event: punctuated turnover in outer neritic benthic foraminiferal faunas from Gebel Aweina, Egypt.** *Israel Journal of Earth Sciences*, 44, 207-222.
- Stassen, P., Steurbaut, E., Morsi, A. M., Schulte, P., and Speijer, R. 2012a. **Biotic impact of Eocene thermal maximum 2 in a shelf setting (Dababiya, Egypt).** *Austrian Journal of Earth Sciences*, 105(1), 154-160.
- Stassen, P., Thomas, E., Speijer, R.P. 2012a. **The progression of environmental changes during the onset of the Paleocene-Eocene Thermal Maximum (New Jersey Coastal Plain).** *Austrian Journal of Earth Sciences*, 105 (1): 169-178.
- Stassen, P., Thomas, E., and Speijer, R. 2012b. **The progression of environmental changes during the onset of the Paleocene-Eocene thermal maximum (New Jersey Coastal Plain).** *Austrian Journal of Earth Sciences*, 105(1), 169-178.
- Stassen, P., Thomas, E., and Speijer, R. P. 2015. **Paleocene–Eocene Thermal Maximum environmental change in the New Jersey Coastal Plain: benthic foraminiferal biotic events.** *Marine Micropaleontology*, 115, 1-23.
- Supko, P. R., Perch-Nielsen, K. et al., 1977. **Initial Reports of the Deep Sea Drilling Project, Volume 39:** Washington (U.S. Government Printing Office).
- Szatmari, P., Conceição, J. C. J., Destro, N., Smith, P. E., Evensen, N. M., and York, D. 2000. **Tectonic and sedimentary effects of a hot-spot track of alkali intrusions defined by Ar-Ar dating in SE Brazil.** In: *31th Geological Congress, Abstracts Volume (CD-ROM)*.
- Takeda, K., and Kaiho, K. 2007. **Faunal turnovers in central Pacific benthic foraminifera during the Paleocene–Eocene thermal maximum.** *Palaeogeography, Palaeoclimatology, Palaeoecology*, 251(2), 175-197.
- Thomas, D. J. 2004. **Evidence for deep-water production in the North Pacific Ocean during the early Cenozoic warm interval.** *Nature*, 430 (6995), 65-68.
- Thomas, D. J., Bralower, T. J., and Jones, C. E. 2003. **Neodymium isotopic reconstruction of late Paleocene–early Eocene thermohaline circulation.** *Earth and Planetary Science Letters*, 209(3), 309-322.
- Thomas, E. 1985. **Late Eocene to Recent deep-sea benthic foraminifers from the central Equatorial Pacific Ocean.** *Initial Reports of the Deep Sea Drilling Project*, 85(OCT), 655-694.
- Thomas, E. 1989. **Development of Cenozoic deep-sea benthic foraminiferal faunas in Antarctic waters.** *Geological Society, London, Special Publications*, 47(1), 283-296.
- Thomas, E. 1990. **Late Cretaceous through Neogene deep-sea benthic foraminifers (Maud Rise, Weddell Sea, Antarctica).** In Barker, P., Kennett, J. P. et al., (eds.), *Proceedings of the Ocean Drilling Program, Scientific Results*, 113: 571-594.
- Thomas, E. 1998b. **Biogeography of the late Paleocene benthic foraminiferal extinction.** *Late Paleocene-Early Eocene climatic and biotic events in the marine and terrestrial records*, 214-243.
- Thomas, E. 2003. **Extinction and food at the seafloor: A high-resolution benthic foraminiferal record across the Initial Eocene Thermal Maximum, Southern Ocean Site 690.** *GSA Special Paper*, 369.
- Thomas, E. 2006. **An ocean view of the early Cenozoic Greenhouse World.** *Oceanography*, 19(4).
- Thomas, E. 2007. **Cenozoic mass extinctions in the deep sea: What perturbs the largest habit on Earth?** *GSA Special Paper*, 424.
- Thomas, E. and Shackleton, N.J. 1996. **The Paleocene-Eocene benthic foraminiferal extinctions and stable isotope anomalies.** *Geological Society, London, Special Publications*, 101: 401-441.

- Thomas, E., Brinkhuis, H., Huber, M. and Röhl, U. 2006. **An ocean view of the early Cenozoic Greenhouse World.** *Oceanography*, 19 (4): 94-103.
- Thomas, E., Zachos, J. C., and Bralower, T. J., 2000, **Deep-Sea Environments on a Warm Earth: latest Paleocene - early Eocene.** B. Huber, K. MacLeod, and S. Wing eds., *Warm Climates in Earth History*, Cambridge University Press, 132-160.
- Tinoco, I. M. 1971. **Foraminíferos e a passagem entre o Cretáceo eo Terciário em Pernambuco.** Doctoral dissertation, Doctoral Thesis, Univ. of São Paulo, Brazil.
- Tjalsma, R. C, and Lohmann, G. P. 1983. **Paleocene-Eocene bathyal and abyssal benthic foraminifera from the Atlantic Ocean.** *Micropaleontol. Spec. Publ*, 4:1-90.
- Tjalsma, R. C. 1977. 9. **Cenozoic Foraminifera from the South Atlantic, DSDP Leg 361, Initial Reports of DSDP Leg 361.**
- Torsvik, T. H., Rouse, S., Labails, C., and Smethurst, M. A. 2009. **A new scheme for the opening of the South Atlantic Ocean and the dissection of an Aptian salt basin.** *Geophysical Journal International*, 177(3), 1315-1333.
- Valentin, J. L. 1995. **Agrupamento e Ordenação.** In: Perez-Neto, P.R., Valentin, J.L. and Fernandez, F.A.S. (eds), *Oecologia Brasiliensis*, Vol. II: Tópicos em Tratamento de Dados Biológicos, p. 27-55.
- Van Andel, T. H. 1975. **Mesozoic/Cenozoic calcite compensation depth and the global distribution of calcareous sediments.** *Earth and Planetary Science Letters*, 26(2), 187-194.
- Van Andel, T. H., Thiede, J., Sclater, J. G., and Hay, W. W. 1977. **Depositional history of the South Atlantic Ocean during the last 125 million years.** *The Journal of Geology*, 651-698.
- Van der Zwaan, G. J., Jorissen, F. J., and De Stigter, H. C. 1990. **The depth dependency of planktonic/benthic foraminiferal ratios: constraints and applications.** *Marine Geology*, 95(1), 1-16.
- Van Morkhoven, F.P.M., Berggren, W.A., Edwards, A.S. et al. 1986. **Cenozoic cosmopolitan deep-water benthic foraminifera,** *Bulletin des Centers de Recherches Exploration-Production Elf-Aquitaine*, Memoire, v.11, p.1-421.
- Viviers, M. C. and Ferreira, E. P. 2006. **Paleocene-Eocene Brazilian sedimentary successions and their "flysch-type" foraminiferal assemblages.** *Anu. Inst. Geocienc.*, 29, (1): 575-575.
- Waśkowska-Oliwa, A. 2005. **Foraminiferal palaeodepth indicators from the lower Palaeogene deposits of the Subsilesian Unit (Polish Outer Carpathians).** *Studia Geologica Polonica*, 124, 297-324.
- Widmark, J.G.V. 2000. **Biogeography of terminal Cretaceous benthic foraminifera: deep-water circulation and trophic gradients in the deep South Atlantic.** *Cretaceous Research*, 21:367-379.
- Winkler, W. 1984. **Rhabdammina-fauna: what relation to turbidites? Evidence from the Gurnigel-Schlieren Flysch.** *Benthos*, 83, 611-617.
- Wood, K. C., Miller, K. G., and Lohmann, G. P. 1985. **Middle Eocene to Oligocene benthic foraminifera from the Oceanic formation, Barbados.** *Micropaleontology*, 1:181-196.
- Zachos, J. C., Röhl, U., Schellenberg, S. A., Sluijs, A., Hodell, D. A., Kelly, D. C., ... and Kroon, D. 2005. **Rapid acidification of the ocean during the Paleocene-Eocene Thermal Maximum.** *Science*, 308(5728), 1611-1615.
- Zachos, J.C., Kroon, D., Blum, P., et al., 2004. Leg 208 Summary. *Proc. ODP, Init. Repts.*, 208: College Station, TX (Ocean Drilling Program).
- Zachos, J.C., Lohmann, K.C., Walker, J.C.G., Wise, S.W. 1993. **Abrupt climate change and transient climates in the Paleogene: a marine perspective.** *Journal of Geol.*, 101: 193-215.
- Zachos, J.C., Pagani, M., Sloan, L., Thomas, E., Billups, K. 2001. **Trends, rhythms, and aberrations in global climate 65 Ma to Present.** *Science*, 292: 686-693.
- Zachos, J.C., Röhl, U., Schellenberg, S., Sluijs, A., Hodell, D.A., Kelly, D.C., Thomas, E., Nicolo, M., Raffi, I., Lourens, L.J., McCarren, H., and Kroon, D. 2005. **Rapid acidification of the ocean during the Paleocene-Eocene Thermal Maximum.** *Science*, 308:1611-1615.
- Zalán, P. V. 2004. **Evolução fanerozóica das bacias sedimentares brasileiras.** *Geologia do Continente Sul-Americano, Beca*, 595-615.